Triangulation methods in engineering measurement.

Stephen Alexander Kyle

Department of Photogrammetry and Surveying
UNIVERSITY COLLEGE LONDON

Submitted for the degree of
Doctor of Philosophy

March 1988

Abstract.

Industrial surveying and photogrammetry are being increasingly applied to the measurement of engineering objects which have typical dimensions in the range 2 - 100 metres. Both techniques are examples of the principle of triangulation. By applying photogrammetric concepts to surveying methods and vice-versa, a general approach is established which has a number of advantages. In particular, alternative strategies for constructing and analysing measurment networks are developed. These should help to strengthen the geometry and simplify the analysis.

The primary results concern the use of non-levelled theodolites, which have applications on board floating objects, and three new suggestions for controlling and computing relative orientations in photogrammetry. These involve reciprocal observations with theodolites, the photographing of linear scales defined by three target points and employing cameras which have been levelled.

As a secondary result, some consideration is given to automation and instrument design. It is suggested that polarimetry could be successfully applied to improve the transfer of orientation in confined situations, such as in mining. In addition, the potential use of electronic cameras as photo-theodolites is discussed.

Contents

ERRATA.

Aberration has been consistently spelled incorrectly as abberation.

P94, line 20. For principal read principle.

P139, line 9. For Imaging read Imagine.

P176, line 8. For superceeded read superceded.

P187, Ref. A2. For british read British.

P203, Ref. L1. For guaging read gauging.

Notation.

For convenience, the following notation and terminology has been adopted :

A,R etc are matrices.
B(m,n) is a matrix of m rows and n columns.
a,r,b are matrix elements, numbered where appropriate. For example, a12 is element a on row 1, column 2.
Mt is the transpose of M
M* it the inverse of M
Groups of matrix elements and partitioned matricies are drawn in square brackets.
U , V , x , y are vectors.
(a,b,c) is a 3-D vector with axial components a,b,c.
U x V is a vector (cross) product.

Multiplication, matrix products and scalar (dot) products of vectors are indicated with "." The context should be sufficient to differentiate between them.

As in Fortran :
- sqrt (..) indicates the square root of the quantity in brackets
- v**2 is the square of value v.
- mod (..) is the magnitude (modulus) of the vector in brackets

The term micron for micrometre is in common usage, and is adopted here.

References to accuracies which are not otherwise qualified should be taken as implying standard errors. The abbreviation "rms" stands for root mean square.

Preface.

This work was undertaken for the challenge and pleasure of the intellectual activity. Unfortunately, it had to be funded out of personal finances, and these would have been insufficient without the help provided by my many friends and colleagues named below.

Lack of proper financing in the field of engineering can make any research activity very difficult, since concrete and practical results are usually expected. Without financing, equipment cannot be purchased, and any hopes of hardware developments, which are a major feature of such research, must be given up. Although some suggestions relating to instrumentation are made, they are not supported by experiment for this reason. I emphasize the point because I feel several of the ideas are worth a closer examination. Indeed, my remarks on an electronic photo-theodolite have much in common with ideas and products from other sources. Prof. Wester-Ebbinghaus, a respected worker in the field of digital photogrammetry, has recently proposed something similar, and current electronic theodolites with built-in CCD cameras simply represent another version of the idea. There can surely be little doubt that the field is commercially interesting and therefore worthy of support.

Fortunately, a concrete result can be reported. This is the development of a set of Fortran 77 programs, known under the collective name of TRIGFIX, which run on a desktop micro-computer. They incorporate most of the geometrical concepts outlined in the thesis and should provide a useful tool for data analysis. It may even prove possible to sell them, and so obtain some financial return for my efforts.

A commercial approach is now almost a necessity in any field of research, and the university authorities have agreed that access to this thesis should be restricted for the next two years. My purpose is to preserve any commercial advantage which might be offered by the ideas on instrumentation, but it is not my intention to prevent bona fide university researchers from using the material.

Given the importance of financing, I also feel obliged to warn other prospective Ph D students of a possible financial impediment to studying. If you return to research at a UK university after a period working abroad, as I did, you may be regarded as an overseas student, whether or not you possess a full British passport. This implies very large fees if you study full-time for a research degree, and no possibility of a grant from the Science and Engineering Research Council. Partly as a result of this, I decided to work instead as a part-time student, at one tenth the fees. In my own situation this was probably the best solution. It also had the advantage that I could then describe myself as either a consultant or student, depending on whether I wished to elicit respect or sympathy.

Despite the difficulties, I have no regrets about undertaking the work. I particularly wish to thank those individuals mentioned below. It is my hope they will share in my pleasure at a successful conclusion, since they have all contributed towards it.

In gratitude to

My supervisor, Ian Harley, for his mathematical abilities and support in our several attemps to find funding.
Peter Scott, my original supervisor and co-worker on the NPL job, who has been particularly helpful with the use of the Metrograph.
Arthur Allan, who originally encouraged me to register for a PhD.
John Gates, now a visiting professor at UCL, but originally in charge of the NPL job which started this work. His extensive knowledge of optics was very informative.
Further colleagues from NPL, Tony Horsfield, Jim Burch, Simon Oldfield, Roger Hunt and Colin Forno, who are particularly valued. Jim was especially helpful with the diffraction grating for the starburst technique. Not only have they all been willing to talk to me at any time, they have on many occasions arranged for NPL facilities to be made available to me.
Ernie Wickens for his help with measurements.
Colin Osborne for manufacturing (and designing) several items of test equipment, and not complaining when I asked for alterations.
Anne Scott and Peter (again) for accomodation at giveaway prices. The food was terrific.
Isobel Hart, for the generous use of her flat when she was away.
Jane Wonnacott for accomodation and supply of gin and tonic.
Keith Greig, with whom I have shared accomodation in more places than either of us can remember, and who still lets me use his spare room.
Mum and Dad, for the calculator (very handy) and the all-important cash injection which paid, amongst other things, for the printing of this thesis.
George Chadwick and Douglas Self for supporting me at the bar. After all, a man has to relax sometime.

Ch. 1 Introduction.

The application of the methods of surveying and photogrammetry to the solution of industrial measurement problems has become fairly well established over the past decade. The extent of this can be seen by the availability of systems based on dual electronic theodolites [F4,F5] and specially developed photogrammetric techniques [A5]. Applications tend to involve objects with dimensions typically in the range 2 - 100 metres, and this is assumed in the work which follows.

The most accurate photogrammetric methods are based on targetted points, optimum geometry and multiple ray intersection. Photographs may then be measured individually or monoscopically, in much the same way as a set of observations are made at a theodolite. This may be described as the mono photogrammetric method, in order to distinguish it from stereo photogrammetry. The latter has a more restricted and usually less accurate geometry, in order to create stereo imagery, but can rely on an object's surface texture for most of the targetting. Despite its tendency to lower accuracy, it remains a useful approach for some engineering problems. Although stereo photographs must be measured in pairs, the mathematical analysis is no different than for two photographs which are monoscopically observed.

Once involved with engineering problems, the application of photogrammetry and surveying demands a different approach from that needed for traditional map making. Engineering objects are very much three dimensional, rather than roughly planar. Although triangulation is essentially non-contacting (one of its attractions to engineers), targetting and illumination can be much more readily controlled than when making a map. There are also more ways of establishing measurement networks than would otherwise be available.

In short, the task is open to a wide variety of approaches. However, this should not make it more complicated, or else the methods will not be adopted. There is therefore scope for extracting the general principles of triangulation, with a view to simplifying the physical and mathematical solution.

The close similarity between surveying and mono photogrammetry is an immediate encouragement to do this. Of course, it is no particular revelation that the subjects are essentially the same, particularly to photogrammetrists. The general case of a non-levelled theodolite, whilst novel to some surveyors, is no different from a camera in normal usage. It is also self-evident that measurements in the photographic image only provide directional information, as does a telescope pointing in a theodolite. It is the method of acquiring the data which is different, and both types of measurement can be treated by the same vector analysis [E14]. Indeed, in its early days photogrammetry was a procedure for terrestrial measurement, closely linked to surveying, and the literature provides a valuable source of general concepts. Unfortunately, these tend to be widely dispersed, and one result of the current work has been to gather a number of them together. Where appropriate, they are contrasted against the ideas developed here.

1.1 Industrial triangulation reviewed.

Several major manufacturers of photogrammetric and survey equipment, and some new entrants to the field, now offer systems tailored to industrial measurement.

Wild in Switzerland offer the RMS 2000 system, based on their electronic theodolite. Their association with the West German firm, Leitz, (which they own) has resulted in Leitz software being incorporated into this package.

As manufacturers of CMMs, Leitz became aware of the alternative approach to coordinate measurement offered by theodolites, and adapted their existing software accordingly. The theodolites are now being offered with motor drives and electronic imaging, and the software for the newer systems has been specially developed for industrial surveying.

Wild also offer software for industrial photogrammetry, notably the BINGO package, primarily for use with their analytical plotters. This program can also process some geodetic measurements. Under their own name, Leitz sell an alternative photogrammetric system, Elcovision. One version is based on the Leica camera and provides a relatively inexpensive facility of interest to groups such as architects, for building elevations and suchlike, and police forces, for measurements at traffic accidents. Another version is directed at the industrial market and uses electronic cameras. This has been developed from "Mapvision" [U4] which originated in Finnland.

Kern, also in Switzerland, are possibly further advanced with their electronic theodolite system, ECDS (Dec. 1987). Together with General Motors in the USA, an automated version, SPACE, has been developed. This can currently operate by having two theodolites sight to well defined targets on the object of interest, or by scanning the object using a laser beam from one whilst tracking the backscattered light with the other [U1,U2].

Kern also offer industrial photogrammetric software, CRISP, for used with their analytical plotter [A6].

In the USA, Keuffel & Esser are active with dual electronic theodolite systems, sold as one variant of their AIMS system. This includes a photogrammetric package as well. K&E have even had one of their theodolites on board the space shuttle [A11], a rather pleasing example of theodolites in use in a non-levelled environment.

Also in the USA, a specialist photogrammetric firm, GSI, currently undertakes the most accurate commercial work. They have developed their own cameras, mono-comparators and software to deal with problems requiring sub-millimetre and micron accuracy [H1].

Amongst the large firms, Zeiss (Oberkochen) do not appear to have the same high profile in the industrial field as the companies above, but they do offer both a theodolite system (IMS) and one based on photogrammetry. Zeiss, a West German firm like Leitz, are also producers of CMMs, and are doubtless aware of the cross connection.

Yet another West German firm, Rollei, have entered the photogrammetric field. Manufacturers of cameras, they have taken up Wester-Ebbinghaus's ideas on digital photogrammetry, and now offer a complete system [U5]. Their camera, with a built-in scanning electronic sensor, probably represents the most well developed implementation of real-time digital photogrammetry in the industrial field. They were also one of the first in the field with a "low cost" option. This relies on a digitizing tablet and personal computer for analysing photographs.

A third variant of the low cost approach exists in the UK, and is called Photometrology. This originated with work done at ICI, who had a need to measure "as-built" process plant [Q1,Q2]. This system can be progressively upgraded, and appears to be particularly well tailored to the production of engineering drawings.

In the field of real-time photogrammetric systems, Leitz and Rollei are not alone. For medical applications, Oxford Metrics sells the VICON system [U11,U12]. This uses conventional television cameras to analyse human gait, by imaging reflective targets attached to the subject. Robots, too, can be measured photogrammetrically by fully electronic means, and the SELSPINE system is manufactured to do just this [U13]. Targets in this case are active, light-emmitting diodes attached to the robot.

None of the above systems is an academic curiosity. They have sold particularly well in the aerospace field, where precision is a high priority. British Aerospace, Westland Aircraft, the European Space Agency, General Dynamics, Boeing and McDonnell Douglas all make use of industrial surveying or photogrammetric methods. Academic researchers, too, have applied their talents to practical applications. The particular example of antenna measurement suggests a real need [K1 - K6].

1.2 Background to the research.

The research presented here has its origins in a project started in October 1980, and sponsored by the National Physical Laboratory (NPL). The work was jointly undertaken by NPL and the Department of Photogrammetry and Surveying at University College London (UCL).

NPL was interested in developing very accurate photogrammetric techniques for the calibration of 3-axis, coordinate measuring machines (CMM). These devices, which are a type of robot, are used to determine the shape and form of industial objects. They have a probe, often mechanical, which can be slid along three mutually perpendicular axes and touched against the side of the object. Each axis is equipped with a linear scale to enable coordinates to be read directly to an accuracy of a few microns. It has a typical measuring volume of a few cubic metres and is of a very large and heavy construction in order to maintain the stability and orthogonality of the axes.

In an initial test to evaluate the potential of photogrammetry, a test object was both photographed and measured by theodolite intersection. Now the camera employed in the test has a significant distortion characteristic, and comparison against some standard was required. Ideally, the standard should be a "perfect" camera, by which is meant "one which functions according to a central projection".

This was approximated with the more accurate theodolite observations, by projecting them onto a plane to create a mathematical "pseudo photograph". Both sets of measurements were then processed by the same photogrammetric bundle adjustment to achieve the comparison. The relevance to the current work lies in the treatment of the theodolite measurements in a photogrammetric fashion.

This was taken a step further when the probe of a CMM was examined by both photogrammetry and theodolite intersection. The CMM was so massive that its supporting block floated in the pitch between it and the retaining pit. The effect was small but measurable, and so the instruments had to be attached directly to the machine in order to view a consistent set of points. The test was then to position the probe at a number of points and compare the three sets of coordinates - from CMM, camera and theodolite. A particularly interesting aspect was that the theodolites could not be levelled due to the tilting CMM, and so their vertical bubbles were clamped. This does not affect the pointings, but instead of being related to the horizontal and vertical, they relate only to the theodolite's internal, non-levelled axes. This is also the case with a camera, whose image coordinate measurements, taken with the principal distance, represent consistent pointings relative to internal, non-levelled axes.

To process the theodolite observations, three positional and three rotational unknowns were assigned to each instrument. (Only one rotation, an unknown horizontal bearing, is required when the instrument is levelled). This is how photogrammetric equations are constructed. It was apparent, however, that the reciprocal observation between the theodolites enabled a direct solution for the relative orientation to be found. Contrast this with the photogrammetric case, where it is rare for a camera to photograph another camera position, although this has been done [G1]. An iterative solution is generally adopted, and this requires initial estimates of parameters by some manual means.

The non-levelled survey is therefore seen to have a geometrical advantage, the more so when it is realized that it has only one failure case, instead of the several in photogrammetry.

Having treated surveying as photogrammetry and uncovered an advantage, the thought occurs that photogrammetry might, with benefit, be turned into surveying. This is one reason for taking a general approach to both procedures, and looking at hybrid techniques. In passing it might be observed that the only difference between the methods, from a geometric point of view, is the presence or absence of a reciprocal observation. Note that the presence or absence of a levelling facility on the instrument is only an apparent difference, since a camera can also be levelled to a sensible degree of accuracy, and with potential benefits.

It was natural that the initial NPL/UCL work would encourage speculation about automated instrumentation. Depending on the procedure adopted, coordinates by triangulation can compare favourably with those from a large CMM. If the CMM can be calibrated by such a method, an external triangulation system might be used for positioning purposes. To be successful it must be fully automatic, and relatively inexpensive, but it offers a degree of mobility which the CMM cannot match. The CMM could itself be of a more flexible or elastic construction, which would offer cost benefits. Currently, internal encoders provide the necessary positional information and the construction must be rigid, robust and relatively expensive in order to achieve a good accuracy.

This concept of robot and external triangulation system also appears in the problem of robot performance measurement. Automated instrumentation is currently being developed for monitoring robot movement, and often uses triangulation to compute position. There is clearly scope to either borrow ideas on automation from this field, or contribute to it.

In surveying and photogrammetry, automation often implies the use of digital images, generated by CCD cameras. Due to their small format, there is a problem in achieving a resolution comparable to conventional methods. An electronic photo-theodolite may avoid the difficulty, and is discussed later. It is similar to an idea recently put forward by Wester-Ebbinghaus [S7], and represents a true hybrid instrument which combines elements of both surveying and photogrammetry.

Some of the work done as part of this research project has already been published. Photogrammetric aspects of the initial NPL work were presented at an international conference in York in 1982 [A3]. The additional investigation of non-levelled theodolites resulted in a further publication [F1], which was itself a summary of a thesis submitted to the Royal Institution of Chartered Surveyors [F2]. The use of scales to solve the orientation problem is discussed in [G4], and the results of a ship deformation measurement involving non-levelled theodolites in [P1].

1.3 Objectives and conclusions.

The main objective of this thesis has been to expose the common threads of surveying and photogrammetry, and examine those which are relevant to industrial dimensional measurement. From a geometrical point of view, these can be presented as two aspects of the same triangulation method.

This can be emphasized by conversion of theodolite and photographic data into a common unit vector format, and subsequent processing by the same computer programs. A package of programs known as TRIGFIX have been developed to demonstrate this.

The exchange of ideas between photogrammetry and surveying has resulted in specific methods for dealing with non-levelled theodolites and the generation of control for photogrammetric orientation.

The generalized method of surveying has made it simpler to analyse data on board floating objects. A practical test supports this, and has also prompted a suggestion for an alignment procedure on board ship.

Surveying with non-levelled theodolites also leads to a more general approach for processing data related to the vertical and suggests a potential development in instrumentation. This would use polarimetry to measure the relative rotation about the baseline between two non-levelled theodolites. Sufficient information is then available to compute a relative orientation in a confined situation such as mining.

The potential for improvements to photogrammetric control is seen in three alternative solutions to the problem of relative orientation between two metric (or calibrated) cameras.

One approach is based on reciprocal measurements between the cameras and one or two theodolites located at the object.

A second approach uses two linear scales, each defined by three target points, as control in the object space.

The third approach is offered only as a suggestion, and requires both cameras (or theodolites) to be levelled.

All three methods avoid photogrammetric failure cases, and offer either a direct solution for the orientation parameters or one which automatically generates trial parameters for an iterative adjustment.

Looking to future developments, an electronic photo-theodolite is discussed and automated triangulation systems briefly reviewed.

Ch. 2 Surveying with non-levelled theodolites.

In conventional use a theodolite is levelled so that its primary axis of rotation is constrained to be vertical. Angles can then be measured with respect to horizontal and vertical planes. This is a sensible procedure given that so many survey measurements are related to the vertical.

Information about the vertical can be also included in another way, as photogrammetry shows. Cameras, which also measure angles, are seldom levelled. However, they still successfully measure the shapes of objects. These are expressed in some arbitrary coordinate system which can be converted into a more suitable system, if additional information is available. For a map there will usually be some ground survey data to enable the photogrammetric measurements to be levelled and oriented with respect to a reference bearing. In the case of industrial objects, existing plans can define design coordinates at critical points, or specify reference axes such as centre lines.

Even this may not be necessary. Often it is an object's shape which must be directly evaluated, to see how well it conforms to a spherical, cylindrical or other design surface. There is not then any special advantage in using a levelled instrument, since the gravity reference gives no more information about shape, although it may help the geometry of the measurements.

Consider the problem of examining a large object, such as an oil platform, which is not exactly level during construction. Measurements related to gravity cannot immediately be related to the object, as the reference Z axis, for example, is not then parallel to the vertical. One approach is to determine the difference between object and gravity related axes. Measurements made with levelled theodolites can then be converted into the alternative system. Another approach is to set the theodolites directly into the object coordinate system, sometimes called the co-planing technique.

By a combination of observation and adjustment, it is possible to arrange for the (non-levelled) horizontal circle to lie in the XY plane of the object. Observations are then mathematically equivalent to those made with levelled instruments, since the common direction of the primary axes of the theodolites functions in the same way as the direction of gravity. Normal survey procedures can therefore be followed. Davis [F3] offers some guidance on these procedures.

On moving or floating objects, a situation which occasionally arises, an interesting possibility is suggested by Brunson [A9]. Dual axis electronic level sensors can continuously monitor the changes of level at the various instrument positions, and can communicate with one another, or with a master unit. Instruments may then be levelled up by arranging for a zero differential signal between the instrument and master. This again ensures that the primary axes point in the same direction. A similar procedure was verbally outlined to me by a British surveyor, Nick Eales.

Yet another alternative is to dispense with either levelling, co-planing or electronic level sensors, and set the theodolites up in an arbitrary, non-levelled position. Coupled with a more general mathematical approach, this is certainly more convenient than co-planing. Compared with the effort of levelling and observing with theododlites which have an automatic index, there may not be much apparent advantage, but this is not an option where the object is floating. The electronic sensors described above may solve this problem, but is is comforting to have alternative tools if these are not available.

Of course, it must be said immediately that survey work on floating objects is only valid if the objects remain sensibly rigid as they move. If they do not, a consistent set of target points cannot be measured within the finite timescale of the observations, and some other method such as multi-camera photogrammetry must be employed.

The non-levelled technique is the subject of the current discussion. In referring to non-levelled theodolites the terms primary and secondary angles or circles will be used. These derive from the tilted horizontal and vertical circles.

2.1 Non-levelled theodolites in practice.

There is no difficulty in using a theodolite without referencing it to the vertical. Provided the vertical circle index and levelling bubbles are not used, the mean of face left and right pointings to a target are correctly located with respect to orthogonal axes within the instrument (section 7.5).

It is usually a simple matter to prepare a theodolite for non-levelled use, and the essential step is to remove the effect of the vertical (and horizontal) circle index. In older model theodolites this is a manually set, split-bubble arrangement, which can be clamped to prevent movement. In some theodolites the index can be physically exchanged with a fixed reference. In others, the tilt of the primary axis is electronically measured, and an appropriate correction applied to both circle readings. If not required, it is simply switched off. In addition to this adjustment, the levelling screws must not be touched, and may be clamped for security.

Users should be aware that two useful features of levelled theodolites are now no longer present.

Firstly, it must be remembered that levelling can provide a check on instrument stability, because a change of tilt is registered by a movement of the bubble. Of course, this could be provided by a completely separate tilt sensor. It should also be remembered that a change of orientation about the vertical cannot be detected by this means.

Secondly, working with levelled instruments simplifies the task of re-locating a given position. This is particularly easy in the horizontal plane. As it is common to separate measurements into the horizontal and vertical, it is not usually so important to re-locate an instrument at the same height. If this is necessary, specialist tools such as scissor jacks enable fine adjustments to be made.

To a certain extent, similar advantages could be available to non-levelled instruments by adopting reference pointings to three nearby fixed marks. Any change of orientation, or relative movement, is detected by differences in the pointings.

Additionally, these marks might be coordinated by taping their separations. They can then be located in the traverse or triangulation network by reversing the resection procedure. Normally, resection locates an instrument with respect to the targets, but the targets can equally well be positioned relative to the instrument. Subsequent resection off the three points would be an option if the station had to be re-located, although the accuracy must be born in mind.

Lastly, the very idea of working with a tilted theodolite must be questioned. The instrument has been designed for levelled use, and the asymmetric loading on the bearings may cause systematic errors. I have not examined this, but have so far found no errors which might be attributed to this cause, despite the fact that I have deliberately set large tilts on instruments of 10 degs. or more. In practice it is unlikely to be a significant problem, as theodolites are difficult to work with if not approximately horizontal. It is not an objective here to advise engineers to attach theodolites at 90 degs. to their mountings, but to deal with tilts of mathematical significance.

2.2 Principle and analysis.

Non-levelled survey measurements can be readily processed in a way similar to photogrammetric observations. This assigns 6 unknown parameters to each theodolite, 3 for position and 3 for rotation. In 3-D levelled surveys there are only 4 unknowns, 3 again for the position of the instrument, and 1 angular unknown which is a horizontal bearing. In the non-levelled case, the additional 2 rotational unknowns deal with the tilt of the primary axis.

Perhaps the simplest way to process the observations is to create a "pseudo photograph" by projecting them onto an arbitrary plane. The equivalent plane coordinates can then be treated as photo image coordinates and processed by standard photogrammetric software. This was done as part of the UCL/NPL accuracy tests [A3]. Although this concept seemed novel at the time, Brown has used the idea as early as 1969 [E6].

Once converted to this format, conventional photogrammetric methods are available for building up information about an object's shape. These are resection, the relative orientation of two sets of observations, and a least squares, bundle adjustment. The photogrammetric practice of using only one instrument can also be employed.

A disadvantage of pseudo-photographs is that not all theodolite pointings can always be projected onto one plane. This happens when the maximum subtended angle reaches and exceeds 180 degrees. It is therefore better to formulate equations in terms of the original angles.

Unfortunately, there still exists a potential problem. If observations are made along the primary axis, the solution for the primary angle is indeterminate. A completely general and robust program should avoid such failure cases, and the current demonstration programs in the TRIGFIX package use a different formulation. Pointings are converted into unit vectors, and three equations generated, one for each element of the vector.

Only two of the equations contribute independent information to the problem, and two ratios of elements could be processed instead. This would involve a choice about the most suitable ratios, and require provision for different formulations depending on the outcome. Instead it is easier to process all three equations, which causes the space angles between the computed and observed vectors to be minimized.

A further refinement to the formulation avoids another potential mathematical singularity. The elements of the rotation matrix, from which the equations are derived, are functions of the three rotational parameters at the instrument. If these are chosen as standard omega, phi, kappa rotations about the axes X, Y, Z, a solution cannot be found for omega and kappa when phi equals 90 degs. Several researchers have suggested that the rotation matrix be expressed in the form dR . Ro, where Ro is a fixed matrix representing the bulk of the rotation, and dR is a variable correcting matrix. Since dR represents a small rotation, the failure case is avoided. In practice it is difficult to tilt a theodolite so much that phi reaches 90 degs., but the TRIGFIX programs also process photo coordinates, converted to a unit vector format, and the problem may more easily occur with cameras.

The equations arising from the mathematical approach just outlined are fully developed in Ch. 7, and are required for a least squares adjustment of an observation network. Hówever, the analysis is not yet complete, for surveying offers another feature which normally has no counterpart in photogrammetry. This is the reciprocal observation which is commonly made between the instruments and which permits a simple computation of relative orientation.

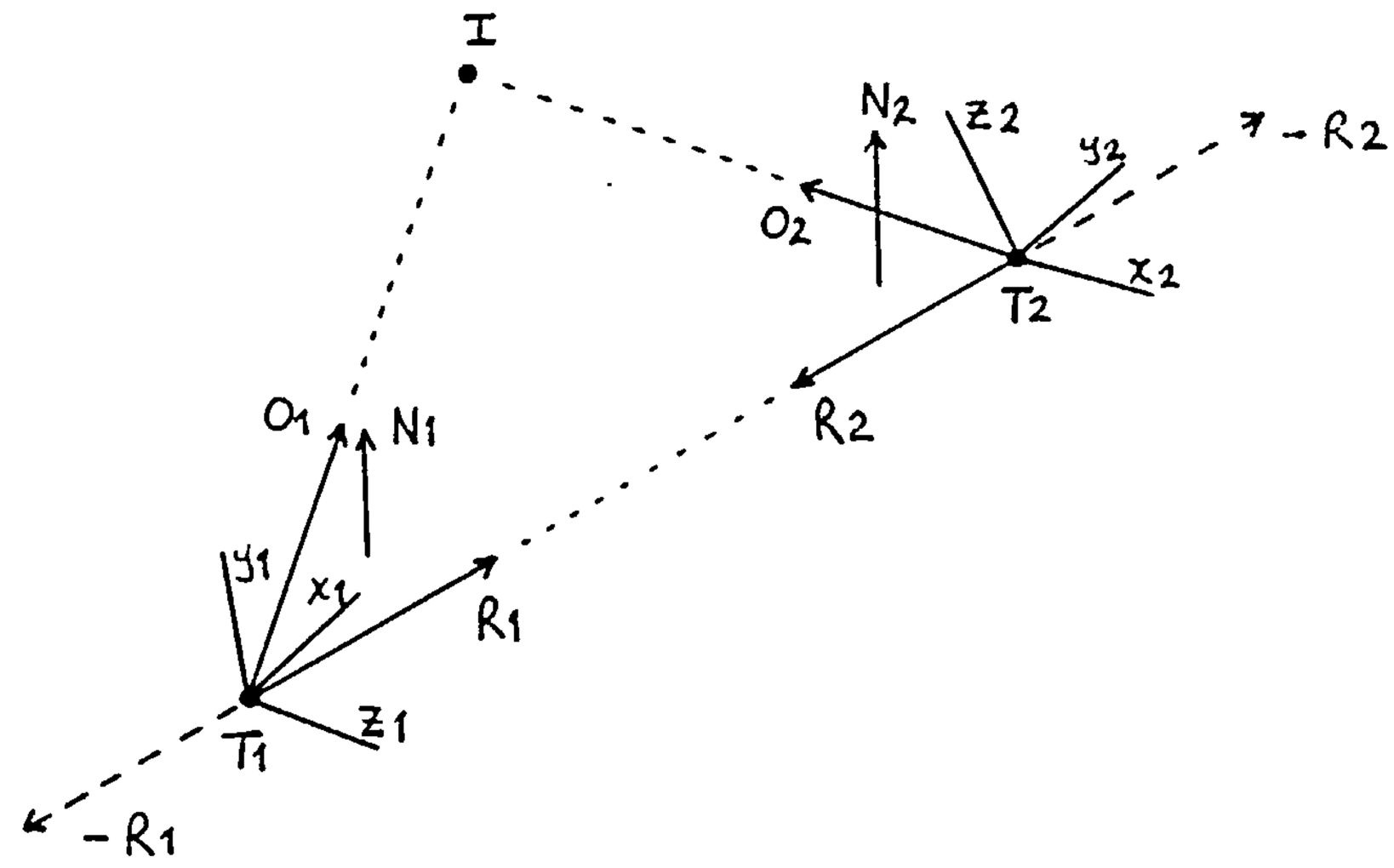

Figure 2.1 Orientation with reciprocal and offset vectors

Fig. 2.1 shows two theodolites, T1, T2, separated by a distance, d, which may be arbitrary. Each measures a reciprocal pointing to the other, and to an intersected target I, offset from the reciprocal line of sight. These are given by unit vectors R1, R2, and O1, O2, with the following elements :

$$R1 = (r11, r12, r13)$$
$$R2 = (r21, r22, r23)$$
$$O1 = (o11, o12, o13)$$
$$O2 = (o21, o22, o23)$$

Evidently T2 can be located a distance, d, along vector R1. The axes of T2 can then be rotated to point R2 in the direction (-R1). Only one degree of freedom then remains, which is a rotation about the baseline between the instruments. This is fixed by ensuring that vector O2 intersects vector O1 at I. The second instrument is then oriented with respect to the first.

This result might be expected analytically. There are :

unknowns = 6 (at T2) + 3 (at I) = 9

equations = 2 per pointing at T1

\+ " " T2

\+ a distance measurement, d

= 9

Although an equality of equations and unknowns is not a rigorous proof, in practice it is sufficient if a "sensible" geometry is selected.

The 6 parameters of relative orientation are easily derived. By inspection, the position of T2 is given by :

d . (r11, r12, r13)

Instead of finding the rotational elements, it is easier to derive the full rotation matrix. The following unit vectors are needed.

With respect to the axes of T2

$\underline{R2}'$ = - $\underline{R2}$

= (- r21, - r22, - r23)

$\underline{N2}$ = perpendicular to the plane of $\underline{R2}$ and $\underline{Q2}$

= ($\underline{R2}'$ x $\underline{Q2}$) / mod ($\underline{R2}'$ x $\underline{Q2}$)

= (n21, n22, n21)

$\underline{P2}$ = perpendicular to $\underline{N2}$ and $\underline{R2}'$

= $\underline{N2}$ x $\underline{R2}'$

= (p21, p22, p23)

With respect to the axes at T1

$\underline{N1}$ = perpendicular to the plane of $\underline{R1}$ and $\underline{Q1}$

= ($\underline{R1}$ x $\underline{Q1}$) / mod ($\underline{R1}$ x $\underline{Q1}$)

= (n11, n12, n13)

$\underline{P1}$ = perpendicular to $\underline{N1}$ and $\underline{R1}$

= $\underline{N1}$ x $\underline{R1}$

= (p11, p12, p13)

The unit vectors, $\underline{R1}$, $\underline{N1}$, $\underline{P1}$ and $\underline{R2}'$, $\underline{N2}$, $\underline{P2}$ represent two sets of corresponding orthogonal vectors. If the axes of T2 are imagined initially parallel to those of T1, a rotation must be applied to make $\underline{R2}'$ parallel to $\underline{R1}$ and $\underline{N2}$ parallel to $\underline{N1}$. ($\underline{P2}$ will then be automatically parallel to $\underline{P1}$). This is simply a re-statement that the reciprocal vectors define the same line, and, together with the offset vectors, the same plane.

From section 7.2, the rotation matrix R is given by :

$$R = \begin{bmatrix} r11 & n11 & p11 \\ r12 & n12 & p12 \\ r13 & n13 & p13 \end{bmatrix} \quad \begin{bmatrix} -r21 & -r22 & -r23 \\ n21 & n22 & n23 \\ p21 & p22 & p23 \end{bmatrix}$$

This is a complete and exact solution, for which there is only one, almost trivial, failure case. This occurs when the intersected point, I, lies on the baseline, or line of reciprocal pointing. T2 is then free to rotate about this line. The case that I is close to the baseline should also be taken as a failure case, when the vectors N1 and N2 cannot be reliably derived. This should be compared with the photogrammetric case of relative orientation, for which there are several object surfaces and instrument positions which do not give a unique solution [E10].

An interesting situation occurs when I is an infinite (or large) distance away from the baseline. In this event, vectors Q1 and Q2 are parallel. This is analagous to the case of levelled instruments, where unit vectors along the primary axes are parallel because they have both been set vertical. Levelling therefore replaces the need for intersecting an off-axis point. However, having seen the equivalence between the situations, it is evident that the gravity vector can take any direction with respect to a theodolite's axes, and not just along the primary axis. This concept is discussed again later.

Finally note that the use of a gravity vector does not necessarily avoid the failure case, as explained below, and that the parallel condition imposes a further constraint on the geometry. As a result, this situation is slightly over-determined.

Three examples of the non-levelled technique follow.

2.3 Dual theodolite intersection of CMM probes.

The method has been used several times to compare intersection coordinates with point coordinates from a CMM. In testing both a large CMM at the Woolwich Arsenal [F2], and a smaller one at the National Engineering Laboratory (NEL) [A2], a frame was constructed which could be bolted onto the CMM. The theodolites were then attached to the frame. This arrangement is necessary because these machines actually tilt, or "float", slightly as the probe is moved.

A target is attached to the probe, and the probe moved to a series of positions. There is no need for the target to be located exactly at the tip of the probe, as it can be safely assumed that the probe does not rotate. The difference between probe and target coordinates is therefore a constant offset. Conventional adhesive targets were used, as well as polished steel balls, reviewed later.

At Woolwich, two Wild T2 theodolites observed 36 points in a volume 0.595 x 0.62 x 1.5 m, from ranges of 2 - 3 m. The data is presented in [F2].

A best fit between theodolite and CMM coordinates gave the following rms values for a steel ball target :

x = 28 microns, y = 31 microns, z = 19 microns.
rms angle residuals were less than 1.5 arc secs.

At NEL, two Wild T2000 theodolites observed 27 points in a volume 0.498 x 0.6 x 0.75 m, from ranges of 1.5 - 2 m. The data is presented in [A2].

Using an adhesive target, the rms values were :

x = 19 microns, y = 11 microns, z = 15 microns.
rms angle residuals were again less than 1.5 arc secs.

2.4 Observation of a large space pyramid.

To demonstrate the technique on a larger scale, a pyramid of points was measured between two buildings. Line lengths were between 25 and 30 m.

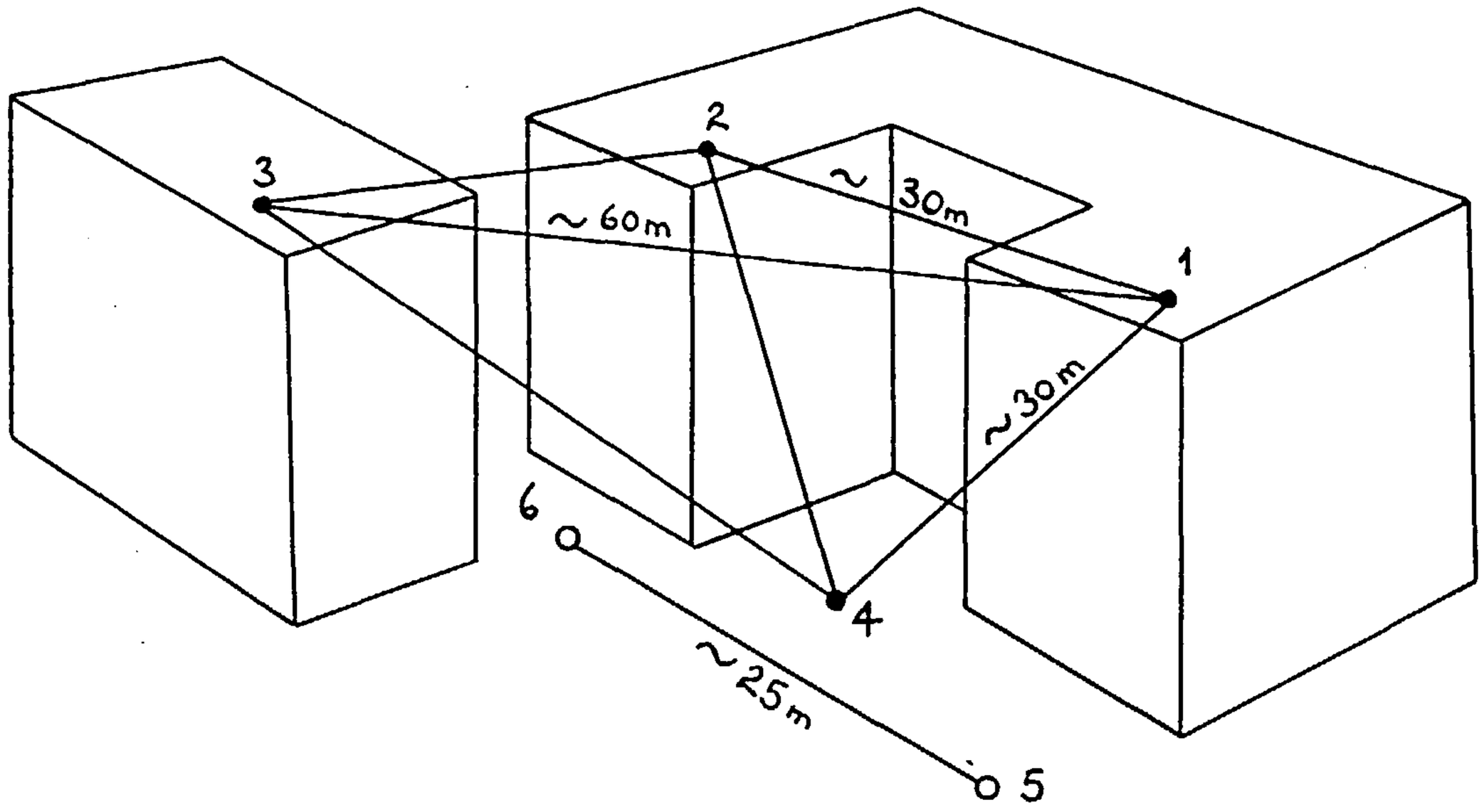

Figure 2.2 Pyramid measurement

All angles were measured between the 4 survey stations, using Vickers 1" theodolites with interchangeable targets. They were set up on tilted tripods, about 2m from a ground mark. At each station all angles were measured by replacing the target theodolites with their targets, and the ground mark was located by direct sighting and taping from the telescope. Scale was introduced by intersecting two ground marks, 5 and 6. Distances were measured by taping to the nearest 0.5cm. As a comparison, the network (i.e. the ground marks), were re-measured with levelled theodolites.

In each test, distances between ground marks were taken as the basis for comparison of the methods. The differences were all 1-2cm, and are given in detail in [F2].

The non-levelled theodolites had relative tilts of up to 20 degs. during this test.

2.5 Theodolite intersection on board an Royal Navy ship.

As part of a contract from the Admiralty Research Establishment, the superstructures of two RN ships were examined for deformation effects. The ships were not in dry dock, but afloat and berthed outside. The deformations were measured by photogrammetry, employing typically 10 - 12 photographs of an 80m length of superstructure. To provide an independent check, a limited number of targets were measured by a survey on board. As the ship was afloat, non-levelled theodolites had to be used.

This presented some practical difficulties. On board, many of the targets can only be viewed very obliquely. To overcome the problem, a hidden point probe was devised which locates on a screw thread around the target, itself supporting two offset targets. All three are then on a straight line, at known separations, and from coordinates of the offset targets the coordinates of the one of interest can be derived. This method is often used in industrial surveying.

The other main problem was the stability of the structure. First attempts at fixing survey points involved clamping theodolites to the railings at the top of the main mast, and to outriggers attached to the deck and cantilevered out from it. Both these attempts failed due to the flexibility of the structure, although the railings were worse. In the end, tripods standing on the deck proved quite stable, although fewer points could be viewed.

The overall rigidity of the ship also had to be checked, for both the photogrammetry and survey. It soon became apparent that only night-time observations would provide a measure of stability, after large differences in pointings between the fore and aft outriggers were measured during the day. When the sun shone on one side of the ship, it distorted by minutes of arc. To quantify the effect, three points were established fore, aft and amidships, and roughly on a line.

On one ship, the outriggers and a clamped position near the bridge were occupied. On the other, it was possible to stand one theodolite on a forward bollard and another on the top of a solid locker box, the third again being located by the bridge. Repeated reciprocal pointings from fore and aft positions to the mid point were made at intervals throughout the night. Changes were of the order of arc seconds, and it was felt that this indicated a sensibly rigid object.

This simple stability test could not detect any twist about the fore - mid and aft - mid lines, which would have been possible had offset points been observed. A full relative rotation could then have been computed. However, this would have been more time consuming at the mid station, when the idea was to check stability within a short time period, but it leads to the suggestion in section 2.6.

After this learning experience, two sets of measurements were carried out on board one ship, in September 1986 and May 1987. The ship was being re-fitted on the first occasion, and had undertaken sea trials by the second. Different visibility problems on each occasion, and the loss of some points, ensured that the same set of targets could not be observed. Although 4 stations had been initially established, and 3 re-occupied (approximately), only the dozen or so points intersected by two of them were available for comparison. Furthermore, there appears to be a problem with the hidden point probes, which often had to be rotated to enable viewing from different directions. Bad pointing residuals indicate that they may not have re-located correctly. As a result, only 5 points could be directly compared.

In summary the results were :

angular rms values in Sept. 86 = 2.2 arc secs

" " May 87 = 1.2 arc secs

average rms coordinate fit using 8 targets = 0.4 mm

Pointings with large residuals were removed from the computation. Instrument separations were about 10 m, and point separations in the range 2 - 20 m. The low residuals indicate consistent results. Although there is not much redundancy in the fit of coordinates, the small value is consistent with a set of stable points.

This application is reported in [P1]. I have not yet found any other written presentation of triangulation on board a floating object. Interestingly, at a conference organized by CERN in April 1986, M. Michel Mayoud from the geodesy group described to me a test he did some years ago. This was the measurement of tank volumes on a floating oil tanker. In common with the above test, measurements required night-time observation and a "quiet" ship. The analytical solution to the problem employed the 6 station parameters listed earlier. Unfortunately, Mayoud's work was not published outside the organization which commissioned the work.

2.6 Orientation transfer.

As part of the ship deformation test, some consideration was given to the relative alignment of various units attached fore and aft to the superstructure. This task is equivalent to a relative (angular) orientation.

In principle, a minimum of three targets attached to an on-board unit could determine its orientation by defining a reference line and plane in a common photogrammetric system. Now, the results suggest that photogrammetry could achieve standard errors in target coordinates of about 3 mm. Unfortunately, this implies that unless the targets are well separated, the reference direction and normal to the plane cannot be found to any great accuracy.

An alternative procedure can be devised with non-levelled theodolites. Each unit must be provided with a mounting to which a metal cube, having two polished faces, can be attached. A precision mounting is necessary so that the cube can always be re-located in the same angular orientation. Its axes can therefore be taken as reference axes for the unit. If need be, these can be further related to some other more convenient set of axes. The positioning of the cube must be such that a conveniently placed theodolite can sight normally onto the polished faces.

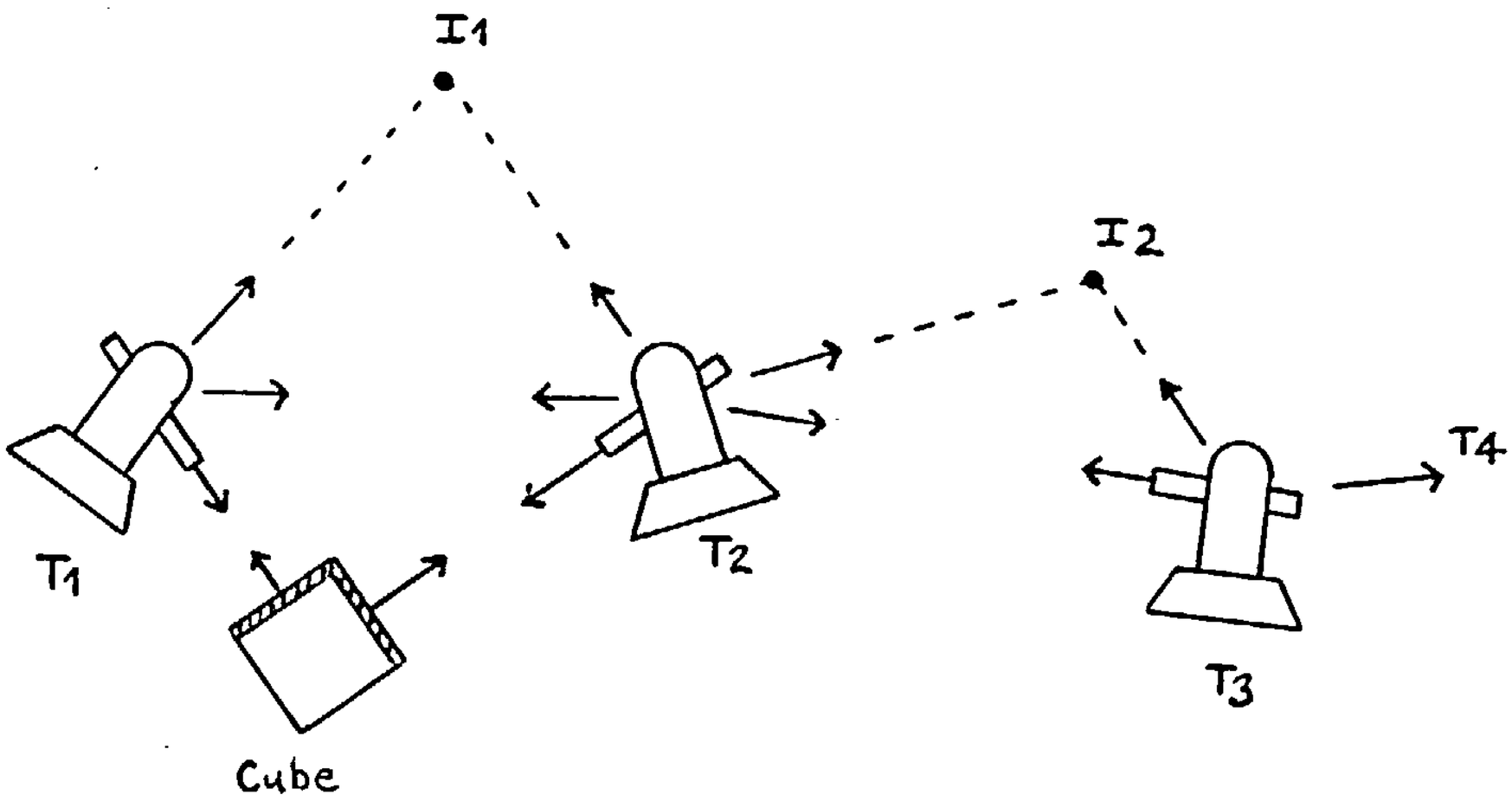

Figure 2.3 Orientation transfer.

Fig. 2.3 shows a cube, perhaps at deck level, with its polished faces looking up at 45 degs. to the horizontal. Theodolites T1 and T2 are set up so that they can auto-collimate onto the polished faces. This technique is explained in [C1,C2] and enables the directions of the mirror normals to be found with respect to each theodolite. However, T1 and T2 can be relatively oriented by reciprocal pointing, and intersecting any convenient offset target, I1. This gives sufficient information to determine the orientation of the cube relative to either. In fact, there is redundant information, since each autocollimation finds two of the angular parameters of the cube. (The third is the rotation about the mirror normal). The orientation at T2 can be further transferred to another theodolite at T3, by reciprocal pointing and offset intersection. This process is continued until another cube can be oriented within the common system.

A very similar method of orientation transfer was verbally outlined to me on a visit to a major aircraft manufacturer. Apparently the method is used in the spacecraft industry, to align separate units attached to satellites. For this application, levelled theodolites are employed in order to avoid the need for offset targets, I1, I2 etc. If the floating structure, or indeed any structure, is relatively open, there should be no difficulty in locating arbitrary offset targets well off the line of sight. Nevertheless, this remains a potential problem, and a solution is offered in section 2.7.

It might also be felt that the location of cubes and theodolites for autocollimation could be awkward. A practical test has not been carried out, and the difficulty may well exist. However, if the idea proves worthy of further investigation, there is undoubtedly potential for designing specialist adapters and items of equipment to ease the problem. The aerospace application makes use of precision XY slides and scissor jacks for the fine location of the theodolites, and this appears to be an acceptable solution. Given the size of components on board ship, it may even be possible to dispense with a reference cube and provide instead a detachable mounting to which a theodolilte may be directly fixed. The orientation of this theodolite then defines the alignment of the item under investigation.

2.7 Direct measurement of rotation.

The previous section mentions the possibility that it might be difficult to find an intersection target off the baseline between two theodolites. This could occur in certain confined situations, such a sighting down a corridor. The obvious practical example is in mining, where it is necessary to transfer a horizontal bearing from the top of a shaft to the bottom. Levelling the instruments at the top and bottom is of no assistance, because the gravity vectors lie close to the reciprocal vectors. This corresponds to the failure case of section 2.2.

A general solution to the problem would be possible if directional information, perpendicular to the reciprocal pointing, could be transmitted along the baseline. Such a property is offered by polarized light, which defines a reference direction within its beam. This section proposes its use in new instrumentation, with the most likely area of application being mining.

It is not the objective here to present the optical and electronics technology for generating and detecting polarized light. Existing research work provides much of this information. Instead, the section attempts to answer some further questions concerning the feasibility of incorporating this property into a practical survey instrument. In developing the proposal, I have had some very helpful discussions with Professor John Gates, who did some of the original polarimetry work at NPL.

2.7.1 Instrumentation.

Polarized light has already been used in the mining industry in Germany [D1]. It enables an instrument to be located at various levels down a shaft, from where points on the wall are coordinated by bearing and distance. This builds up a picture of the shaft for monitoring purposes. The beam of polarized light, apparently of fairly large diameter, is transmitted vertically down the shaft. The plane of polarization provides a horizontal reference direction for the instrument, which is positioned within it. The wide beam simplifies the task of moving and setting up the instrument again. Unfortunately, the method achieves a relatively low angular accuracy of 0.3 gon in setting the reference direction, with little expectation of significant improvement.

However, two papers from NPL [D3,D4] show that an accuracy of a few arc seconds is possible. This depends on a sensitive method of detecting the crossed position in which an analyser, located in the transmitted beam of light, is set at right angles to the plane of polarization.

By oscillating this plane, an out of balance signal, due to a departure of the analyser from the crossed condition, can be detected to a high precision. The later paper describes a polarimeter based on modern laser technology, with applications in the field of alignment and angle measurement. The earlier paper explicitly suggests the application of orientation transfer in pit shafts.

A polarimeter is therefore available which can measure rotations with an angular accuracy roughly compatible with the horizontal and vertical pointings of a theodolite of one arc second resolution. I suggest that such a device be attached to theodolites, in order to measure a tertiary angle of rotation about the line of sight. The device should be able to function as a transmitter (polarizer) or receiver (analyser) of polarized light.

Ideally, the polarimeter would operate co-axially, in the manner of a laser eyepiece, although there may be safety problems with reciprocally sighted laser beams. However, the beam does not have to be viewed by the observer, but sensed only by the electronics, and a filter arrangement may solve the problem.

If an offset polarimeter is attached to the theodolite, in the manner of many EDM instruments, there may be problems if the theodolites have varying tilts. The rotation sensors may not then be correctly aligned.

Alternatively, an attachment could operate perpendicular to the line of sight and trunnion axis, as well as through the centre of rotation. By rotating the telescope through 90 degs. about the trunnion axis, the rotational measurement will operate correctly along the original line of sight.

Regardless of the adopted solution, there are a number of geometrical problems to be resolved. To simplify the following discussion, the "set" condition is assumed to be achieved when the beam polarizer and analyser are parallel, not crossed at right angles.

2.7.2 Rotational ambiguity.

There are two positions for the set condition, separated by 180 degs. This ambiguity needs to be resolved, perhaps with a coarse optical setting based on sighting an asymmetric target at the transmitting instrument.

2.7.3 Ambiguity when sighting near the primary axis.

There is an apparent ambiguity if either reciprocal pointing is close to the theodolite's primary axis. In this case, primary and tertiary rotations take place about the same axis, and an alteration in one is exactly compensated by a corresponding change in the other. In fact, every combination will give the same value for the horizontal pointing of the plane of polarization. The solution is to clamp the horizontal circle in any position, since all horizontal angles give the same value for the reciprocal pointing, i.e. the vector (0,0,1). Alternatively, the theodolites can be tilted so that the primary and tertiary axes no longer coincide.

2.7.4 Datum errors.

In addition to an ambiguity of +/- 180 deg, there are two other sources of datum error in determining the offset rotation.

Assume that the transmission plane of polarization is nominally perpendicular to the trunnion axis. Ignore the fact that it may be convenient to rotate this plane around the line of sight, as the argument is not affected. The plane cannot be exactly normal to the trunnion axis, so giving a transmission datum error, e, indicated in the next figure.

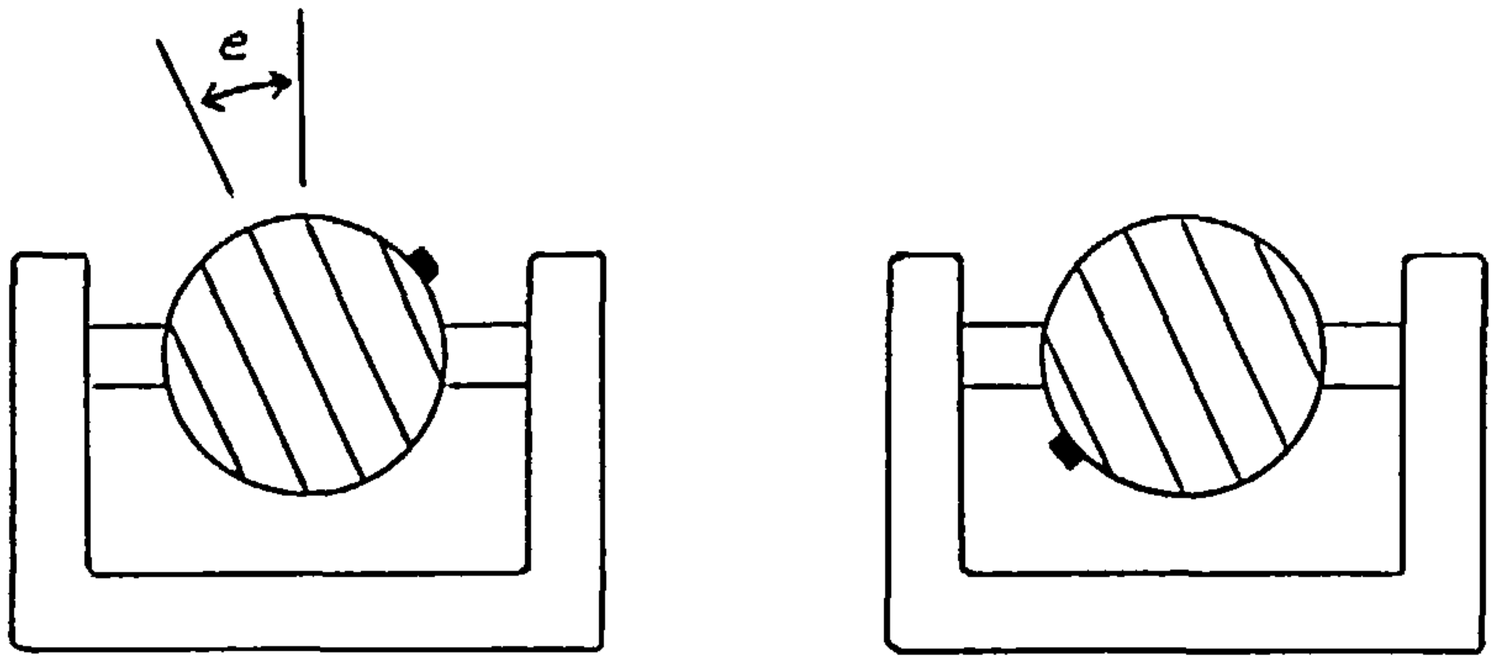

Figure 2.4 Transmission datum error

This is not removed on telescope reversal. A similar error occurs at the receiving end, if the datum position which corresponds to a zero rotation is not normal to the trunnion axis.

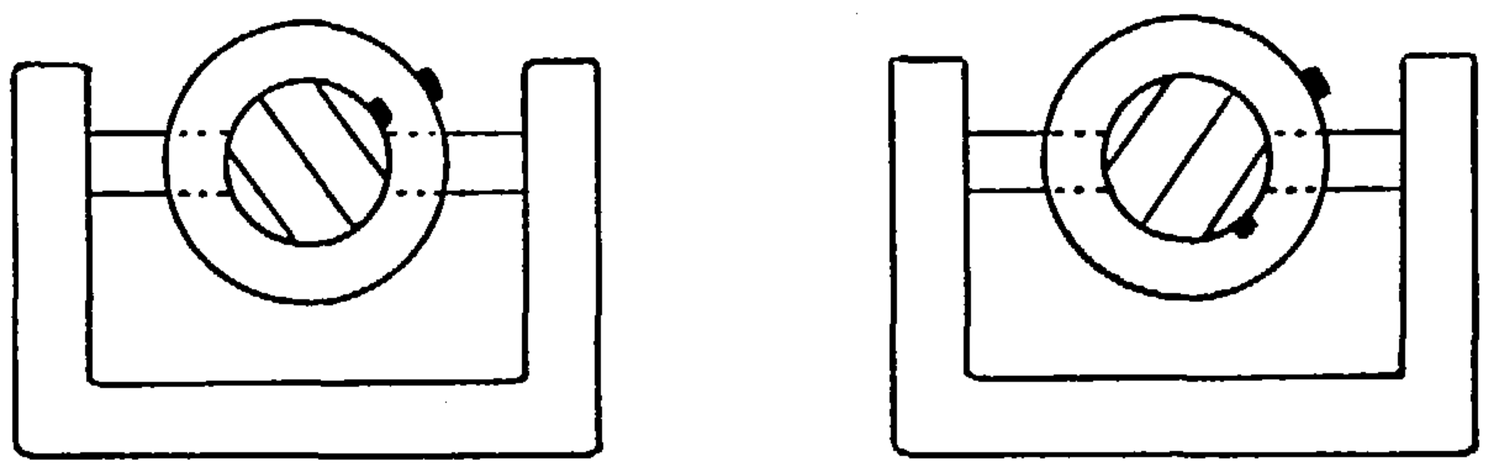

Figure 2.5 Removal of transmission error

Fig. 2.5 shows that the problem would be solved if polarizer and analyser could be independently rotated about the trunnion axis. However, it may be difficult to ensure that this axis of rotation is identical with the trunnion axis.

Alternatively, for any pair of instruments the combined transmission and receive error can be determined by calibration in the following way.

Both theodolites are set up, possibly non-levelled, and oriented as usual with a reciprocal observation and intersection of a common point. Additionally, the tertiary angle of rotation, t, is measured. From the known relative orientation, the correct value, T, can be computed, giving an equation such as :

$$T + Et + Er = t$$

Et is the transmission error at one instrument, Er the receive error at the other. From the equation, (Et + Er) is found.

This must be done in both directions, since transmit and receive errors for each instrument may not be the same, although instrument design may make it so, if the polarizer on transmission functions as the analyser on reception.

Where more than two instruments are in use, it is clearly unreasonable to calibrate every possible pair of instruments. Fortunately, a calibration technique involving three instruments, set up in a triangle, would solve the problem. In this case, there are 6 unknowns (Et and Er at each station). The tertiary angle is measured, forwards and backwards, along each of the three lines. This gives 6 measurements. Also, the correct orientations are determined by external means, so giving 6 equations in 6 unknowns of the form above.

Since Et and Er are now absolutely known for these three instruments, any of them can be used as a reference for calibrating others.

2.7.5 Disturbing influences.

The measurement of the relative rotation about the reciprocal line of sight, will be subject to systematic error if external magnetic and electric fields are present. If these have oscillating components, the averaged error rotation will be zero for effects which are linear functions of the field, but constant fields parallel to the line of sight may cause a significant error. However, it appears that this error is removed by measuring in both directions.

The disturbing influence gives a "twist" to the plane of polarization, which is in the opposite direction when the sign of the disturbance changes.

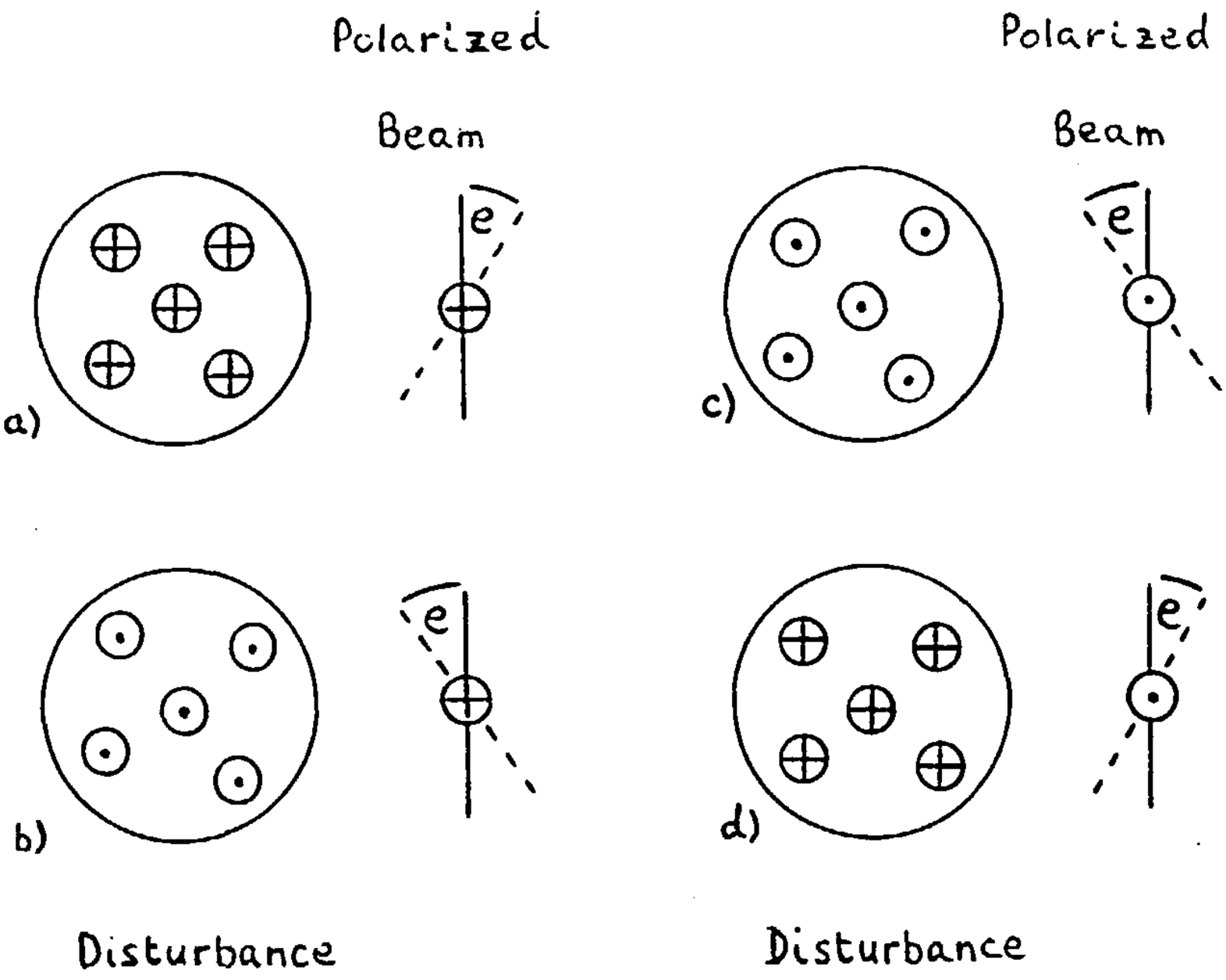

Figure 2.6 Disturbing influences

Figs. 2.6 (a) and (b) show this effect, and (c) and (d) are obtained by viewing (a) and (b) from the other side of the page. If polarized light is transmitted to a plane mirror and reflected back to the transmitter, figures (a) and (d) show what happens. In the absence of a disturbance, no relative rotation is detected. When a disturbance is present, twice the error angle is measured. In a two-way measurement, the following is obtained.

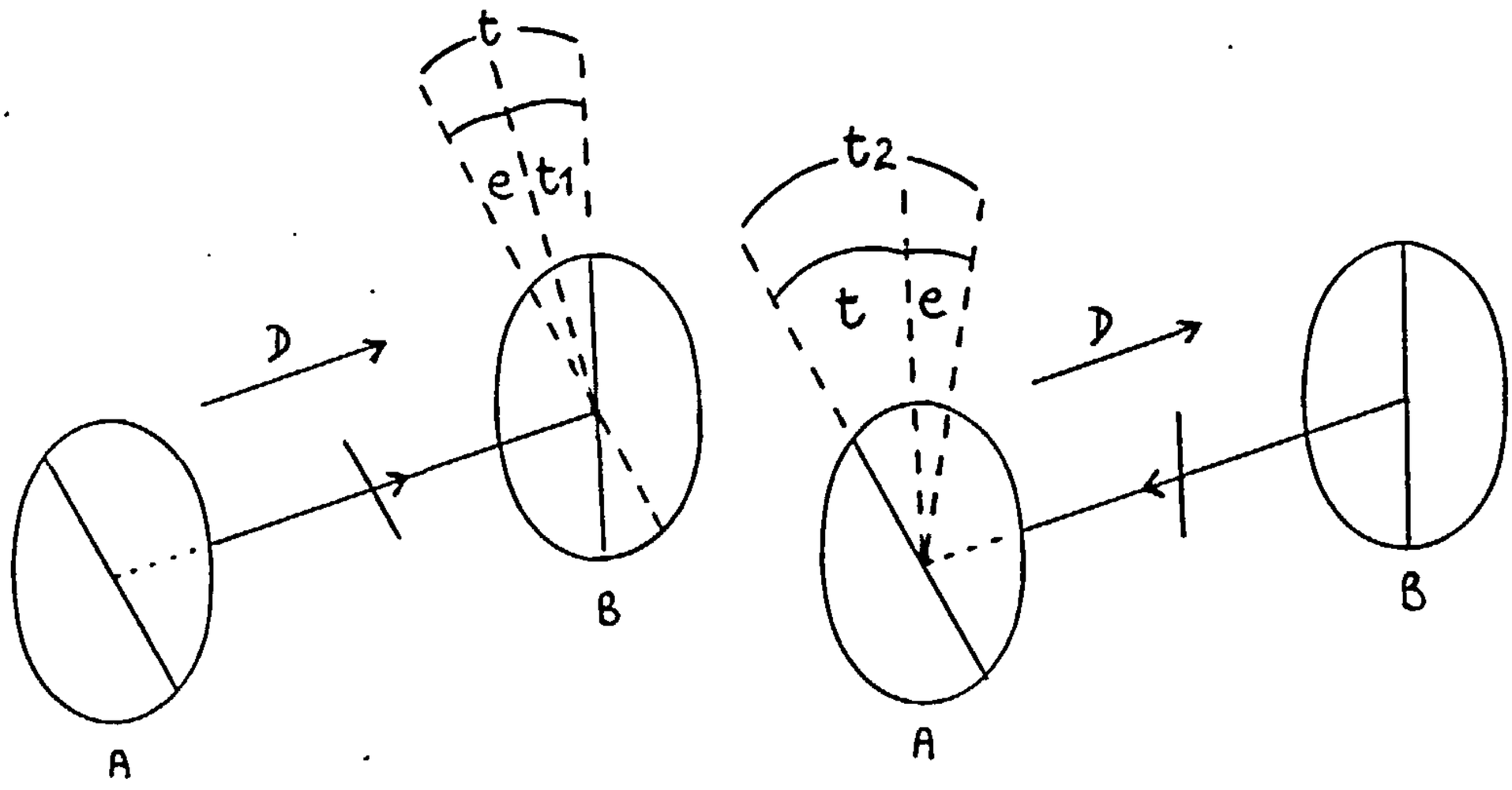

Figure 2.7 Effect of disturbance on rotation

Transmitting from A to B in fig. 2.7, the measured rotation is (t-e). When transmitting from B to A, the rotation is determined as (t + e). Consequently, the mean of the two values is correct.

Although the actual rotation measurements would be made at both ends, the result of the two way measurement should be applied as though made one way only.

2.7.6 An equivalent observation equation.

A rotational observation between two stations has an analogy with a distance measurement between them. For the distance observation, an equation containing only position parameters and measured distance is obtained. For rotation measurement, only the 3 observed angles and the two rotation matrices, each defined by 3 unknowns, need be involved.

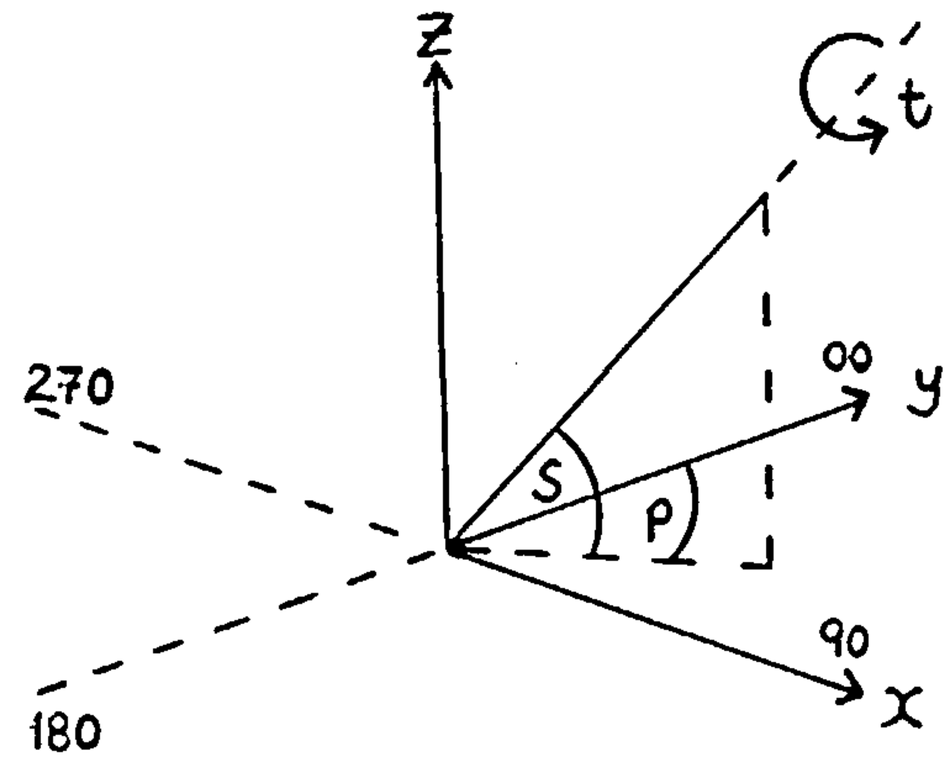

Figure 2.8 Triple angle measurement

Let instrument axes be defined as in fig. 2.8, where p,s are the primary and secondary angles, and t is the tertiary rotation angle.

Let the transmitted polarization vector be vt = (0,0,1) when p,s are zero.

Suppose at the transmission station 1 the instrument is defined by an rotational orientation matrix R1, and observes angles p1 and s1 to station 2. Then the transmitted vector becomes :

$$vt = R1 \cdot Rp1 \cdot Rs1 \cdot (0,0,1)$$

where Rp1 is the rotation matrix corresponding to rotation p1 about Z, and Rs1 is the same for rotation s1 about X.

A similar analysis at the receiving end, which additionally measures a tertiary angle, t2, gives the receiving vector as :

$$vr = R2 \cdot Rp2 \cdot Rs2 \cdot Rt2 \cdot (0,0,1)$$

where Rt2 is a rotation matrix about Y.

Clearly, vt and vr should represent the same vector, hence the angle between them should be zero, i.e.

arc cos (vt . vr) = 0 + e , where e is a residual angle

vt . vr is a dot product.

2.7.7 Combination with EDM.

Before leaving this section, it is difficult to resist a final speculation. The technique of modulating the plane of polarization of a laser beam is also used in some EDM instruments. Could both functions be combined ?

2.8 Observing the gravity vector.

Having removed gravity, it will now be put back, but in a more generalized form which may offer advantages. This form has already been indicated. Rather than arranging that the gravity vector lies along the primary axis of a theodolite, its actual direction is physically observed with the telescope and expressed as a component along each axis.

It is then located to an accuracy consistent with that of other pointings.

When constructing a rotation matrix, dr.Ro, for a set of observations, Ro can be selected to align the gravity pointing parallel to the system Z axis (assumed to define the vertical). The small corrective matrix, dr, may then cause it to tilt slightly, depending on which of two options is selected. If the corrective matrix is expressed in terms of omega, phi, kappa rotations about the x,y,z axes, these options are :

a) constrain the gravity pointing to stay on the Z axis by fixing omega = phi = zero. Any value of kappa only causes a change in horizontal bearing.
b) assume there is a degree of uncertainty in observing the direction of gravity, and treat omega and phi as observations of nominal value zero, but correspondingly weighted to allow for this uncertainty.
These options are also mentioned by Wester-Ebbinghaus [E7].

There are a number of ways in which the gravity vector might be physically observed. These are in addition to conventional levelling, and the measurement of primary axis tilt by striding level or vertical circle bubble.

2.8.1 Autocollimation using a horizontal liquid surface.

Since an undisturbed liquid surface can be treated as a perfectly horizontal plane mirror, a telescope autocollimated onto such a surface must be pointing along the vertical. A suitable surface is a mercury pool mirror. However, a much cheaper and less toxic liquid is any reasonably viscous, black oil. This was suggested by research work at Trent Polytechnic which successfully used an oil surface to create a laser plumb-line. A weak but adequate reflection is obtained with the autocollimation eyepiece of the Wild T2000. The eyepiece available at UCL for a Wild T2 is not as strongly illuminated, but still observable, and was used in the test described below.

A major practical problem with a liquid surface is how to point the telescope at it. Ideally, a dish containing the liquid would be placed on the (roughly level) alidade of the theodolite, immediately underneath the telescope. (Proximity makes no difference to autocollimation). Unfortunately, there is no room on a T2000 to do this. On a T2 it is indeed possible to locate a small oil bath in a position which still permits the telescope to be pointed downwards. However, the dish must have such a small diameter that meniscus effects cause the surface to be curved, and autocollimation cannot be obtained.

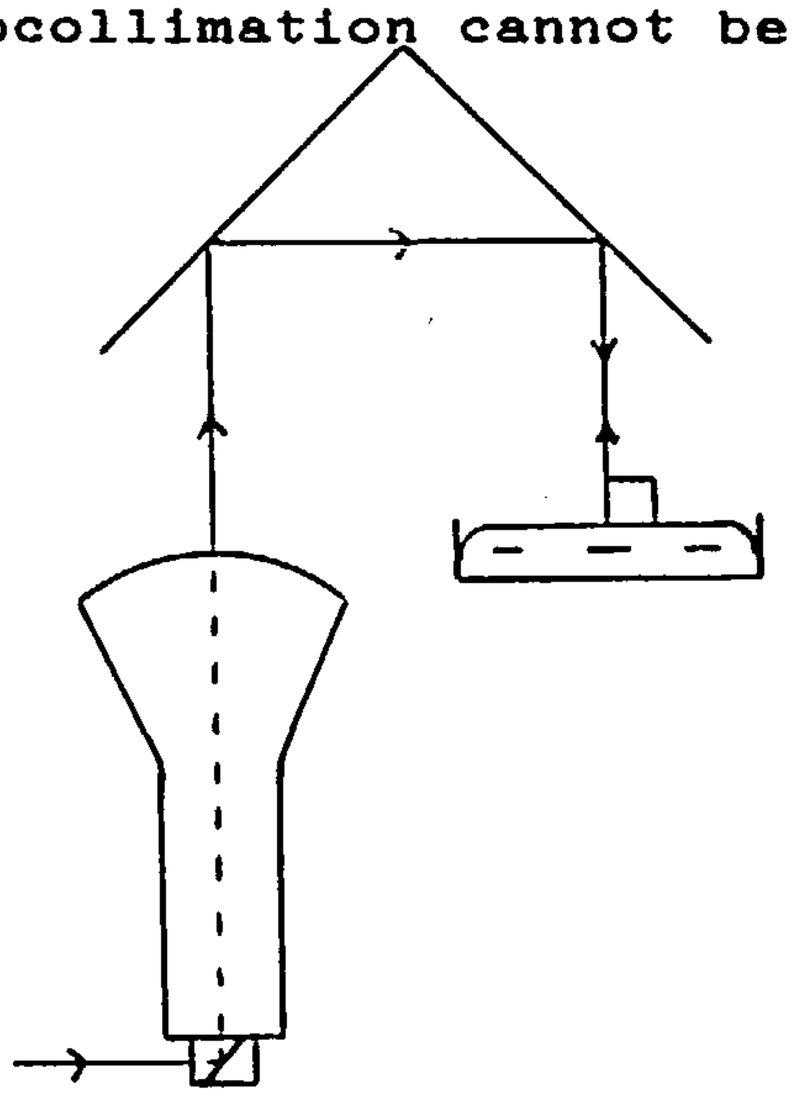

Figure 2.9 Autocollimation using a liquid surface.

Dr. Peter Scott has suggested one alternative, shown in fig. 2.9. If the telescope looks vertically up, onto a corner cube reflector, the line of sight could be displaced sufficiently far off to the side that an off-axis liquid surface could be viewed. This has not been tried. Instead it proved easier to clamp a T2 in a tilted position so that a downward vertical line of sight did not pass through the base. With a tilt of some 23 degs., a faint but observable autocollimation image of the cross-hairs could be observed in an oil pool underneath. This pool covered the base of a bucket, and the meniscus effects were not present. Test measurements were carried out as explained in section 2.9.

2.8.2 Autocollimation to find two horizontal pointings.

A vertical line need not be directly observed. If two horizontal pointings can be found, preferably at about 90 degs. to one another, the vector cross product of the two corresponding unit vectors must be a vector in the direction of the vertical.

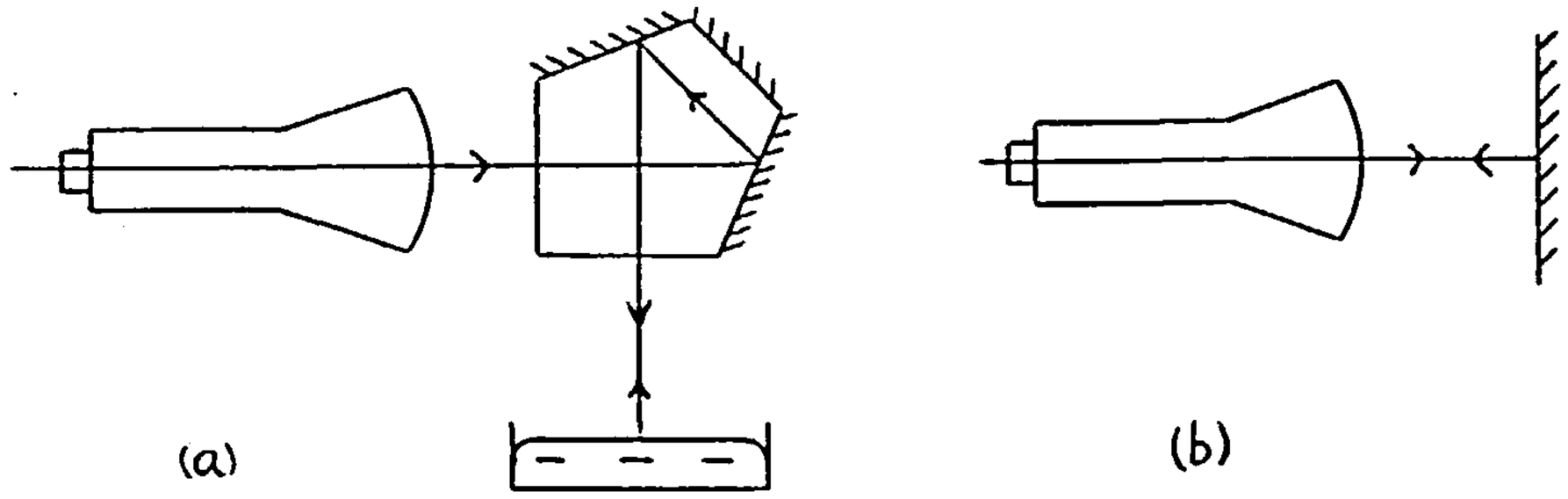

Figure 2.10 Observing a horizontal pointing.

In fig. 2.10(a), a pentaprism has been attached to the objective of a telescope, which turns its line of sight through 90 degs. (An attachment such as this is commercially available, for example from Wild Heerbrugg). By adjusting the telescope pointing and angular position of the prism, autocollimation could be obtained from a surface as indicated. The telescope is then pointing horizontally. In fig. 2.10(b), autocollimation is obtained off a plane mirror with its reflecting surface set vertical. Again the line of sight is horizontal.

2.8.3 Vertical and horizontal pointings by autoreflection.

As an alternative to autocollimation, autoreflection can be used. This is based on the property that the line joining an object and its plane mirror image is perpendicular to the mirror surface. Unlike the case with autocollimation, the mirror surface must be positioned such that the image is at least as far away as the minimum focussing distance. Therefore it must itself be at least half this distance away from the theodolite (i.e. about 1m for many theodolites).

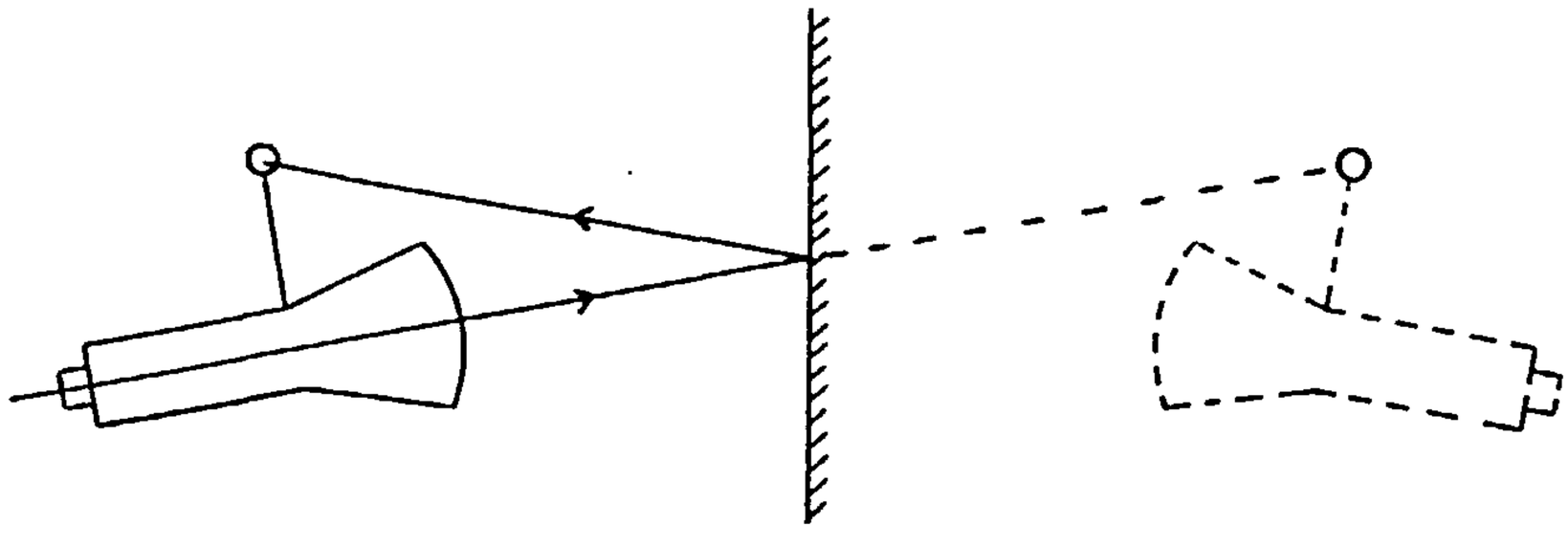

Figure 2.11 Pointing by autoreflection

Fig. 2.11 shows the situation where an off-axis telescope target is available. Although the line of sight is not now perpendicular to the mirror surface, the sign of the error is changed by reversing the telescope position. The same philosophy lies behind reciprocal pointing with offset targets, outlined below.

The method is much more suitable for use with an oil surface, because it is easy to manufacture a bright, luminous target which gives a good reflection. However, unless it is displaced to the side of the telescope, a very excessive tilt may be necessary in order to view it in both telescope positions. A fibre optic is available at UCL, which could be taped to the side of the telescope in a suitable position. Unfortunately, this is currently too bright to be of use, and so the idea has not been tried in practice.

2.9 Theodolite intersection with observed gravity vector.

As a demonstration, a comparison test was carried out in a basement laboratory at UCL. A number of targets were intersected by two conventionally levelled theodolites, which produced reference coordinates in horizontal and vertical planes. Two non-levelled theodolites were then set up, and one of these observed the gravity vector by autocollimation onto a horizontal pool of black engine oil. The orientation procedure was selected to make the gravity pointing define a Z axis of coordinates, and the targets were again intersected.

The second set of coordinates was compared with the first by a transformation which involved a shift, scale change and alteration of horizontal bearing only. (A scale change was necessary as an independent scaling length was not measured by the non-levelled theodolites). A transformation of this form preserves the gravity reference in order to make a valid comparison.

The rms results of the fit in microns were :

x = 65 microns, y = 83 microns, z = 86 microns.

The results are given in the appendix, Data Sets 2. They are similar to other comparisons of coordinate sets, created by both levelled and non-levelled theodolites. See for example, Data Sets 1.

2.10 Levelling a 3-D traverse.

The previous section shows how it is not necessary to level both instruments in order to obtain horizontal and vertical coordinates of the targets. In fact, in any multi-station network it is only necessary to level one of the instruments to do this. This was demonstrated by a short test traverse described in [F2].

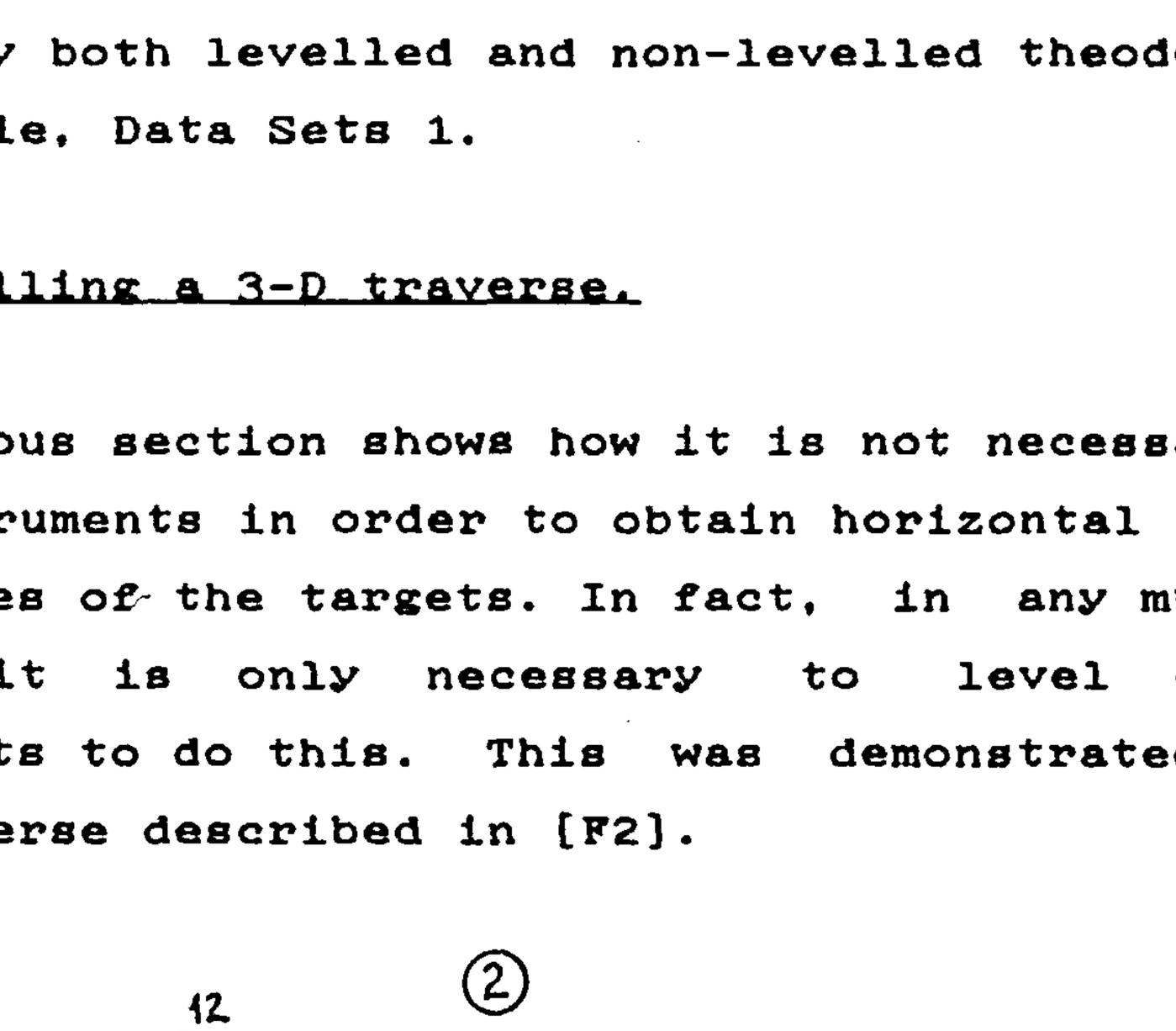

Figure 2.12 3-D traverse.

Five traverse stations were set up, using a conventional procedure in which every station was levelled, and an alternative procedure in which only one was levelled. Between every pair of stations there was an offset point which enabled a relative orientation to be computed. Ground points were located by height of instrument, or bearing and distance, as for the 3-D triangulation. Side lengths were taped to 0.5cm. In the second survey, the levelled instrument defined the system, creating Z values which were equivalent to heights.

Again line lengths between both surveys disagreed by no more than 1cm, and height differences by no more than 1.5cm.

When traversing with a mixture of levelled and non-levelled theodolites each line requires an offset point for orientation unless the neighbouring instruments are both levelled. Also the line length must be measured as usual. One method might employ EDM instruments, although care must be taken to interpret the distance correctly.
Interchangeable targets are designed for level use, and may be offset from the theodolite's nominal centre in the vertical direction. A correction must, in general, be applied to account for a relative tilt of the primary axes. Another method intersects two off-axis points with a known separation. This is common technique in industry, where the two points are the ends of a scale bar. A careful check should be made to ensure that the scale is transfered sufficiently accurately. If it is possible to use the same offset point for more than one traverse line, scale may only need to be defined on one of the lines concerned. From fig. 2.12 it can be seen that scale generated on line 2-3 results in a known length for line 3-234. This in turn provides scale for line 3-4.

2.11 Potential advantages of observing the gravity vector.

Several advantages might be claimed for this method of including gravity information.

a) Avoiding problems with steep sights.

It is a well known problem in surveying that steep sights lead to errors in computing a traverse, or transferring orientation. A residual tilt of the primary axis primarily affects the horizontal angle, and the error is not removed by transiting the telescope. Instead, careful measurements with a striding level are often made to determine the tilt.

If non-levelled theodolites are used, no assumptions are made about angles being horizontal or vertical, and errors are virtually eliminated on telescope reversal. If a steep sight is a potential problem on a traverse, for example when changing floor levels in a tall building, it may be possible to sight an orienting target through openings in the walls. If so, the two theodolites concerned can be non-levelled, thereby avoiding the problem.

b) Accurate introduction of the vertical.

Observing the gravity vector should be at least as accurate as setting up with the plate bubble, possibly more so, and I would welcome comparison tests.

2.12 General remarks.

The following comments close some remaining gaps in this presentation of close range surveying.

2.12.1 Refraction.

It is assumed that refraction effects are negligible over the ranges of interest, and that obvious sources of heat and cold are removed from the measurement field. Burch [C3] states that if the air temperature has a vertical gradient of 1 deg. Celsius per metre, a line of sight pointing roughly horizontally will bend at the centre by 50 microns on a line of length 20 m. This is an angular error of about 1 arc sec., in the presence of some significant refraction. The small error supports the view that the tests described here will not be adversely affected by this effect.

2.12.2 Reciprocal pointing.

At close ranges it is unreasonable to assume that interchangeable theodolite targets will re-locate to within, say, 10 microns of the theodolite's rotation centre. If this is not the case, angular errors may arise. Also, if simultaneous intersection of targets from two theodolites is required, both instruments must remain in position, and cannot be exchanged for targets without an inevitable loss of angular reference.

The most elegant solution to the problem has been adopted in the Wild T2000, which has a target inside the telescope, positioned such that its image is at the rotation centre. Each theodolite need only look down the telescope of the other to achieve reciprocal pointing.

This solution is only available with a particular theodolite, and alternatives are required. One of these involves the reciprocal sighting of cross-hairs, and is outlined in detail by Kissam [C1]. However, I have personally found the method to be tedious and time consuming, although a brightly illuminated graticule may help. I prefer the third alternative, which is to use an external telescope target for which there are two forms, concentric and offset.

The first is nominally concentric with the line of sight. The only difference with the solution implemented on the T2000 is that the target moves slightly whilst its host telescope is directed at the other. Once the reciprocal pointing is achieved, the baseline is established. Dr. Arthur Allan has used a target like this at UCL, by having crossed pairs of wires in front of the objective. These are sometimes not as easy to sight as conventional 2-D targets, which could be formed by concentric rings deposited onto an optical cover glass. See, for example, the cover glass target on a Rank Taylor Hobson alignment telescope [C2]. Note also that small targets concentric with the line of sight will not seriously impair the view. At greater distances, a large bulls-eye surrounding the telescope barrel would suffice.

The second form of target, which is easy to manufacture, is offset from the line of sight, attached perhaps to the top of the telescope barrel. (Unless well manufactured, concentric targets are effectively of this form). Again, each target moves whilst its host telescope is manipulated. Provided the reciprocal direction is not close to the primary axis, this is a stable "iterative" procedure, because the target movement is very small compared with the movement of the searching line of sight from the observing instrument. This is not the case for a pointing along the primary axis. In this rare instance, the difficulty can be resolved by using an earlier suggestion, which is to deliberately tilt the theodolites, or by using a truly concentric target. However, the offset target itself requires a little more analysis.

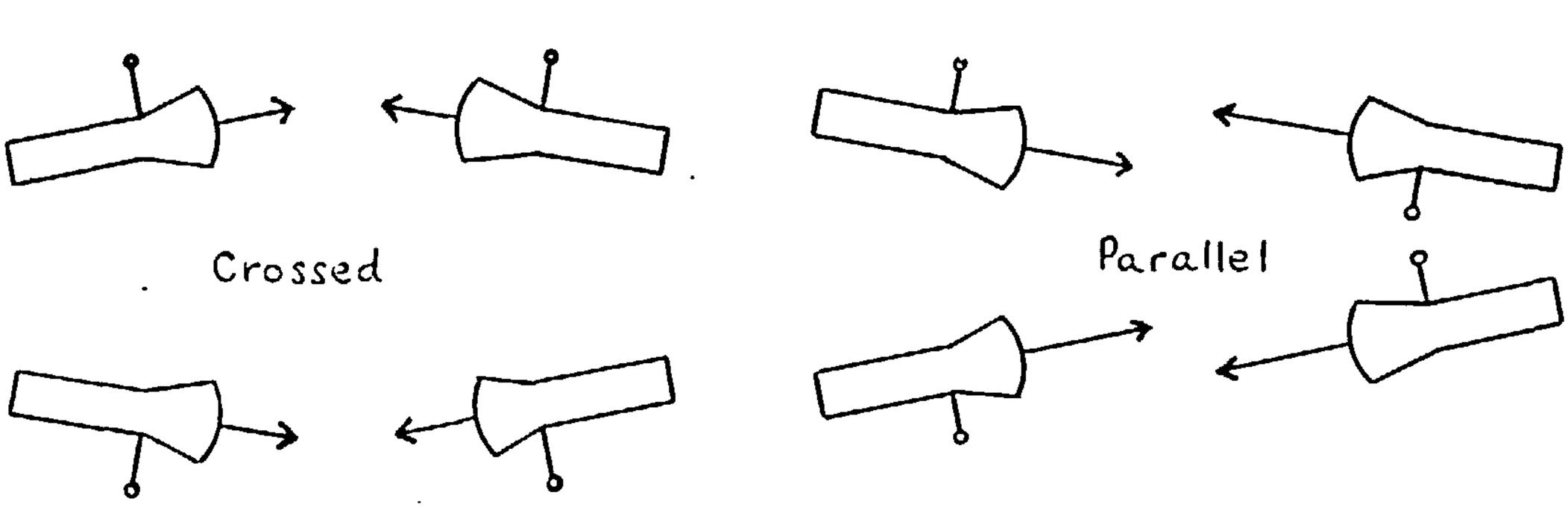

Figure 2.13 Reciprocal pointing with offset targets.

Fig. 2.13 shows that reciprocal pointings can be made with the lines of sight either in the "crossed" or "parallel" condition, but do not point along the baseline as required. Fortunately in either case, telescope reversal creates a situation which is symmetrical about the baseline, and the sign of the error vector is reversed. It can be seen that this is true when the target telescope points in the same direction after reversal. In fact, since it is likely that it also points at an offset target which changes position, the situation is slightly altered. Fortunately, the pointings on face left and right vary by positive and negative amounts which have substantially the same magnitude, and the symmetry is preserved.

Although these differences are equal for most practical purposes, it is not strictly correct that the mean primary and secondary angles of face left and face right give the direction of the baseline.

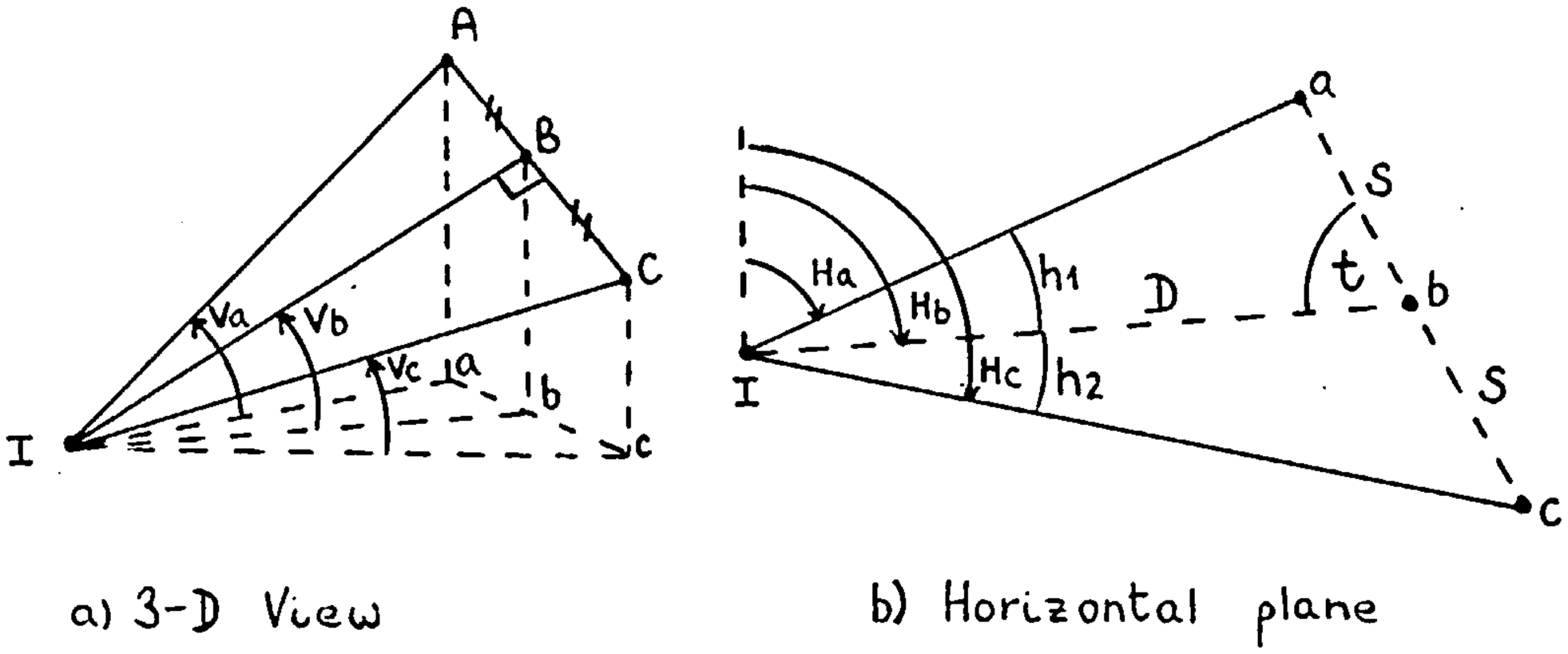

a) 3-D View b) Horizontal plane

Figure 2.14 Reciprocal vectors from one theodolite.

Fig. 2.14 shows the view from a levelled theodolite, in which target positions A and C are symmetrical about the baseline IB. Triangle IAC is therefore isosceles. In general A and C will have different horizontal and vertical values. It is clear that the mean of the vectors IA and IC is correctly a vector in the direction IB. The direction of this vector is <u>not</u> given by the mean horizontal and vertical angles to A and C. To appreciate the reason, consider the horizontal view in fig. 2.14 (b), where a,b,c are vertically below A,B,C.

Point b still bisects ac, but triangle Iac is not isosceles. Given that :

$$Ia = IA \cos (Va)$$
$$Ic = IC \cos (Vc)$$

then Ia is not equal to Ic since Va is not equal to Vc.

Hence the subtended angles h1 and h2 are not equal, and the direction to b is not given by the mean horizontal angle.

This only has significance at close ranges. In practice, mean values are correct if A and C have the same horizontal or vertical angle, and errors completely negligible if their horizontal or vertical separations are small. It is usually easy to arrange matters to achieve this condition, but exceptions will inevitably occur. A numerical example will give an idea of the magnitude of the effect.

Again considering fig. 2.14(b), the instruments are separated by a distance, D, in the horizontal plane, with the offset given by S at an angle, t, to the pointing.

From the sine rule :

$$S / \sin (h1) = D / \sin (t + h1)$$

expanding

$$\sin (t).\cos (h1) + \cos (t).\sin (h1) = (D / S) . \sin (h1)$$

or

$$\sin (t) . \cot (h1) = D/S - \cos (t)$$

hence

$$\tan (h1) = \frac{\sin (t)}{(D/S - \cos (t))}$$

and by a similar analysis

$$\tan (h2) = \frac{\sin (t)}{(D/S + \cos (t))}$$

When the offset lies in the vertical plane then

t = 0 deg., and h1 = h2 = 0 deg.

When A and C are at the same height, then

t = 90 deg., and h1 = h2 = arc tan (S/D)

If t = 45 deg., S = 1.5 cm and D = 3 m, then

h1 = 00 deg 12 min 12 sec
h2 = 00 deg 12 min 07 sec

In this realistic example the difference is small, although measurable and systematic.

In passing it should also be mentioned that when using offset targets instrument errors are not strictly removed by transiting. These errors are functions of the nominal horizontal and vertical angles, which are unchanged only if the same target is observed. It is actually a different target position which is sighted on telescope reversal, but again effects will negligible, particularly if the theodolite is well adjusted before use. If it is felt that this could be a problem, reciprocal pointing using both the "crossed" and "parallel" conditions will virtually eliminate instrument errors.

I have discussed reciprocal pointing with offset targets in some detail, because the method has only recently been of use. Consequently, I have not found any other alternative descriptions, and these may not exist.

Despite the fact that I prefer to use offset targets rather than cross-hairs, a comparison of techniques would be a valuable exercise. A proper evaluation should also investigate internal telescope targets and exchangeable targets. Although I have not carried out such a test, there has been no indication in numerous measurements to date which suggest that offset targets introduce significant errors.

2.12.3 Targetting.

Two convenient types of target have been successfully used in this work.

a) A polished steel ball.

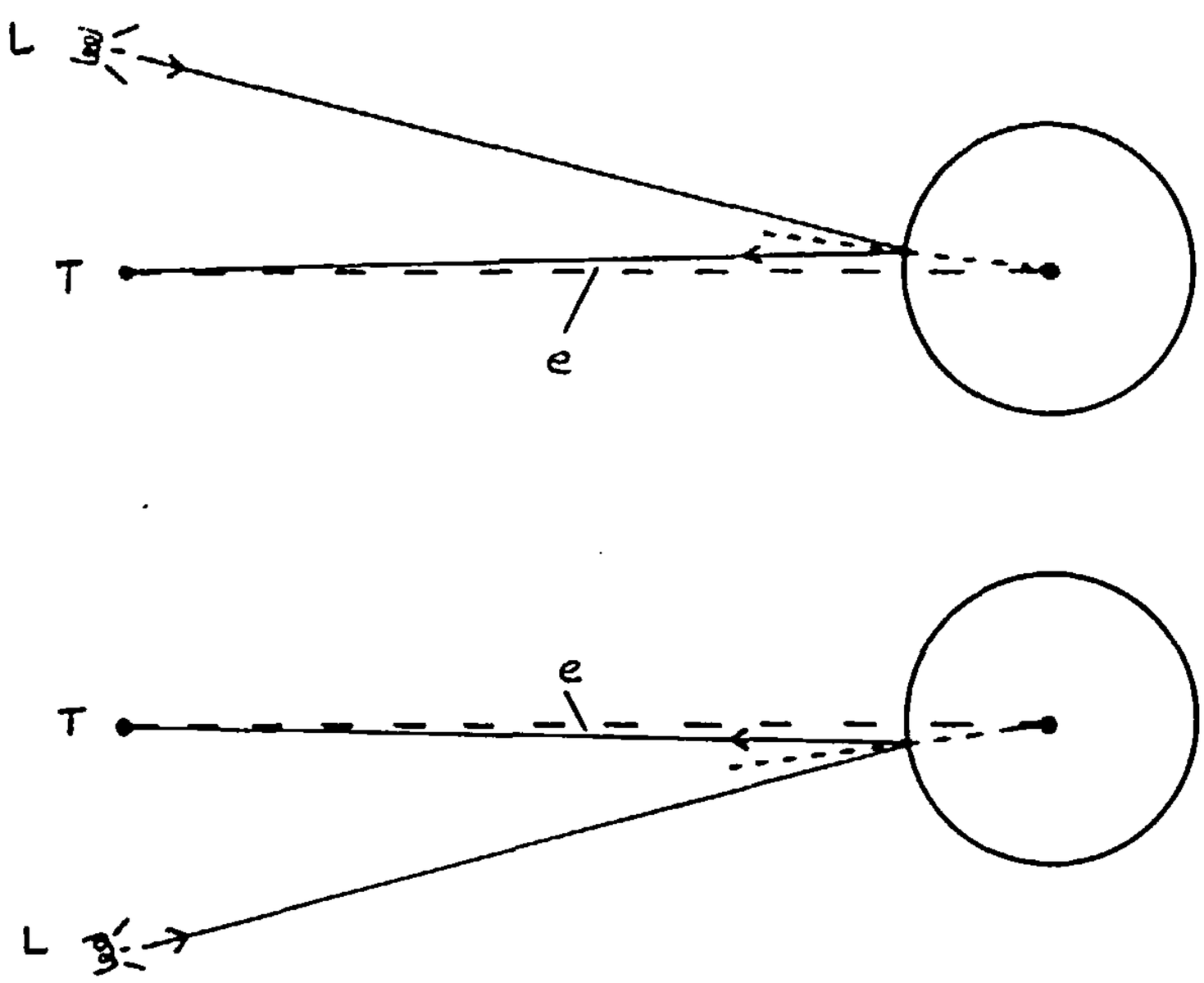

Figure 2.15 Steel ball target

A telescope can view the reflection of a lamp or similar, attached externally to its barrel. Although the reflection does not appear at the centre of the ball, which constitutes the target, the error is removed on reversal. This target was first suggested by Dr. Peter Scott, and is convenient for viewing from all directions.

b) Retro-reflective material.

Retro-reflective material was first used by Brown for photogrammetric purposes [A5]. It gives a very strong reflection when illuminated by a source close to the viewing position. For use with the ball target, Simon Oldfield at NPL has manufactured a compact and powerful fiber optic illuminator, and a similar device was later built at UCL. This was then employed on the ship survey, for which photogrammetric retro-reflective targets had been prepared. They worked just as well for survey targets, indeed almost as well as self-luminous ones. I would recommend their further use, particularly with black, rub-down lettering to create suitable target designs.

This completes the treatment of surveying in a photogrammetric fashion, and the inverse problem of considering photogrammetry from a survey point of view will now be addressed. In particular, photogrammetry requires the introduction of two features, reciprocal sighting and the measurement of the gravity vector.

Ch. 3 Camera behaviour.

In order to introduce reciprocal observations into photogrammetry, either directly between instruments or by replacing them with targets, a unique target point must be mechanically established on the camera. If cameras created images according to a central projection, there would be no difficulty in doing this. The target point would be the (unique) projection centre. There are two real-life examples of such imaging. The first is the NPL Centrax camera [A4], in which the target point lies at the centre of the concentric spherical lens elements. The second is the pinhole camera, where the pinhole represents the target. Unfortunately, in conventional cameras, the imaging process is more complicated. This chapter therefore attempts to answer some pertinent questions.

1) Is it reasonable to identify a single point as the projection centre ?
2) If so, can this point be easily found ?
3) If not, does it matter ?

The first step in finding answers is to decide on the most suitable model for the camera. When a model has been found, it is possible to convert a real photograph into one which would have been taken by a nearby pinhole camera, and use that instead. This conversion is also known as camera calibration. The differences between the real camera and pinhole model are known as distortion.

Camera calibration is done this way because the mathematics of a central projection are so simple, although it is mentioned later that triangulation networks need not depend on central projections for their solution. However, the pinhole camera will be taken as a standard, for comparison with more complex models. This commonly accepted view is stated, for example, by Ziemann [B6]. He also remarks that for most applications a single projection centre exists.

This would be the equivalent pinhole, and it would obviously solve the current problem if it always had a fixed relationship to the actual camera. It could then be marked with a target.

Unfortunately, the work of Scott [B11] and others, suggests that there is not a unique projection centre, and so the discussion will develop his model first.

3.1 Basic requirements.

It seems fairly obvious that a lens with fixed glass elements will always process incident light in the same way. It seems equally obvious that the position of the imaging sensor, be it film, plate or electronic chip, cannot affect how the light traverses the lens. The position of the image plane is dependent only on the independent need to obtain a sharp image of the object being examined. If a projection centre or target point can be identified, it will be a property of the lens, and not the lens/image combination. Once identified, it should remain fixed with respect to the lens, regardless of the focal distance. Equally, any distortion will be caused by the lens, and cannot, in a real sense, be altered by re-focussing. The discussion therefore assumes that the elements are supported in a sensibly rigid mount. Over long periods there should be no movement which significantly affects how it creates images.

In principle, a camera is adequately defined by a model of the lens, and separate parameters to define the image. The lens could be described by the designer's ray tracing program, which requires a knowledge of the refractive index of each element, its thickness and surface curvatures, and its position on the axis. This is a complicated description, and one which still fails to deal with the manufacturing inaccuracies which give rise to "decentring" distortion. It exists because the individual components of a compound lens cannot be placed exactly on the same optical axis.

Given its complexity, a model of this form is impractical. Therefore it will be assumed that the simplest description, consistent with the limits to measurement precision, is the one required.

Most photogrammetric camera models take this approach. Additionally, they tend to treat the lens and image as a combined unit, rather than explicitly separate them. In practice, this may amount to much the same thing. Usually, there is separate provision to allow for variable stretching and contracting within the image surface, and any departures of this surface from a true plane. Also, if photographs have been taken with the same camera at the same focal settings, variable parameters such as principal distance and radial distortion may be constrained to have the same value in the relevant photographs. Both these features are an acknowledgement that the lens and image are separate entities. The analysis will, therefore, concentrate on the lens.

3.2 Optics and Scott's model.

A lens has a limited size and a relatively small aperture. As a result, only narrow cones of light can be admitted from any object point. In choosing a representative line of sight from the camera to the object, it is clear that one of the rays within this cone is a sensible candidate. To appreciate this, it is only necessary to imagine another small object inserted into the cone, such that the light from the first is extinguished. The second point now has the same image position, and the two object points define a line which can be interpreted as the line of sight to both. If the camera functions as a central projection, several such lines within the field of view should intersect at a single projection centre. Object space geometry, so defined, can then be compared with the geometry of the image space to derive a suitable camera model. This is essentially Scott's calibration method [B10]. The principle is easily understood and has some physical meaning.

In theory it could be used to define the projection centre, independently of any constructional features on the lens.

However, it would still be useful if a particular feature of the lens represented the projection centre, as is the case with the Centrax and pinhole camera. This would avoid the necessity to set up a radiating target field to create the intersecting lines of sight. It might also be more accurate to identify the projection centre directly on the lens. The feature most likely to correspond to this point is the centre of the entrance pupil. This is the image of the aperture viewed from the object side of the lens. It is the hole into which the object space rays apparently travel, hence the suspicion that it corresponds to the pinhole. From the image side of the lens, the apparent position of the aperture is the exit pupil, from where the object rays appear to emerge and converge to a focus. The two pupils are not necessarily in the same position, which leads to the concept of separate object and image space projection centres.

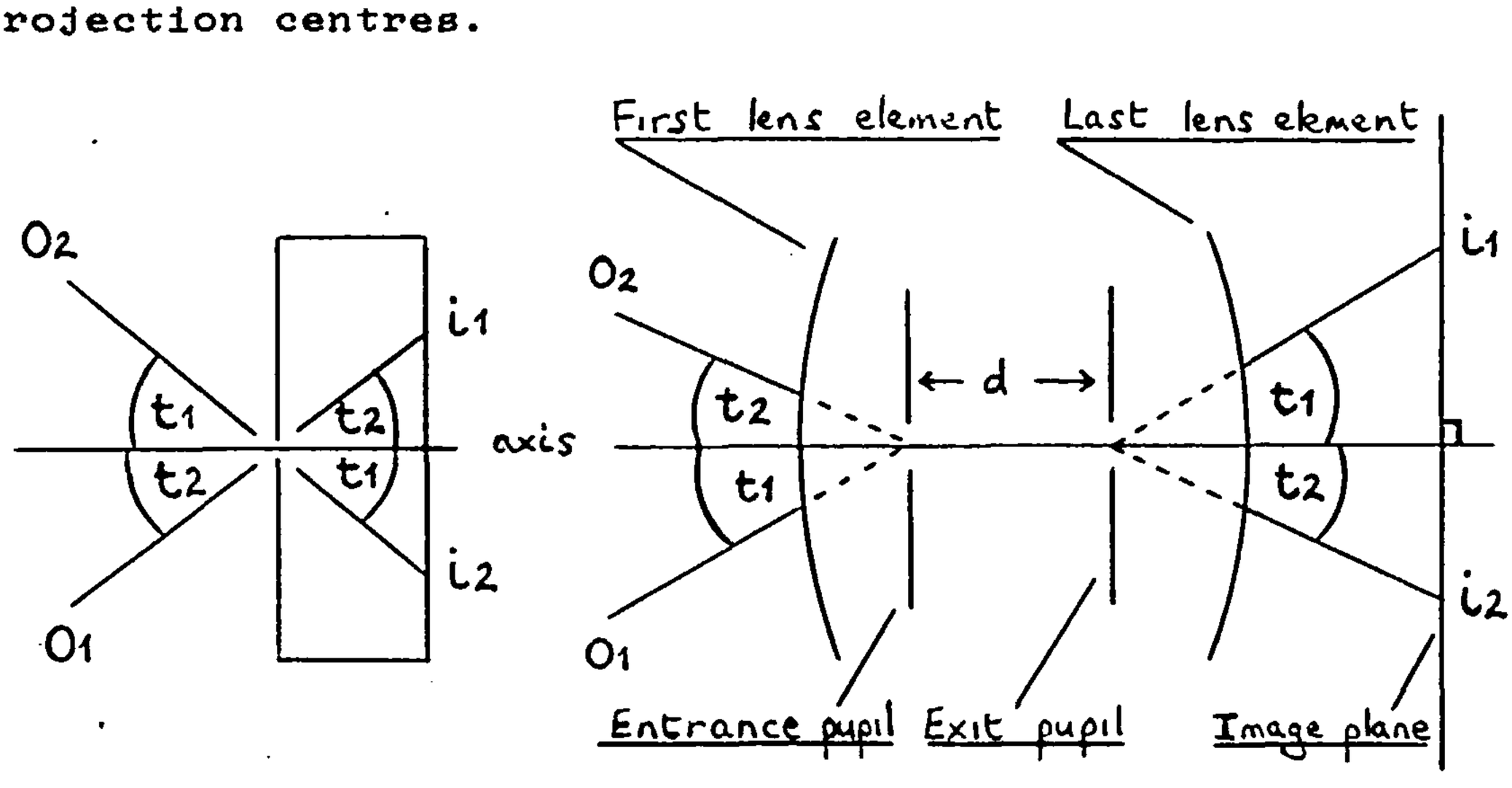

Figure 3.1 Pinhole camera and simplified real camera

In (a) a pinhole camera is shown subtending equal angles in object and image space. In (b) the first simplified camera model shows the same angular relationships, but with two separate projection centres separated by a distance, d.

This creates no difficulty in processing, as the exit pupil and image plane may be imagined shifted to the left so that the pupils superimpose, and effectively create a pinhole camera. The pupils, of course, are not small points like pinholes, and treating them as projection centres requires further justification.

The diameter of the entrance pupil determines the size of the cone of light accepted from any object point. In the middle of this cone is the principal ray, which passes through the centre of the pupil. It is clearly stated by Finsterwalder and Schwidefsky [B3,B4] that the centre of the entrance pupil is the projection centre in object space. This might be expected by imagining what happens as the aperture shrinks. The object rays then form an ever narrowing cone, until only the principal ray is left. A second object point, on the principal ray of the first, is similarly affected. Both principal rays are then seen to be the same, and clearly represent the line of sight described above. Of course, this thought experiment cannot be executed, because diffraction effects make it impossible to restrict a cone of light to a single ray. In addition, some assumptions are made which may not be true. Since it is sometimes suggested that the node is the projection centre [A1], the optical process will be considered in a little more detail.

A compound lens is represented in fig. 3.2 by an optical axis and two principal planes normal to it.

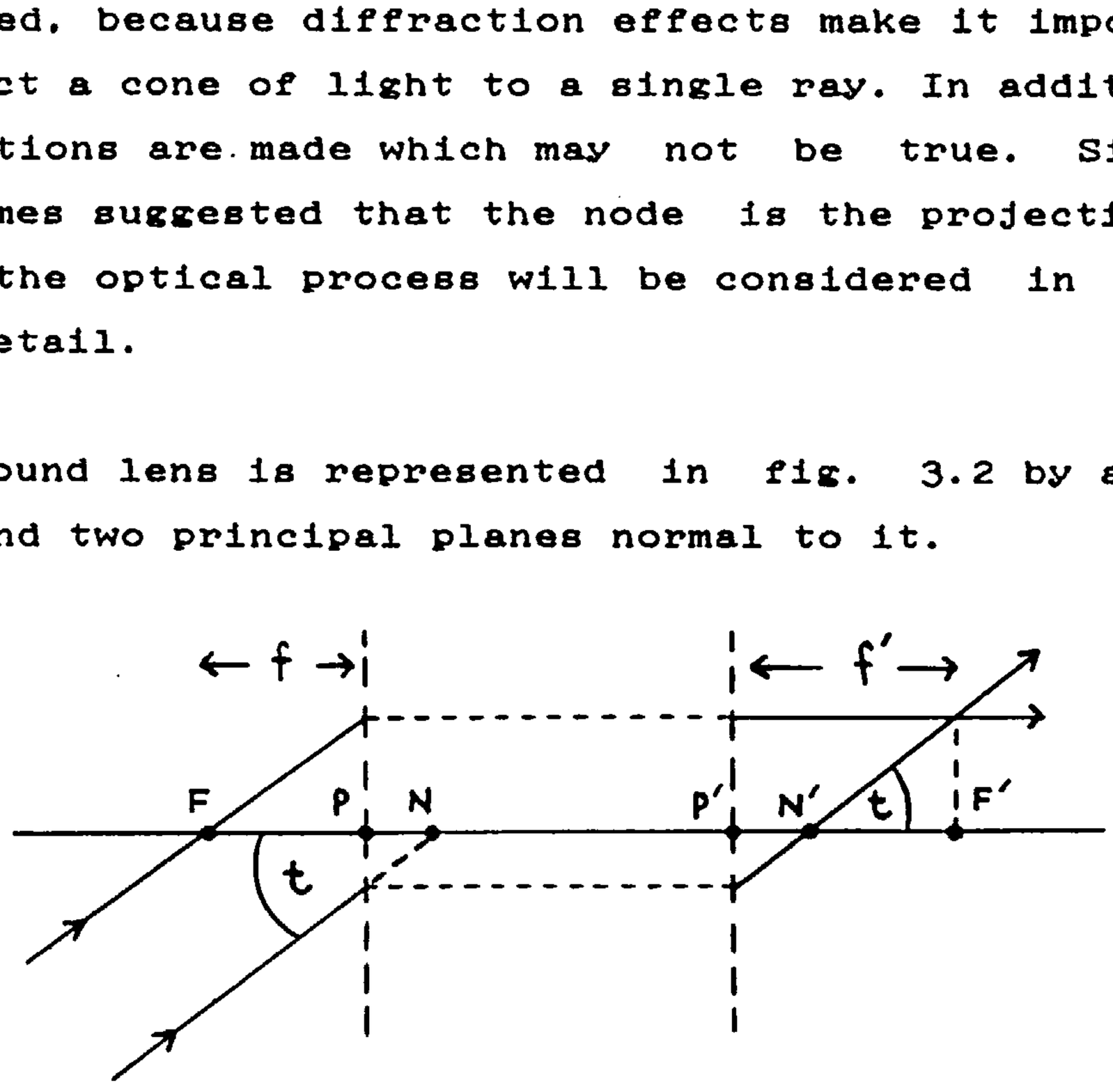

Figure 3.2 Cardinal points in an optical system

The (optical) principal points are at P and P', foci at F and F'. The focal lengths f and f' are equal only if the object and image spaces have the same refractive index. This is commonly the case, the refractive index being that of air. The nodes at N and N' are axial points such that if a ray enters at N, it leaves N' at the same angle, t, to the axis. Given this property of equal angles in object and image space, it is no surprise that the nodes are sometimes identified as the projection centres. Instead it should be appreciated that the cardinal points are primarily used to construct object/image pairs, and are strictly only valid for rays lying close to the axis. (Note Schwidefsky's comments, p48). Now consider the pupils again.

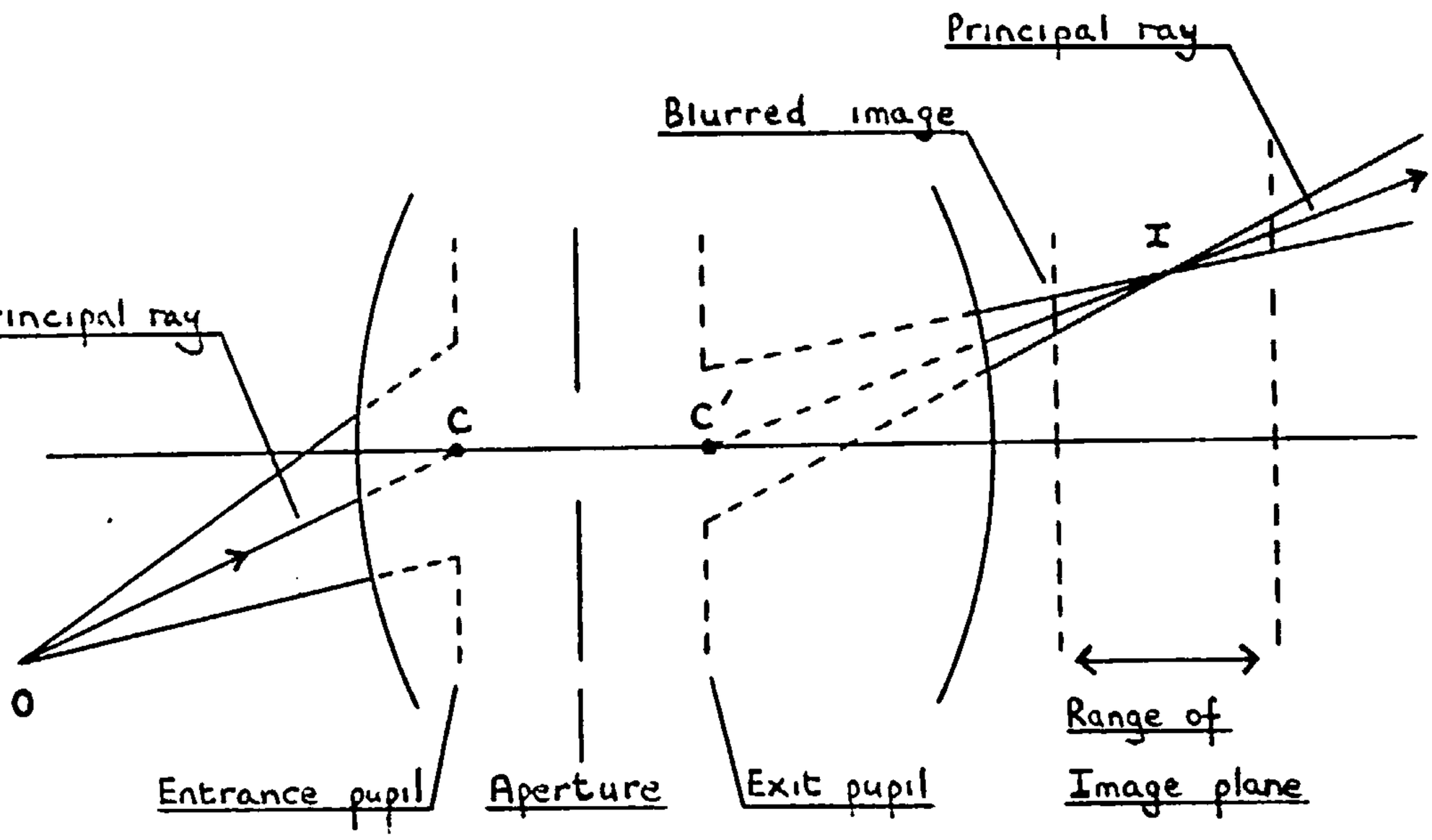

Figure 3.3 Pupils

Fig. 3.3 shows how the images of the (limiting and circular) aperture, seen from both sides of the lens, determine the actual rays of light accepted from object O, and converged to its image at I. Since image distances vary, a compromise position must be selected for the image plane. This is restricted to limits which depend on how much blurring is acceptable. Using the simplified concept of rays, the blurred image of the point is a small circle with its centre located on the principal ray.

(Note that the light emerging from the exit pupil forms an oblique cone. An image plane parallel to the aperture plane intersects it in a circle). For the moment, this ray will be taken as defining the imaging geometry. If the image plane intersects a short length of this ray, near the true image point, an acceptable image is produced. This concept gives rise to the next diagram.

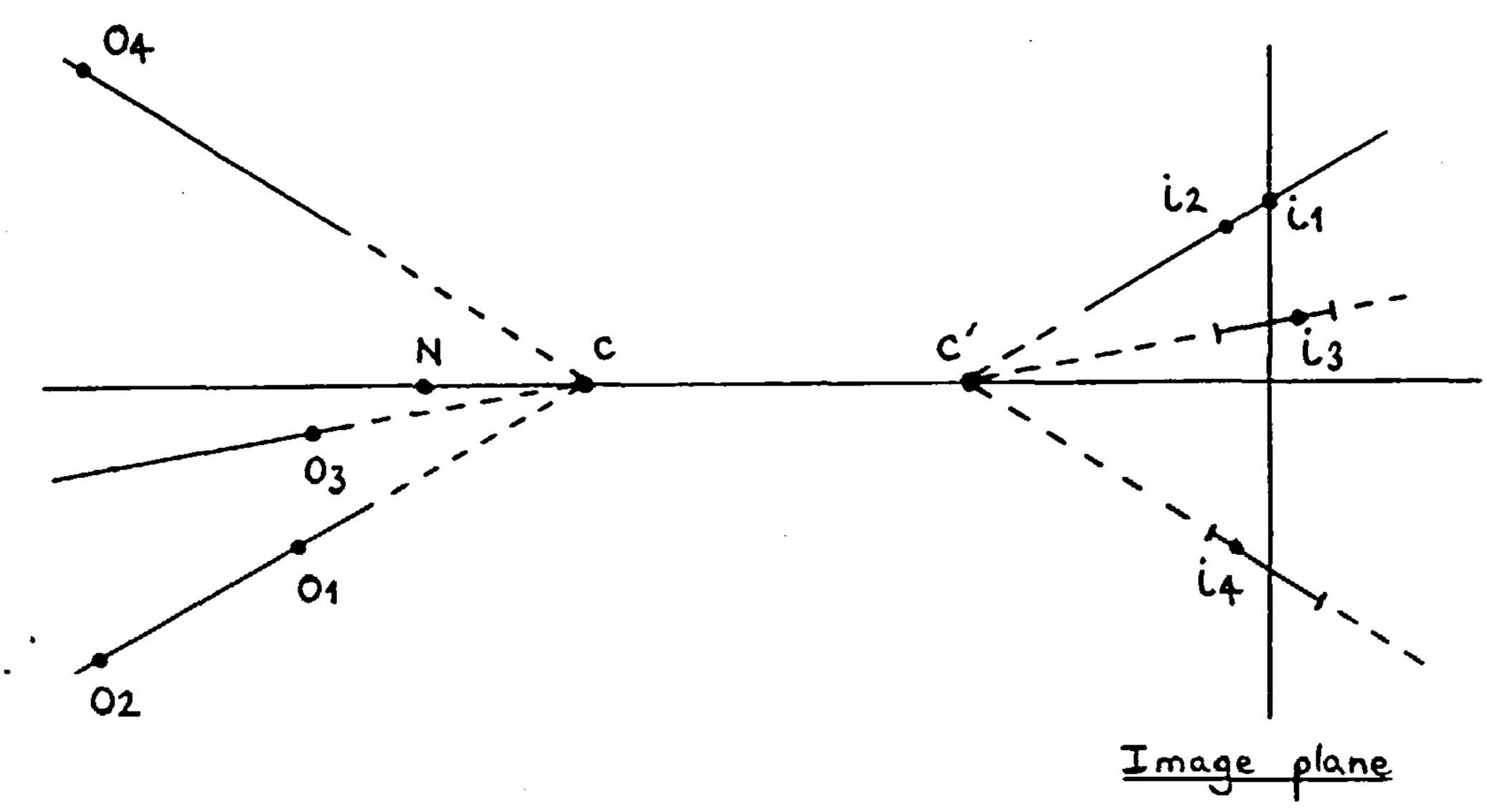

Figure 3.4 Geometry of imaging.

Only principal rays are shown, provisionally intersecting at the pupil centres C and C'. Two points, O1 and O2 have the same principal ray. They do not have the same image positions in 3-D space, but on the plane the blurred image of one is superimposed on the sharp image of the other. The front node, N, is shown in a different position from the pupil centre C, which in this diagram acts as a single projection centre.

To reinforce the fact that this geometry is influenced by the pupils, consider the effect of moving the aperture (assumed to remain the limiting aperture).

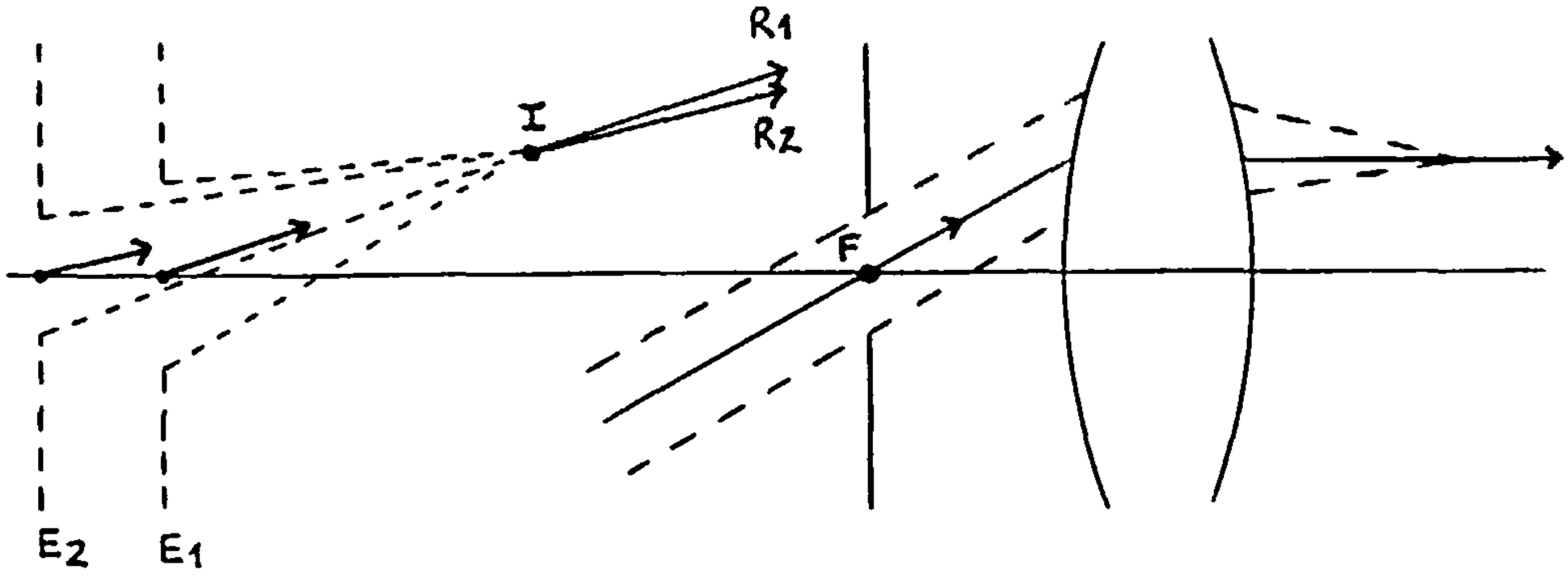

Figure 3.5 Shift of Aperture and Telecentric stop

In fig. 3.5 (a), a movement of the aperture shifts the exit pupil along the axis. A different principal ray is obtained, at a different angle to the axis. However, the true image position in 3-D space remains fixed at I, and would be computed at this position by constructing rays through the nodes. The nodes, therefore, only help to find the spatial image, and say little about the effective projection geometry. Had the lens in fig. 3.4 been fixed in position and the aperture moved, points O1 and O2 would have had different principal rays and, consequently, different image positions on the plane. Despite the fixed lens, the projection centre would have moved, giving a slightly different perspective view.

It might still be felt that a nodal ray is present within the cone of light from the object, and thereby influences the geometry. The extreme example of a telecentric stop, fig. 3.5b, shows how this is not the case. Here the principal ray is forced through the focus, and must emerge parallel to the axis. A nodal ray does not even exist. (The telecentric lens makes use of the fact that shifting the image plane along the axis does not cause a shift of the image point).

It might seem a little hard to reject the nodes as useful only for predicting image positions. They do, after all, have the useful property of subtending equal angles in object and image space. If a lens is constructed to approximate to a central projection, good use could surely be made of this.

In fact, it might be expected that matters are arranged so that the nodes coincide with the centres of the pupils. Welford [B1] suggests this is the case, by indicating that lenses are often designed in which the pupils nearly coincide with the principal planes. Their centres are therefore close to the principal points. Since the nodes also coincide with the principal points when the front and rear focal lengths are equal (a common occurance), it is clear that the nodes are usually close to the projection centres. Schwidefsky also points out that in symmetrical lenses there is an exact coincidence of pupil centres and nodal points. Nevertheless, it is still more accurate to describe the pupils as the <u>physical</u> projection centres. Schwidefsky [B4] emphasizes this several times.

This raises another issue. If the principal rays only pass close to the nodes, subtended angles in image and object space cannot be equal. Yet another modification must be made to the camera model.

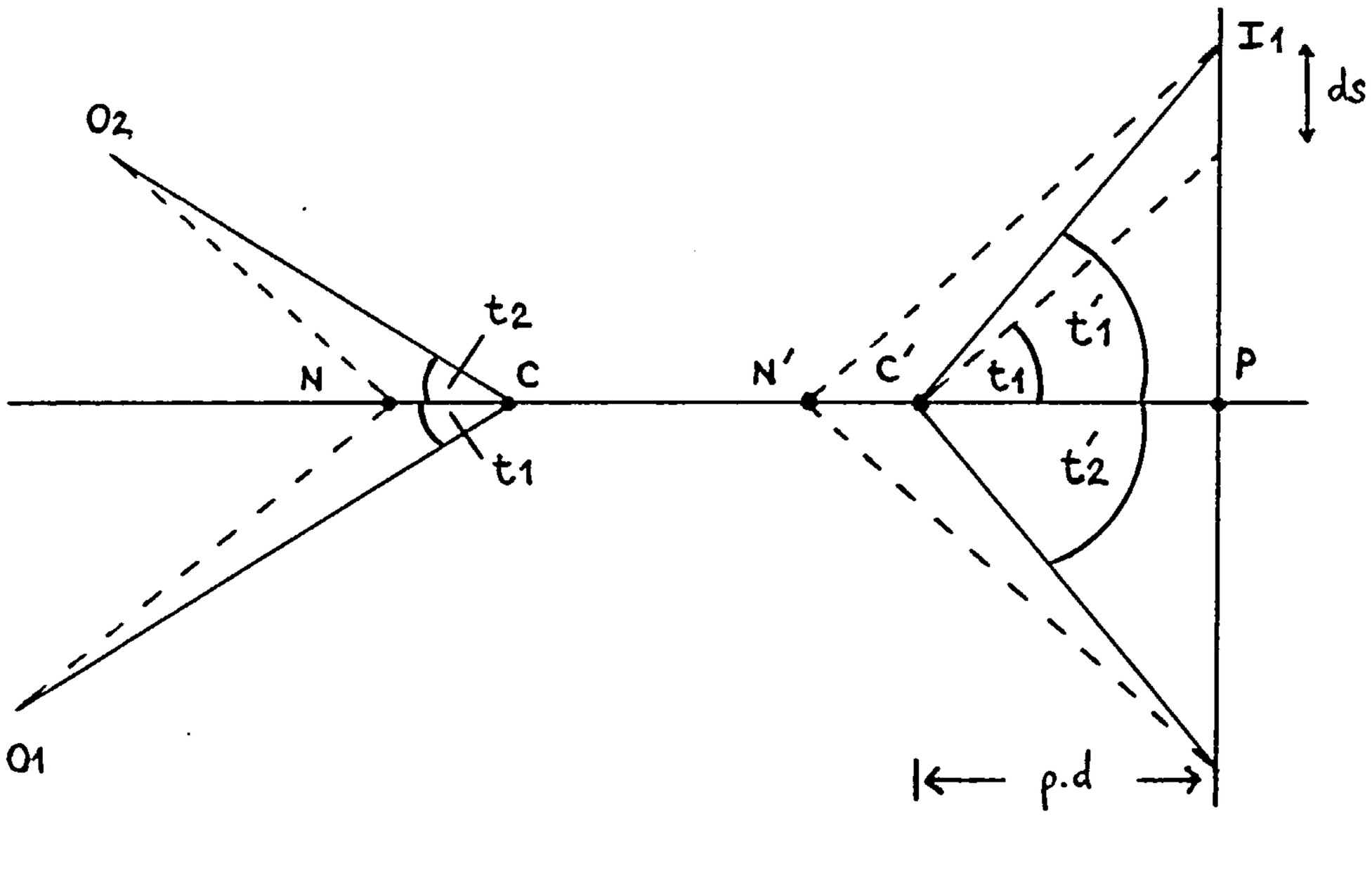

Figure 3.6 Close range model

(N.B. In fig. 3.6 a point, P, is shown. This is the photogrammetrist's principal point, the intersection of the axis with the image plane. This is not one of the optician's principal points which will not now be further discussed).

The revised diagram is a description of image distortion. The angles subtended in image space must be converted by a process of calibration, to derive the true angles subtended in object space.

Distortion need not necessarily be considered only in angular terms, but in the context of close-range measurement and 3-dimensional objects it is convenient to do so. The angular correction to photogrammetric measurements will be called the distortion characteristic, and other camera defects designated abberations.

For the next stage in deriving a camera model, fixed front and rear projection centres, C and C' are assumed. It might seem sensible to define a fixed principal distance, C'P, and derive a function which shifts an image point, I1, by an amount ds. The new position of the image, combined with the principal distance, pd, gives a vector of the correct direction. Alternatively, a vector with the correct direction can be found by keeping the image fixed in position, constructing a nodal ray through N', and altering the pd to N'P.

Adopting this second approach it would be found that N' was not generally a fixed distance from P for varying values of t. This leads to the conclusion that the projection centre, erroneously taken here as the nodal point, varies its position with incident angle. As it happens, this is true, but the wrong arguments are used in the deduction.

Another false deduction can be made about this model, and is most easily seen in the special case where a fixed principal distance can be associated with every image point, even though angular distortion is present.

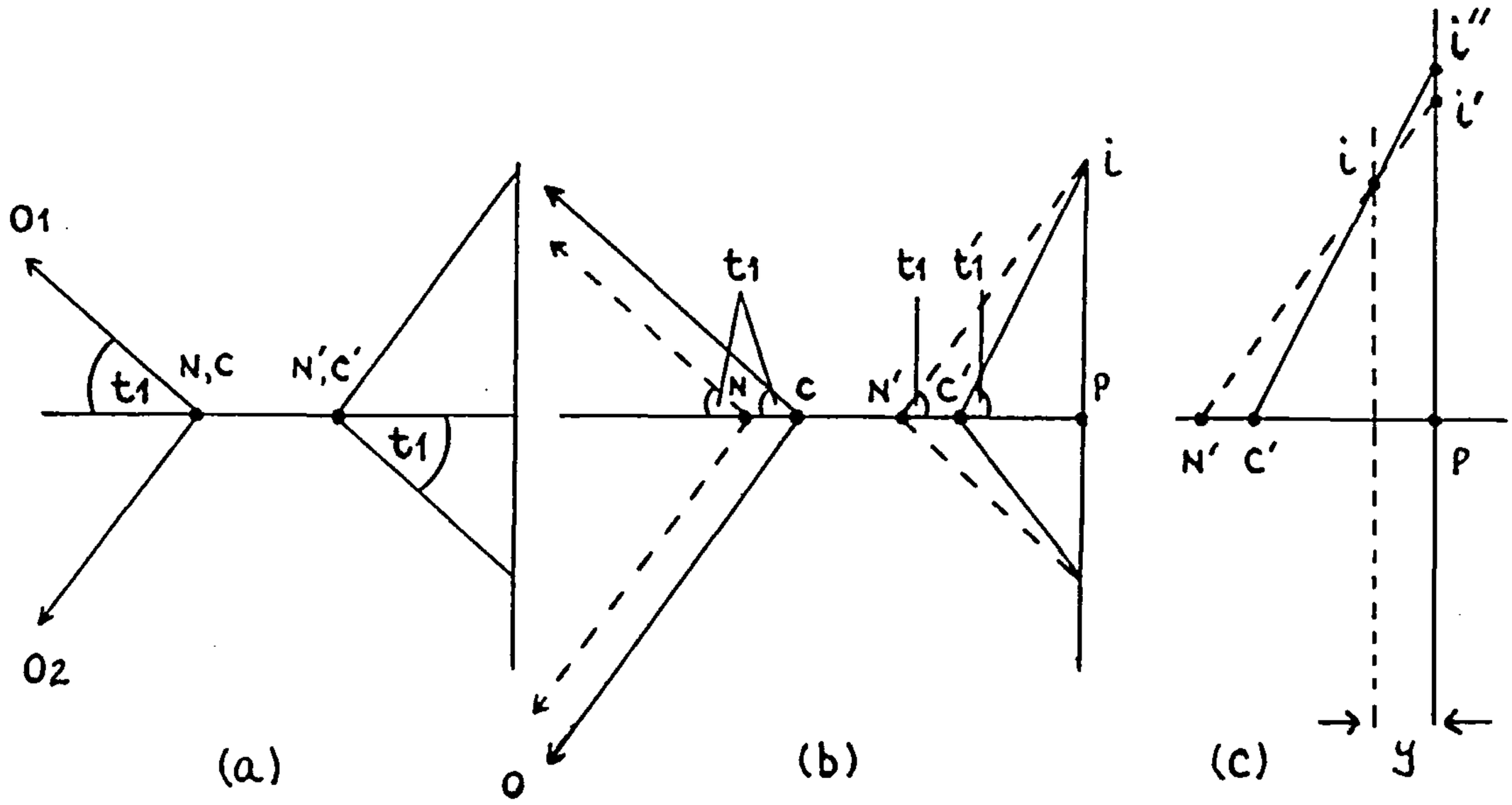

Figure 3.7 Distortion created by aperture movement.

Fig. 3.7 (a) shows a distortion-free camera at infinity focus, nodes and pupil centres coinciding. In fig. 3.7 (b), the aperture is then moved slightly to the right, causing a similar movement of the pupils. Although the object space projection centre, C, has moved, this has no effect on angles subtended by objects at infinity. In contrast, different angles are now subtended at C'in the image space. However, distortion is not detected because the images do not move. In the special case of objects at infinity, every 3-D image point falls on the same image plane, and all rays, nodal, principal or otherwise, still pass through this point despite the aperture movement. The same principal distance, N'P, associated with each set of unaltered image coordinates, continues to give the correct direction to the associated object point. This is the diagram shown by Finsterwalder [B3, p35].

In fig. 3.7 (c), the camera is re-focussed for near objects, by moving the image plane an amount, y, away from the lens. Now the images do not move to i', but to i''.

Distortion then becomes apparent, since it is no longer possible to associate each image position, i'', with a new fixed principal distance, (N'P' + y), and arrive at the correct object space directions.

In this situation, the deduction which would be made is that the distortion characteristic has changed (from nothing to something significant), when it manifestly has not. Had a close-range distortion characteristic been defined, based on a fixed value for C'P and an image shifting function, it would only be necessary to re-scale image coordinates at infinity focus by an amount :

$$(C'P + y) / C'P$$

The same distortion characteristic could then be applied. (This could also be deduced from the fact that the distortion characteristic is angular in nature, in this case).

This analysis is not the one given by Scott. He points out that a distortion characteristic based on a varying principal distance, cannot simply be altered by increasing each pd by an amount, y. If this is done, there is an apparent change in the characteristic which, in a real sense, is not present. Despite a different approach, the same conclusion is obtained.

Now, many camera models developed in close-range photogrammetry consider the situation to be exactly as described. That is, there are single projection centres in the image and object spaces, a nominal but initially unknown principal distance, and distortion expressed as an image shift which may be both radial from the axis, and normal to such radii (hence the term tangential). Murai has reviewed and tested several models [B9]. These models do not, and need not, indicate if the projection centres are the centres of the pupils, which is implicit in the discussion so far.

Unfortunately even with this model, it is still found that the distortion characteristic varies with focussing distance, and Scott has examined a further modification.

He suggests that there cannot be a single projection centre, with or without additional (angular) distortion. Perhaps this is not surprising, since lenses are axially symmetric rather than being built up from spherical surfaces centred on a common point, as is the case with the Centrax. They cannot then present the same imaging properties in all directions. Undoubtedly, for rays which are significantly off-axis, and for which simplified lens formulae based on cardinal points are no longer valid, the axial position of the entrance pupil can be expected to change.

This movement of the pupil is known as pupil abberation [Bi2], and Scott argues that it is responsible for a variation of the distortion characteristic with focussing distance. If the projection centre varies with the angle of the principal ray to the axis, a simple diagram shows why a central projection can only be created by admitting a variable distortion characteristic.

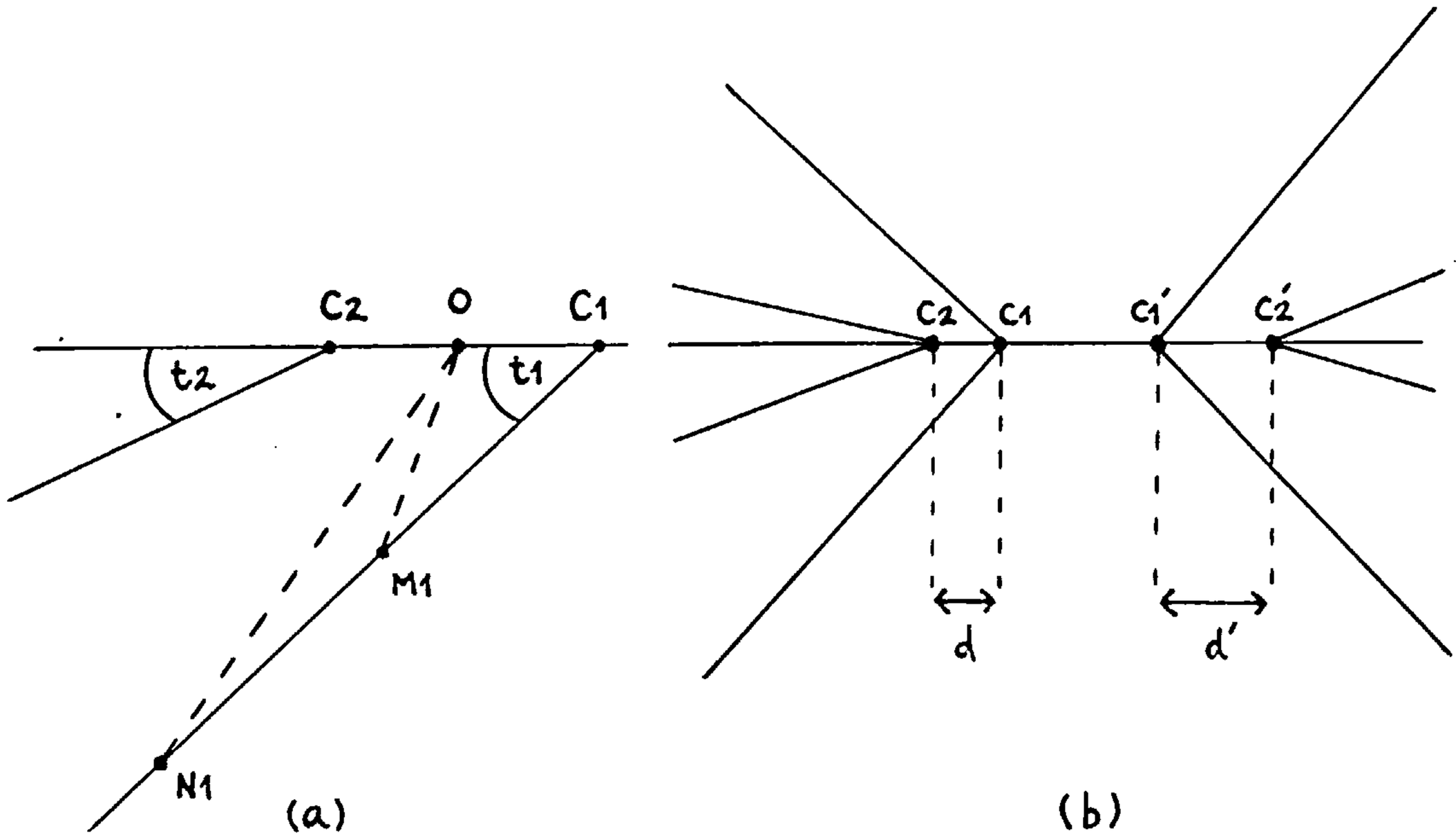

Figure 3.8 Variable projection centre, Scott's model.

For different directions, t1 and t2, there is a different effective projection centre, C1 and C2. An equivalent pinhole camera, which is the result of the modelling/ calibration process, has its pinhole at O. The rays OM1 and ON1, to two targets which have the same image position in the real camera, are different. This means that different adjustments must be made to the images of M1 and N1, because they are at different distances from the lens. They will therefore separate in the adjustment process. This, in turn, implies that the distortion characteristic varies with distance. Of course, the further M1 and N1 are from the lens, the smaller the difference between the adjustments. The effect will only be noticed at very close ranges, and when the separation of C1 and C2 is relatively large. This is Scott's argument, which he supports with direct measurements of the varying position of the exit pupil. For the lens he used, which had a significant distortion characteristic, the range of movement was around 0.2 mm. For lenses whose elements are roughly symmetric about the aperture, a similar movement could be expected for the entrance pupil. (A figure quoted in [B10] derives from intersecting space rays, and the value given may be adversely affected by the intersection geometry.) Thompson [B12] also quotes two figures for exit pupils, from a small 0.3 mm to a large 10 mm. These probably relate to aerial survey cameras given the subject matter of his paper.

By taking account of this abberation which is probably different for each pupil, the next development of the camera model is shown in fig. 3.8b.

Before considering the implications of pupil abberation, further potential complications must be dealt with. Here, I am grateful to physicists Simon Oldfield and Professor John Gates for discussions which emphasized that wavefronts will not necessarily pass through a lens in the straightforward way which an analysis with rays predicts.

So far, the principal ray through the centre of the pupil has been proposed as the effective line of sight. This would give a convenient mechanical reference when searching for a projection centre. However, the wavefront might be abberated in such a way that it cannot converge to a reasonable point, and the central ray is no longer a reliable guide to the effective position of the image. Coma illustrates the problem. The comet-shaped image spot caused by a small point object is radially offset from the image position predicted by ray optics.

If the effective line of sight does not pass through the pupil centre, then a change in the diameter of the aperture would be expected to alter the distortion characteristic. This could also be argued from the observation that a larger aperture accepts more of the wavefront. The warping effects of abberations on the wavefront would then become even more apparent. Conversely, a very small aperture processes such a limited extent of the wavefront that it can be considered spherical, and expected to converge to the point predicted by ray optics. Additionally, it would also be heavily diffracted. This description agrees with the one given in [B5]. It implies that apertures should be as small as possible to minimize the effect of abberations, and preferably of constant diameter to preserve the same distortion characteristic.

There still remains another problem. This concerns variation of the apparent position of the entrance pupil with the distance of a point from the lens. This should not be confused with its variation with angular offset, explained above. Oldfield made the comment that points at different distances from the lens generate wavefronts of different curvatures, and there is no guarantee that these pass through the lens in the same way. Also, Gates has remarked that a near point lying on the principal ray of a far point might "see" the entrance pupil in a different position. For the surveyor, the consequences would be that a line of sight cannot be uniquely defined by two points lying on it.

In fact, curved "lines of sight", rather than straight ones, would then be defined. As an analogy, consider a fixed theodolite telescope whose collimation error varies with focus. A target, moving towards the instrument and whose image remains on the cross-hairs, will trace out a curved line in space.

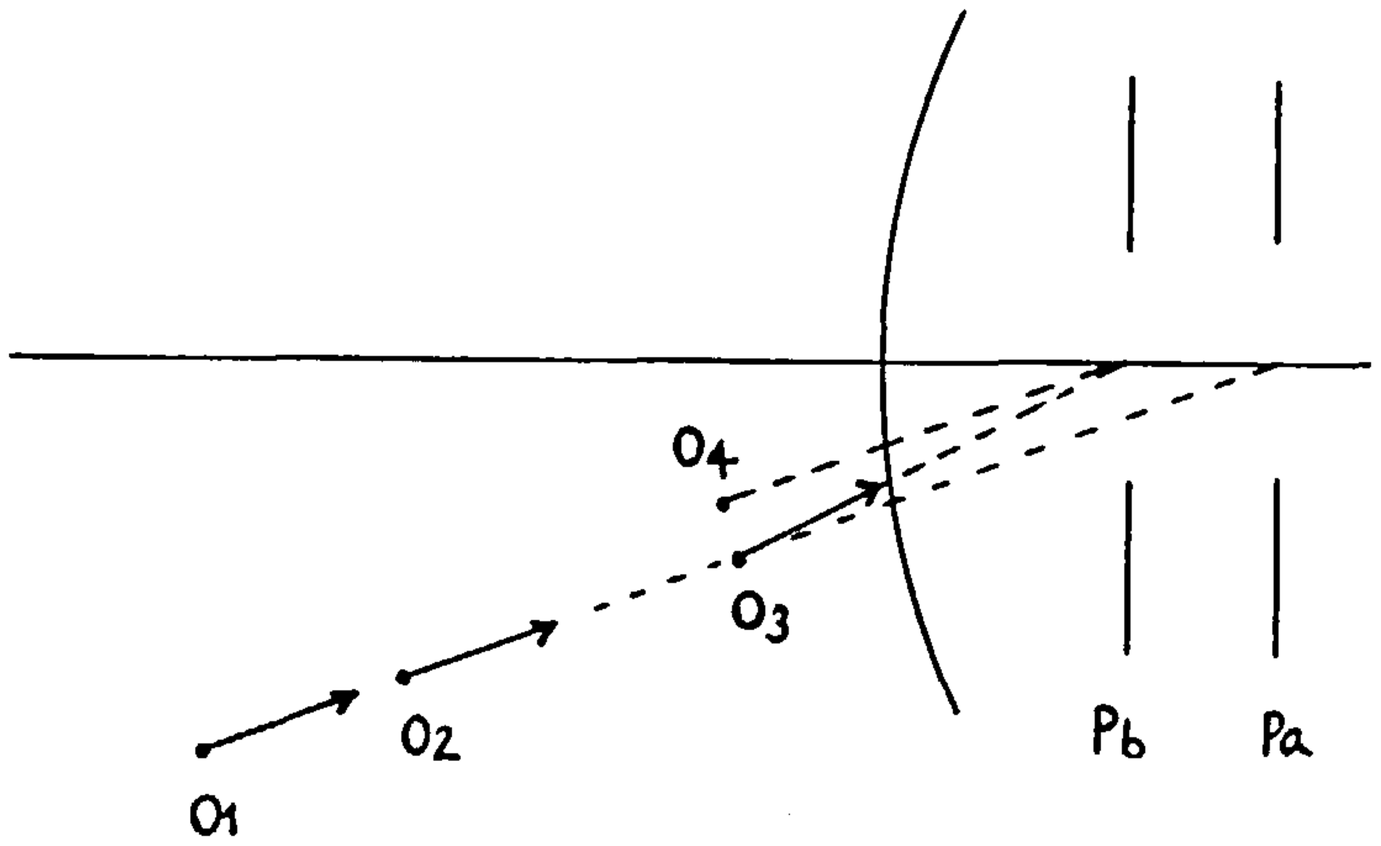

Figure 3.9 Pupil shift with distance

Fig. 3.9 shows two points, O1 and O2, at some distance from the lens, and which effectively have the same principal ray passing through the entrance pupil at Pa. Point O3 lies on this ray, but is closer to the lens and sees the pupil at Pb. From the camera's point of view, O3 subtends a larger angle with the axis than O1 or O2. The same angle is actually subtended by a point O4, close to O3 but nearer the axis. Following the analogy with a theodolite, it can be seen that a sequence of targets with the same image point will then fall on a curve, not a straight line.

3.3 Other camera models.

Before deciding on the importance of this model, it is worthwhile looking at another source of camera calibration.

This is primarily the work of D.C. Brown [B8]. He and his colleagues at GSI currently do the most accurate commercial work in industrial photogrammetry.

Since they use non- metric lenses in their cameras, they have developed a comprehensive camera model based on the physics of the imaging process. By taking equal care in removing distortions of the image plane itself, typical photo residuals of around 1 micron are obtained. They regularly work with focal lengths in excess of 200 mm [H1], so this corresponds to an angular standard error of about 1 arc sec.

To achieve this high accuracy, Brown finds that distortion corrections are functions of object distances. He offers no explanation for this, probably as it has no immediate relevance to his work, but the above model obviously offers one possibility. As he makes no reference to pupil abberation, he may not have investigated movements of the projection centre. Indeed, in his development of an equation to account for variation of distortion with distance [B7], he assumes a fixed projection centre in image space. This allows him to re-scale distortion functions onto different planes. The error may not be significant when applied to the depth of field of lenses with long focal lengths, which is the case considered by Brown. Thompson [B12] gives a numerical example which supports this statement, provided the pupil abberation is only a few tenths of a millimetre.

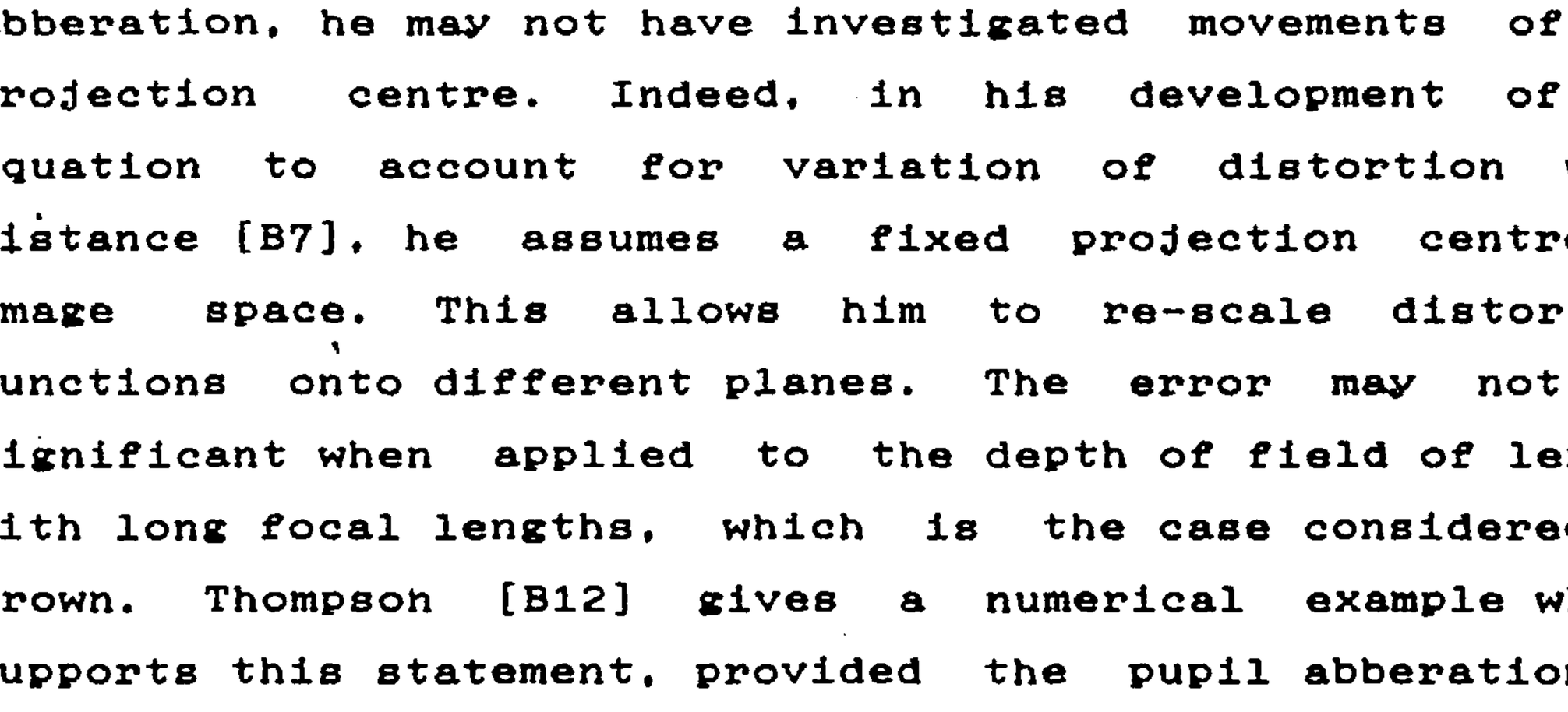

Figure 3.10 Angular distortion as a function of distance.

Fig. 3.10 shows a simple scheme in which the projection centres in object and image space are fixed. In this case, there is no distortion at infinity focus, and the images of O1 and O2, at infinity, subtend the same angles with the axis on both sides of the lens. Close up, the situation is different. A near point at O3, on the line of sight to O1, has its principal ray in image space altered by a small amount of angular distortion, and now superimposes with the principal ray to I2. Use of a re-scaled image position and constant distortion function would lead to error, since I3 then moves to the position of I2, and no correction would be applied (no distortion at infinity focus). Distortion as a function of object distance is needed.

In this model, targets on lines radial to the front projection centre have different image positions. Conversely, if targets at different ranges have the same image position, they must lie on a curved line. (It might be objected that they could lie on some other straight line, but this is an admission that Scott's model is the better description).

Once again there is the suggestion that lines traced out by targets with the same image position are curved, and it would be most interesting to test this. A potential method based on electronic imaging is outlined in chapter 8. However it is more than likely that Brown's work supports the view that there is some movement of the projection centre, which he accommodates by adopting a calibration which is dependent on focussing distance.

3.4 Adopting a projection centre.

From the above discussion, a complicated picture of the camera emerges. A surveyor could easily be discouraged from seeking a projection centre which he or she could target. In my opinion this is too pessimistic.

It seems clear that the effective projection centre in object space will be close to the axis of symmetry of the lens, itself close to the effective camera axis, and that the main uncertainty will be its position along this axis. It most probably lies within the range of positions taken up by the entrance pupil.

Provided this movement is confined within a volume which is small in comparison to the separations between instruments, or instruments and object, it will be sufficiently accurate to represent it by a single point. The movement of the projection centre in image space is almost of no importance. On the image side the task is to find some calibrating function which converts image coordinates into directions which closely approximate the lines of sight to the object. (This is very much Thompson's view in [B12]. Furthermore, as he is dealing with objects at infinity, the movement of the projection centre in object space is also of little importance).

At close ranges it may be possible to tolerate a relatively large uncertainty in the position of the perspective centre. Imagine a camera target in error by 0.5 mm along the camera axis, sighted by a theodolite. When the reciprocal observation is on axis, there is no error. 30 degs. off axis and 5 m away, the theodolite pointing error is about 10 arc secs. Clearly this reduces with greater separation of the instruments. An additional reduction in error may be achieved by positioning the target for the benefit of off-axis rays, as this is the case for which the axial positioning error is most critical.

The tests I carried out at UCL employed a metric camera, the Wild P32, which has a maximum 60 degree field of view. Such cameras have been deliberately constructed to function as central projections, within specified tolerances which provide a fairly high accuracy. Scott's work indicated pupil movements of around a few tenths of millimetres for a lens with significant distortion.

It therefore seems reasonable to expect that the entrance pupil on metric cameras can be used to identify the projection centre within about 0.1mm. Indeed, some workers would expect this uncertainty to be within tens of microns [G3].

The manufacturer maintains that distortion in the P32 is no more than +/- 4 microns. For a typical standard error in image coordinates of 3 microns, at the fixed principal distance of about 70mm, an equivalent angular accuracy of some 10 arc secs. is obtained. If reciprocal observations are to be employed, there seems little point in making these significantly more accurate. From the numerical example, a target error of +/- 0.5 mm can be tolerated at close ranges, which is considerably more than anticipated.

This argument applies to metric cameras. However, even non-metric cameras can achieve good results by adopting a model which assumes a fixed projection centre and variable angular distortion. Murai's work [B9] supports this view. He concludes that with a simple calibration model, an Olympus OM1 can give as good an accuracy as a Wild P32. It is to be expected then, that results obtained here may be readily applied to non-metric cameras, at this level of accuracy.

Where uncertainty remains, operating with instrument separations of greater than 5 or 10 m should avoid major difficulty. This range still covers many industrial measurement problems, such as those associated with ship sections [P1 - P6], bridges [R1] and pipework [Q1,Q2]. Even so, reciprocal observations at closer ranges may still be viable. Metric cameras, treated as pinhole cameras, have achieved good, sub-millimetre results when used to measure antennae [K1 - K5]. Perhaps the method only fails at higher accuracies, such as GSI obtain, and for the moment no attempt will be made to examine such cases.

In the event that a single projection centre cannot be well enough defined for accurate reciprocal observations, the exercise is still not wasted. The observations can be then be employed to generate automatically the starting values of all parameters for a subsequent optimum solution. This avoids the need for manual estimation, which greatly eases the computational effort. Optimizing programs exist which can then process all the observations, including the poor reciprocal measurements, to give the best answer which fits the facts. A typical example of a suitable program is the MOR package described by Wester-Ebbinghaus [E7].

Finally, if a camera model really requires a different projection centre for each pointing, this can be directly incorporated into a triangulation network, without the need to create an equivalent pinhole camera. The laser tracking system developed by Parker [U17] demonstrates this. A laser beam is pointed in two directions by reflecting off two rotating plane mirrors. The mirrors do not have the same centre of rotation, and so the laser beam is not directed through a unique point. The device does not function as a central projection, but this does not prevent coordinates of a target point from being successfully and accurately computed. The mathematics of the projection are given by Mayer [U19].

Ch. 4 Reciprocal observations in photogrammetry.

It has been shown how a relative orientation between two instruments can be directly computed, provided that reciprocal sighting and pointings to a single common offset target are available. Normally the reciprocal measurements are absent in photogrammetry, either because a single camera records all the photographs, or the restricted field of view makes it impossible to record both the object and another camera position. Consequently, the relative orientation of two photographs must usually start with trial values for the 6 external orientation parameters, followed by an iterative solution which requires a minimum of 5 common target points. Very often, trial values cannot be automatically generated and must be estimated by whatever means are available, such as roughly taping distances from object to camera. This is unsatisfactory, occasionally difficult and potentially unreliable. There are methods which lead directly to the solution, without the need for estimating parameters, given a minimum of 6 or 8 common targets. These are mentioned at the end of the chapter. However, certain geometrical configurations will still cause problems. Hofmann [E10] presents a definitive outline of photogrammetric failure cases, such as the arrangement where target points and camera stations lie on the same cylindrical surface. Granshaw [E9] discusses the orientation problems which arise when the targets are "badly distributed", for example when they fall within a relatively narrow band on a photograph.

If reciprocal observations can be introduced into a photogrammetric network, parameters can be determined automatically and potential failure cases will be avoided. The intention here is to target the entrance pupil as the most likely projection centre, and then use theodolites in the object space to establish the appropriate reciprocal pointings. This amounts to a form of control, but one which may be easier to create than a set of well-distributed and fully coordinated reference points.

4.1 Targetting the projection centre.

In general it is not convenient to place a target at the projection centre, somewhere in the middle of the lens. Conceivably, if the aperture was a fixed size circular hole, concentric rings could be painted around it to act as a target, but this would still only be useful within certain close ranges. The NPL CENTRAX is unusual in that the centre of the spherical lenses is the required point. This could easily be found with a theodolite telescope, using the reflection of an illuminating lamp attached to the barrel. The method is the same as for the steel ball target described in section 2.12. It is not suggested that this is of any practical use, because the CENTRAX would require a special target at the theodolite. It is also likely to have a higher angular accuracy than the theodolite, which may not make the approach worthwhile.

On conventional lenses, a target can be identified within the lens by 4 co-planar targets surrounding it on the outside. These define a quadrilateral whose diagonals intersect at a virtual point. By adjustment, this virtual point can be made to coincide with the projection centre. When such a target is photographed, it is only necessary to intersect the diagonals created by the 4 image points, in order to deduce the position of the projection centre.

Although this "4-point target" will be observed by theodolite rather than photographed, the data reduction is very little more complicated. In fact, the TRIGFIX software converts the pointings into the format of a "pseudo-photograph", reduces the data, and converts the result back into theodolite format.

A target of this type is suitable for fairly close ranges. At longer ranges a single large conventional target should suffice, for example a bulls-eye with its centre removed. In this case the centre can be easily estimated.

A disadvantage of the external target as described, lies in the mechanism of adjustment. Three degrees of freedom must be built into the support in order to move the virtual point onto the projection centre. A more elegant solution was suggested by Professor Ian Harley. He pointed out that if the relative positions of 5 points lying on a plane are known in object space, the imaged position of the fifth can be deduced from the imaged position of the other 4. This is a property of projective transformations [A1]. Clearly, the 4 points form the external target and the fifth is the projection centre. It will be shortly explained how the relative positions of all 5 can be found. If the fifth does not then lie in the plane of the 4, it is only necessary to rotate this plane through a line joining two of the targets, in order to make the necessary adjustment. Only one degree of freedom is involved, which in a practical target could be very simply implemented.

4.2 UCL 4-point camera target.

For the tests at UCL, a fairly elaborate design of 4-point target was adopted.

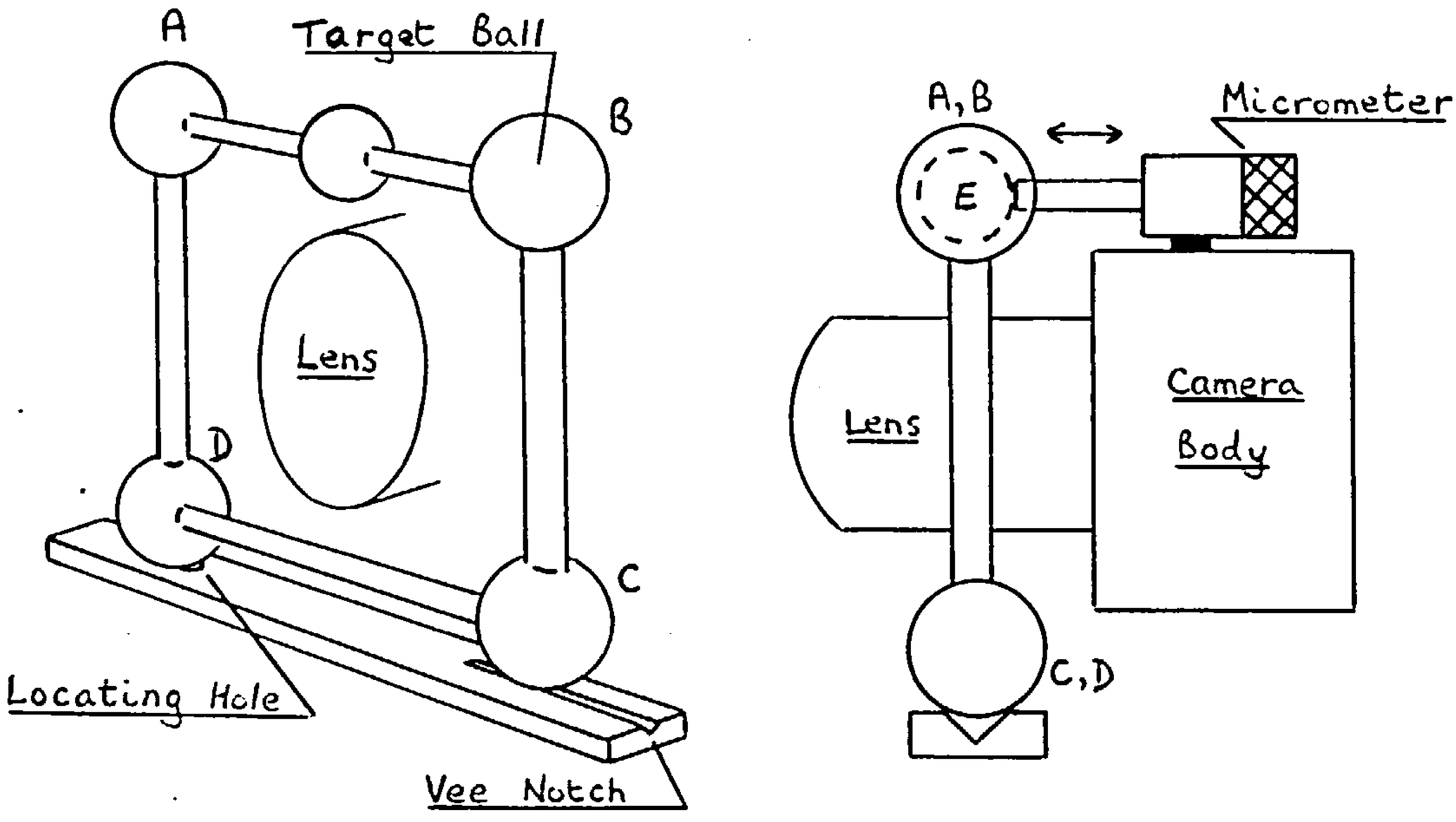

Figure 4.1 4-point camera target

Fig. 4.1 (a) shows the original concept of 4 polished target balls, A,B,C,D, located on a frame around the target. D rests in a locating hole, C in a vee notch. A micrometer attached to the camera body contacts another ball E, spring loaded against it. The 4 target balls form a nominal plane rectangle, with the entrance pupil of the lens nominally at the centre of this. (Wild state the position of the projection centre on a P32 to the nearest millimetre). By altering the setting on the micrometer, the plane rotates about the line CD. The movement of E can then be closely represented by a short straight line, perpendicular to this plane, whose length is the change in micrometer setting. Any shift of E is nominally twice the relative shift between the plane and the projection centre. An offset of the projection centre from the plane can therefore be removed by setting twice the value on the micrometer.

The arrangement was originally chosen because the balls can be used as targets by theodolites (section 2.12), and because the rotation axis is automatically forced through two of the targets. Unfortunately, the aluminium balls, chosen as being easier to work than steel, were abraded along "lines of latitude". As a result, the reflection of the illuminating source at the theodolite was diffracted along a "line of longitude". This no longer offered a sharp target point. To avoid the problem, the frame had to be modified and the balls rejected as targets.

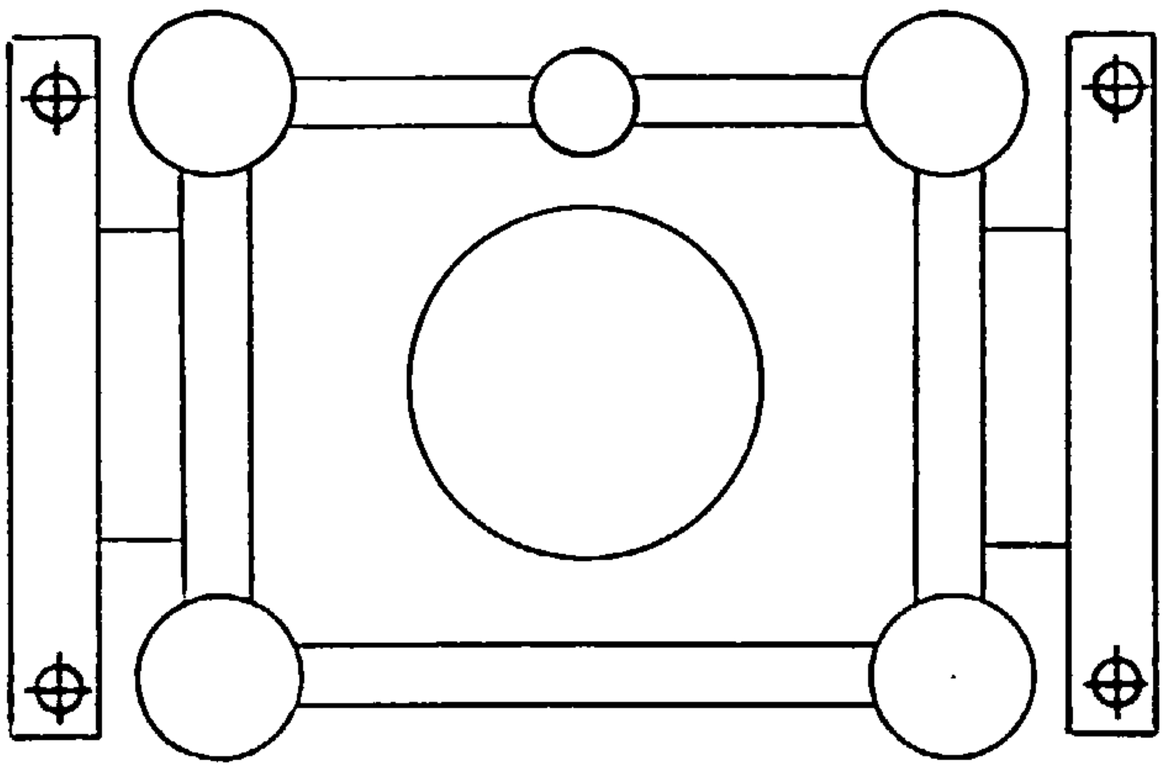

Figure 4.2 Modified target.

Fig. 4.2 shows the modified frame. Two additional brackets, supporting conventional 2-D targets, were attached. These were positioned just to the side of balls A,B,C,D. An adjustment was provided for two of the new targets, to enable all 4 to be located in a plane. This was not quite the same plane as defined by the 4 balls, nor was the rotation axis directed through the new targets at C and D. However, this made a negligible difference. For practical purposes, the movement of E was still perpendicular to the plane, and twice the relative movement required at the projection centre. The targets at C and D were so close to the rotation axis that for small rotations they were not shifted by a detectable amount.

This 4-point target frame is obviously a cumbersome prototype. Some comments on more practical frames may be of interest.

There is no reason why a target should not be attached to the screw thread or bayonet mounting at the front of most lenses. It should be sufficiently accurate to assume axial symmetry, with a single adjustment for axial position. Standard spacing shims and washers could be used for this. As for the target design, bulls-eyes are general purpose and simple. Professor Harley has also suggested vertical and horizontal lines, made so with the aid of a simple bubble attachment. For roughly horizontal pointings, this makes a good target to observe with a levelled theodolite.

Note that when designing any such external targets, the lens projects in front of its surface, and may obscure parts of it from off-axis positions.

By attaching the target to the lens, the projection centre is identified in an unambiguous way. As an alternative, it would be possible to devise an interchangeable camera and target mount. This must avoid the feature, often seen, where the camera can rotate in its mounting, but not about its projection centre. Consider the P32, used in conjunction with a T2 as a photo-theodolite.

The T2 can be replaced by a target, but the direction and magnitude of the offset of the camera's projection centre from this target must be taken into account. A true reciprocal pointing is not obtained. Other metric cameras such as the Jena UMK10 and Wild P31 can be located in supports which fit into standard tribrachs, but again the rotation axis does not pass through the projection centre.

4.3 Calibrating the projection centre and 4-point target.

Two methods were considered for finding the relative positions of the projection centre and the 4 camera targets. Using either method an adjustment could be made, although it will soon be appreciated that the first is easier than the second. As there are two methods, one could be compared against the other.

4.3.1 The Metrograph method.

Dr. Peter Scott has developed an instrument called the Metrograph [A10]. It is essentially a small, 3-axis coordinate measuring machine whose probe is the virtual image of a light spot in a semi-reflecting, plane mirror. With an object behind the mirror, the light spot is moved on three orthogonal axes until its virtual image appears to be coincident with a selected point on the object. Operators use their stereoscopic vision to achieve this condition.

With a little care, and using well defined target points, it should be possible to obtain coordinate accuracies better than 0.1mm. This is suitable for the present task. By its nature, the Metrograph is particularly useful for measuring other virtual images, such as the entrance pupil. If the back of the P32 is opened, the edge of the aperture is easily seen against a bright background. Formed by the leaves of the aperture, this edge is a symmetrical pentagon whose 5 points can be coordinated by the virtual probe of the Metrograph. The mean value of these is taken to be the centre of the entrance pupil and projection centre.

It is a simple and speedy procedure to repeat the measurement of entrance pupil and 4 target points, and make the adjustment for co-planarity. Two sequences should be enough to establish a best-fitting plane from which the 5 points have offsets no greater than, say, 50 microns. From the coordinates, two parameters may be computed, which are representative of the target. These are the values J and K defined below.

Data Sets 6 in the appendix show two measurements of an adjusted target, separated by two months and performed by two different Metrographs, which support the accuracy statement given above.

4.3.2 The resection method.

A resection produces coordinates of a "best estimate" projection centre with respect to control point coordinates. It is based on an assumed camera model, rather than the assumption that the entrance pupil represents the projection centre.

With the aid of a dual theodolite arrangement, it is easy to intersect the 4-point camera target as well as all, or a sub-group, of a set of control points. By taking a resection photograph at the same time, this establishes the target frame in the same coordinate system as the control points and the resected camera position. Once again, an appropriate adjustment can be made. However, this strategy involves considerably more effort and inconvenience than the approach with the Metrograph. There is a need for :

- a dual theodolite intersection for each adjustment (in case the camera moves)
- computation of the theodolite measurements (an on-line system was not available at UCL)
- development of the photo plate
- measurement of the photo plate
- computation of the resection

In addition, it appears that the positional accuracy of the resection may not be much better than 0.5mm. For several of the tests, a number of control points were established on two walls forming the corner of a basement at UCL. In this position they are unlikely to be undisturbed.
Unfortunately, this is not necessarily the most suitable geometrical configuration for achieving an accurate resection. It would be far better if the points were arranged to radiate away from the selected camera position. As it is, the camera views the inside of a corner, with the targets radiating from the corner itself.

Data Sets 3 in the appendix show typical resection results. For a standard, non-levelled resection, the error estimate in position is around 0.5mm. The computation has treated observations as unit vectors, but a conventional photogrammetric treatment gives a similar answer. Further, the control data is treated as "perfect". These are derived from theodolite intersection, and the independent measurements shown in Data Sets 1 suggest that they are good to an accuracy of some 0.05 mm, or 10 times better. This error will not significantly affect the estimate of the resection accuracy. It was thought that more targets on the walls would help improve matters, but doubling the number had little effect. The only improvement came when additional targets were positioned in the triangular-shaped, "dead space", between the camera and corner. This was done for a camera calibration (data not presented here), which improved the estimate of positional error to about 0.2 mm.

Despite this potential source of improvement, the resection method for calibrating the 4-point target was not pursued. It is worth noting, however, that a low accuracy for the resected position of the projection centre does not necessarily imply that it is an ill-defined point. It may well be that the overall geometry of the situation is ill-conditioned.

The classic case of attempting a camera calibration by perpendicular viewing of a planar set of control points may underline the reason. No matter how well defined the projection centre, the geometry does not permit its accurate determination.

4.4 Computing the perspective centre from 4 target images.

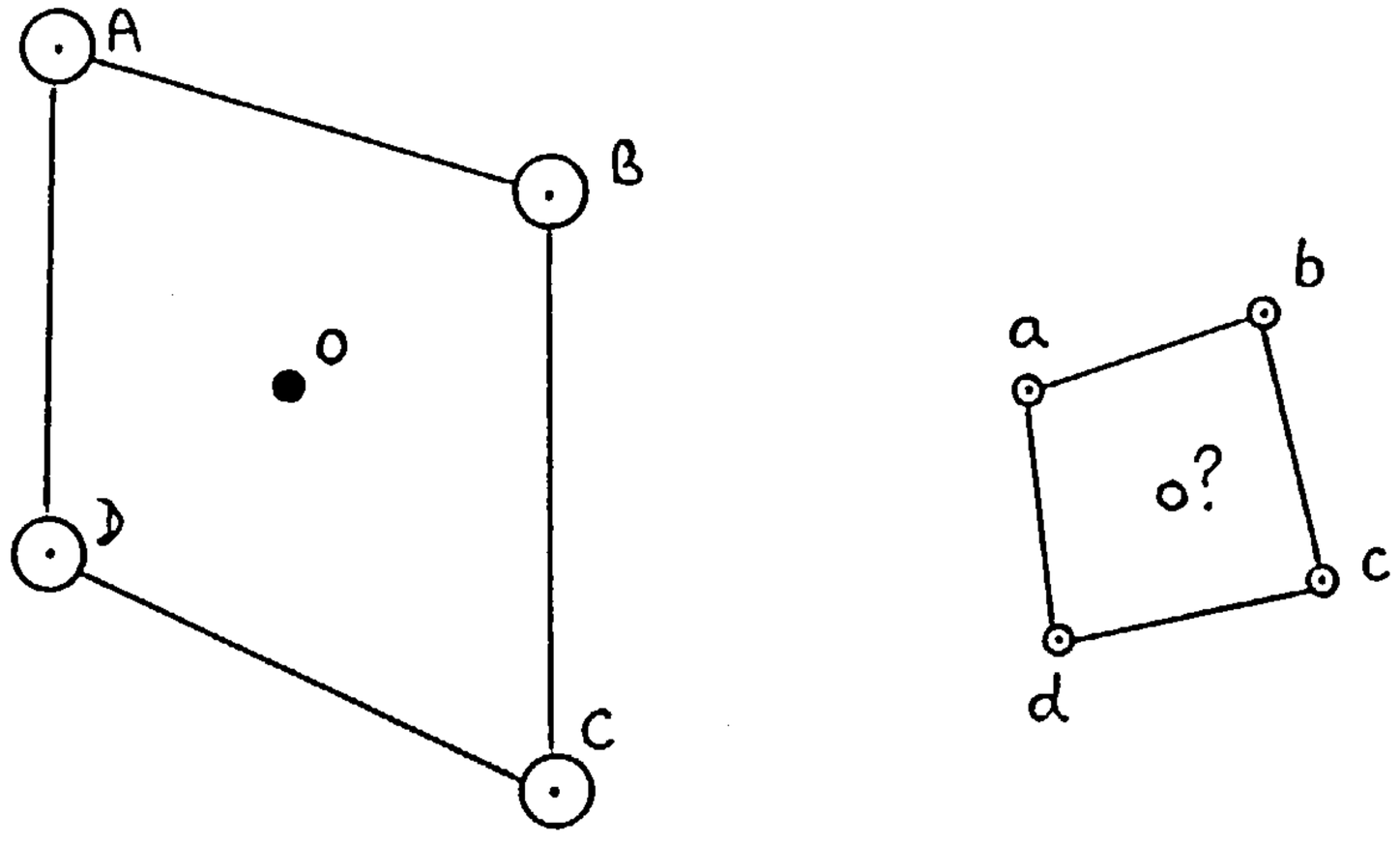

a) Target Frame b) Image

Figure 4.3 Viewing the 4-point target

After adjusting the 4-point target, the projection centre, O, is known with respect to A,B,C and D in object space. However, when sighted by a theodolite or photographed by a camera, only the images a,b,c and d are seen. The mathematical task is to determine the imaged position of the perspective centre, o, given only these 4 target images. The following analysis assumes that theodolite pointings are converted into pseudo photographs.

My solution uses two properties of perspective imaging and one reasonable assumption.

- straight lines image to straight lines.
- lines can be divided into parts whose ratios remain the same in object and image space (cross ratios).
- the projection centre, O, is somewhere in the middle of the frame.

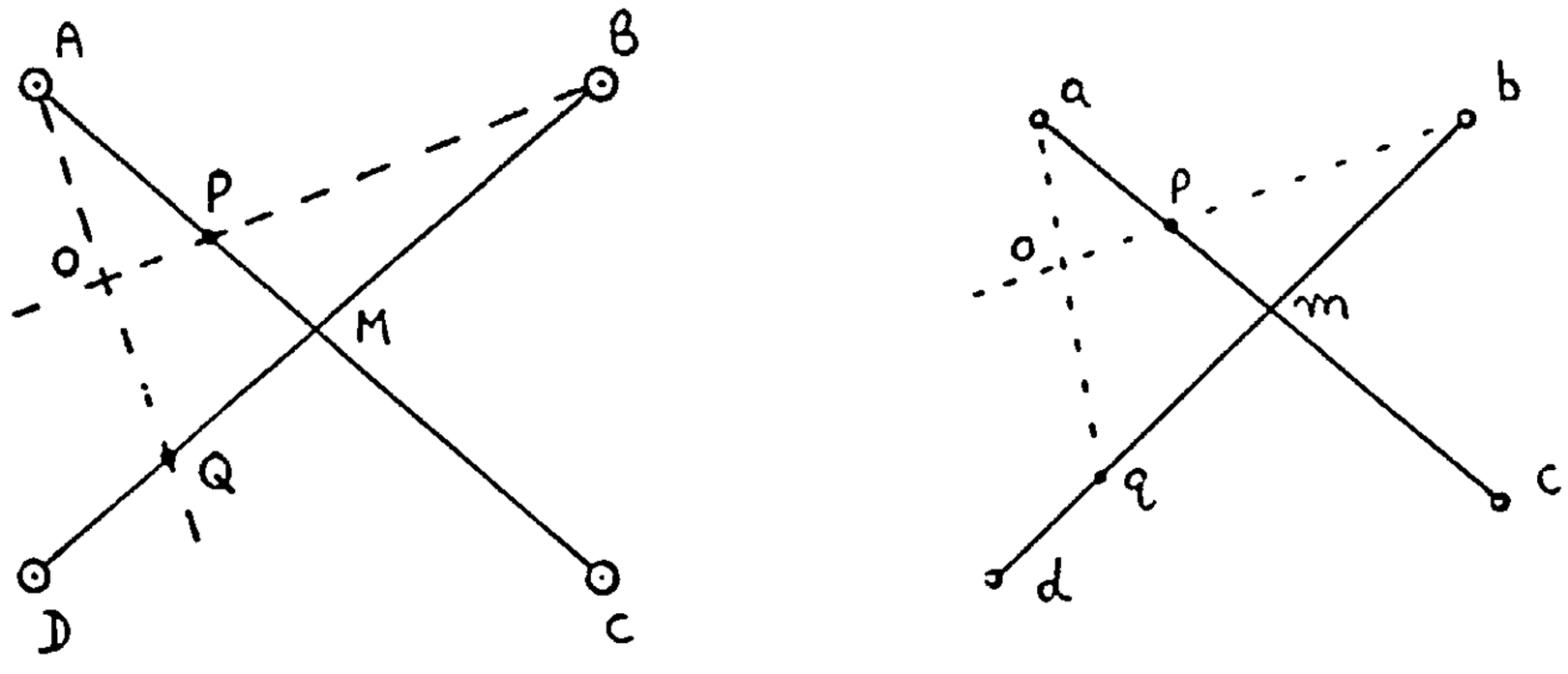

a) Object b) Image

Figure 4.4 Perspective centre defined by intersecting lines.

The essential step in the solution is to re-define O as the intersection of lines BP and AQ, where P lies on the line AC, and Q lies on the line BD. (For a reasonable intersection, O must lie near the middle of the frame). If the images, p of P and q of Q, can be computed in the image space, then o must lie at the intersection of bp and aq.

It is evident that the intersection, M, of diagonals BD and AC is immediately found as the intersection, m, of bd and ac in image space. Now consider the plane through the line APMB and the camera's perspective centre.

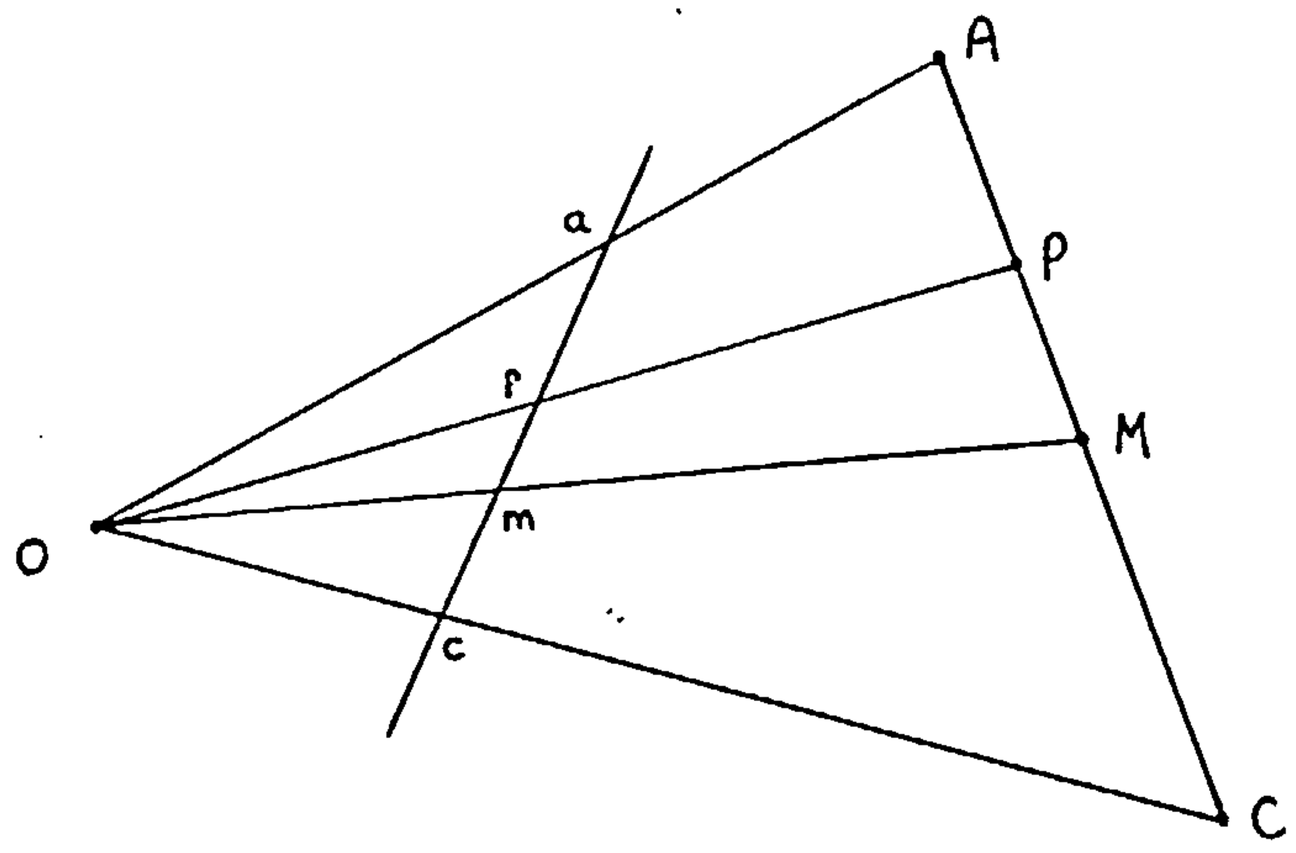

Figure 4.5 Cross ratios.

As fig. 4.5 shows, this plane also contains the images of A,P,M and C. Images a and c are directly recorded, m deduced from the intersection of diagonals as explained. The position of p is as yet unknown.

Applying the sine rule :

$$AP / \sin(AOP) = AO / \sin(APO)$$

and

$$AM / \sin(AOM) = AO / \sin(AMO)$$

hence

$$AP / AM = \sin(AMO)/\sin(APO) \cdot \sin(AOP)/\sin(AOM)$$

similarly

$$CM / CP = \sin(CPO)/\sin(CMO) \cdot \sin(COM)/\sin(COP)$$

Noting that

$$\sin(APO) = \sin(CPO)$$

$$\sin(AMO) = \sin(CMO)$$

we get

$$AP/AM \cdot CM/CP = \sin(AOP).\sin(COM) / \sin(AOM).\sin(COP)$$

Since this ratio of lengths only involves the angles subtended at O, it can be immediately stated that

$$AP/AM \cdot CM/CP = ap/am \cdot cm/cp$$

$$BQ/BM \cdot DM/DQ = bq/bm \cdot dm/dq$$

Re-writing the order, two known constants, J and K, can be defined.

$$J = (AP / CP) / (AM / CM)$$

$$= (ap / cp) / (am / cm)$$

$$K = (BQ / DQ) / (BM / DM)$$

$$= (bq / dq) / (bm / dm)$$

J and K are computed from the object space coordinates of A,B,C,D and O. The quantities (am/cm) and (bm/dm) can be derived in image space. Consequently, only (ap/cp) and (bq/dq) are unknown, and can be found from the relationships above. With these, it is possible to compute image coordinates for p and q, i.e.

$$xp = xa + \{ ap / (ap + cp) \} . \{ xc - xa \}$$

or

$$xp = xa + \{ (ap/cp) / (ap/cp + 1) \} . \{ xc - xa \}$$

Similar expressions are found for yp, xq and yq. The lines bp and aq can then be intersected to find o.

4.5 Theodolite targets.

The theodolite position must be photographed by the camera. It may be possible to use an interchangeable target, if this re-locates with an error smaller than the typical coordinate accuracy expected from the photography. This approach really requires interchangeable targets for the cameras as well, so that all theodolite pointings can be made using pre-targetted camera positions, and vice-versa.

It is more convenient if the theodolite, like the camera, can be combined with its own target. Since the rotation centre is mechanically well defined, two targets symmetrically located about the centre would suffice. Provided the theodolite is pointing roughly at the camera, the mean of the unit vector pointings to these targets gives the direction of the reciprocal vector.

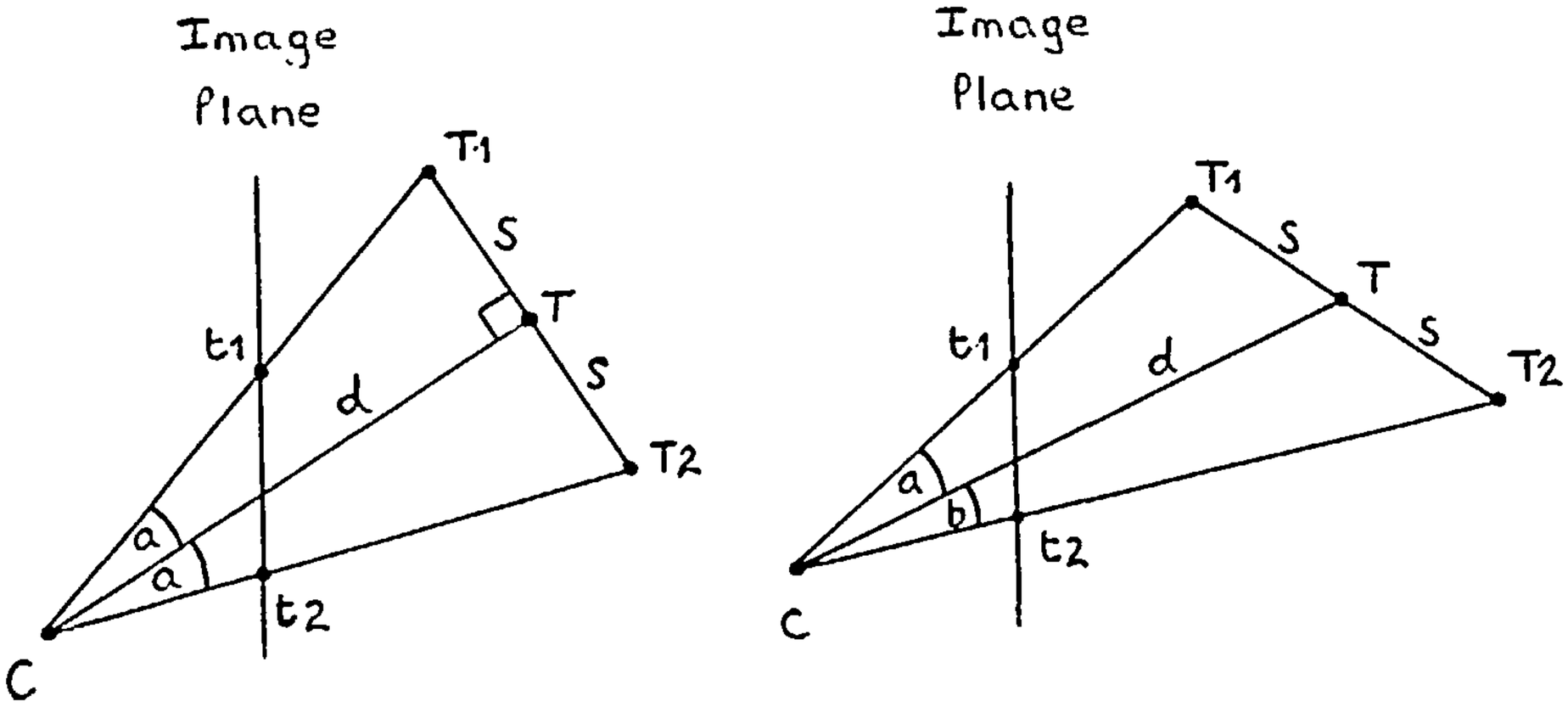

Figure 4.6 Imaging two offset theodolite targets

The analysis is very similar to that required for reciprocal pointing between theodolites, section 2.12. The current situation is shown in fig. 4.6 (a), where the targets form an isosceles triangle with the camera. The mean position of their images, t1 and t2, does not necessarily indicate the direction to the theodolite at T, hence the reason for using the direction of the meaned unit vectors to t1 and t2. Where the theodolite is not pointed at the camera, as in fig. 4.6 (b), the offset distances, s, subtend unequal angles a and b at the camera, and the mean vector is then also incorrect. Fortunately, where the offset distance, s, is small in comparison with the instrument separation, d, angles a and b are nearly equal. Furthermore, the separation of t1 and t2 will then be sufficiently small for their mean image position to represent the theodolite position to a good accuracy.

Another option, used in the tests below, is a target concentric with the telescope barrel. After sighting the 4-point camera target, and roughly pointing the telescope at the entrance pupil, a bulls-eye on a lens cap was slipped over the telescope objective. For a lens cap 5cm from the rotation centre, an instrument separation of 5m, and a mis-pointing equivalent to 5cm at the camera, the lens cap target is only 0.5mm off the reciprocal line.

This rather large pointing error would be a relatively small 6 microns in a P32 image (principal distance 65mm). It is assumed that for a correct reciprocal pointing, a lens cap concentric with the barrel has its centre on the line of sight.

4.6 Geometrical configurations.

Once it has been decided to include reciprocal observations in photogrammetric measurements, the options increase for the design of triangulation networks. To indicate the possibilities, a selection of simple arrangements will be presented.

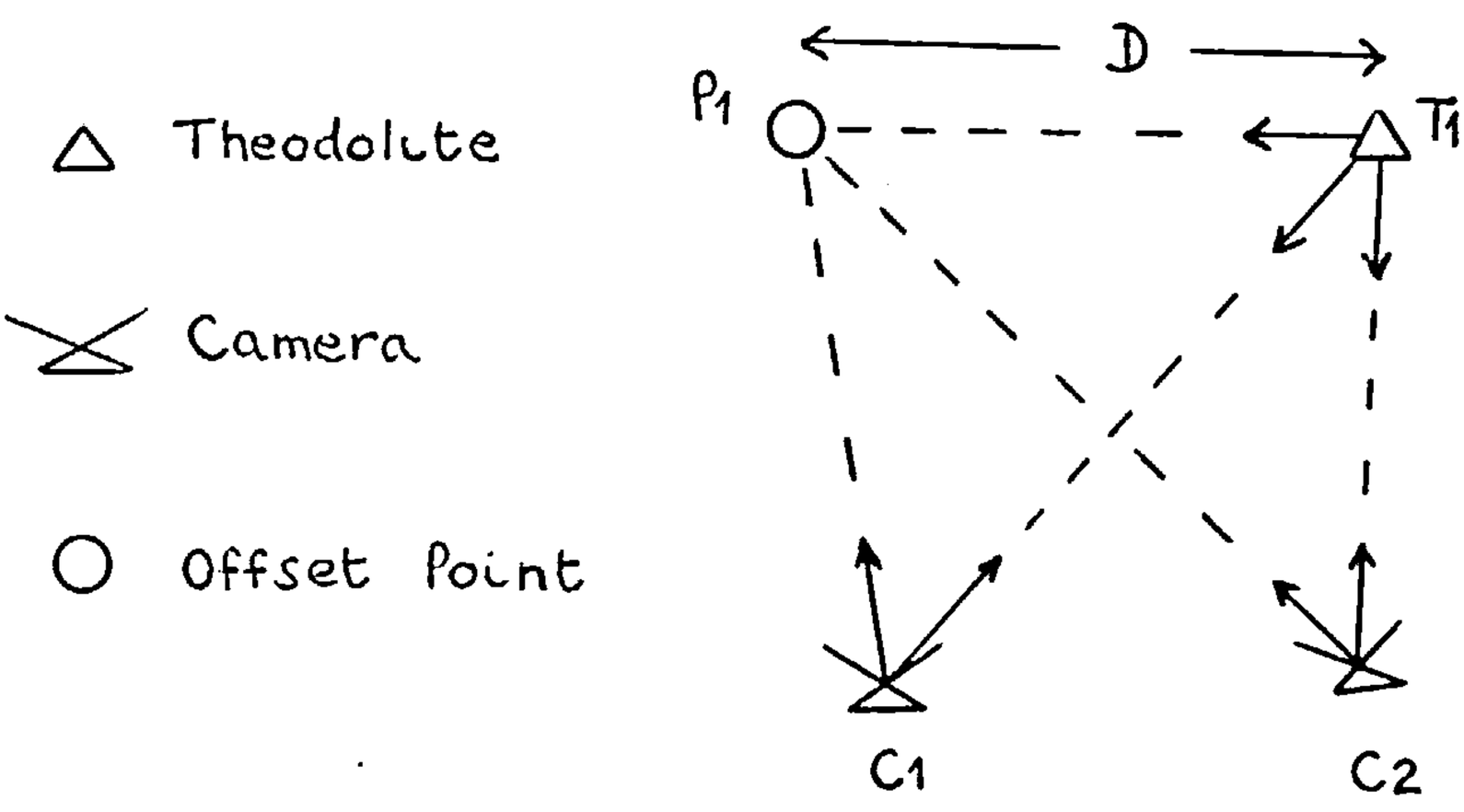

Figure 4.7 Minimum measurement.

Fig. 4.7 shows perhaps the easiest way of orienting two cameras. By locating a single theodolite and one offset targetted point within the overlap between the photographs, C1 and C2 can be relatively oriented in both positional and angular terms. If the distance, D, between T1 and P1 is measured, correct scale is introduced. Otherwise the model is at an assumed scale.

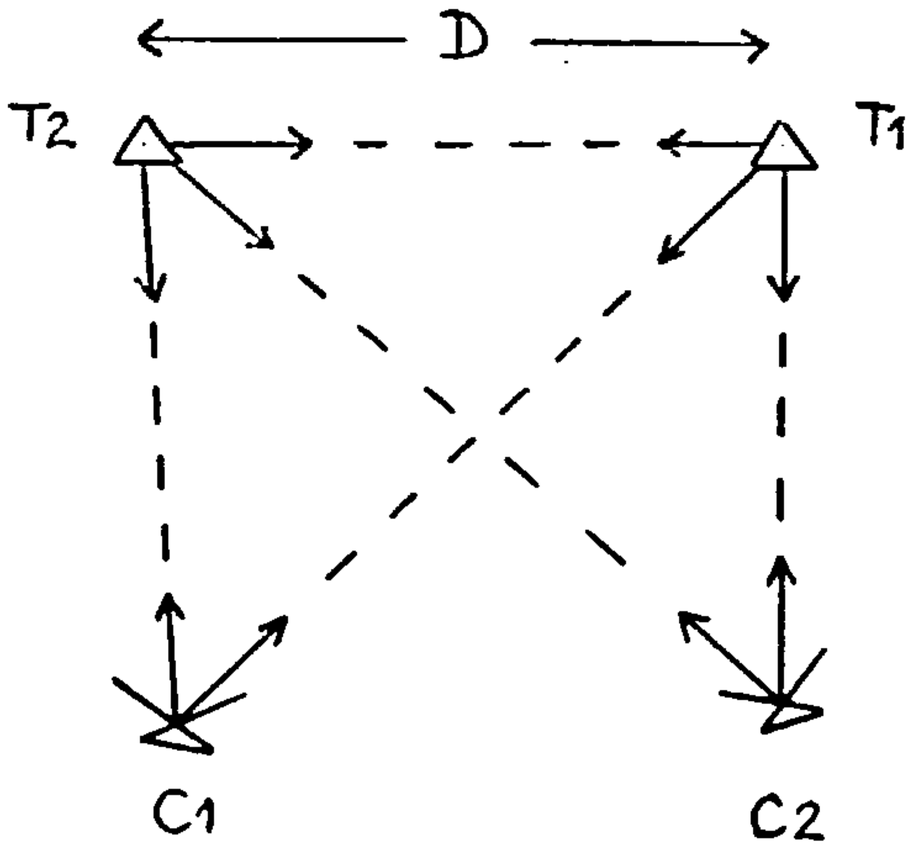

Figure 4.8 Fully observed, minimum solution.

Fig. 4.8 is simply an improvement on fig. 4.7, in which the offset point is replaced by a second theodolite. More observational effort is rewarded by greater redundancy.

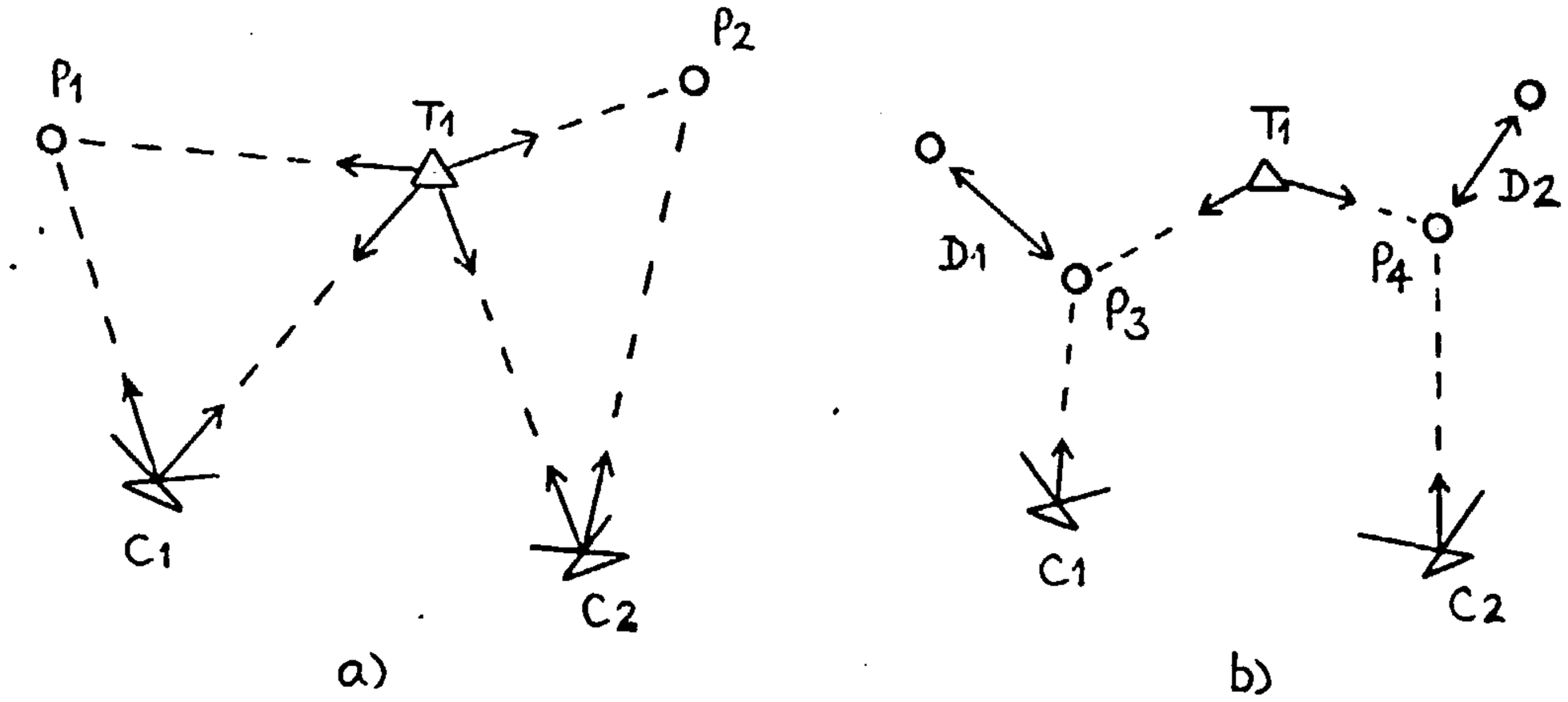

Figure 4.9 Potential scale error.

Fig. 4.9 shows a potential failure in the relative orientation between the cameras. For whatever reason, each uses a different offset point when orienting to the common theodolite. If distances T1->P1 and T1->P2 are not measured, then there is no common scale for the oriented pairs T1/C1 and T1/C2. For an arbitrary length T1->C1, T1->C2 will, in general, be incorrect. If distances cannot be measured directly from the theodolite, other solutions are available. For example, all three instruments could include a common offset point, as in fig. 4.7. Fig. 4.9 (b) shows another possibility. Two separate scaling lengths, defined with additional offset points, P3 and P4, are included between each camera and theodolite. This ensures the correct lengths for lines T1->C1 and T1->C2.

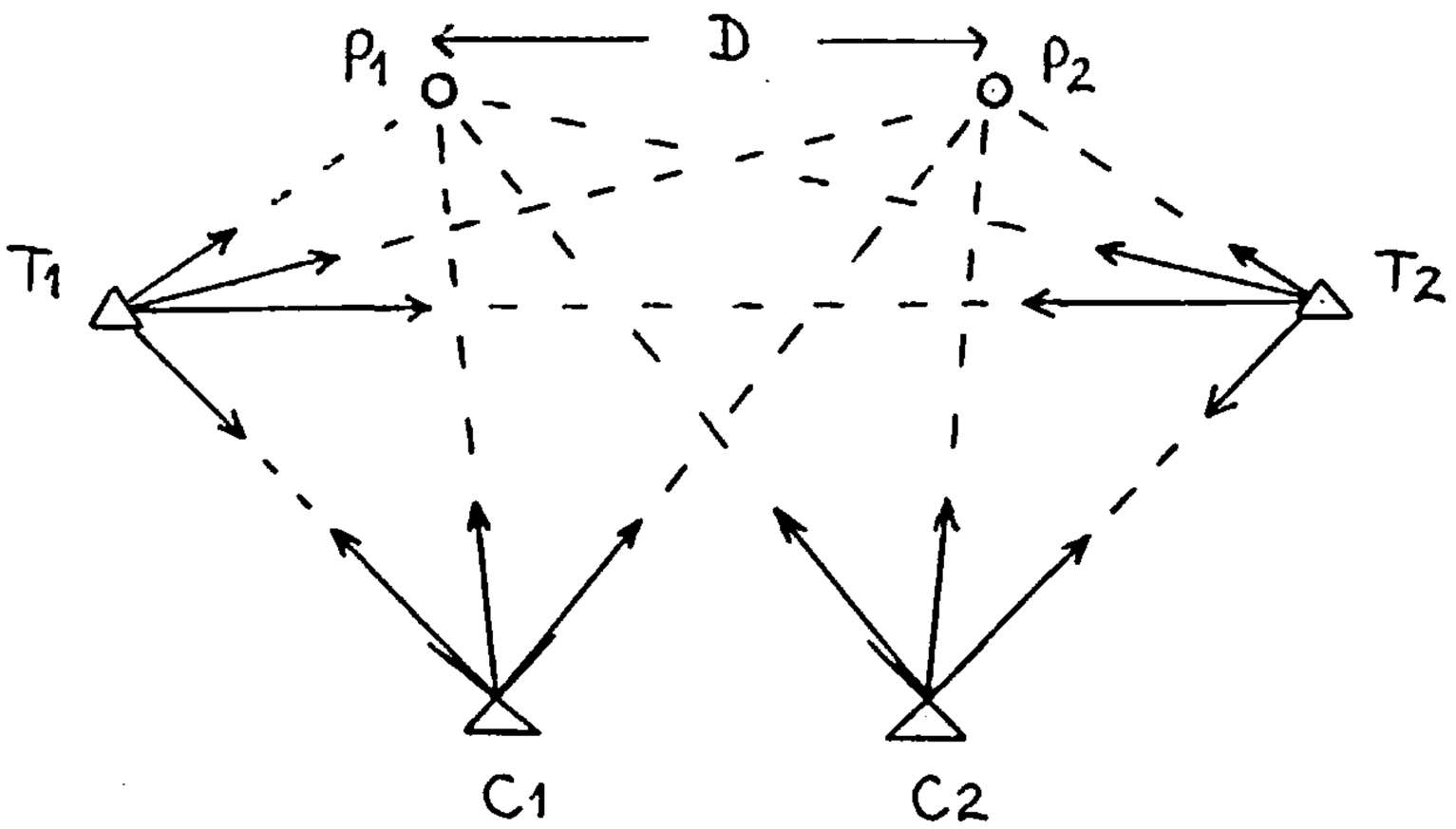

Figure 4.10 Improved geometry for stereo photographs.

In stereo photography, the overlap may only cover some 60 % of a photograph. This may limit the angle subtended at the camera by a theodolite and offset point. The smaller this is, the less the accuracy of relative orientation. Fig. 4.10 seeks to make best use of each camera's field of view. The offset targets represent the extent of the stereo overlap. T1 and T2 are outside the overlap, and can only be seen from C1 and C2 respectively. Nevertheless, a full orientation is possible, at either an assumed or known scale, depending on whether or not the separation between P1 and P2 is known.

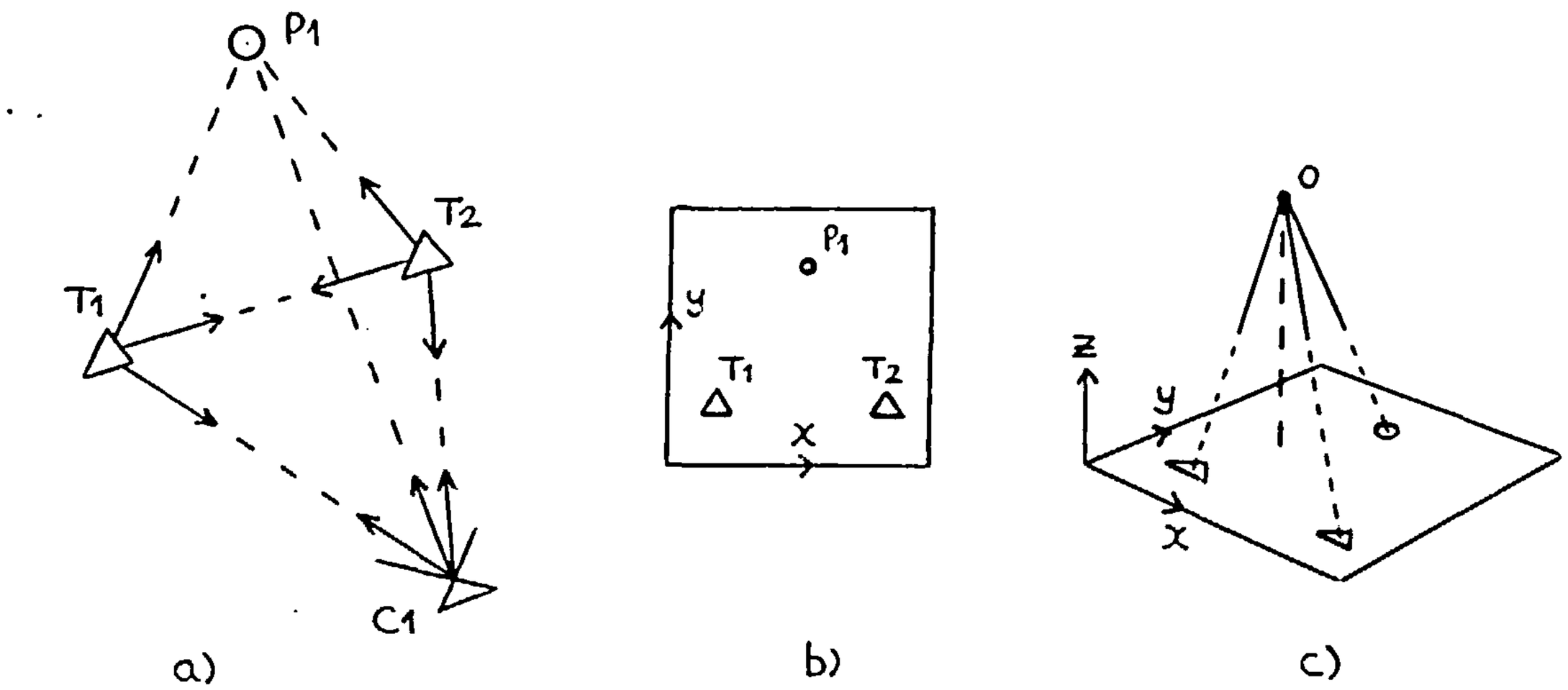

Figure 4.11 Camera calibration.

Another arrangement provides sufficient information to calibrate a metric camera for an unknown principal distance and principal point. These represent three unknown positional variables in the image space. Fig. 4.11 (a) shows how two theodolites intersect the camera perspective centre and a single offset point. The theodolites and offset point are arranged such that they define a triangle in the image, fig. 4.11 (b). Accepting that the projection centre is identified by a target on the lens, regardless of the uncertainty in the camera's internal geometry, then the space angles between the rays in object space are determined. These must equal the space angles in image space, and the task in fig. 4.11 (c) is to position the internal projection centre to achieve this condition. The solution is simply a space resection, and resembles a 3-D version of Burnside's field calibration [A1].

The above outlines hardly represent an exhaustive list of possibilities, but may serve to encourage more constructive ideas. Of course, theory should be supported by practice. To demonstrate the principal of employing reciprocal observations, two tests were carried out. Both attempted to orient two cameras with a common theodolite and common offset point. The arrangement is the first one discussed in this section. As a check, further common points were included in each case.

4.7 Dual camera intersection of a test field.

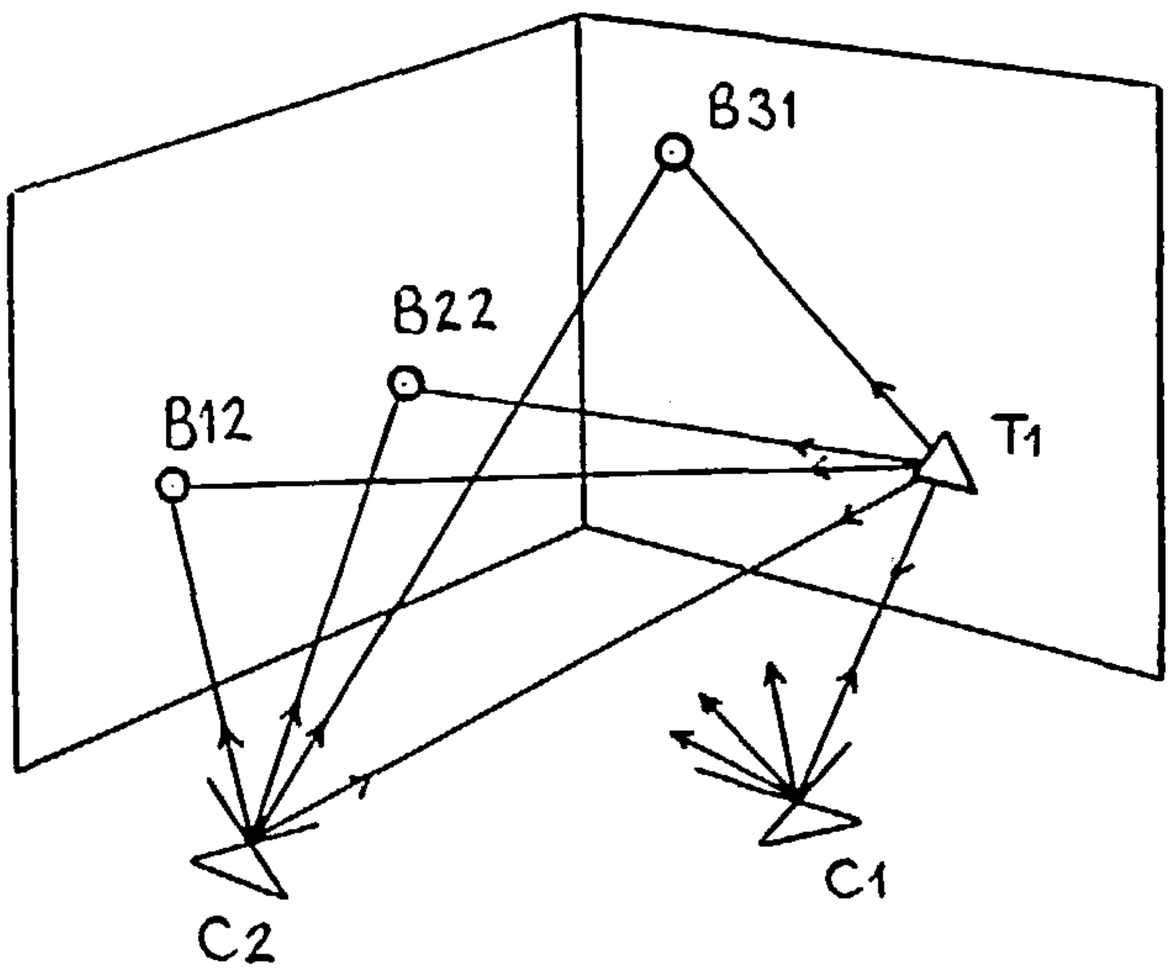

Figure 4.12 Intersection of test field.

The basement control field mentioned earlier was photographed from two positions. At each position, reciprocal observations were established to a common theodolite. The theodolite intersected three of the control points to provide the necessary orientation information. Scale was not independently measured.

The analysis oriented camera C1 to theodolite T1 with the aid of the reciprocal observation. Their separation was assigned a value of unity. This gave values to the separations T1->B12, T1->B22, and T1->B31. Using the reciprocal observation, C2 was then oriented to T1, taking the longest of the theodolillte/target separations as a scaling length.

With these computed orientation elements, all the common observations between C1 and C2 were intersected. The orientation parameters were not further optimized for the intersection, and the resulting rms angular residual had a value of 8.5 arc secs. Coordinates obtained in this way were transformed onto existing values derived from a dual theodolite intersection and the differences taken as a test of quality. The best-fitting transformation involved 7 parameters to allow for a shift, rotation and scale change.

This was a true close range test, with instrument separations of the order of 4 metres. The measurements are presented in the appendix, Data Sets 7 (intersection residuals not given). From the 7 parameter transformation, an rms lack of fit of approximately 0.35 *mm* is indicated. This can be compared with another measurement of the same set of targets. Again two photographs were used in a test designed to derive orientation elements with the aid of scaling distances (see Ch. 6). The final optimized orientation is a conventional one, which does not involve reciprocal observations and treats all target points as unknown. A best fit to the same control gives an almost identical result. See Data Sets 5.

I consider this accuracy to be consistent with that which can be expected from a P32, and consistent with a successful identification of the projection centre to better than 0.1 mm.

4.8 Portico test.

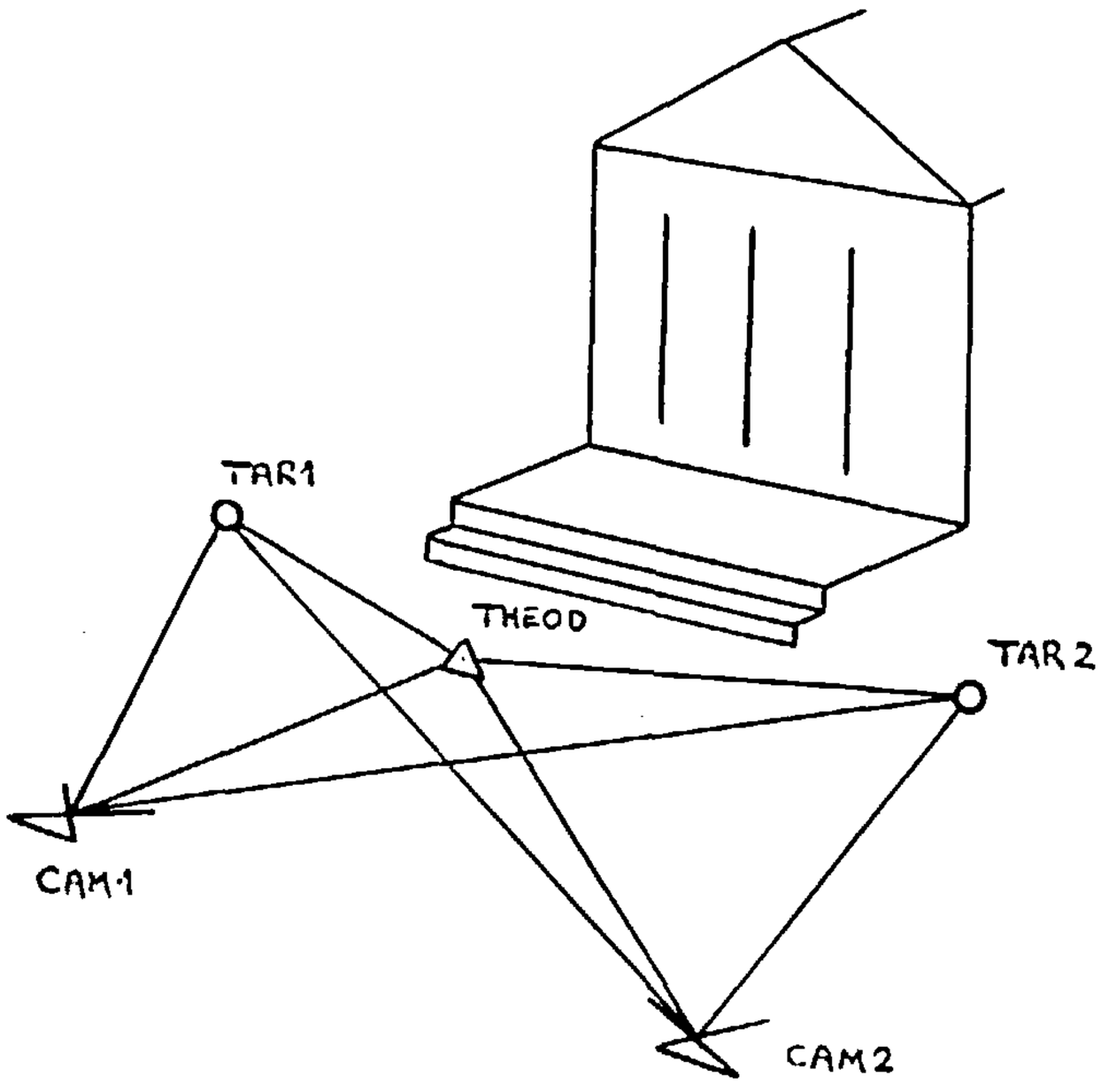

Figure 4.13. Portico test.

An analogous test was carried out on a much larger object. This was the Portico in the main court at UCL. It is regularly used for tests, and control coordinates are available for a number of points of detail on the facade. These are not targetted points, and their coordinates are expected to have an accuracy of a centimetre or two.

The test employed only two offset targets, visible from both camera stations. They were well-defined, standard Wild targets which locate in Wild tribrachs. The theodolite was positioned fairly close to each camera station, in order to ensure good imaging of the bulls-eye target attached to its lens cap. Unfortunately, this resulted in a poor intersection at TAR1 from THEOD and CAM2, and of TAR2 from THEOD and CAM1. The value was 14 degs. in both cases.

The orientation pattern follows the one outlined for the previous test, with scale for the THEOD/CAM2 combination being taken from the line THEOD -> TAR1. For this reason the intersection angle at TAR1 from THEOD and CAM2 should have been larger, as TAR1 is not so well defined by this pair. However, a successful result was obtained, and the main data are presented in the appendix, Data Sets 8. Although the angular residuals of the intersection had an rms value of 25 arc secs., the coordinates still fitted to the 9 control points with an rms lack of fit of about 1 cm. (The angular residuals are not presented. The rms value is based on the rejection of one point with a large residual of 71 arc secs.)

As a comparison, the photographs were re-measured independently, without making use of the reciprocal observation data. A standard orientation program on the Kern DSR 11 analytical plotter gave residuals of fit to control of 1.8 cm in plan and 1.5 cm in height.

Orientation based on reciprocal measurements therefore appears once again to give results as good as those obtained from a conventional technique. The poor quality of the intersection residuals should, perhaps, be put in perspective. At a principal distance of 65 mm (Wild P32), an angular error of 25 arc secs. is approximately equivalent to an image coordinate error of 8 microns. For untargetted points this is an entirely respectable result. Furthermore, it could be further optimized with a full adjustment involving all theodolite and camera measurements.

4.9 Potential advantages of the method.

The introduction of reciprocal observations can be seen as a way of controlling the relative orientation of two photographs. Depending on the geometrical configuration it may be very economical in terms of the additional effort required, and I suggest below two potential applications where the technique may offer a very good solution.

The method can also be interpreted as a convenient means of transferring information about orientation and level from a theodolite to a camera. This makes sensible use of the special features offered by a theodolite, such as the facility to determine accurately the direction of the vertical, pick up information from all directions or establish a precise position. As in the examples above, the camera then fills in the detail.

There is another way of transferring information from a theodolite to a camera, by adopting a photo-theodolite combination. The P32 is designed to function together with a Wild T2 in this way. It attaches to the theodolite's telescope, and can be adjusted so that the camera axis is parallel to the telescope axis and the x axis of photo-coordinates is horizontal when the theodolite is level. I have carried out this adjustment according to the instructions in the handbook, and found it a very tedious and awkward procedure. Once adjusted it is assumed that the orientation of the camera is mechanically linked to that of the theodolite. When the latter is found, the former is known.

It is unreasonable to expect that this adjustment can be made to a high accuracy, nor can it be assumed that the relationship is maintained when re-locating the camera back onto the telescope. (It really would be tedious to make the adjustment for every measurement). Admittedly, a 4-point target must be calibrated if reciprocal observations are to be used, but this was very easily done with the Metrograph. Furthermore, there appears to be no real need to re-calibrate the 4-point target after it has been dismantled and then returned to the camera. The same settings still apply.

If the method is accepted as offering potentially higher accuracy than a photo-theodolite, there are two particular problems where it might be fruitfully applied.

Long thin objects, which only occupy a small proportion of a camera's field of view, do not offer an ideal distribution of points for a good conventional relative orientation. An obvious example is a bridge or an aircraft fuselage, and some of the difficulties which arise are discussed by Erlandson and Veress [G3]. If dynamic considerations do not complicate matters, the simple form of control sketched out in fig. 4.7 may offer the solution. Here the theodolite and offset point themselves only occupy a narrow band on the photograph, and could be positioned directly on the bridge or next to the aircraft.

Another application could be the measurement of process plant, already well established [Q1,Q2]. Sample photographs presented in [Q2] would suggest it is not particularly easy to distribute sufficient control points to tie together stereo models or resect camera positions. I would also imagine that individual pairs do not generally have well distributed orientation points. Since a theodolite traverse or triangulation will inevitably form part of the job, the task might be much more efficiently performed if survey and photogrammetric observations were fully integrated.

I offer one final thought in this section. Reciprocal observations lead to a more flexible construction of triangulation networks. It is often the case that optimum intersection geometry requires strongly convergent camera views. Both features improve the strength of a network but may make it impossible for neighbouring photographs to be viewed as stereo pairs. These require camera axes to be approximately parallel. I suggest that current technology may enable an engineer to design a network for optimum strength whilst still obtaining stereo coverage. With electronic image processing it is no longer difficult to digitize an image and transform it from one plane to another. Sharply convergent images which cannot be viewed stereoscopically can be re-projected onto parallel planes for comfortable viewing.

The idea goes little further than some established practices, such as the digital ortho- photos shown to me by colleagues at the University of Karlsruhe. Indeed, one of those colleagues was using the approach to simplify image correlation on existing stereo photography.

4.10 The method in perspective.

Establishing a reciprocal observation, or integrating survey and photogrammetric observations, are not such novel concepts, although other sources do not make the points presented here.

Hofmann-Wellenhof [E16] mentions an analysis of orientation by von Sanden, dated 1908, in which the latter uses the "Kernpunkt" to compute the relative orientation. It is defined as the position in one image at which the projection centre of the other would appear. This also represents the reciprocal pointing. Von Sanden did not work with an actual reciprocal pointing, but apparently managed to derive it by processing the observations to 8 common points. He chose this route as a direct means of determining the orientation elements.

A reciprocal pointing has been employed in the real application of tunnel calibration. The opportunity arose because the situation enabled cameras to point at one another. In this case the reciprocal pointing, or von Sanden's Kernpunk, can be physically measured. Ethrog and Schmutter [G1] discuss their method. Rather than attach a target around the lens, they chose an interchangeable camera/target combination. Also, they do not adopt a general analysis, but treat this very much as a special case. Their solution is to convert image coordinates to those which are obtained when the camera axes are superimposed, and claim results as good as conventional methods provide.

Reciprocal observations also involve the integration of survey and photogrammetric measurements. Many adjustment programs simultaneously process both types of observations, and the paper by Wester-Ebbinghaus [E7] is a good source of reference. His own Multi-image ORientation (MOR) program is comprehensive, and I have little doubt it could process observations of the type I have described. However, its very generality prevents it from illuminating the points made here. Also, the inclusion of a camera's projection centre in a combined network is still described in terms of a conventional photo-theodolite. No suggestion is made that it be explicitly targetted in order to enable the deliberate inclusion of reciprocal observations. Furthermore, the paper does not address the problem of generating trial parameter values to initiate the adjustment. Reciprocal observations offer one way of doing this. If need be, they can then be discarded, or given a low weight which amounts to much the same. Of course, Professor Wester-Ebbinghaus is aware of the need for the direct computation of trial parameter values, and he has informed me that this is under investigation at his institute.

The direct determination of orientation parameters brings me to my last point. My solution has been to make additional observations in order to establish the reciprocal pointing. Von Sanden found a way of determining this with the help of 8 common points. This avoids additional effort in observation and can be adopted in the normal photogrammetric case. Hofmann-Wellenhof sets himself the same problem, namely the direct derivation of orientation parameters in the normal case. One route he describes is to re-define the variables in order to obtain a set of linear equations for which direct solutions are available. This approach requires more than the minimum 5 points for a conventional relative orientation, and again the minimum is 8. (The Direct Linear Transformation [E15], works in a similar way, and another 8-point solution is presented by Longuet-Higgins in [E16]).

Hofmann-Wellenhof then proceeds to demonstrate how a direct solution can be derived with only 6 common points.

The existence of such solutions does not necessarily make redundant a technique based on reciprocal observations. There still remains the problem of failure cases and poorly conditioned situations which the method can resolve. It also succeeds in turning photogrammetry into surveying, which may make the use of photographs more palatable to surveyors.

Ch. 5 Photogrammetry with levelled cameras.

Now that reciprocal observations have been introduced into photogrammetry, the one remaining difference with surveying is the ability to level the instrument. Some metric cameras are equipped with bubbles to enable the camera axis to be set horizontal. This can involve a rather tedious adjustment procedure, which may not provide the most direct connection between the gravity vector and the camera axes.

This chapter will outline some other ways in which a camera may be levelled. These demonstrate principles, rather than practical application, although the plumb-line technique offers a reasonable method of checking how well a metric camera has been levelled by using its bubbles. There are also potential advantages in removing two of the camera's unknown rotational parameters. This side effect of levelling will be explored in the next chapter.

5.1 Including gravity information in a photograph.

Gravity information can be introduced indirectly into a photogrammetric procedure, for example by resecting the camera position using control points with horizontal and vertical coordinates. The components of the Z (vertical) axis along the camera axes can then be found. Also, the previous chapter has explained how a camera can be relatively oriented to a theodolite. If the theodolite is levelled, then the gravity information is effectively transferred to the camera. In yet another scheme, targetted points on a plumb-line can be used to impose a constraint in the object space. The constraint is that these points lie on a straight line parallel to the Z axis. Note that in all these methods, the solution still employs 6 unknown parameters at the camera.

A photo-theodolite, such as the P32/T2 combination, enables a camera to be directly levelled. Once adjusted, the camera's x and z (optical) axes are both horizontal when the theodolite has been levelled and set to a zero vertical angle. The camera's y axis is then vertical. Any subsequent tilt of the camera can is given by the vertical angle reading. The adjustment has established a mechanical link between theodolite and camera.

As there is no recommendation to make the adjustment every time the camera is mounted onto the theodolite, the assumption must be made that the relative orientation between the instruments is stable.

In the case of the P32 there is a further mechanical link between theodolite and camera. It is not the camera but the support ring which attaches to the theodolite, and the camera itself rotates within this ring.

Both these features are potential sources of error, and in my view it would be better to attach a bubble or level sensor directly to the camera body, in order to remove them. A calibration procedure, rather than an adjustment, would determine the relationship of the gravity vector to the camera axes when the bubbles were centred. Several possibilities can be envisaged which introduce gravity information directly into the image, and which can form the basis of a calibration.

For a camera at infinity focus, and tilted sufficiently to include a zenith or nadir point, an approach based on autocollimation could be used. A separate, vertically mounted collimator is needed [C2], which directs its light into the camera. If the zenith or nadir are not available but the horizon is in view, then two horizontally pointed collimators will achieve the same result.

The problem with collimated light is the requirement that the camera be focussed at infinity. This is not an option at the close ranges of interest here.

Autoreflection might be considered instead. Two plane mirrors, set vertically at the edges of the field of view, define horizontal reciprocal pointings.

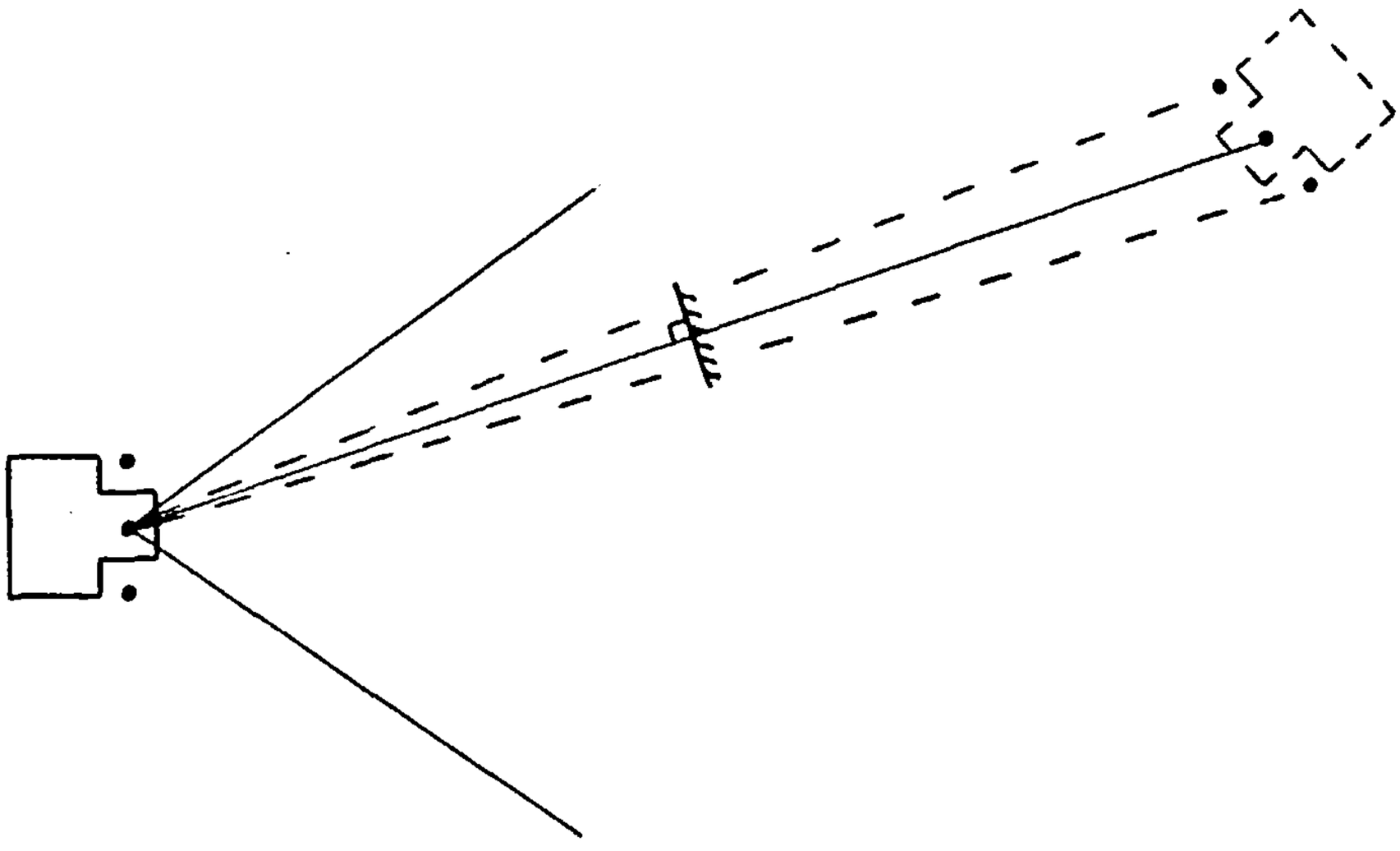

Figure 5.1 Horizontal pointing by autoreflection.

Fig. 5.1 shows the principle. The mirror must be at least half the minimum focus distance away from the camera, with linear dimensions at least half those of the camera target.

However, the simplest method is to image at least two plumb-lines in the field of view. Unlike the plumb-lines mentioned above, targets are not required. Instead, the line images give sufficient information to compute the direction of the gravity vector with respect to the camera axes. Clearly, the method only works when the view is roughly horizontal, but this is often the case in engineering applications.

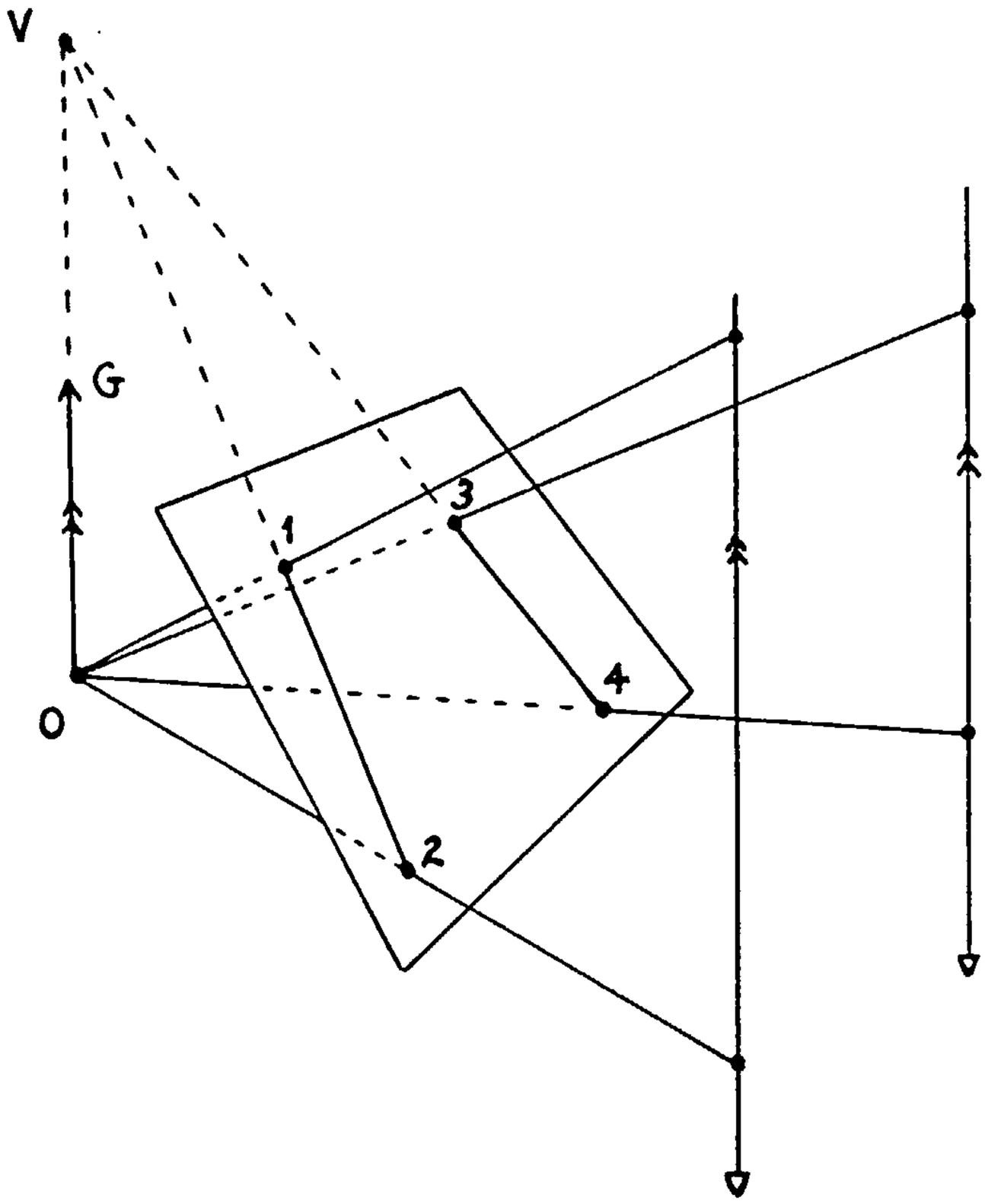

Figure 5.2 Plumb-line images

Fig. 5.2 shows a positive image of two plumb-lines, each identified by two arbitrarily selected points. Evidently, the plane formed by the perspective centre, O, and points 1 and 2, is vertical. The same applies to the plane of O, 3 and 4. Unit vector pointings, $\underline{U1}$, $\underline{U2}$, $\underline{U3}$, $\underline{U4}$ are derived for each target. From these, two horizontal vectors, $\underline{H1}$ and $\underline{H2}$, are obtained :

$$\underline{H1} = \underline{U1} \times \underline{U2}$$
$$\underline{H2} = \underline{U3} \times \underline{U4}$$

A correctly vertical vector, $\underline{V}$, then follows :

$$\underline{V} = \underline{H1} \times \underline{H2}$$

This may be converted into a unit gravity vector, $\underline{G}$:

$$\underline{G} = \underline{V} \; / \; \text{mod}\, \underline{V}$$

This vector is known with respect to the camera axes, which effectively levels the camera. If need be, observations can be converted into horizontal and vertical angles.

For a unit vector pointing, $\underline{U}$:

zenith angle, $z = \arccos (\underline{U} . \underline{V})$

vertical angle, $v = 90 - z$

A horizontal component, $\underline{H}$ is most simply computed from the vertical plane as :

$$\underline{H} = \underline{U} \times \underline{G}$$

This is actually at right angles to the true horizontal pointing. It is not important as horizontal angles are measured with respect to an arbitrary datum and all are affected in the same way. The datum is selected by choosing the longest horizontal vector, $\underline{Ho}$. All horizontal pointings are then converted into unit vectors, $\underline{H}'$:

$$\underline{H}' = \underline{H} / \text{mod } \underline{H}$$

Horizontal angles, h, are then given by :

$$h = \arccos (\underline{H}' . \underline{Ho}')$$

5.2 Accuracy of estimation using imaged plumb-lines.

The accuracy with which the gravity vector may be determined expresses how well the camera may be levelled. A simplified analysis can be made, in order to develop an appreciation of the principal variables.

If a camera points horizontally at a set of vertical lines, these appear as parallel lines in the photograph. Tilting the camera up or down causes all the lines to converge to a single vanishing point, v. The vanishing point is found by intersecting the image plane with the vertical planes defined by the plumb-lines and perspective centre. These lines of intersection are the plumb-line images. Since the vertical planes also intersect to create the gravity vector, $\underline{G}$, v lies on this vector also. An uncertainty in the direction of $\underline{G}$, corresponding to a levelling error, can therefore be interpreted as an uncertainty in the position of v.

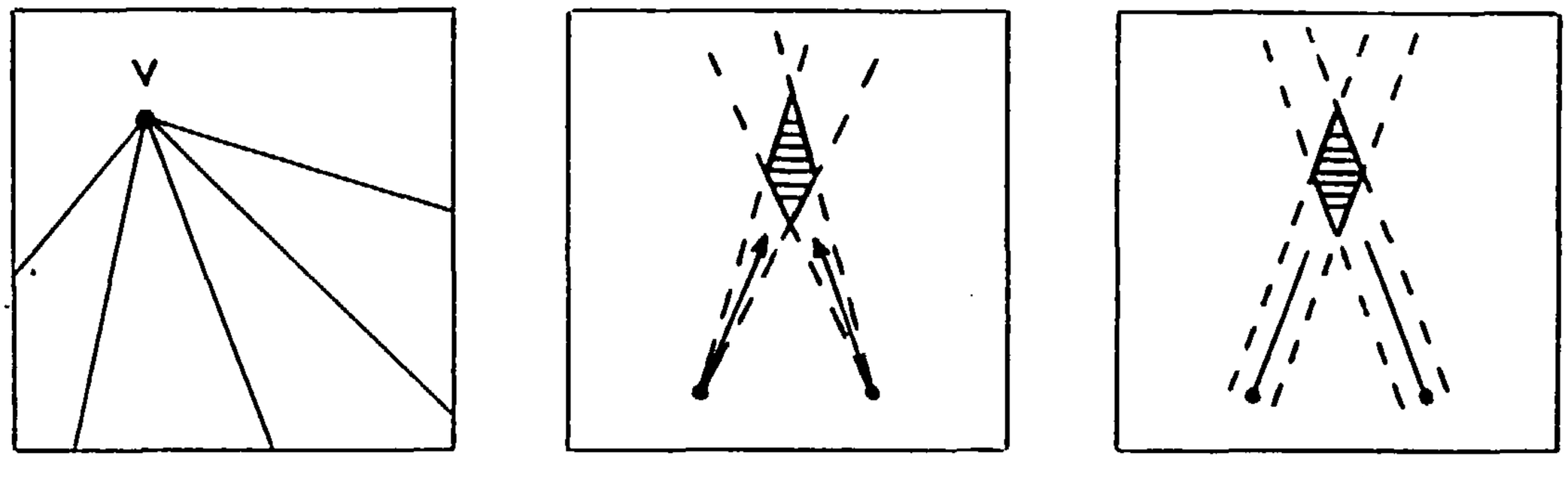

Figure 5.3 Intersecting plumb-line images.

Fig. 5.3(a) shows the situation in the image. Given any two plumb-lines, the position of v is affected by an error in the measured direction of the lines (fig. 5.3(b)), and a positional error in the lines themselves (fig. 5.3(c)). The simple analysis will concentrate on the separation of the lines, and their intersection angle. It will be immediately apparent that the directional accuracy will improve for longer lines. Also, the method of finding $\underline{G}$, by computing vectors normal to the vertical planes, suggests that the planes should subtend as wide an angle as possible.

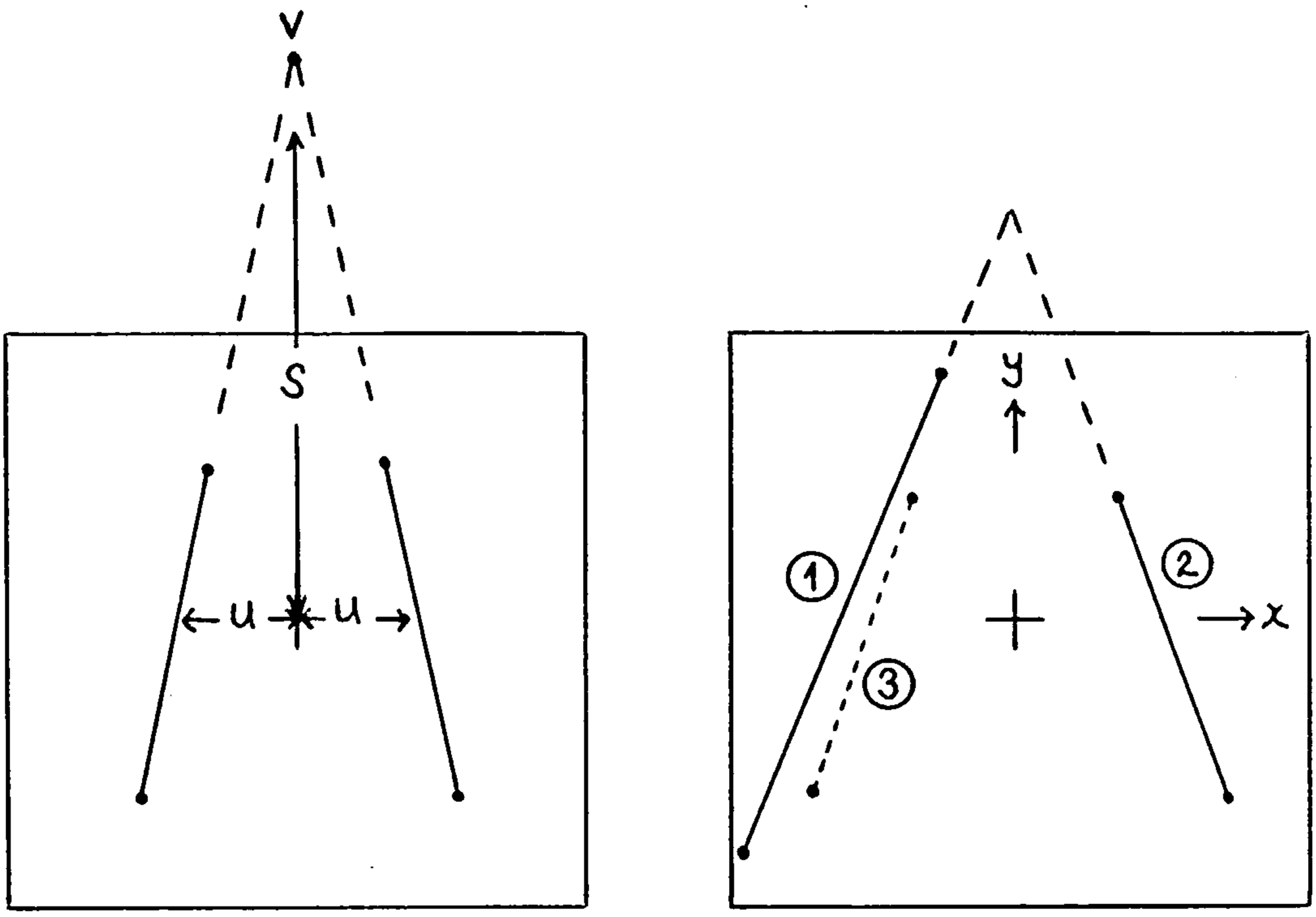

Figure 5.4 Symmetrical and asymmetrical cases.

As a further simplification, it will be assumed that the two plumb-lines are of the same length, and symmetrically disposed about the principal point. Fig. 5.4 (b) shows that this is not the general case in practice, but by selecting a symmetrical counterpart, line 3, to the short line 2 near the y axis, a "worst case" is created which should still provide a good guide.

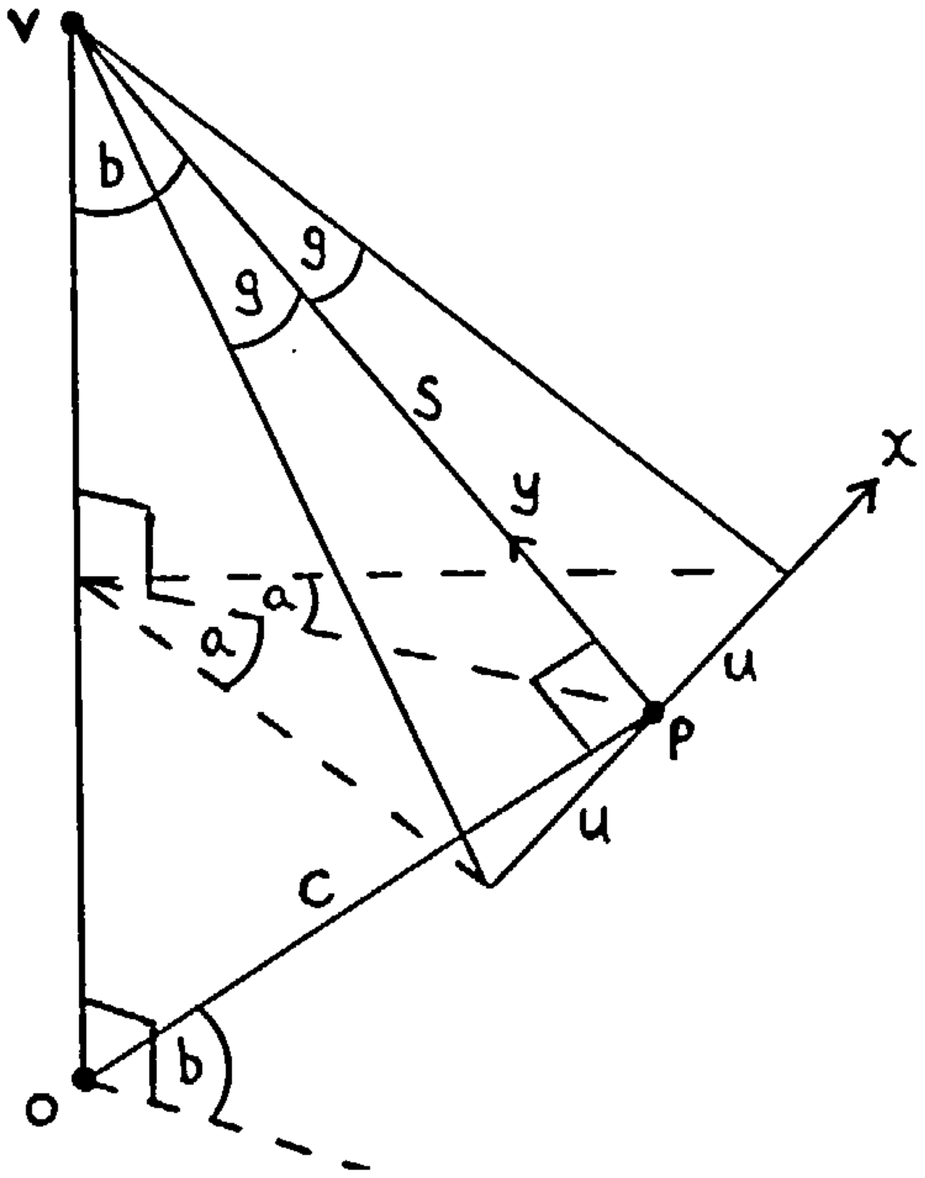

Figure 5.5 Intersection geometry

The intersection geometry is represented in 3-D in fig. 5.5. The tilt, b, of the camera axis, op, is also the angle between the gravity vector, ov, and the y axis. Given a camera principal distance, c, the following relationships are obtained.

$$\tan b = c / s$$

$$\tan g = u / s$$

or

$$\tan b = c \,.\, \tan g / u$$

for small b, and hence small g,

$$b = c \,.\, g / u$$

Also

$$\sec^2 b \,.\, db = (c/u) \,.\, \sec^2 g \,.\, dg - (c/u) \,.\, \tan g \,.\, (du/u)$$

or

$$db = (c/u) \,.\, (\cos^2 b / \cos^2 g) \,.\, dg - (c/u) \,.\, (\cos^2 b \,.\, \tan g) \,.\, (du/u)$$

for small b, g

$$db = (c/u) \,.\, dg - (c/u) \,.\, g \,.\, (du/u)$$

and for near horizontal pointings where g is very small, this further reduces to

$$db = (c/u) \,.\, dg$$

i.e. an error in u does not affect the determination of tilt. (v is then at infinity, and any error is parallel to the direction of the gravity vector, G).

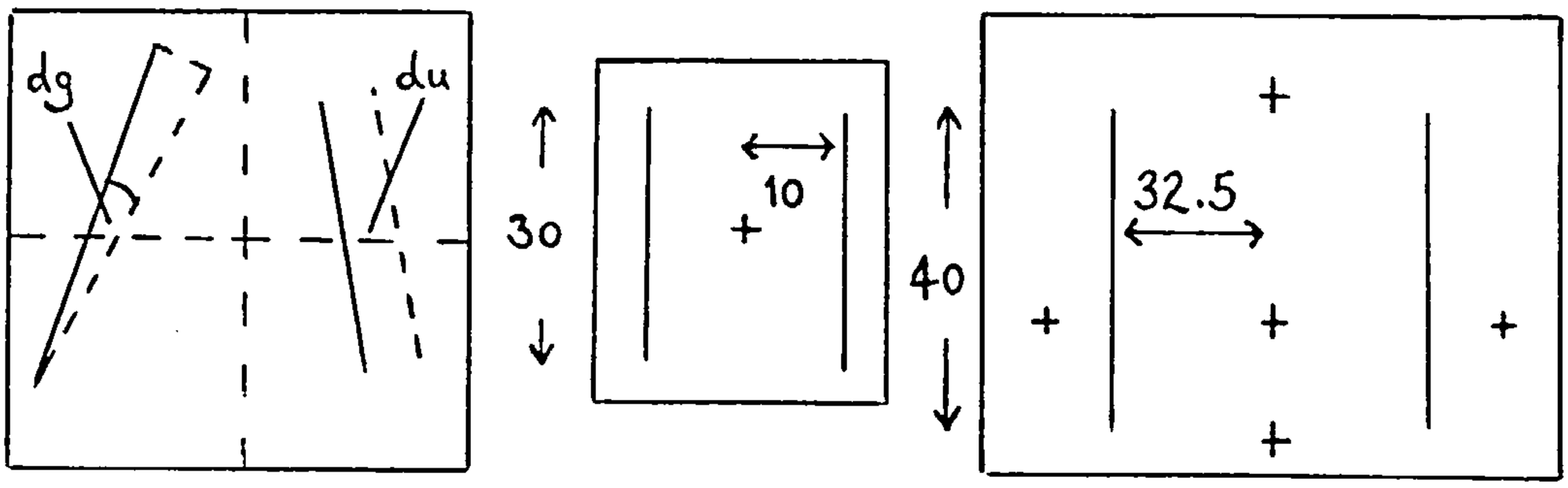

(a) Errors (b) 35mm camera (c) WILD P32, 65mm p.d. 50mm p.d.

Figure 5.6 Errors and camera formats

Fig. 5.6 shows the errors, and how two plumb-lines might image on both a 35 mm camera and a P32. Plumb-lines are shown towards the edge, and of reasonable length. The following table can be constructed, which gives the tilt error for errors dg and (du/u).

Angle of tilt b	35 mm camera (50 mm pd)	P32 (65 mm pd)
small	db = 5.0 . dg	db = 2.0 . dg
10 degs.	db = 4.9 . dg - 0.2 . (du/u)	db = 2.0 . dg - 0.2 . (du/u)
40 degs.	db = 3.0 . dg - 0.5 . (du/u)	db = 1.4 . dg - 0.5 . (du/u)

If du is an error of 2 microns, and dg is caused by an offset at one end of the plumb-line by 2 microns, typical errors are :

dg = 12 secs for small format
= 10 secs for larger format

(du/u) = 36 secs for small format

= 12 secs for larger format

For the P32, estimation of tilt should be good to about 20 arc secs. with minimum data. In practice, several plumb-lines, each defined by a number of points, would be expected to achieve a result good to a few arc secs.

5.3 Resection test for a levelled camera.

The validity of the method was checked with a simple test carried out in a basement at UCL. The results are presented in the appendix, Data Sets 3.

Control points were established in one corner of the basement by theodolite intersection in a levelled frame of reference. Two plumb-wires were suspended in front of the test field and a photograph taken.

A straight line was fitted through 8 points on each plumb-line image. Taken with the projection centre, each then defined a vertical plane, as described above. The components of the gravity vector along the camera axes were then computed.

Using the remaining images of 9 control points, a 3-D resection was performed. This gave the rotation matrix of the camera. It is explained in section 7.1 that the columns of the matrix can be interpreted as unit vectors along the camera's tilted x,y and z axes. Since gravity is the vector (0,0,1) in the reference system, its scalar product with each axial unit vector should again give the same components. Further, these components form the bottom row of the rotation matrix.

For convenience the resection was run twice, forcing a levelled resection in one case. This means that the pre-computed gravity vector was constrained to remain parallel to the system Z axis. The bottom row of the rotation matrix in this case therefore represents the components of the gravity vector as computed from the plumb-lines.

The angle between these two vectors, which should represent the same thing, is 27 arc secs. In a camera which can be roughly equated with a 10 sec. theodolite, this is a respectable result. However, the test is a limited one because the camera had to point roughly horizontally to image a good length of plumb-wire, and this is a condition which helps to minimize errors.

5.4 Calibration of bubbles.

If it proves an advantage to level a camera, then plumb-lines in the object space are unlikely to be very convenient. Finding points from which to suspend them, and keeping them steady, may be difficult in practical situations. Far better to have an accurate bubble on the camera which finds the vertical within a few arc seconds. Once set up with the help of the bubble, it is only necessary to determine where the gravity vector actually is. Photographing a set of plumb-lines should enable this to be done also to an accuracy of a few arc seconds. The simple test above gave a reasonable accuracy with only a small number of points on two wires. A number of well spaced plumb-lines covering the full image format, and digitized with 20 or 30 points each should be sufficient. Plumb-lines can also be used to calibrate a camera for lens distortion [B8], which offers an additional benefit.

Two objections can be raised about the use of bubbles as opposed to plumb-lines. Firstly, the bubble implies a stable camera position, as well as a stable object, whereas plumb-lines only require the object to be fixed.

Secondly, a bubble restricts the pointing, preventing the camera from looking up or down if this were more convenient.

Both points are valid. The stable camera position is perhaps not such a loss if the object is itself fixed. Regarding the other objection, it may be possible to permit camera tilt and measure this with a clinometer. The philosophy here is that a sufficient degree of flexibility is obtained if the camera is provided with a single axis about which it can rotate. In the direction parallel to this axis it should be kept level with a precision bubble.

Typically, the tilt axis would be the x axis, and this would enable the z or optical axis to be pointed up or down. The calibration must then be performed with this axis tilted twice, preferably in the extreme up and down positions. The other axis must be kept level. From the two computed directions of the gravity vector the axis of tilt can be derived. At intermediate positions the clinometer measurement provides sufficient information to interpolate the direction of gravity.

Clinometers with arc second precision are commercially available, for example from Rank Taylor Hobson.

If the extremes of the range of tilts require plumb-lines which are too long, the gravity information might be most easily introduced by reciprocal observation to a levelled camera, orienting on an offset point.

Ch. 6 Resection and routes to orientation.

This chapter suggests ways in which levelled instruments and optical distance ranging (or tacheometry) could enable the parameters of relative orientation to be directly computed. The methods deal with the case that reciprocal observations between instruments cannot be introduced. This may happen when only one instrument (theodolite or camera) is available. Alternatively, the measurement task may be dynamic, with a moving object or camera, and a reciprocal observation may not be possible. Lastly of course, it is intrinsically valuable to have other options available. One of the methods, based on ranging to two scale bars, has been identified as convenient and simple to implement. It has, therefore, been programmed into the TRIGFIX package.

Resection has been included in the title because the essence of the methods is to locate a single instrument with respect to an object, based on a knowledge of some control information. When a second instrument has been located in the same way, each is effectively oriented to the other.

A conventional resection offers this possibility. It is an established procedure in surveying to observe 3 existing control points with a levelled theodolite. This provides the data necessary to derive the horizontal and vertical position of the instrument. Position is computed firstly in the horizontal plane, then in the vertical direction. The method can be generalized into three dimensions. See, for example, Smith and Hunt [E11,E12], who provide direct solutions for position and angular orientation. Once again a minimum of 3 targets with existing coordinates is necessary. The solution provides up to 4 possibilities for instrument position in this case, and a 4th. control point will normally resolve the ambiguity. In passing it is worth mentioning that an improvement to both methods is outlined in section 7.4.

Another direct solution can be obtained from the Direct Linear Transformation (DLT), first proposed by Abdel-Aziz and Karara [E15]. The DLT was primarily designed to process non-metric camera data, and does this by re-arranging the unknowns in a photogrammetric solution in terms of 11 parameters which are inter-dependent. The method can also be applied to metric camera data, which can be considered a special case of non-metric data. There is also no reason why the solution should not be configured in terms of theodolite angles as well. To solve for the 11 unknowns, 6 existing control points are required which generate 12 equations (2 per pointing). In most cases a solution is possible.

All the above methods of resection require a number of targets with known coordinates. Such information could be provided by a dual theodolite intersection, which would involve a reciprocal pointing to avoid the very difficulty under discussion. Existing design coordinates of critical points on the object might also be used. This may seem an odd approach in cases where the task is to check the design, but the purpose need only be the automatic estimation of initial values. The design information may then be ignored in a subsequent optimum analysis.

The next sections consider other ways of creating and applying control information.

6.1 Resection on two coordinated points.

If horizontal and vertical coordinates are known for two targets, it is possible to compute the instrument orientation by measuring horizontal and vertical angles to each. The instrument has 4 unknowns, 3 of position and 1 of rotation, and each pointing generates 2 equations, or 4 in all. This suggests that a solution exists, and the method will be called a 2-point resection. It is applicable to cameras as well as theodolites, since it has been shown in Ch. 5 how they may also be calibrated to produce horizontal and vertical angles.

The technique can be interpreted geometrically, by considering the subtended horizontal angle and the two vertical angles.

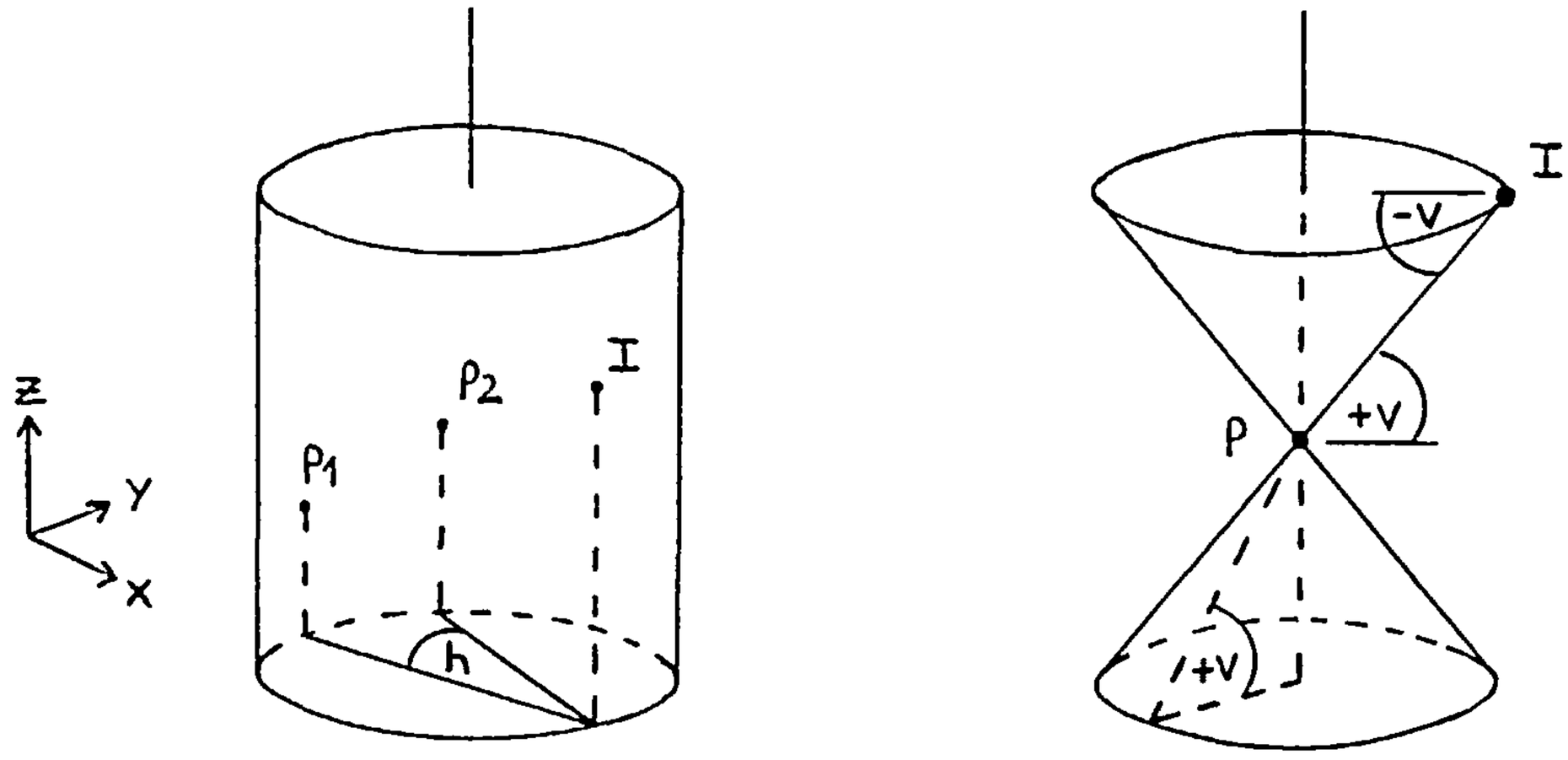

Figure 6.1 Resection surfaces in a 2-point resection.

In the horizontal XY plane, the subtended horizontal angle, h, locates the instrument, I, on a resection circle. Viewed in 3 dimensions, this positions the instrument on a cylindrical surface whose axis is vertical.

The vertical angle from the instrument to either target point, P1 or P2, can be reversed by changing the sign of the angle. This information is sufficient to place the instrument on a conical surface. The axis of the cone is vertical, with its apex at the target point.

The instrument therefore lies at the intersection of two cones and a cylinder. In general, there are 4 solutions for this intersection. Some of these may be immediately rejected, since one half of each conical surface is not relevant. This is the upper or lower half, depending on whether the observed vertical angle is respectively positive or negative. Before continuing, two failure cases should be noted.

If the observed vertical angle to one point is zero, the upper and lower cones reduce to a horizontal plane. This intersects with the cylinder to place the instrument on a horizontal circle. No problems arise provided the vertical angle to the second point is not also zero, i.e. provided both are not on the same level as the instrument. In this event, the second conical surface reduces to the same horizontal plane and no further information is obtained.

If both targets are vertically above one another, the subtended horizontal angle is zero and a cylindrical surface cannot be defined. The instrument then lies on the intersection of two cones with the same vertical axis, which is again a horizontal circle.

To avoid the failure cases, the subtended horizontal angle must be non-zero, and at least one of the vertical angles must also be non-zero. Given these conditions a simple analysis is possible.

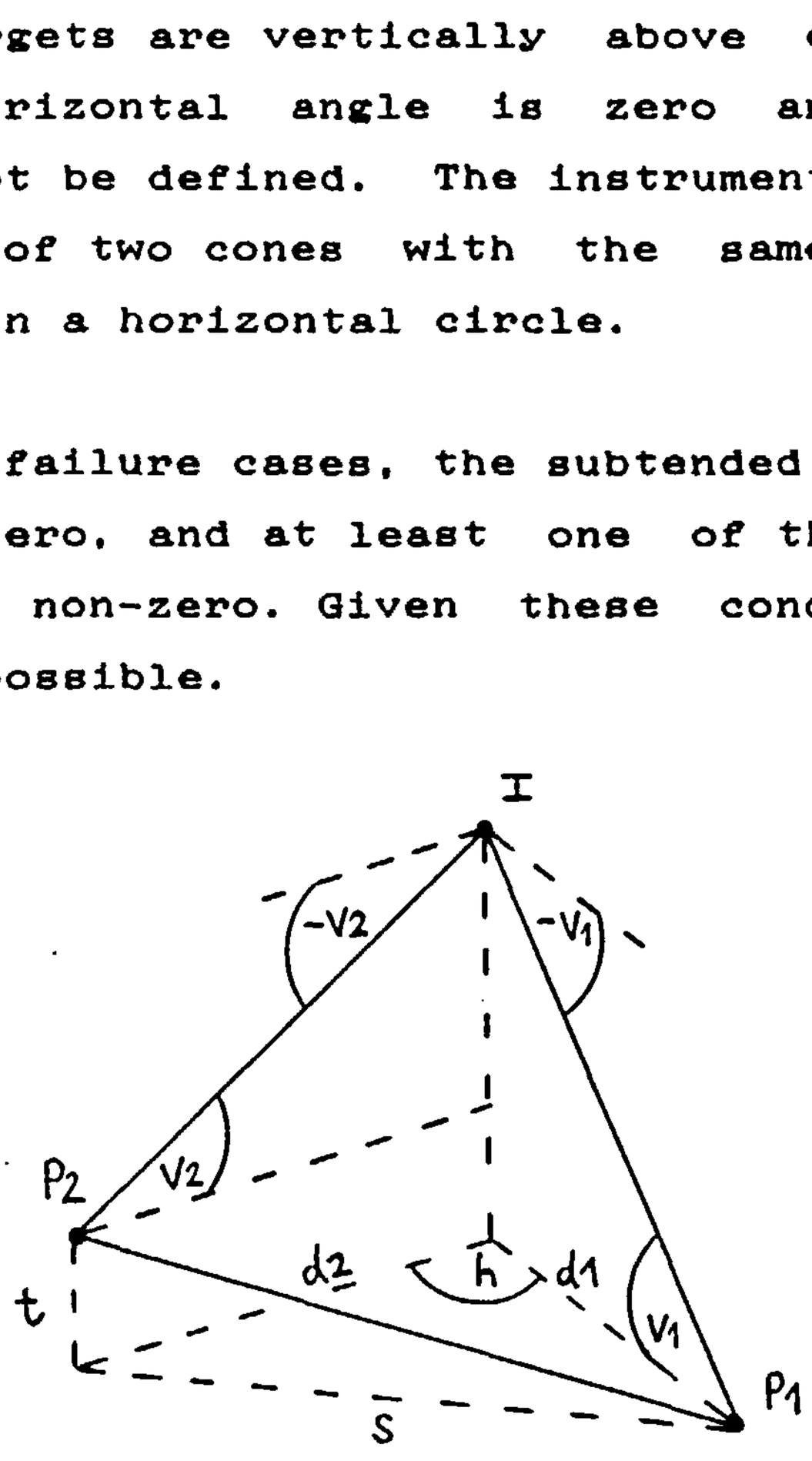

Figure 6.2 Analysis of a 2-point resection.

Fig. 6.2 shows the two target points, P1 and P2, separated by a horizontal distance, s, and vertical distance, t. The instrument is a horizontal distance d1 from P1 and d2 from P2. It measures a subtended horizontal angle, h, and angles of depression v1 and v2.

The relative height of I above P1 can be computed from either P1 or P2, i.e

$$d1 \cdot \tan(v1) = t + d2 \cdot \tan(v2) \qquad (i)$$

Assuming v1 > v2, divide through by tan (v1) to obtain,

$$d1 = t / \tan(v1) + d2 \cdot (\tan(v2) / \tan(v1)) \qquad (ii)$$

(The analysis continues in a similar way if v2 > v1).

Applying the cosine rule to the horizontal triangle in the diagram,

$$d1^{**}2 + d2^{**}2 - 2.d1.d2.\cos(h) - s^{**}2 = 0 \qquad (iii)$$

Substituting for d1 from (ii)

$$k1 \cdot d2^{**}2 + k2 \cdot d2 + k3 = 0 \qquad (iv)$$

where

$$k1 = 1 + \{\tan(v2)/\tan(v1)\}^{**}2 - 2.\cos(h).\{\tan(v2)/\tan(v1)\}$$
$$k2 = 2.t.(\{\tan(v2) / \tan(v1)^{**}2\} - \{\cos(h) / \tan(v1)\})$$
$$k3 = \{t/\tan(v1)\}^{**}2 - s^{**}2$$

Equation (iv) is a quadratic offering up to two solutions for d2. Substituting each into (ii) gives the corresponding value of d1. It is then a simple matter to derive the height of the instrument from (i). The other angles of the horizontal triangle can then be found, for example by application of the sine rule. There is then sufficient information to compute the angular orientation of the instrument from the bearing of the line P1 -> P2.

It would be quite easy to create the necessary control information with the aid of a scale bar which has been levelled or set up with a known tilt. The origin of co-ordinates can be placed at one of the end points, with the direction to the other defining, say, the XZ plane. The second point then has a Y value of zero, and its remaining X and Z coordinates are easily computed from the known length and tilt. Note that a bar with zero tilt must be positioned above or below the instrument to create the conical resection surfaces.

This is not in itself a very practical or useful procedure. There are potentially two solutions, and a third point is needed to resolve the ambiguity. This could be located on line with the end points of the scale bar, and at a known separation from either. It can then be assigned coordinates. However, with three control points now known in a levelled system, a standard plane resection can be computed. In fact, this method was described to me by Dr. R Clayton of the CEGB, who has used it to position a single theodolite when intersecting targets. Nevertheless, the mathematics might form the basis of a method of relative orientation when target coordinates are unknown, but the instruments are levelled.

6.2 Relative orientation with three target points.

Consider the case that two instruments are levelled and each measures horizontal and vertical angles to three common points.

For a relative orientation one instrument can define the axes of the reference system. The definition must be such that the measured gravity vector represents one of the axes, conveniently taken as the Z axis.

At the other instrument, 4 unknown parameters must be defined, 3 of position and 1 of rotation. For each target there are 3 unknowns, giving a total of 9. The sum of instrument and target unknowns is 13.

There are a total of 3 pointings from each instrument. Each pointing generates 2 equations, or a total of 12. If a distance is measured for scale, or one is assumed in order to create an arbitrary scale, a further equation is obtained. There are therefore as many equations as unknowns and a solution potentially exists. It will be called a 3-point relative orientation.

By inspection some failure cases can be identified, and deduced from the measured angles. Let the fixed instrument be I1, the moving instrument be I2 and the 3 common target points be P1,P2 and P3. The failure cases, in which corresponding rays still intersect, are :

a) P1,P2 and P3 all on the same vertical line. For a given scale, I2 may then take up any position on a horizontal circle which has this line passing through its centre. In each instrument horizontal pointings to all 3 targets are the same.

b) P1 and P2 on the same vertical line, P3, I1 and I2 on the same horizontal plane. Failure case as in (a). In each instrument horizontal angles to P1 and P2 are equal and the vertical angle to P3 is zero.

c) P2, P3, I1 and I2 on the same horizontal plane. For a given separation of P1 and I1, I2 may again take any position on a horizontal circle lying on this plane and centred on a vertical line through P1. Vertical angles to P2 and P3 are zero from both instruments.

d) P1,P2,P3,I1 and I2 all lie in the same horizontal plane. I2 may be placed anywhere on this plane. All vertical angles are zero.

This list is not intended to be exhaustive, but to demonstrate that the method may fail. Fortunately, in a real situation there should be rather more than three points available.

It may then be possible to chose the most suitable by examining the data and rejecting those which indicate a known failure case. Any remaining ambiguities should not cause serious difficulties as the relative orientation is intended to be a robust procedure. It is based on an automatic, "trial and error" search for suitable values which can initiate a conventional least squares solution. This optimum solution should be designed so that the gravity observations can be constrained to lie close to the Z axis. An excess of points over the minimum three will not only permit this constraint to be optional, but should enable the correct solution to be identified if several sets of initial conditions have been generated.

With this goal in mind, a solution for relative orientation can be developed.

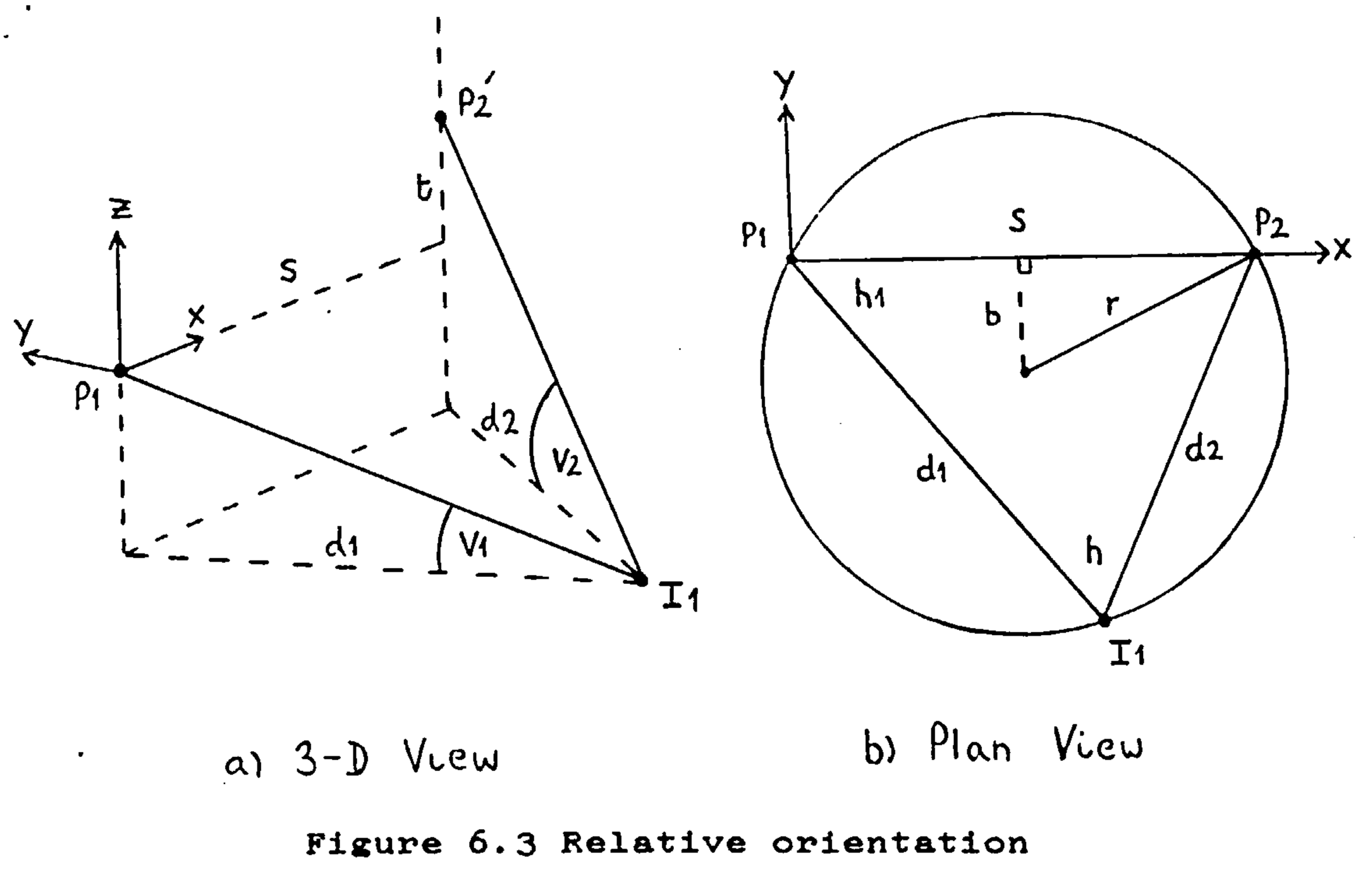

a) 3-D View

b) Plan View

Figure 6.3 Relative orientation

Fig. 6.3 shows two of the three points which have a horizontal separation. For a relative orientation scale is arbitrary, and the horizontal separation, s, may be given any convenient value such as unity. The origin of co-ordinates is located at target P1, and the direction to the second target, P2, defines the XZ plane. The height of P2 relative to P1 is currently unknown.

The diagram also shows one of the two instruments, and the associated angular measurements to P1 and P2. The parameters of the resection circle, shown in the plan view of fig. 6.3(b), are easily established and do not require a knowledge of the vertical position of P2.

Since the angle subtended at the centre is twice that subtended at the instrument,

radius of resection circle, $r = s / (2.\sin(h))$

offset of centre from chord P1 - P2, $b = r.\cos(h)$

In outline, the automatic "trial and error" method proceeds as follows :

a) I1 is stepped around the resection circle in equal increments.

b) In each position, horizontal distances d1 and d2 to P1 and P2 are computed. The angle, h1, is also computed. This effectively gives the bearing of line P1 -> I1 and hence the angular orientation of I1.

c) The height of P2 above P1 can be derived for the current position of I1 from the expression,

$$t = d2.\tan(v2) - d1.\tan(v1)$$

d) Instrument I2 can now be resected with respect to targets P1 and P2', where P2' is the current position of P2 as derived from step (c). The basis of the resection is the quadratic equation developed in section 6.1, taking due regard for any failure cases.

e) The intersection of the third target, P3, from the current positions of I1 and I2 is examined, and the minimum separation of the rays in the vertical direction recorded. This is most easily done by computing a horizontal intersection of P3 from a knowledge of the horizontal positions and bearings of I1 and I2. From the horizontal ranges I1 -> P3 and I2 -> P3, two values are found for the height of P3. Their difference is the required separation.

Ideally, potential solutions are signalled when the test parameter changes sign from one position of I1 to the next. Unfortunately, random variations in pointings and poor geometry may ensure that the solutions are not so well defined. In such cases, it may be possible to eliminate invalid solutions if rather more than three target points are available.

There has been insufficient time to investigate the 3-point relative orientation in detail, but it represents a novel use of gravity information as control. Here it is purely a property of the instrument, and control information on the object is not required. Of course, vertical angles of a sensible magnitude must exist. This excludes views which are essentially upward or downward, and requires the object to have some reasonable vertical extent. Clearly the only area of application can be close range. It is also obvious that the technique may not be applicable in dynamic situations. In order to be levelled, the instruments must be fixed. Movement of the object can then only be permitted if levelled cameras are used, one at each observing position, and simultaneously released. Otherwise the object will have a changing relationship with the direction of gravity during the measurement procedure, which invalidates the analysis.

6.3 Resection on two vertical scale bars.

Now that gravity information has been seen to be useful when applied at the instrument, its exclusive application at the object will be investigated.

Although relative orientation is a procedure which is independent of scale, and although scale is not an essential ingredient in every engineering measurement, in most cases scale information is present. Consider therefore two vertical scale bars in the object space, or two plumb-lines each supporting two targets with known separations.

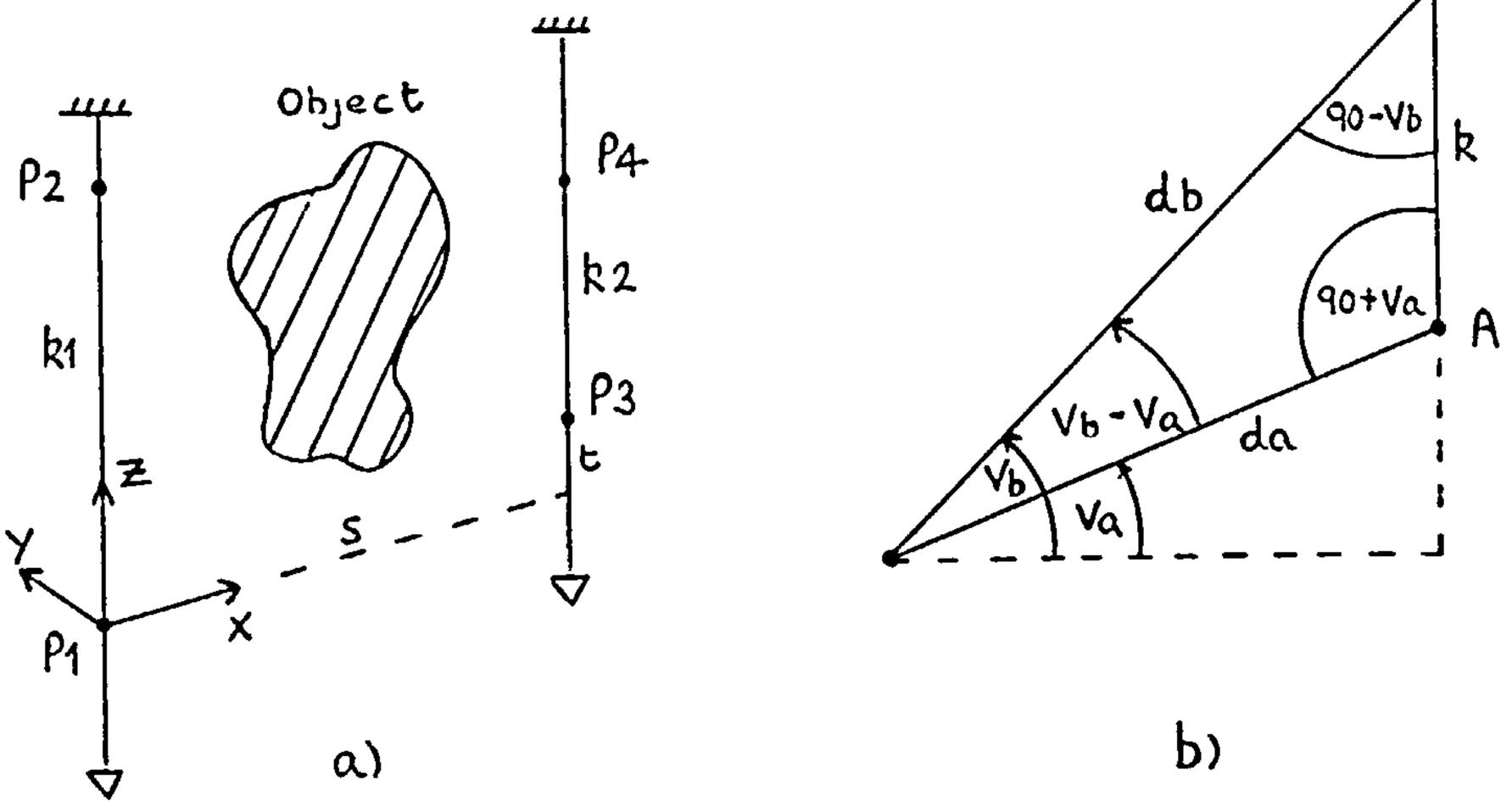

Figure 6.4 Observing vertical scales.

In fig. 6.4 (a), target P1 defines the origin of coordinates and the direction of the plumb-lines is parallel to the Z axis. Both plumb-lines define the XZ plane. There is an unknown separation, s, between the plumb-lines, and an unknown height, t, of target P3 above P1. In this situation it is evident that the 4 targets involve only 2 unknown coordinates, since P2 and P4 are shifted by known vertical amounts, k1 and k2 above P1 and P3 respectively.

A non-levelled theodolite or metric camera which observes these 4 points has 6 unknown parameters of position and angular orientation. There are 8 unknowns in total. However, each observation gives 2 equations, or 8 in all. Again a solution is expected. Following the previous pattern, this will be known as the 4-point resection (or relative orientation).

There should be no difficulty in configuring an optimum solution which fixes the coordinates of the 4 targets in such a way that 2 unknown parameters of position remain. Alternatively, the use of other constraints may achieve the same effect.

For example, the known separations P1 -> P2 and P3 -> P4 can generate 2 distance equations, and the verticality of each plumb-line provides 2 further constraints. Regardless of the optimum solution, trial parameters of orientation are readily found using an established surveying technique. This is vertical staff tacheometry.

Fig. 6.4 (b) shows vertical angles, va and vb, measured from instrument, I, to two targets A and B, on a plumb-line and separated by a distance, k. From the sine rule,

$$k / \sin(va - vb) = da / \cos(vb) = db / \cos(va)$$

hence

$$da = (k . \cos(vb)) / \sin(va - vb)$$
$$db = (k . \cos(va)) / \sin(va - vb)$$

If the vertical angle from an instrument to each target is known, the distance to each target can easily be computed. Knowing the distance and the observed unit vector, it is a simple matter to locate each target in the local system of the instrument. Although this positions the targets with respect to the instrument, the effect is the same as that produced by a resection, which positions an instrument with respect to the targets. Two issues must now be addressed.

Firstly, the derivation of the vertical angles. There has been no requirement that an observing instrument be levelled. However, as Ch. 5 has shown, the direction of the vertical at an instrument can be deduced from observations to two plumb-lines, which is the current situation. Consequently, pointings can be converted into horizontal and vertical angles and the above procedure applied.

Secondly, the computation of relative orientation between two instruments. It has been stated that once each is positioned with respect to an object, their own relative positions can be determined. So far, this has not been shown, but one method will be briefly outlined.

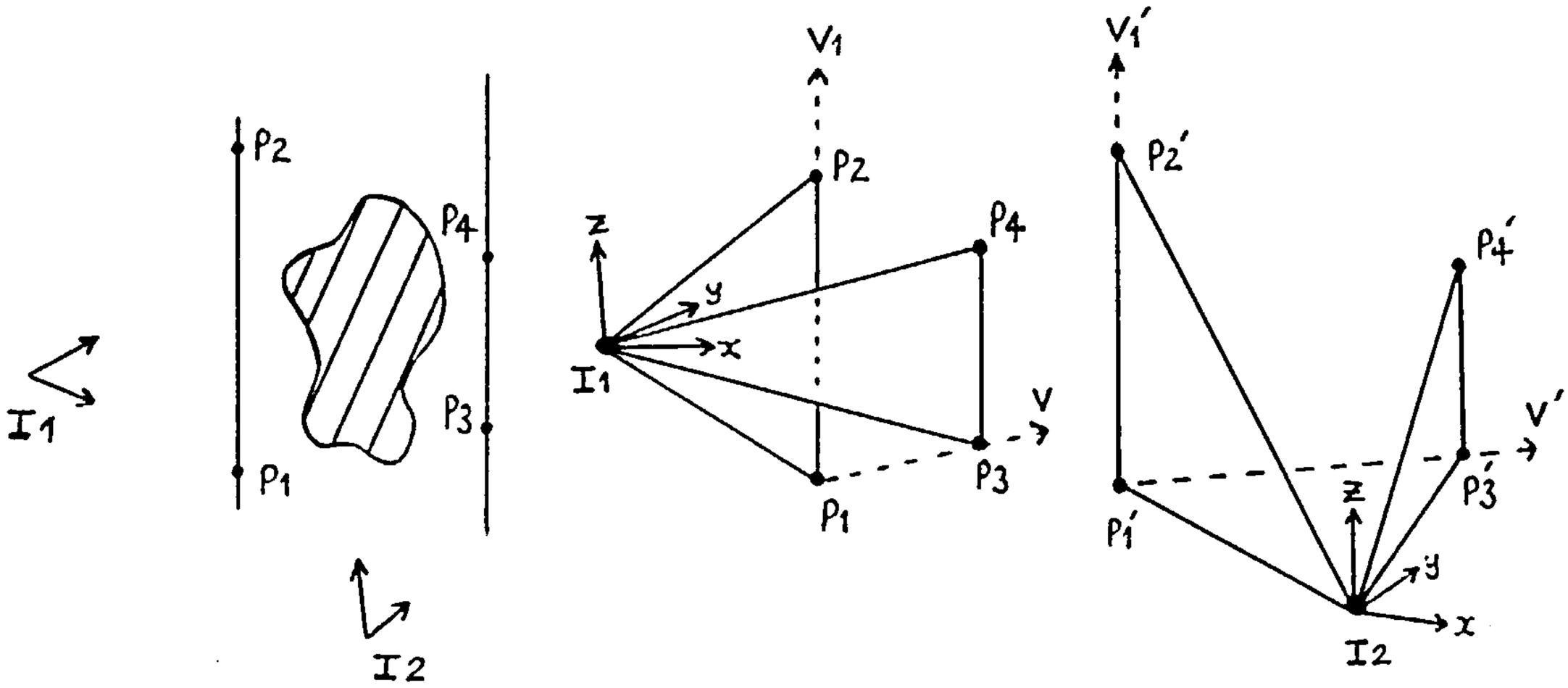

a) b) c)

Figure 6.5 Relative orientation on two vertical scales.

Fig. 6.5 (a) shows the observing situation. In diagram (b) the 4 targets have been located in the local system of I1. In (c) they are located in the system of I2, and accented to indicate that they have different values here. On a 3-D plot, I1 and I2 should superimpose, since they are provisionally located at the origin, but the diagrams have been separated for clarity.

Unit vectors $\underline{V1}$ and $\underline{V}$ respectively define directions P1 -> P2 and P1 -> P3. They have counterparts $\underline{V1}'$ and $\underline{V}'$ as indicated.

If I2 and its axes are considered rigidly attached to points P1',P2',P3',P4', the relative orientation of I2 with respect to I1 can be derived from a shift and rotation. The shift causes P1' to mate with P1, and the rotation turns V1' parallel to V1 and V' parallel to V. Due to observation errors and possibly poor geometry, it cannot be expected that the 4 target points define the same shape with respect to each instrument, and so the fit will not be exact. However, it should be adequate to provide a good approximation to the parameters of relative orientation.

The shift is readily found from the difference between coordinates of P1' and P1. The rotation matrix is derived as follows.

Compute unit vectors $\underline{V2}$ normal to $\underline{V1}$ and $\underline{V}$, and $\underline{V2}'$ normal to $\underline{V1}'$ and $\underline{V}'$, i.e

$$\underline{V2} = (\underline{V1} \times \underline{V}) / (\text{mod } \underline{V1} \cdot \text{mod } \underline{V})$$
$$\underline{V2}' = (\underline{V1}' \times \underline{V}') / (\text{mod } \underline{V1}' \cdot \text{mod } \underline{V}')$$

Complete the orthogonal set by creating $\underline{V3}$ normal to $\underline{V1}$ and $\underline{V2}$, and $\underline{V3}'$ normal to $\underline{V1}'$ and $\underline{V2}'$, i.e.

$$\underline{V3} = \underline{V1} \times \underline{V2}$$
$$\underline{V3}' = \underline{V1}' \times \underline{V2}'$$

It is shown in section 7.2 that each set of orthogonal unit vectors can be regarded as defining two rotation matrices, R and R', where the columns of each are the unit vectors themselves. The relative rotation of the accented set with respect to the unaccented set is then given by (R . R't).

It only remains for the position of I2 with respect to I1 to be found. This is done by applying first the shift to the initial position of I1 at (0,0,0), and then applying the rotation. The final position is the one required.

Since plumb-lines are used to define the object reference system, the 4-point relative orientation can only function with a fixed object, although a moving camera may be used to measure it. However, camera or theodolite views of the object cannot be used if pointings are close to the vertical. In this case, the direction of gravity cannot reliably be determined from the observations to the plumb-lines or vertical scale bars. Indeed, as shown in Ch. 5, these lines must also subtend "reasonable" angles even if the pointings are within a suitable range.

The size of the subtended angle has a further influence on the accuracy of the instrument - target separations. An error analysis of the ranging technique will not be made, because the primary purpose is the relative orientation and not the location of the targets. However, it is evident that small subtended angles will not give accurate values of separation. This may give rise to significant differences in the set of points defined by P1,P2,P3,P4, and P1',P2',P3',P4', which would result in a low accuracy in the determination of the orientation parameters. Given that there are a number of sources of low accuracy in this respect, the method is only recommended for initiating an optimum solution, as suggested above.

6.4 Resection on two linear scales.

Plumb-lines are restrictive, and it would be more convenient if two linear scales could be set up in any orientation. A gravity reference would not then be required, and the scales could be set up in positions suitable for upward or downward viewing if this were advantageous. They could even be fixed to a moving object.

A solution is possible if three targets with known separations are available on each of two straight lines, corresponding to the plumb-lines above. Whilst this may suggest the introduction of a 6-point orientation, the number can be reduced to 5, because both lines can, for a reason given below, share a common end. The method will therefore be called the 5-point relative orientation.

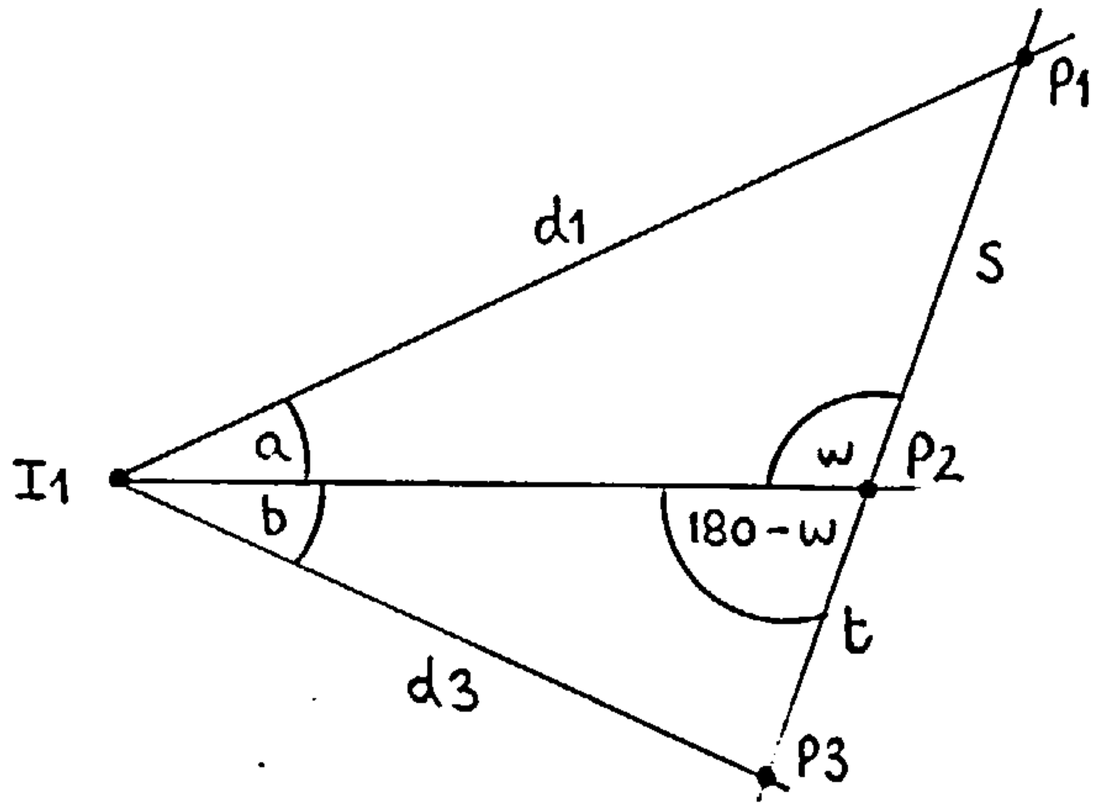

Figure 6.6 Three pointings to a linear scale.

Three target points, P1,P2,P3 are located on a straight line, with separations s and t as indicated in fig. 6.6. Neighbouring points subtend space angles a and b at an instrument I. The space angles are easily found from the scalar product of the of the observation unit vectors to each point. As with the plumb-lines, the task is to find distances d1 and d3 to the end points P1 and P3.

From the sine rule,

$$d1 / \sin(w) = s / \sin(a) \quad \text{(i)}$$

$$d3 / \sin(180 - w) = t / \sin(b)$$

or

$$d3 / \sin(w) = t / \sin(b) \quad \text{(ii)}$$

From (i) and (ii)

$$d1 = k \cdot d3 \quad \text{(iii)}$$

where

$$k = (s / t) \cdot (\sin(b) / \sin(a)) \quad \text{(iv)}$$

Let

$$u = s + t \quad \text{(v)}$$

$$c = a + b \quad \text{(vi)}$$

From the cosine rule

$$u^2 = d1^2 + d3^2 - 2 \cdot d1 \cdot d3 \cdot \cos(c)$$

$$= k^2 \cdot d3^2 + d3^2 - 2 \cdot k \cdot d3^2 \cdot \cos(c)$$

$$= d3^2 \cdot (1 + k^2 - 2 \cdot k \cdot \cos(c))$$

therefore

$$d3^2 = u^2 / (1 + k^2 - 2 \cdot k \cdot \cos(c)) \quad \text{(vii)}$$

d3 can be found from this expression, and d1 from equation (iii).

This provides the mechanism for locating the end points of two linear scales, each defined by 3 targets. The remaining part of the analysis follows the pattern outlined in the previous section. Here it should be noted that only 3 of the 4 end points are needed for the derivation of shift and rotation. This justifies the initial comment that 2 end points may be common, thereby reducing the total number of control targets to 5.

The scales may be positioned in any convenient orientation which offers "reasonable" subtended angles. For the reasons given in the last section, an error analysis of the expressions for distance is not of prime importance. As a practical guide, I would suggest that the scales be of the same size as the object, if not larger. In fact, it is not uncommon to place graduated scales or levelling staffs on either side of an object, and I would suggest that this is a reasonable approach to take. The two most extreme points which are still visible, and a third roughly half way between them, should be selected on each scale. For large objects, or as an alternative, two stretched wires, each supporting three targets, would provide a very convenient form of portable control. These amount to little more than a form of tape measure, which may well be additionally needed for scale determination. In this form it would be particularly easy to manufacture wires with a common and targetted hinge, giving a true 5-point relative orientation.

A disadvantage of linear scales and stretched wires is that they may not correctly define a straight line. This is another potential source of error, but I emphasize that the main objective is to generate starting values for an iterative solution. It should not be difficult to manufacture scales which are good enough for this purpose.

6.5 Tests of orientation by optical distance ranging.

Of the three techniques of orientation presented, the previous one can be identified as the easiest and most convenient general method. It has therefore been programmed into the TRIGFIX package.

As a practical demonstration, a set of reference targets was intersected in two ways. Firstly by a single theodolite from two positions, secondly by a single metric camera from two positions. To enable a 5-point orientation to be computed, three adhesive targets were attached to each of two levelling staffs. These were simply used as scale bars and not set vertical. The targets were placed by eye using the graduations.

The staffs themselves were in two parts, and bent slightly at the join. As a result, an orientation based on these targets is poor. In the appendix, Data Sets 4 show the figures for the theodolite, which are better than those for the camera given in Data sets 5. An optimum orientation then followed in each case, taking the parameters already derived as starting values. All points were treated as unknowns, including the scaling targets.

For the theodolite test the optimum result was as good as a dual theodololilte intersection with reciprocal pointings. A best fit of 17 reference targets to existing data (not listed) was :

rms x = 0.057 mm, rms y = 0.078 mm, rms z = 0.036 mm

A similar fit was carried out for the photogrammetric test, which has been listed to provide a comparison for the test represented in Data Sets 7. The reference coordinates are, in fact, those derived from the equivalent theodolite test. In this case, the fit between 16 targets shows residuals :

rms x = 0.377 mm, rms y = 0.385 mm, rms z = 0.273 mm

6.6 Concluding comments.

The methods presented in this chapter are principally intended for the automatic generation of trial orientation parameters. This is a worthwhile goal and one which is often neglected. Hunt's comments support this opinion [E11].

The techniques are characterized by the use of some additional control information. This implies some extra effort by the engineer undertaking the measurements, but this is relatively small. Levelling instruments or including scale information is already a feature of many tasks, and in some cases the suggestions above may simply make better use of existing data. I would also maintain that levelling bubbles and collapsible scale bars represent a very convenient and portable form of control. Other methods, for example, depend on the creation of control points by dual theodolite intersection, or bearing and distance using a single theodolite coupled with an EDM unit. These may be more time consuming, and involve additional equipment which may not be available. Of course, different types of control may produce different qualities of result, and comparisons would be advisable.

It might still be felt that there is too much effort involved, or that the methods cannot be made to work for every pair of instruments in a network. However, in a practical multi-station network, only a few pairs of instruments, and possibly only one, need be oriented by one of these techniques. (This also applies to the introduction of reciprocal observations). From these, further targets can be intersected, from which other instruments can be positioned by a standard 3-D resection.

Further research should consider a detailed error analysis. This would determine the accuracies and geometrical configurations which enable the computed orientations to be accepted without further optimizing.

Ch. 7 Mathematics and software.

This chapter presents a number of mathematical features which I have used in analysing the triangulation problem. These have been incorporated in the TRIGFIX demonstration programs. Parts of the presentation are simply re-statements of existing theory, but this makes it easier to place my own ideas in context. Sections with novelty value are preceeded by "*".

7.1 Rotations.

In the TRIGFIX programs, the general rotation matrix, R, has the form :

$$\begin{bmatrix} r11 & r12 & r13 \\ r21 & r22 & r23 \\ r31 & r32 & r33 \end{bmatrix}$$

It pre-multiplies vectors to rotate them from their current position to their final position.

If an instrument axes are imagined initially parallel to the reference system axes, and represented by unit vectors, then the columns of R give the unit vectors of these axes after rotation.

$$R\begin{bmatrix}1\\0\\0\end{bmatrix} = \begin{bmatrix}r11\\r21\\r31\end{bmatrix} \qquad R\begin{bmatrix}0\\1\\0\end{bmatrix} = \begin{bmatrix}r12\\r22\\r32\end{bmatrix} \qquad R\begin{bmatrix}0\\0\\1\end{bmatrix} = \begin{bmatrix}r13\\r23\\r33\end{bmatrix}$$

x axis y axis z axis

This point of view provides a convenient way of comparing rotation matrices associated with an instrument, and which have been computed in different ways.
The comparison uses the angle between corresponding column vectors in the different matrices, determined from their dot product. For matrices R and R' :

axis	angle	value
x	tx	arc cos (r11.r'11 + r21.r'21 + r31.r'31)
y	ty	arc cos (r12.r'12 + r22.r'22 + r32.r'32)
z	tz	arc cos (r13.r'13 + r23.r'23 + r33.r'33)

This gives a meaningful comparison, in much the same way as the difference of two computed instrument positions. It is also one which does not rely on any particular definition of the three independent elements of the matrix and consequently has no "failure case" (below).

When specifying a rotation matrix, it is common to do so in terms of just three independent quantities. Very often these are taken as angular rotations omega (w) about the x axis, phi (p) about y and kappa (k) about z. Each has an associated matrix, respectively O,P and K. The actual rotation matrix, R, is then given by :

$$R = O \cdot P \cdot K$$

Here the rotations can be interpreted in two ways.

1) first omega, then phi, then kappa about the current positions of the axes (the moving instrument axes).
2) first kappa, then phi, then omega about the fixed reference system axes.

In terms of the individual O,P,K matrices, R =

$$\begin{bmatrix} 1 & 0 & 0 \\ 0 & \cos w & -\sin w \\ 0 & \sin w & \cos w \end{bmatrix} \begin{bmatrix} \cos p & 0 & \sin p \\ 0 & 1 & 0 \\ -\sin p & 0 & \cos p \end{bmatrix} \begin{bmatrix} \cos k & -\sin k & 0 \\ \sin k & \cos k & 0 \\ 0 & 0 & 1 \end{bmatrix}$$

which gives matrix elements :

$$r11 = \cos p \cdot \cos k$$

$$r12 = -\cos p \cdot \sin k$$

$$r13 = \sin p$$

```
r21  =    sin w . sin p . cos k  +  cos w . sin k
r22  = -  sin w . sin p . sin k  +  cos w . cos k
r23  = -  sin w . cos p

r31  = -  cos w . sin p . cos k  +  sin w . sin k
r32  =    cos w . sin p . sin k  +  sin w . cos k
r33  =    cos w . cos p
```

From this it can be seen that

```
w = arc tan ( - r23 / r33 )
p = arc sin ( r13 )
k = arc tan ( - r12 / r11 )
```

However, when phi = 90 deg., w and k are indeterminate, since the elements r11, r12, r23, r33 then have the value zero. Any program which uses w,p,k as the three rotational parameters, and explicitly solves for them, will fail in this case. (A similar problem occurs if R is specified in the format of a Rodrigues matrix [E5]).

In industrial work, which should be treated as a general case, it is not valid to assume that phi can never approach 90 degs. It is equally unsatisfying to assume it will never exactly equal 90 degs.

The preferred solution is to express the rotation matrix, R, as the product of two matrices :

$$R = dR \cdot Ro$$

Ro is a fixed matrix which describes the bulk of the rotation, and whose 9 elements are computed by direct or approximate means, without recourse to any particular three rotational parameters. (See the example below).
dR is a matrix providing a small additional 3-D rotation. Since it is small, the failure case is avoided, and any convenient set of three rotational parameters can be used to specify it. This is discussed by Granshaw [E8], Hunt [E11] and Wester-Ebbinghaus [E7].

TRIGFIX programs treat the dR matrix as derived from three small rotations, first k, then p, then w, taken about fixed system axes. This makes it easier to deal with the gravity vector. Since an instrument can be levelled by observing the direction of the gravity vector with respect to its own axes, Ro can be chosen such that, when applied to the instrument, the gravity vector is rotated parallel to the system Z axis, taken as representing the vertical axis. The further application of dR has the effect of tilting the gravity vector slightly. This tilt is due entirely to w and p. Consequently, w and p may be fixed at zero to achieve the same effect as an absolutely levelled instrument, which is the normal survey case. This can be done using both SURV3D [F2] or TRIGFIX. Alternatively, they may be free to vary, but two additional weighted observations can be included which ensure that the tilt does not become large. A proposal for this is given below and a similar technique is used by Wester-Ebbinghaus [E7].

When formulating equations, particularly for iterative solutions, it is convenient to simplify the form of dR. By expressing the general form, given above, in terms of small angles, dR becomes

$$\begin{bmatrix} 1 & -k & p \\ k & 1 & -w \\ -p & w & 1 \end{bmatrix}$$

and the elements of R become

$$\begin{aligned} r'11 &= r11 - k.r21 + p.r31 \\ r'12 &= r12 - k.r22 + p.r32 \\ r'13 &= r13 - k.r23 + p.r33 \\ \\ r'21 &= k.r11 + r21 - w.r31 \\ r'22 &= k.r12 + r22 - w.r32 \\ r'23 &= k.r13 + r23 - w.r33 \end{aligned}$$

$$r'31 = -p.r11 + w.r21 + r31$$
$$r'32 = -p.r12 + w.r22 + r32$$
$$r'33 = -p.r13 + w.r23 + r33$$

The simplified form of dR may be convenient, but is not itself an orthogonal matrix. Therefore, in any solution for w,p,k, dR must be derived from the correct form of the matrix product, O.P.K. In some iterative solutions it is a further convenience to "update" Ro by pre-multiplying with dR. In this event, elements w,p,k always have the value zero at the start of an iteration. However, if a problem requires a large number of iterations before converging to a solution, the repeated updating of Ro by matrix multiplication may itself cause it to become non-orthogonal. This is caused by the limits to precision inherent in the computer. The problem can be avoided by passing the updated value of Ro through a routine which forces it to be orthogonal, such as the Schmidt procedure [E5].

* 7.2 Computing a relative rotation.

Relative rotations occur frequently in triangulation problems, and a very good approximation can often be found directly from available space vectors. These approximations give true orthogonal matrices and this section examines the general case.

The objective here is to find a rotation matrix which will line one set of vectors up with another, so that corresponding vectors are parallel.

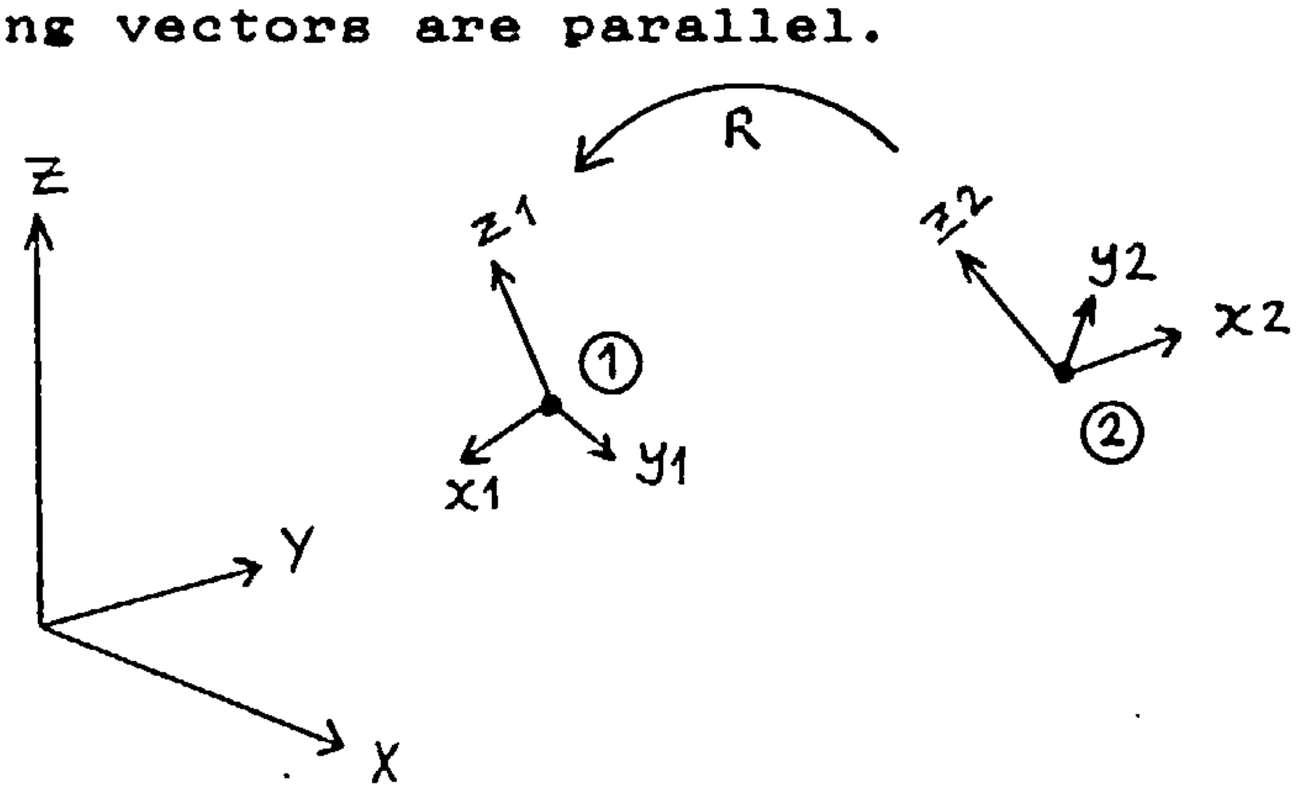

Figure 7.1 Relative rotation

Fig. 7.1 shows two objects in some reference system, each defined by an origin and three orthogonal axes.

Let $\underline{x1}$, $\underline{y1}$, $\underline{z1}$ and $\underline{x2}$, $\underline{y2}$, $\underline{z2}$ represent unit vectors along these axes. The elements of $\underline{x1}$, etc, can also be written as a row matrix, X1, etc.
The rotation, R, which when applied to object (2), rotates $\underline{x2}$ parallel to $\underline{x1}$, etc., can be constructed directly from these 6 vectors.

Imaging each set of axes is initially parallel to the system axes, X,Y,Z. If R1 rotates (1) into its present orientation, and R2 does the same for (2), then from 7.1 above :

$$R1 = [\ X1t \quad Y1t \quad Z1t\ ]$$
$$R2 = [\ X2t \quad Y2t \quad Z2t\ ]$$

If the additional rotation, R, is now applied to (2), this causes its axes to be parallel to those of (1). But this combined rotation will achieve the same effect as R1,

$$\text{hence} \qquad R \,.\, R2 = R1$$
$$\text{and} \qquad R \,.\, R2 \,.\, R2t = R1 \,.\, R2t$$

but R2t is the inverse of R2

$$\text{hence} \qquad R = R1 \,.\, R2t$$

and R1, R2 are directly computed from the axial unit vectors above.

This method can be used in several apparently diverse instances. Two examples follow, and two more appear in the main text. These are the direct computation of relative orientation (section 2.2), and a relative orientation based on scale lengths (section 6.3). The latter is essentially the same as the resection case in section 7.4.

* 7.3 Shift and rotation for a 3-D fit.

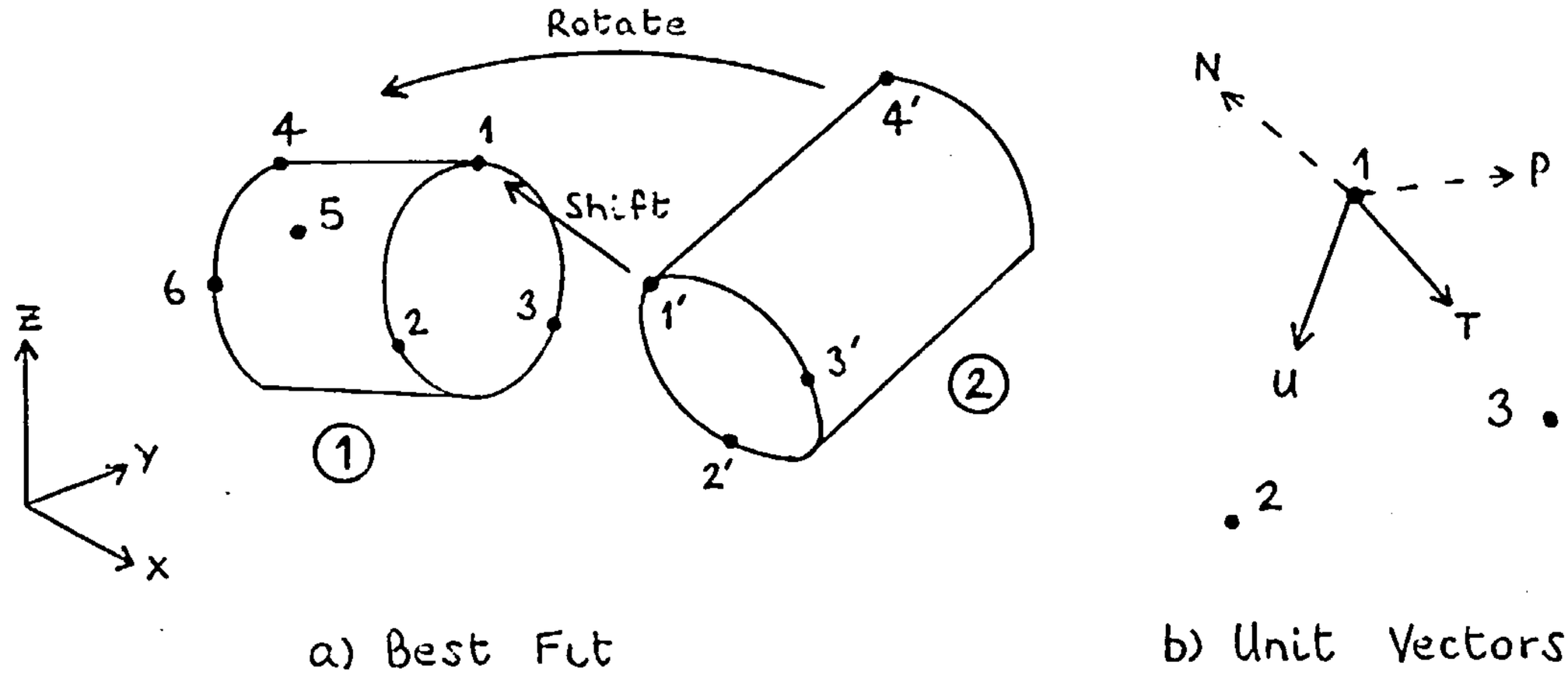

a) Best Fit b) Unit Vectors

Figure 7.2 Best fit.

Fig. 7.2 shows two independent measurements of an object, with the result that it is specified by two different sets of coordinates. By applying a shift and rotation to set (2) it may be directly compared with set (1). In general a best fitting transformation is required, but the bulk of the rotation can be determined by taking just three of the common points.

Evidently the shift is easily found by forcing any two corresponding points together, eg 1' to 1. Only a rotation about point 1 then remains to cause the other points to fit together.

Compute the following unit vectors :

1) U from 1 to 2 in object (1), U' from 1' to 2' in object (2)
2) T from 1 to 3, and T'.
3) P perpendicular to U and T, and P'.
   P is obtained from the cross product
   (U x T) / mod (U x T)
4) N normal to U and P, and N'.
   N is again found from a cross product U x P.
   Note that mod (U x P) = 1.

Evidently U , N , P and U', N', P' correspond to the axial vectors in fig 1, and the rotation matrix can be immediately computed.
(Note that this is an over-determined problem, and the fit will only be exact at point 1).

* 7.4 Position and orientation for a 3-D resection.

Two direct methods of space resection, by Smith [E12] and Hunt [E11], solve the problem by first computing the distance from the instrument's origin to three points on the object. Two further steps to the solution follow. Firstly, the position of the instrument with respect to the object is found by intersecting three spheres. Secondly, the corresponding rotation matrix is computed. When finding the instrument position, the ambiguous "mirror image" case must be discarded. A simpler solution is available than that provided by Smith or Hunt, and which avoids the need for considering the ambiguous case.

Evidently, once the distances from instrument to object points have been computed, object point coordinates can be derived with respect to the instrument axes.

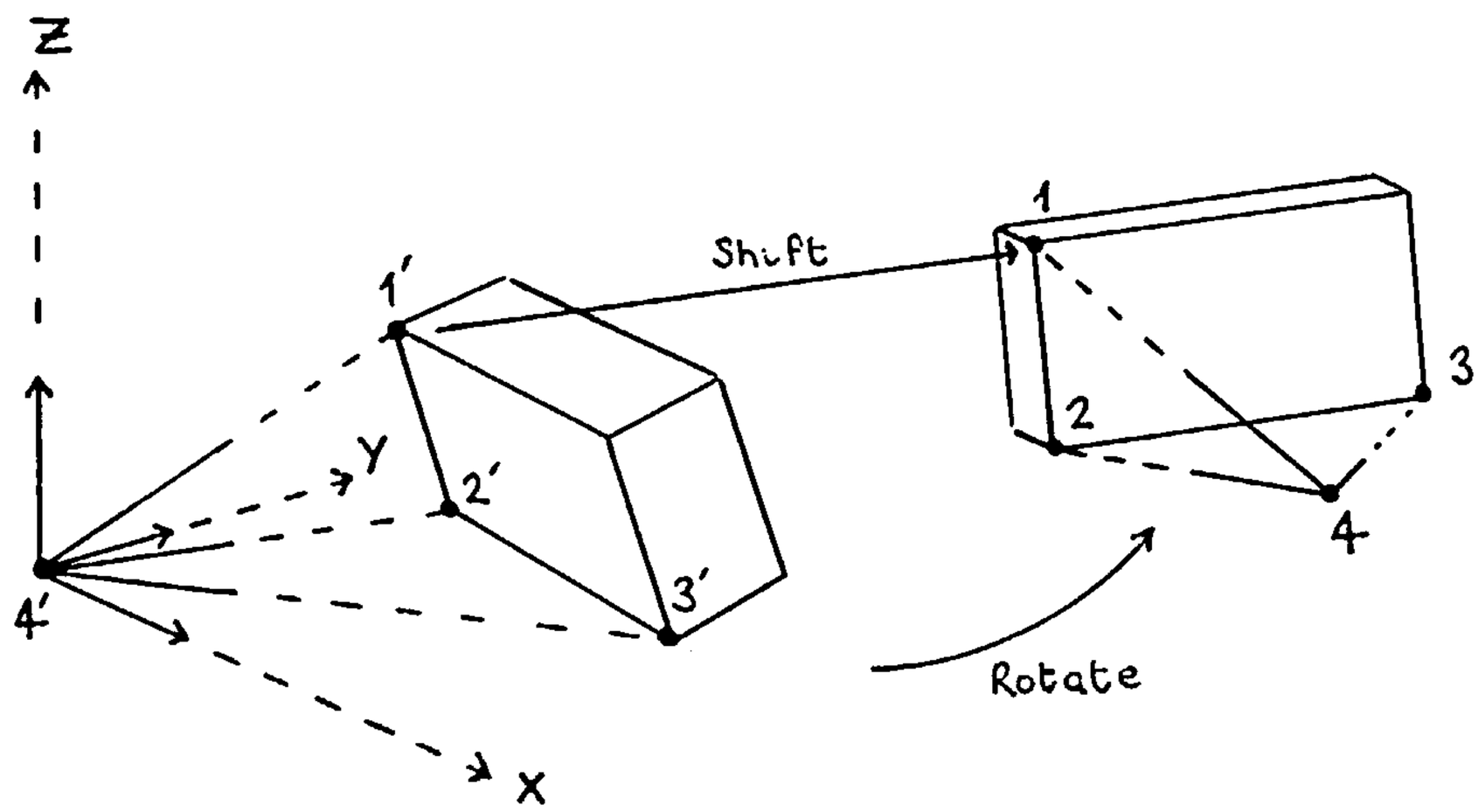

Figure 7.3 Resection

Fig. 7.3 shows the situation, in which the instrument has been provisionally located at the reference system origin, its axes lined up with the reference axes.

Point 4' is the instrument origin, with initial coordinates (0,0,0). 1',2',3' are the computed object points, 1,2 and 3 are the actual points, and 4 shows the actual position of the instrument.

The situation has now become the same as the best fit described in fig 2. The shift is found by comparing coordinates of 1' and 1, and the computation of the rotation matrix follows the scheme in 7.3 above. The shift, followed by a rotation about point 1, is then applied to a point located at (0,0,0), i.e. point 4', so providing the resected instrument position. The mirror image case, where 4 is found behind the plane of 1,2,3, does not develop.

7.5 Instrument pointings.

In a properly levelled theodolite, the mean of face left and face right pointings gives horizontal and vertical components of a pointing to an object. If the theodolite has not been levelled, the vertical angle readings can be correctly measured with respect to the (non-levelled) plane of the horizontal circle, provided the index is fixed. This provides consistent pointings within an orthogonal set of instrument axes. Again, the mean of face left and face right gives the required value. For convenience, the terms horizontal and vertical will be used.

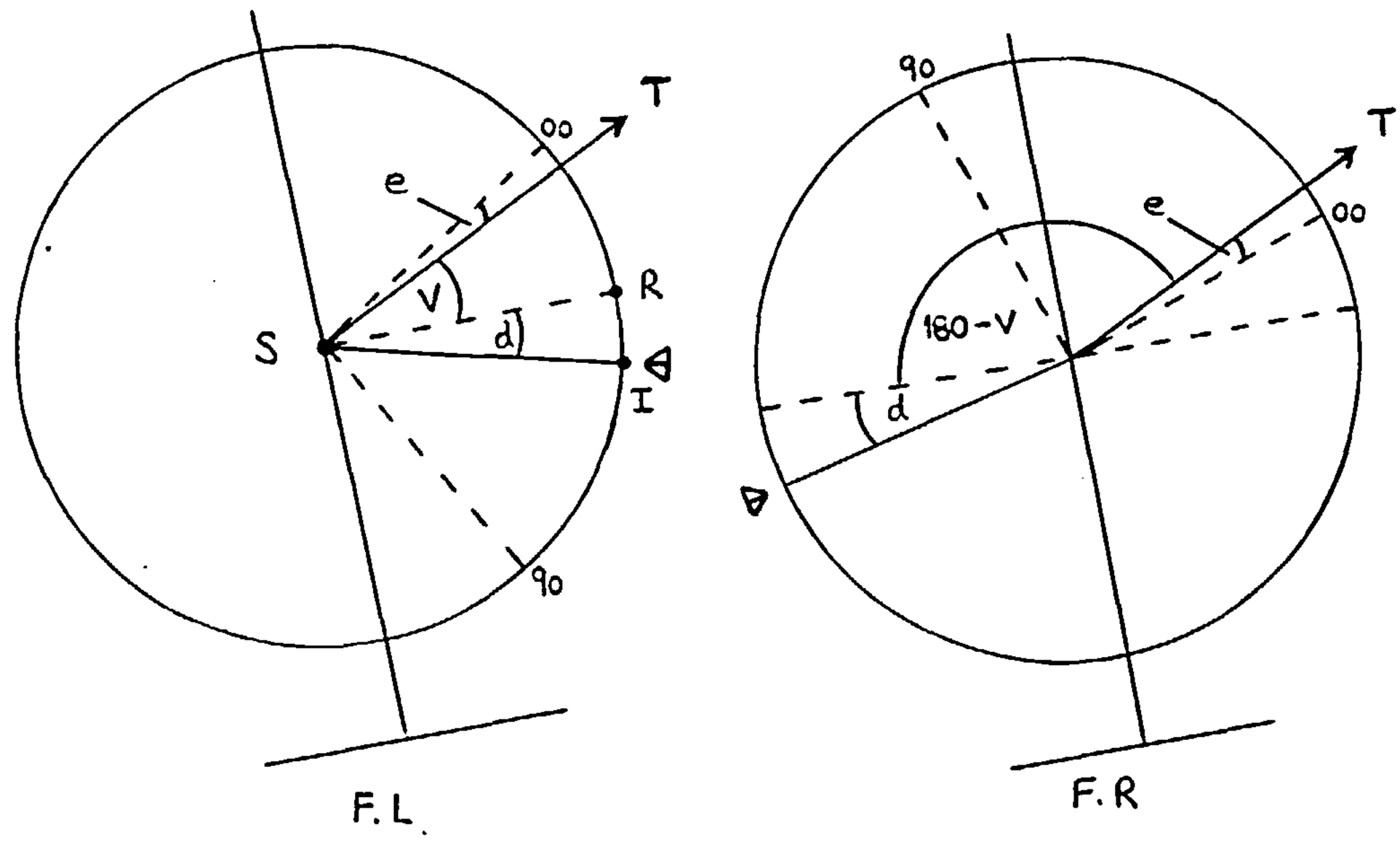

Figure 7.4 Non-levelled theodolite pointings on two faces

In fig. 7.4 the zero mark does not correspond with the line of sight (collimation error), and the index has not been fixed on the line SR, parallel to the horizontal circle (index error).

Measured vert. angle on f.l, $a = v + e + d$

" f.r, $b = 180 - v + e + d$

hence $a - b = 2 . v - 180$

or $v = 90 + (a - b) / 2$ in this case.

The errors, e and d, do not appear when computing the vertical angle using both faces. As with levelled theodolites, it is possible to make an adjustment such that the reading on one face is sufficiently accurate. In this case, set $d = - e$.

When formulating equations in terms of unit vectors, an orthogonal set of axes must be defined on the theodolite.

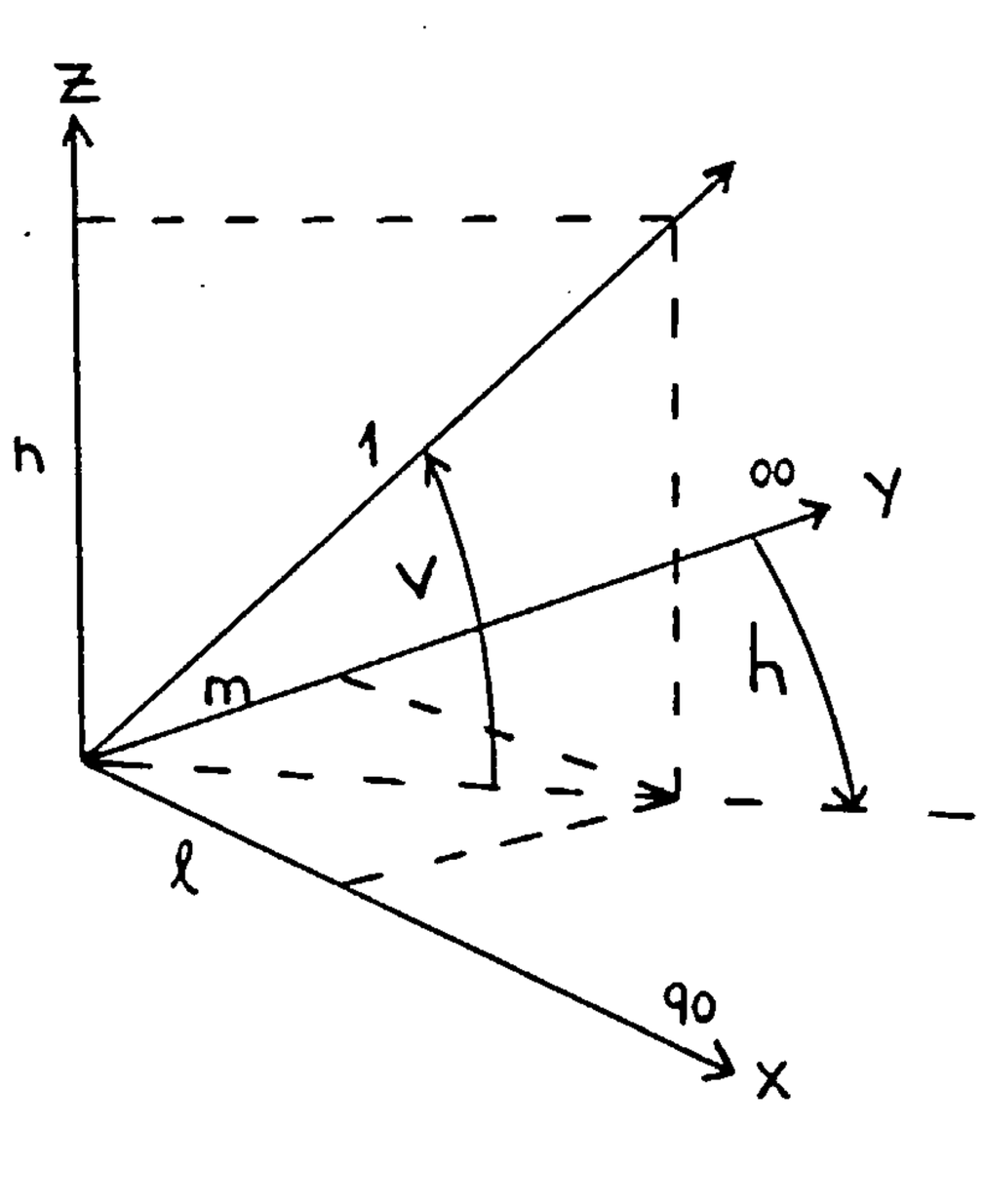

Figure 7.5 Theodolite axes and unit vector pointing

In the absence of any convention, I have chosen the +Y axis to lie along the zero degrees line of the horizontal circle, and +X along 90 degrees. For a right handed system, the primary axis, Z is then positive "up", when the theodolite is levelled.

It might seem natural to consider X and Y the other way around, giving the usual mathematical convention for increasing horizontal angles, but then Z must be positive down. I find this more of an inconvenience than the loss of the mathematical convention.

For a unit vector with elements (l,m,n) :

```
l  =  sin h . cos v
m  =  cos h . cos v
n  =  sin v
```

The equivalent unit vector pointing for a camera is easily stated.

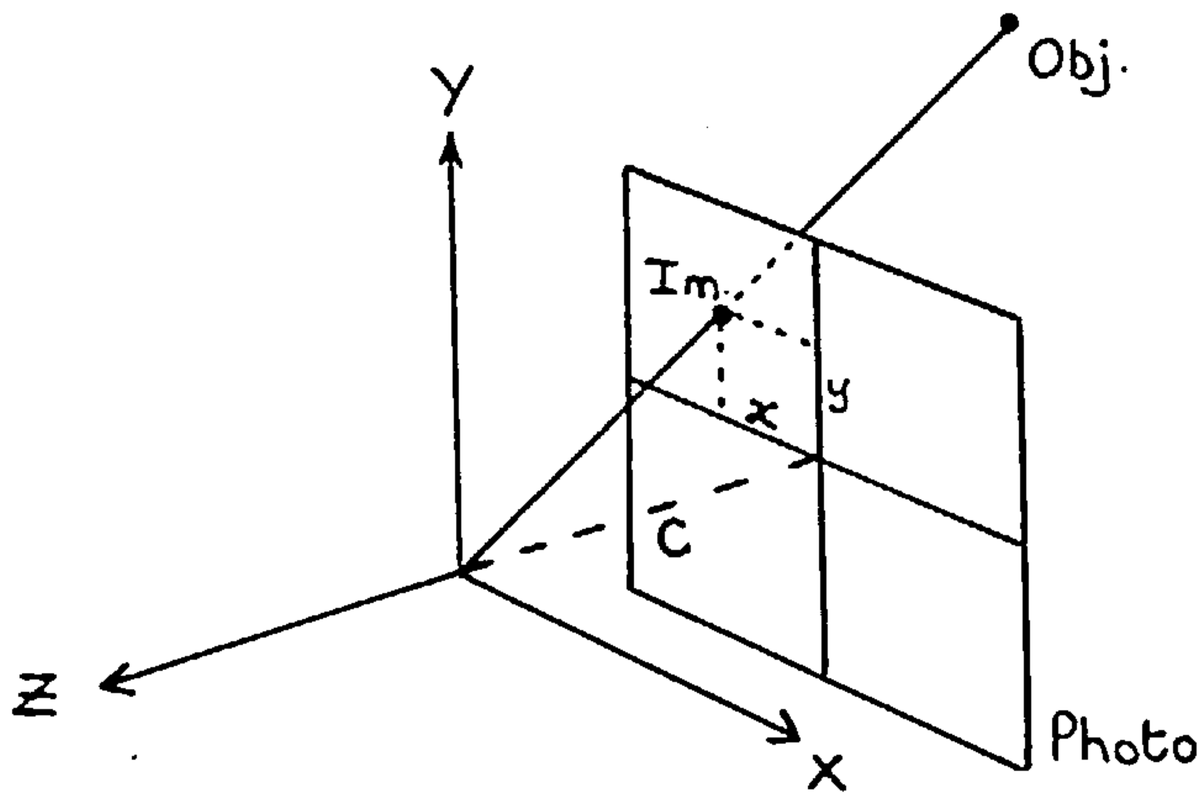

Figure 7.6 Camera vector

Fig. 7.6 shows the image of an object on a positive photograph. Image coordinates are (x,y) and camera principal distance is c. The observed vector is (x,y,-c). This has length, d, given by

```
d  =  sqrt ( x**2  +  y**2  +  c**2 )
```

and the unit vector components are

```
l  =  x / d
m  =  y / d
n  = -c / d
```

For both theodolites and photographs, the general equations relating instrument to object point are given by :

$$R \cdot \begin{bmatrix} l \\ m \\ n \end{bmatrix} = \begin{matrix} = \\ = \\ = \end{matrix} \quad 1/D \quad \begin{bmatrix} X - x \\ Y - y \\ Z - z \end{bmatrix}$$

R is the rotation matrix which rotates the pointing parallel to the space ray connecting instrument and target

l,m,n are the elements of the pointing

X,Y,Z are the target coordinates

x,y,z are the instrument coordinates in object space

D is the separation of instrument and target

This equation can be re-written

$$\begin{bmatrix} l \\ m \\ n \end{bmatrix} = 1/D \quad Rt \cdot \begin{bmatrix} X - x \\ Y - y \\ Z - z \end{bmatrix}$$

which gives known instrument measurements on one side, and unknown instrument and object parameters on the other.

* 7.6 Vector observations.

The previous discussion indicates how theodolite and (metric) camera observations can be reduced to the same format. Non-metric cameras can be included if pre-calibration is acceptable. Devices such as the electronic photo-theodolite can also generate vector observations. It is therefore convenient to convert diverse forms of observation to this common format, and then continue with standard procedures for solving triangulation problems.

The vector equations in 7.5 can be linearized as follows. Expanding :

$$\begin{aligned} l &= 1/D \{ r'11 \cdot (X-x) + r'21 \cdot (Y-y) + r'31 \cdot (Z-z) \} \\ m &= 1/D \{ r'12 \cdot (X-x) + r'22 \cdot (Y-y) + r'32 \cdot (Z-z) \} \\ n &= 1/D \{ r'13 \cdot (X-x) + r'23 \cdot (Y-y) + r'33 \cdot (Z-z) \} \end{aligned}$$

An observation equation is established by the relation :

$l = l' + v_l$, i.e.

computed value = measured value + residual

l can be written (lo + dl), where lo is its value close to a solution, and dl a small correction. lo is found by substituting approximate values for the rotation matrix, target and instrument positions in the equations above.

This leads to the general linearized form :

$$lo + dl = l' + v_l$$

$$dl = (l' - lo) + v_l$$

but

$$dl = f_1.dX + f_2.dY + f_3.dZ + f_4.dx + f_5.dy + f_6.dz + f_7.dw + f_8.dp + f_9.dk$$

$$= (l' - lo) + v_l$$

where the differential elements have now become the unknowns.

Coefficients, f1 - f9 for an "l" equation, g1 - g9 for "m", and h1 - h9 for "n" are obtained as follows.

$$f_1 : \quad r_{11} / D - (X-x)/D \,.\, lo/D$$

$$f_2 : \quad r_{21} / D - (Y-y)/D \,.\, lo/D$$

$$f_3 : \quad r_{31} / D - (Z-z)/D \,.\, lo/D$$

$$f_4 : \quad - f_1$$

$$f_5 : \quad - f_2$$

$$f_6 : \quad - f_3$$

$$f_7 : \quad - r_{31} \,.\, (Y-y)/D + r_{21} \,.\, (Z.z)/D$$

$$f_8 : \quad r_{31} \,.\, (X-x)/D - r_{11} \,.\, (Z-z)/D$$

$$f_9 : \quad - r_{21} \,.\, (X-x)/D + r_{11} \,.\, (Y-y)/D$$

$$g1 : \quad r12 / D - (X-x)/D \cdot mo/D$$

$$g2 : \quad r22 / D - (Y-y)/D \cdot mo/D$$

$$g3 : \quad r32 / D - (Z-z)/D \cdot mo/D$$

$$g4 : - g1$$

$$g5 : - g2$$

$$g6 : - g3$$

$$g7 : - r32 \cdot (Y-y)/D + r22 \cdot (Z.z)/D$$

$$g8 : \quad r32 \cdot (X-x)/D - r12 \cdot (Z-z)/D$$

$$g9 : - r22 \cdot (X-x)/D + r12 \cdot (Y-y)/D$$

$$h1 : \quad r13 / D - (X-x)/D \cdot no/D$$

$$h2 : \quad r23 / D - (Y-y)/D \cdot no/D$$

$$h3 : \quad r33 / D - (Z-z)/D \cdot no/D$$

$$h4 : - h1$$

$$h5 : - h2$$

$$h6 : - h3$$

$$h7 : - r33 \cdot (Y-y)/D + r23 \cdot (Z.z)/D$$

$$h8 : \quad r33 \cdot (X-x)/D - r13 \cdot (Z-z)/D$$

$$h9 : - r23 \cdot (X-x)/D + r13 \cdot (Y-y)/D$$

In the TRIGFIX demonstration software, all three equations are generated, and processed, for every pointing. This does not imply that all three are independent, which is evidently not the case. Since (l,m,n) is a unit vector, once any two elements are specified, the other is immediately defined. Conventionally, different equations would be developed for different types of pointing. For example, two equations representing horizontal and vertical angle observations for theodolites, or two representing x and y photo coordinates for cameras. This is not necessarily a preferable approach, as will be seen shortly.

As regards the vector, only the ratio of elements is of real importance, as these contain the all-important directional information. Two independent equations could therefore be developed using, say, l/n and m/n.

However, a choice must be made as to which combination is suitable, for the one just given will obviously fail when n is zero or very small. In fact, the largest of l,m or n, chosen as the denominator, will give the most stable solution, and this will not necessarily be the same choice for all pointings at one instrument station. Although this approach has been already been implemented [P2], the use of three equations avoids the need to make a choice. Of course, making a choice probably results in less computing time than the processing of an additional equation, but TRIGFIX makes use of a least squares algorithm which can be considered to be fairly efficient, and which may offset the disadvantage. In any case, additional off-line processing time, which could only amount to minutes, is not a serious objection. More critical, perhaps, is the question whether this is a valid technique.

A pragmatic response is to say that any technique which fits the facts is as good as any other. Furthermore, creating additional equations which contain no new information is not a novelty. Burnside [A1], for instance, describes something similar.

Then again, it might be felt that the linearized formulation will cause the vectors to depart from unit length, but, if so, this is not relevant. The observed vectors are deliberately manufactured to have unit length, and are not altered in the solution. They are simply compared with some mathematically derived unit vectors, and the purpose of the solution is to provide an estimate of instrument parameters which improves the fit. The fit is represented by the space angle between the vectors, which seems a logical criterion. That this is so, can be seen from the three equations.

$$l = l' + vl \qquad \text{or} \qquad l - l' = vl$$
$$m = m' + vm \qquad\qquad m - m' = vm$$
$$n = n' + vn \qquad\qquad n - n' = vn$$

The residuals represent the components of the small vector difference (dV) between computed and measured unit vectors (L - L'). Now, the least squares minimizes the sum of the elements (v**2), and these may be grouped together in the following way :

summation = (v1**2 + vm**2 + vn**2) .. + similar terms

= dv**2 . . .

where dv**2 is the length of the small difference vector. However, since the measured and observed vectors are of unit length, dv is numerically the space angle between the vectors in radians. The least squares solution, therefore, minimizes these space angles.

To emphasize the merit of minimizing the space angles, consider the effect of equally weighted photo and theodolite observations. This approach would normally be adopted if every pointing is equally valid. Pointings which, for different reasons, are good or bad, raise a separate issue which should not be confused with the next argument.

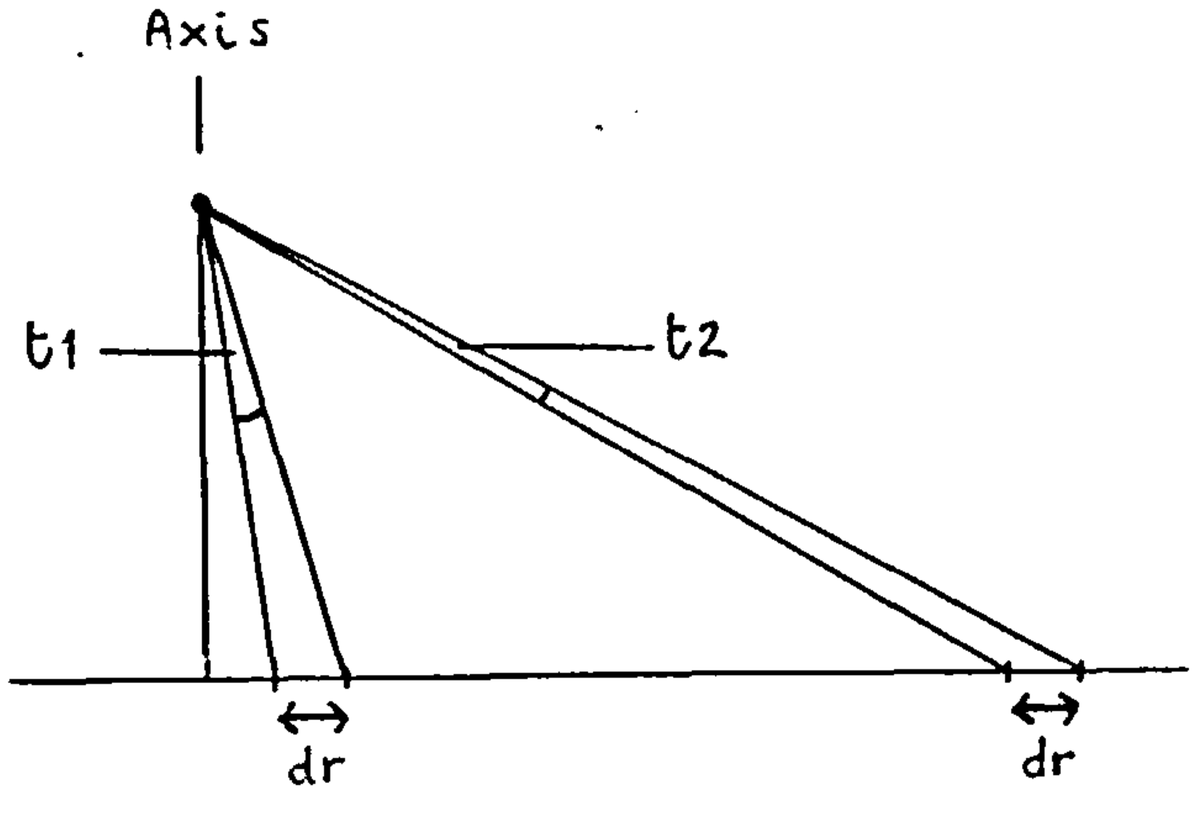

Figure 7.7 Photo observations

Fig. 7.7 shows photo coordinates close to the axis and at the field edge. These are assumed to have the same degree of uncertainty, which would be the case if they were given equal weighting. However, this ensures that the angular uncertainty at the edge, t2, is smaller than its counterpart, t1, near the axis.

Consequently, the implication is that pointings near the edge are more accurate than those near the axis. This conflicts with the knowledge that photographic quality, and therefore pointing precision, falls off at the field edges.

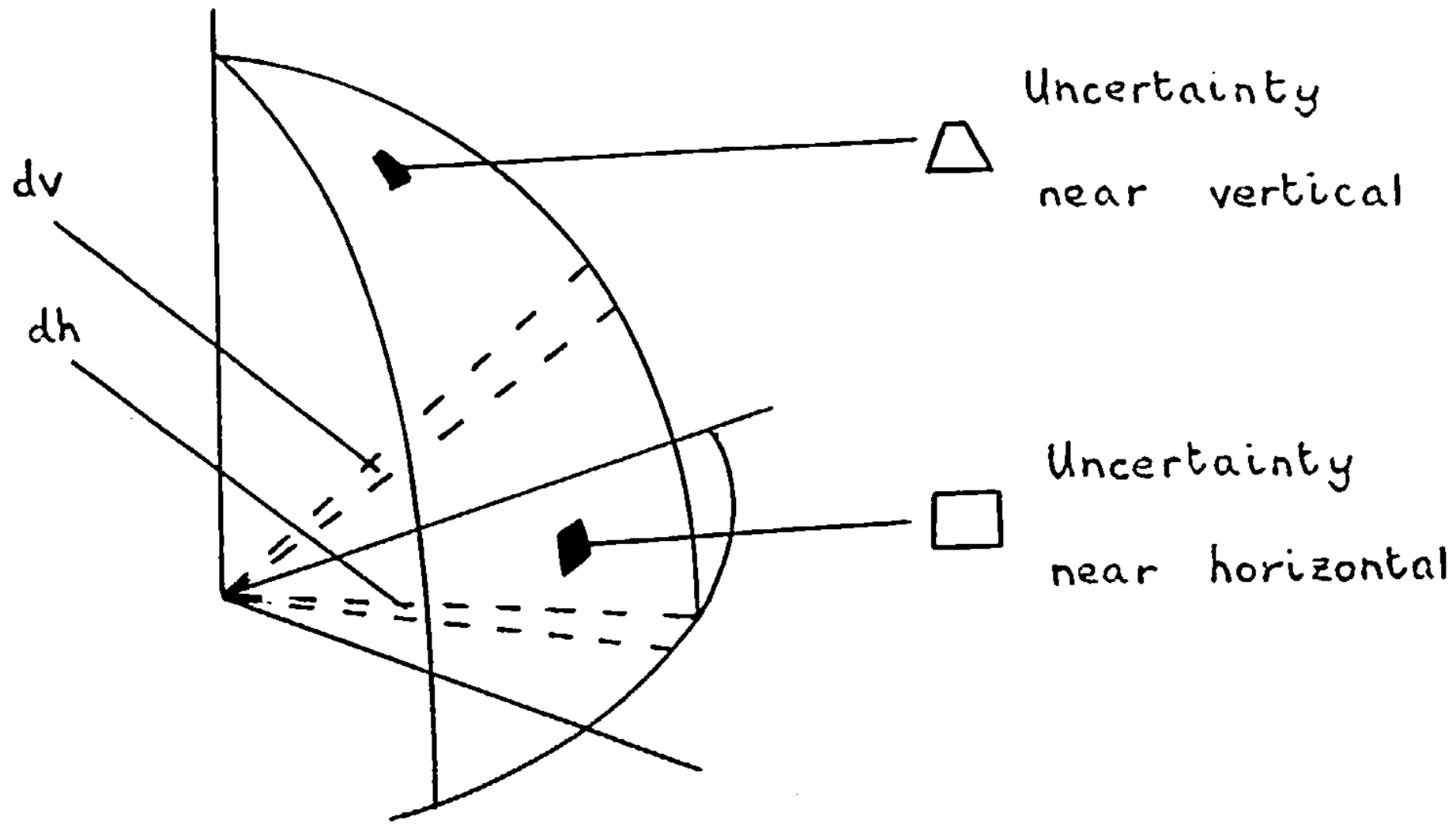

Figure 7.8 Theodolite observations

A similar problem develops with theodolite observations. If an equal uncertainty is assigned to vertical and horizontal angles, a smaller area of uncertainty in the actual pointing is obtained near the primary axis than near the horizontal. Are zenith pointings, then, more accurate than others? This particular problem is resolved when it is realized that the horizontal pointing is indeterminate on the primary axis. For this reason, observation equations developed for horizontal and vertical angles are not as general as those based on vectors.

There is, of course, no objection to constructing a weighting system which takes account of where a pointing lies within the field of view. Lower weights could then be given to image coordinates on the edges of photographs, and horizontal angles would be given progressively lower weights as their associated vertical angles approached +/- 90 degrees. Unfortunately, the weight should be zero on the primary axis, an act which will not be lightly tolerated by a computer program.

Either way, much the same effect is achieved by the vector approach, and the main justification is that the uncertainty in pointing is as much due to the observer (human or electronic), as it is due to the physical construction of the reading device.

A final comment about vector observations concerns levelling. Currently, TRIGFIX keeps an instrument level by holding w = 0 and p = 0. A possible alternative is to treat it as another vector observation, which also means it can be given a weight. The observation is slightly different from the others, since there is no target involved. The following approach is suggested.

Let (lg,mg,ng) be the observed gravity unit vector. In a conventionally levelled theodolite this would be (0,0,1), a pointing along the primary axis. The rotation matrix is such that this vector is rotated into the position (0,0,1), i.e.

$$R \cdot \begin{bmatrix} lg \\ mg \\ ng \end{bmatrix} = \begin{bmatrix} 0 \\ 0 \\ 1 \end{bmatrix}$$

By transferring R to the right hand side, three equations are again developed as before. This time lg, mg and ng are only dependent on the elements of the rotation matrix, and other parameters do not appear.

7.7 Standard least squares solution.

The problem is to solve the equations :

$$A \cdot X = L + V \qquad (1a)$$

where A is a coefficient matrix of order (m,n)
and each row of A represents an observation equation.

X	col. matrix of	n unknown parameters
L	col. "	n constant values
V	col. "	residuals

For Vt . V a minimum, the least squares solution is

$$At \cdot A \cdot X = At \cdot L \qquad (1b)$$

Each equation may be multiplied by a factor, z, using a diagonal matrix, Z, where Zt . Z = W, and the elements of W represent observation weights.

$$Z \cdot A \cdot X = Z \cdot L + Z \cdot V$$

where Z is order (m,m). This can be written,

$$A' \cdot X = L' + V'$$

For V't . V' a minimum,

$$A't \cdot A' \cdot X = A't \cdot L' \qquad (2a)$$

ie, for Vt . Zt . Z . V = Vt . W . V a minimum,

$$At \cdot W \cdot A \cdot X = At \cdot W \cdot L \qquad (2b)$$

which is the standard solution for weighted observations.

Since (1b) and (2a) have the same form, weights are easily included by modifying each observation equation by the appropriate factor, z.

7.8 Givens rotations.

Let R be an orthogonal matrix such that

$$R \cdot A = \begin{bmatrix} U \\ 0 \end{bmatrix}$$

where U is upper triangular of order (n,n), 0 is order (m-n,n).

hence, $$A = Rt \cdot \begin{bmatrix} U \\ 0 \end{bmatrix}$$

and substituting in (1) for Vt . V a minimum

$$[\ Ut\ Ot\ ]\ .\ R\ .\ Rt\ .\ \begin{bmatrix} U \\ O \end{bmatrix}\ .\ X\ =\ [\ Ut\ Ot\ ]\ .\ R\ .\ L$$

i.e. $$Ut\ .\ U\ .\ X\ =\ [\ Ut\ Ot\ ]\ .\ \begin{bmatrix} T \\ L' \end{bmatrix}$$

where T is (n,1), L' is (m-n,1) and where

$$R\ .\ L\ =\ \begin{bmatrix} T \\ L' \end{bmatrix}$$

i.e. $$Ut\ .\ U\ .\ X\ =\ Ut\ .\ T \qquad (3a)$$

or $$U\ .\ X\ =\ T \qquad (3b)$$

which is easily solved by back substitution.

and note $$At\ .\ A\ =\ Ut\ .\ U \qquad (4a)$$

$$At\ .\ L\ =\ Ut\ .\ T \qquad (4b)$$

7.8.1 Note 1

$$At\ .\ A\ =\ N\ =\ Ut\ .\ U$$

where N is the normal matrix

hence $$N^*\ =\ U^*\ .\ U^{*t} \qquad (5)$$

Since N* gives statistical information, such information is easily derived from U by the procedure in (5)

7.8.2 Note 2

$$Vt\ .\ V\ =\ [\ A\ .\ X\ -\ L\ ]t\ .\ [\ A\ .\ X\ -\ L\ ]$$

$$=\ [\ Xt\ .\ At\ -\ Lt\ ]\ .\ [\ A\ .\ X\ -\ L\ ]$$

$$=\ Xt.At.A.X\ -\ Xt.At.L\ -\ Lt.A.X\ +\ Lt.L$$

and substitute for At . A and At . L from (4) to obtain

$$Vt\ .\ V\ =\ Xt.Ut.U.X\ -\ Xt.Ut.T\ -\ Tt.U.X\ +\ Lt.L$$

but $U \cdot X = T$

also $R \cdot L = \begin{bmatrix} T \\ L' \end{bmatrix}$

hence $Lt \cdot L = [\ Tt\ L't\ ] \cdot \begin{bmatrix} T \\ L \end{bmatrix}$

or $Lt \cdot L = Tt \cdot T + L't \cdot L$

therefore

$Vt \cdot V = Tt.T - Tt.T - Tt.T + Tt.T + L't.L$

$Vt \cdot V = L't \cdot L$

7.9 Givens rotations in practice.

The matrix, R, is a product of k matrices, Rk . Rk-1 ... R1, and each is chosen to operate only on an upper and lower row of A. If the rows are p and q, then each R has elements such as :

	col p		col q	
	0	0	0	0	0
	0	0	0	0	0
row p	0	r(p,p)	0	r(p,q)	0
	0	0	0	0	0
row q	0	r(q,p)	0	r(q,q)	0
	0	0	0	0	0

The non zero elements are the 4 elements of a plane rotation matrix which can be written as :

$$\begin{bmatrix} c & s \\ -s & c \end{bmatrix}$$

where $c^{**}2 + s^{**}2 = 1.$

When the R matrix is multiplied out, corresponding elements, g and h of the upper and lower rows, are transformed into g', h', where :

$$g' = c.g + s.h$$
$$h' = -s.g + c.h$$

The rotating elements, c and s, are chosen to convert the first non-zero element of the lower row of A to zero. This lower row of A can be interpreted as the incoming observation equation, imagining them processed sequentially.

It is conceptually simpler to imagine the observation equations (1a), augmented by a set of n null equations [E3],

$$\begin{bmatrix} 0 \\ A \end{bmatrix} . X = \begin{bmatrix} 0 \\ L \end{bmatrix} . \begin{bmatrix} 0 \\ V \end{bmatrix}$$

The solution remains the same, but now the rotations are chosen to reduce A to zero, and fill the upper matrix, initially null, to form the upper triangle, U, i.e.

$$R . \begin{bmatrix} 0 \\ A \end{bmatrix} = \begin{bmatrix} U \\ 0 \end{bmatrix}$$

and

$$R . \begin{bmatrix} 0 \\ L \end{bmatrix} = \begin{bmatrix} T \\ L' \end{bmatrix}$$

In this procedure, the incoming equations have their coefficients, a, rotated up into U, and their constant elements rotated up into T (to leave a residual amount, L', used for finding the least sum of squares).

If U currently has its elements filled, the general action is as follows, accented elements are those affected by the rotation.

```
u u u u ....    u' u' u' u' ....    u  u  u  u  ....
0 u u u ....    0  u  u  u  ....    0  u' u' u' ....
0 0 u u ....    0  0  u  u  ....    0  0  u  u  ....
0 0 0 u ....    0  0  0  u  ....    0  0  0  u  ....

a a a a ....    0  a' a' a' ....    0  0  a' a' ....

initial state   after 1st. rotn.   after 2nd. rotn.   etc
```

The incoming row is processed with row k of U, where k is the column position of its first non-zero term (from the l.h.s). Although the rotation is applied to all elements of the "u" and "a" rows, the first (k-1) elements in both are zero, and remain unchanged. In this way the incoming row is reduced to zero, and U preserves its form.

Now consider the action in detail, with a rotation chosen to operate on the first row of U and a new observation equation, ie

```
 c   s          u1   u2   u3   ....   un          t
-s   c          a1   a2   a3   ....   an          1
```

Take d = sqrt (u1**2 + a1**2)

and c = u1 / d

s = a1 / d (6)

Apply the rotation to get

```
          u1'  u2'  u3'  ....  un'          t'
         (= d)

          a1'  a2'  a3'  ....  an'          1'
         (= 0)
```

where

$$u_i' = c \cdot u_i + s \cdot a_i$$

$$a_i' = -s \cdot u_i + c \cdot a_i \qquad (7)$$

$$t' = c \cdot t + s \cdot l$$
$$l' = -s \cdot t + c \cdot l$$

and $u1' = d$

$a1' = 0$ as indicated

As presented, a square root is needed for each rotation, and 4 multiplications for each conversion. Gentleman shows how an improvement can be made [E1].

Take the case that the observation equation is weighted with the factor, w. As explained above, this can be accommodated by multiplying through by z, where z**2 = w. (Note also that w and z can be unity in what follows.) Also factorize each element of the "u" row and obtain :

	p.1	p.p2	p.p3	.....	p.q
equivalent to	u1	u2	u3	.....	t
and	z.a1	z.a2	z.a3	.....	z.l

as a modified "a" row.

After rotation these become

	p'.1	p'.p2'	p'.p3'	.....	p'.q'
equivalent to	u1'	u2'	u3'		t'
and	0	z'.a2'	z'.a3'	.....	z'.l'

Clearly, p' = d = sqrt (p**2 + z**2 . a1**2)

or p'**2 = d**2 = p**2 + z**2 . a1**2 (8)

Make the following <u>definition</u> :

z' = (p . z) / d

or z'**2 = (p**2 . z**2) / (p**2 + w . a1**2)

= (p**2 . z**2) / p'**2 (9)

Now substitute p.pi, for ui, z.ai for ai, etc, in (7)

Note from (6) that c = u1 / d

s = a1 / d

hence c = p / d

s = z.a1 / d

Obtain p'.pi' = c . p.pi

\+ s . z.ai

or pi' = (p**2 / d**2) . pi

\+ ((z**2 . a1) / d**2) . ai

or pi' = (trf1) . pi

\+ (trf2) . ai

where (trf1) = (p**2 / d**2)

= (p**2 / p'**2)

(trf2) = (z**2 . a1) / d**2

= (z**2 . a1) / p'**2 (10)

Also obtain

z'.ai' = - s . p.pi + c . z.ai

from (9) z' = (p . z) / d

((p.z)/d) . ai' = - ((z.a1) / d).p.pi + (p/d) . z.ai

or ai' = - a1 . pi + ai (11)

similarly q' = (trf1) . q + (trf2) . 1

1' = - a1 . q + 1 (12)

This re-structuring permits the storage of p**2 instead of p, and w (=z**2) instead of z. Furthermore, only d**2 and not d appears, which avoids the computation of square roots (apart from the small number needed below).
Also, once (trf1) and (trf2) are computed, there are only 3 multiplications to update pi and ai, as opposed to 4.

Finally, since w is stored, not z, the same equation can be processed again with a negative weight, in order to remove it from the equations [E1].

The procedures in equations 8 - 12 have been written for rotation of the incoming equation against the first row of U. It is then rotated against all the other rows of U to reduce all its elements to zero.

In a computer algorithm, p**2 is stored on the diagonal elements of U, and the other elements of U and T in their factorized form. Before a back substitution can be carried out, it is necessary to

- take square roots of diag. elements of U
- convert the factorized elements to their correct format.

Note that z is initialized with the weight of the current equation.

* 7.10 Initializing the U and T matrices.

The above procedure requires non-zero values on the diagonal matrix, U, otherwise a factor p cannot be found to start the process.

Cox [E3] explains how processing the first n equations, when U starts off as a null matrix, is slightly different. This might initialize diagonal elements to non-zero values, but this is not certain. Instead, the following procedure is used. Imagine n "pseudo" equations are created, one for each parameter, and which have the form

$$0.x1 + 0.x2 .... + 1.xi .... + 0.xn = 0 + vi \quad \text{(weight =1)}$$

for an iterative solution

$$0.x1 + 0.x2 .... + 1.xi .... + 0.xn = ki + vi \quad \text{(weight =1)}$$

for a direct solution

In the iterative case, the equation states that parameter xi has a trial value of zero, which is the starting point for any solution.

In the direct case, the equation states that parameter xi has some trial value ki. Usually a good estimate of all parameters will be available from an approximate solution to any problem. (In theory, this is not necessary and arbitrary values, say zero, could be used).

These pseudo equations are then processed, followed by the real equations. Then the pseudo equations are removed, by re-submitting them with negative weights (=-1). This apparently pointless procedure has the advantage that the pseudo equations initialize the U matrix to a unit matrix, and T to a vector of zeros or constants. The real equations can then proceed without any further modification.

Adopting this process, the structure of the equations to be solved now becomes (for an iterative solution) :

$$\begin{bmatrix} 0 \\ I \\ A \\ I \end{bmatrix} \cdot X = \begin{bmatrix} 0 \\ 0 \\ L \\ 0 \end{bmatrix} + \begin{bmatrix} 0 \\ Vp \\ V \\ Vp \end{bmatrix} \quad \begin{matrix} \\ \text{(weights +1)} \\ \text{(weights w)} \\ \text{(weights -1)} \end{matrix}$$

where I is a unit matrix.

Although the initializing pseudo equations are processed simply by making U a unit matrix and T a zero column, they can only be removed by processing in the same way as real equations.

* 7.11 Fixing parameters.

If some parameters are to be fixed, the obvious method is to remove them as unknowns from the equations, but this is not the only choice.

It is convenient to formulate many problems as though all parameters were unknown, and then provide some standard way of fixing a subset which may vary. For example, a general space resection would set all 6 instrument parameters variable if it were a full 3-D resection (3 position, 3 rotation), but only 4 if a plane resection (3 position, 1 rotation).

In a computer program this could be done by using some additional arrays :

Marker	1	1	1	0	1	0	0	1 ...
Column number	1	2	3	0	4	0	0	5 ...
Parameter	x1	x2	x3	x4	x5	x6	x7	x8 ...
Coefficient	c1	c2	c3	c4	c5	c6	c7	c8 ...

Here parameters x4,x6,x7 are to be fixed, and are marked with zeros in the marker array. Variable parameters are marked with corresponding unity values. If the fixed variables are removed as unknowns, then the 4th position in the parameter array is actually used by x5, the 5th by x8, etc. It is only necessary to condense the coefficient array so that the correct values match up with the correct column numbers before processing. The solution vector is then correspondingly expanded to match up again with the unknowns. Only those with non-zero marker or column numbers are updated.

Alternatively, imagine the fixed parameters carried in the solution. If a parameter is fixed, its coefficient is zero. By multiplying each element of the marker array with the corresponding coefficient, the correct coefficients can be obtained.
Additionally, for each fixed parameter, include a pseudo equation of the form above.
Finally, re-arrange the parameters so that the first ones are the fixed ones. The observation equations then have the form :

1	0	0	0	0	0	0	0	x4	0	v4
0	1	0	0	0	0	0	0	x6	0	v6
0	0	1	0	0	0	0	0	x7	0	v7
0	0	0	c1	c2	c3	c5	c8	x1	11	v1
0	0	0	.	.	.	.	.	x2	12	v2
0	0	0	.	.	.	.	.	x3	12	v3
0	0	0	.	.	.	.	.	x5	15	v5
0	0	0	.	.	.	.	.	x8	18	v8

etc

This is the same as

$$\begin{bmatrix} I & 0 \\ 0t & A \end{bmatrix} \cdot \begin{bmatrix} X' \\ X \end{bmatrix} = \begin{bmatrix} 0 \\ L \end{bmatrix} + \begin{bmatrix} V' \\ V \end{bmatrix}$$

where fixed and unknown variables have been split up into X' and X. (Note that the zero matrices are of different orders.)

The standard solution is given by :

$$\begin{bmatrix} It & 0t \\ 0 & At \end{bmatrix} \cdot \begin{bmatrix} I & 0 \\ 0t & A \end{bmatrix} \cdot \begin{bmatrix} X' \\ X \end{bmatrix} = \begin{bmatrix} It & 0t \\ 0 & At \end{bmatrix} \cdot \begin{bmatrix} 0 \\ L \end{bmatrix}$$

which reduces to

$$I \cdot X' = 0$$

or $X' = 0$ as required

and $At \cdot A \cdot X = L$ standard solution

The solution of equations is not affected by re-ordering the parameters, and so this solution will hold in the original case. It is obvious that the technique can be combined with the procedure for initializing the U and T matrices. The steps are as follows :

1) Initialize U,T with pseudo equations.
2) Form the marker array.
3) Compute all coefficients as though all parameters were variable.
4) Use the marker array to reduce coefficients of fixed parameters to zero.
5) Process the observation equations as usual.
6) Remove all initializing equations EXCEPT those corresponding to parameters with zero values in the marker array.

Ch. 8 Automation.

The previous chapters effectively conclude the research program of the thesis. It is my intention here to make suggestions for future work and speculate on the possibilities for industrial photogrammetry and surveying. Much of this derives from unsuccessful efforts to find support for a research proposal which was intended to develop new instrumentation. The ideas were based on the application of electronic imaging, and lead logically to a discussion of fully automatic measuring systems. These tend to be of a hybrid nature, employing both survey and photogrammetric concepts. It is therefore entirely appropriate that they appear in a thesis which presents a general approach to triangulation.

In the search for existing ideas, a number of papers dealing with robot performance measurement were discovered. These come from sources not directly related to photogrammetry and surveying, but a common feature is the use of triangulation to derive target coordinates. The information which these sources offer is quite extensive, and the application is rather different from the analysis of static objects which form the bulk of current industrial photogrammetry and surveying. Although it is obvious that robot movement can be analysed by the methods presented here, full automation is a distinct advantage in dynamic situations.

Robot performance measurement is an interesting task. Typically there is a need for both static and dynamic information. For example, the static question of whether the robot's encoders will always return it to the same position, and the dynamic question of exactly which path is taken when it moves from point to point.

Parker [W1] reviews the problem, describing some of the methods used by mechanical engineers as well as the application of survey and photogrammetric techniques.

Warnecke and Schiele [W2] supply similar information and mention the dual theodolite approach. Interestingly, both these papers report on a technique which a surveyor would recognize as trilateration, and which positions a robot dynamically by continuously measuring its distance to three fixed points. Priel and Schatz [W3] hope to develop a photogrammetric approach

Surveyors and photogrammetrists have their own motivations for investigating automated instruments. Ideally, the speed and convenience of data acquisition, as offered by photogrammetry, should be combined with the immediate results which surveying can provide. The major impediment to the photogrammetric approach is the photo-chemical processing stage, and some form of electronic imaging is needed. As implied, surveying may be too slow on site, unless there are only a small number of points to be measured. Avoiding the human operators and motorizing the instruments is an obvious route to consider. Even at this early stage, both comments immediately suggest some form of photo-theodolite.

8.1 Electronic imaging and the photo-theodolite.

To surveyors and photogrammetrists, automation often suggests electronic imaging with "CCD" arrays. This is the route being taken by digital photogrammetry and automated survey systems. Considerable support is available from the technology of image processing, and photogrammetric ideas are readily applied. However, they are not the only possible sensors. The potential application of polarimetry, outlined in Ch. 2, demonstrates an alternative.

Very briefly, CCD arrays are "Charge Coupled Devices". These electronic, solid state sensors produce a charge in response to incident light. They can therefore record a photographic image as a pattern of charges, rather than a varying deposit of silver as in a conventional photograph.

Conductors on the surface set up "potential wells" into which the charges from a local area flow and are held, until read out and recorded. Effectively, each well has averaged out the charge in its local area. This creates a digitized image composed of picture elements or pixels, each recording the local average gray level, or intensity of the image.

An area array sensor sets up a rectangular array of such pixels. In television applications the pixels typically number about 400 x 300. For scientific work larger arrays are now available, such as the Kodak Megaplus offering 1320 x 1035 [S1].

A linear array sensor generates only a single line of pixels, but offers more pixels in one direction, possibly up to 5000. A full 2-dimensional image can be created by mechanically scanning this array across an image plane.

CCD arrays offer the considerable advantage of image stability. Geometrically, the pixels are in well-defined positions, although cameras developed for television applications are not ideal in this respect. From optical image to computer frame store, where the pixel values are held, data are distorted and possibly lost. This is not an inherent feature of such devices, and when properly designed for measurement purposes, as is the Megaplus, the problem should not exist. The other advantage of solid state arrays is that deformations associated with films and plates are avoided.

Probably the most important question to be asked in connection with CCD arrays is what effective resolution they can offer. Since any new instrument will be essentially an angle measuring device, it is convenient to think of resolution in angular terms. To be useful, this must be competetive with current instrumentation.

Working with a one second theodolite such as a Wild T2, I have obtained typical residual pointing errors of 1 - 2 arc secs.
A Wild P32 metric camera, with a principal distance of 65mm, has typically shown image residuals of 3 - 6 microns. These are roughly equivalent to 10 - 20 arc secs.
My own and other work with a Zeiss Jena UMK 10 metric camera, principal distance 100 mm, suggests that residuals of 2.5 microns could be considered a good result. (See some of the papers on antenna measurement in the reference list). This resolution is approximately equivalent to 5 arc secs.
It therefore seems reasonable to state that any new angle measuring instrument should aim at a pointing accuracy of 5 arc secs. or better.

Before considering what a CCD array might achieve, it must be remembered that the position of a target in an image can be determined to better than a single pixel. The extent to which image coordinates can be interpolated as fractions of a pixel is clearly of immediate importance. The smaller the fraction the better the pointing resolution. It will depend on the quality and nature of the target's image, as well as the image processing algorithm used to find its centre. Buechli et al [S4] give a simple argument to explain why it should be possible to interpolate to a small fraction of a pixel. Imagine that each pixel can recognize 300 gray levels, and the perfectly sharp edge of a target image, black on one side, white on the other, moves across a pixel. Obviously, 300 separate increments in movement can be detected as the gray level changes, and in principle the interpolation factor is 1/300. They report just such a high interpolation factor, but it is much more common to read of factors around 1/10 pixel. This is quoted, for example, by Luhmann [S6], although Zhou [S5] manages 1/20 and Dennison and Stanton [S3] suggest 1/50. If a little optimism may be permitted, I would suggest 1/20 as a realistic figure for well defined targets.

To estimate the angular resolution associated with a CCD instrument, which must be some form of camera in the context of the current discussion, it is only necessary to consider the angular field of view divided by 20 times the maximum number of pixels in one direction. Imagine a 50 deg. field of view offering 5 arc sec. resolution. With this facility, fixed camera positions, total object coverage and a respectable coordinate accuracy should be possible. Unfortunately, the CCD array must then have 1800 x 1800 pixels, which is not a realistic option at present. However, the Megaplus might manage 10 - 15 secs. and offer serious competition to the P32.

A linear array scanned across the image field could certainly achieve this resolution, although the scanning mechanism must be very precise. I prefer the solution adopted by Wester-Ebbinghaus and Rollei, in which a small area array is stepped across the back of the camera [U5]. Precise positioning is provided by a reseau plate. In each stepping position the array images 4 of the reseau crosses, which enables this portion of the full image to be located in a common coordinate system. The final image is built up as a composite. Due to the accurately manufactured reseau, stepping need only be precise enough to ensure 4 reseau crosses are imaged each time.

The other way of employing a small array is to scan it by rotation. Wester-Ebbinghaus has himself recently proposed this idea [S7]. His arrangement is exactly the electronic equivalent of the conventional photo-theodolite. His proposal is to attach a CCD camera to the telescope of a theodolite, much as a P32 is attached to a T2. Knowing the orientation of the camera with respect to the theodolite, the data from the small format, narrow angle sensor can be incorporated in a common reference system. He clearly envisages adjusting all data together in a program such as MOR [E7], outlined in Ch. 4.

The rotational scan, embodied in an electronic photo-theodolite, is my own preference. It has the advantage that moving objects such as robots can be tracked. Contrast this with the linear scanning methods above which operate in a systematic way and can only analyse static objects.
Furthermore, the facility to view in almost all directions makes it particularly easy to establish reciprocal observations with another instrument. I would also go further than Wester-Ebbinghaus, and specify two further features of this instrument.

Firstly, the camera's projection centre should be located at the centre of rotation, which simplifies the geometry. In the event that there remains an offset, or the projection centre cannot be defined by a single point, an analytical approach such as described by Mayer and Parker could be adopted [U19].

Secondly, the angle of view should be as wide as possible, consistent with the required pointing accuracy. Several reasons justify the suggestion.

With a wider angle, faster scans of static objects are possible. It is also advantageous for the tracking mechanism, which does not then need a very sensitive response to object movement. (Once the field of view is wide enough, the instrument need not itself move).

Wide angles further simplify the task of tracking multiple targets. For example, three points on an object can define both its position and angular orientation. If these could be simultaneously intersected from two positions, all 6 parameters could be continuously monitored. Multiple targets may also appear as external lens targets, mentioned in Ch. 4. The electronic photo-theodolite could then easily sight to a conventional camera operated from an unstable position.

Lastly, the wider the angle, the shorter the focal length. This implies a greater depth of field, and for a given application it may well be possible to adopt a fixed focus. With fewer moving parts, the internal geometry of the instrument is more stable and improved accuracy should be the result. Admittedly, the relative aperture will be smaller, and the optical resolution would not be as high. However, this is unlikely to be a problem with the proposed targetting.

To give an idea of a suitable field of view, consider a Megaplus imaging chip combined with a 20 mm lens. The sensor area is approximately 7 mm wide and high, with approximately 1000 pixels in each direction. This gives an angular field of view of about 20 degs., and with 1/20 interpolation the pointing accuracy is around 3.5 arc secs. It would then be appropriate to incorporate 1 arc sec. angular encoders in the photo-theodolite, and realistic to expect better than 5 arc secs. pointing accuracy overall.

In targetting, my preference is to avoid the direct use of an object's surface texture, and so stereoscopic methods and correlation techniques are not considered here. Targets are much easier to identify unambiguously, which simplifies the task of automation. If they can be optically distinguished from their background, this greatly reduces the information to be processed and further assists computation. Three options appear regularly.

1) Brightly illuminated, retro-reflective targets result in images which are virtually "star fields", i.e. sharply defined targets set against a black background.

2) Self-luminous targets can be colour coded and observed with corresponding filters. If this is not sufficient to isolate them from the background, they can additionally be pulsed (intensity modulated) to help pick them out.

3) A scanning laser spot and appropriate colour filter works in a similar way. By illuminating a small part of the object's surface a single point is effectively isolated.

Once isolated targets are accepted, multi-ray intersections may be employed to improve coordinate accuracy.
Furthermore, image abberations are acceptable provided they are systematic or, preferably, symmetrical about the nominal image position. The CENTRAX demonstrates this principle very well. Its images are virtually useless as conventional photographs, as they suffer from extreme spherical abberation. However, isolated points image with a well defined ring pattern which is the key to a very accurate measurement of their image coordinates. Low optical resolution and out-of-focus effects should not, therefore, necessarily affect instrument performance.

This discussion has lead to some concrete ideas for a future hybrid instrument, the electronic photo-theodolite. There is still a need to discuss calibration, and perhaps the specification of one or two more design features, but a brief discussion of competitive ideas will help put it in perspective.

8.2 Review of automated triangulation systems.

I designate as purely photogrammetric those systems which employ fixed cameras for triangulation.

The Rollei system has already been introduced, and qualifies as purely photogrammetric since the camera is fixed, despite a mechanical scan to build up a full image. The system is still under development, but is likely to produce the most accurate results in digital industrial photogrammetry. Complete images are obtained which can be analysed by the full range of image processing techniques.

Mapvision [U4] has been under development in Finland over the past 4 years, and has recently been taken up by Wild-Leitz as part of the Elcovision system. 4 CCD cameras view an object illuminated by a scanning laser spot. A single point measurement takes 1.5 secs.

Although the camera geometry is not given, it is implied that the field of view covers objects of interest and achieves an accuracy of 1 : 10 000 within this field. This is not particularly high for industrial work, although the authors seem to think that there are applications.

The Vicon system [U11] is certainly not high accuracy, but is applied in a field where the accuracy is sufficient. The application is the analysis of human gait. Typically, 4 vidicon (rather than CCD cameras) point towards a test area, and the subject, wearing small adhesive retro-reflective targets, walks through. Around each camera lens is an infra-red stroboscopic lamp, and in front of the lens an infra-red filter. This freezes an image on each camera frame of the targets, and the sequence of corresponding frames provides an analysis of the movement a few minutes after recording the data. The system has been sold commercially.

Another system in commercial use is Selspot [U13]. Light emitting diodes (LED) are used as self-luminous targets for cameras which have position sensing devices (PSD) in the image plane. The PSD operates by finding the centre of gravity of an image spot within its sensitive area. It can therefore only observe one target at a time. Multiple targets are observed by sequentially illuminating them, and the system can handle up to 16 cameras and 128 targets. Sold as the Selspine Robocheck, a dual camera arrangement is used for robot calibration, and is supplied with specially tailored software.

Moving on to pure surveying systems, these are theodolites which have been modified with motor drives and CCD camera viewing down the telescope. Both Wild [3] and Kern [U1,U2] have developed commercially available versions, although I have not yet obtained information on specific applications. Although these systems can be fully remotely controlled, they still provide all the necessary functions for manual use.

This may well be an intermediate step taken by the manufacturers because it is simpler to develop existing instruments rather than move directly to a robot theodolite. However, dual purpose instruments seem to me to be unnecessarily complicated and are inevitably expensive. I believe the cheapest instrument possible should be one of the development goals.

Theodolites modified in this way are obviously very similar to my proposals for an electronic photo-theodolite. The field of view of a telescope is around 1 - 1.5 degs. and so much less than I suggest. Automatic focussing is also a requirement which I would prefer to avoid, but unlike the suggestion from Wester-Ebbinghaus, the camera view is here co-axial with the telescope view.

The closest example I have found to the electronic photo-theodolite has been described by Foud [U7]. He has taken a video camera with a 4 deg. field of view, and supported it in a rotating mount. The suggested application is architectural. Two devices are levelled and scan the building horizontally and vertically. A reciprocal pointing provides a horizontal reference. Unfortunately, the author is much too vague on details such as calibrating and targetting the devices, and it is difficult to judge if he has succeeded in constructing an accurate instrument.

The final three examples still employ triangualtion, but the instrumentation cannot be described as camera, theodolite or photo-theodolite.

CODA 3 [U10] is an instrument which scans fan-shaped beams of white light through the measurement volume. Targets are small corner-cube reflectors, colour coded for identification purposes. A single scanning unit makes a measurement by recording the encoder angle when a return flash is seen. Three scanning units are fixed in a rigid box. Two rotate about vertical lines, with their beams in vertical planes. A common target can therefore be placed on the intersection of the planes, which is a vertical line.

The other unit scans its beam about a horizontal axis and finds the position of the common target along the vertical line. Targets are therefore located by the intersection of three planes rather than two rays, but the principle is still one of triangulation.

Professor Graham Parker at Surrey University is developing a laser tracking system capable of locating a point moving at 5 m/s to an accuracy of 0.1 mm. The device has already been mentioned. Each tracker contains a laser beam and two mirrors rotating about orthogonal axes. The beam is reflected off the mirrors towards a corner cube reflector attached to a robot. A sensor detects the return beam and uses any offset to correct the pointing. Two such devices intersect a single target point.

As Mayer points out [U19], this only gives positional and not rotational information about the robot. He then proposes the use of three instruments, each individually tracking a single reflector on a cluster of three. The relative positions of the three targets are known. Although each is not fixed by intersection, but located on a line in space, there is still sufficient information to determine all 6 orientation parameters of the cluster. This is not surprising, as the situation is no different from a space resection.

Mayer's idea has similarities with my suggestion that two photo-theodolites could track and intersect three target points to do the same thing. In fact, if the relative positions of the targets are known, only one photo-theodolite is, in principle, necessary. Although very economical, I would be doubtful about the accuracy, given subtended angles which are rather small for accurate resection. Still, returning to the idea of two photo-theodolites, it is worth noting that they need not each track the same targets. A good solution may be possible if they each point roughly at right angles to one another and track different target clusters, assuming relative target positions are known.

The minimum configuration for a solution is two targets for one instrument, one for the other. Two for each is already over-determined.

The final example has more similarity with theodolite technology. Lau et. al. at the US National Bureau of Standards also propose a laser tracking system [U15]. In this arrangement, a single mirror is rotated about two axes to direct a laser beam onto a target attached to a moving robot. There is only one centre of rotation, unlike Parker's system, and a direct analogy with an automated theodolite. The target is most interesting. It, too, is a plane mirror, actively controlled about two axes to return the laser beam back to the tracking instrument. This could be described as a miniature theodolite, and the situation is one in which two theodolites maintain a reciprocal pointing.

The NBS development incorporates an interferometer in the laser, to measure the separation of the mirrors to a high accuracy. The surveying analogy with an EDM measurement along a traverse line is inescapable. However, it is apparent that only 5 of the 6 orientation parameters at the target can be determined. The missing 6th. is a rotation about the connecting line. The authors themselves point out the close similarity with surveying and the fact that not all degrees of freedom (orientation parameters) are obtained at the target.

It is difficult to resist the question of how all 6 parameters might be derived. Each instrument cannot simultaneously sight an offset point. Conceivably, each could be levelled. The difficulty at the target instrument is the effect of movement on a level sensor. Accelerations cannot be distinguished from the effects of gravity, but they might be separately monitored by accelerometer. Even if this were possible, or accelerations were negligible, the dynamic response of the sensor could cause difficulties.

Adding a polarimetry measurement to the laser system would be a solution, at the expense of a complicated instrument. If the interferometric measurement were removed, relative separation could be computed by having a separate instrument track another single point on the robot.

This discussion on alternatives will be concluded by a brief outline of a novel idea which I proposed some time ago, but which may have been superceeded by other events.

8.3 Starburst images.

Despite the conclusion that it is necessary to scan a CCD array in order to obtain high resolution pointings, I was reluctant to discard the concept of a fixed, wide angle camera of, say, 50 degs. field of view. Linear arrays can subtend such a wide field, but unfortunately these only give a line image, and once again scanning seems to offer the only method of covering a full field of view. However, if unconventional images are accepted, alternative approachs are possible. These rely on creating line images of targets which are active light sources.

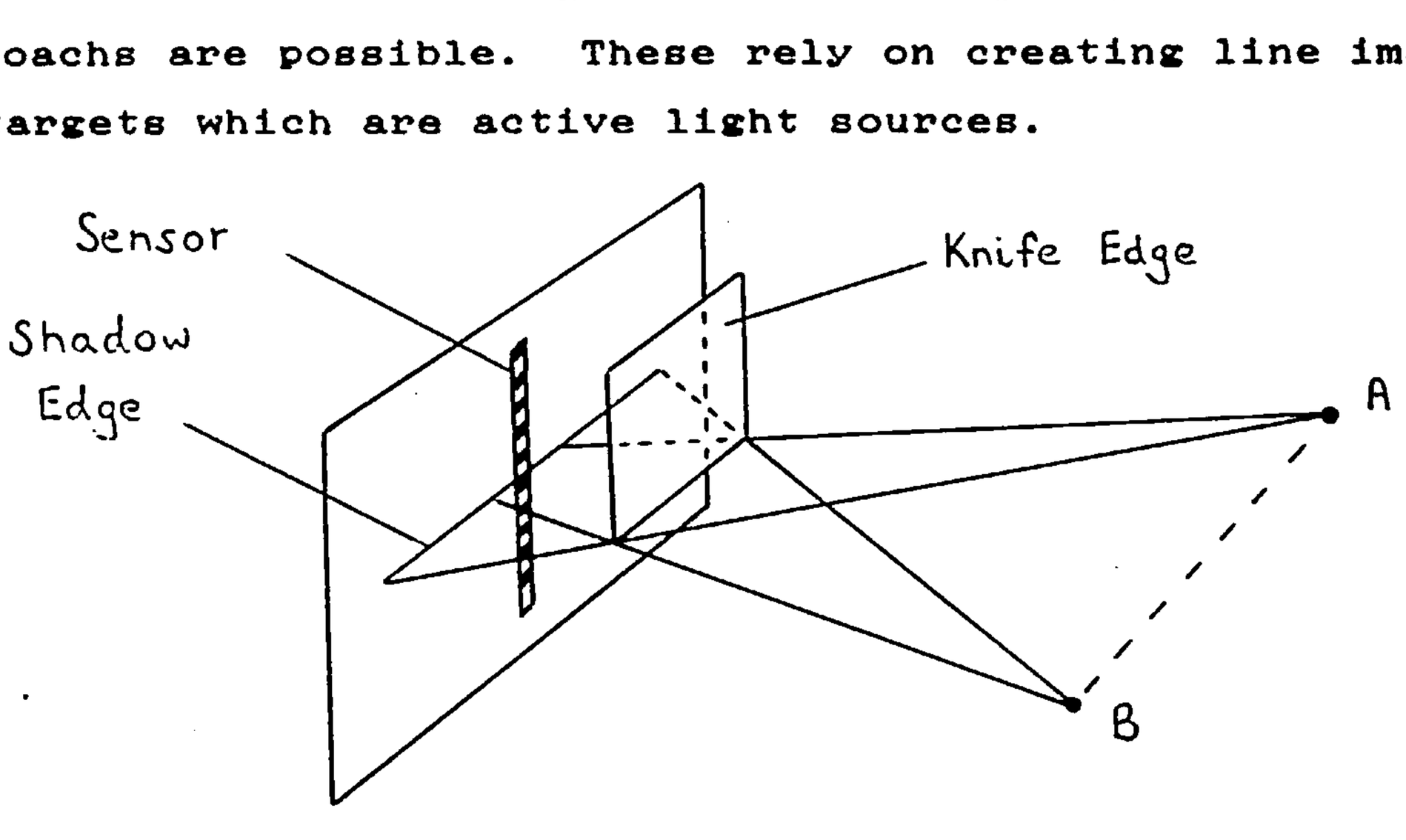

Figure 8.1 Shadow sensor.

Fuchs et. al. [T2] describe a shadow sensor, shown in fig. 8.1. A knife edge is fixed a short distance from a linear array, with the array aligned perpendicular to the edge. A luminous target at point A casts a shadow of the edge on the sensor, and the position of the edge is easily detected.

The information is sufficient to place A on a plane. This can be seen by considering a second point B which casts a shadow on the same point of the array. The plane is defined by this point and the line of the knife edge. If three such devices are employed, any point can be fixed in space by the intersection of three planes.

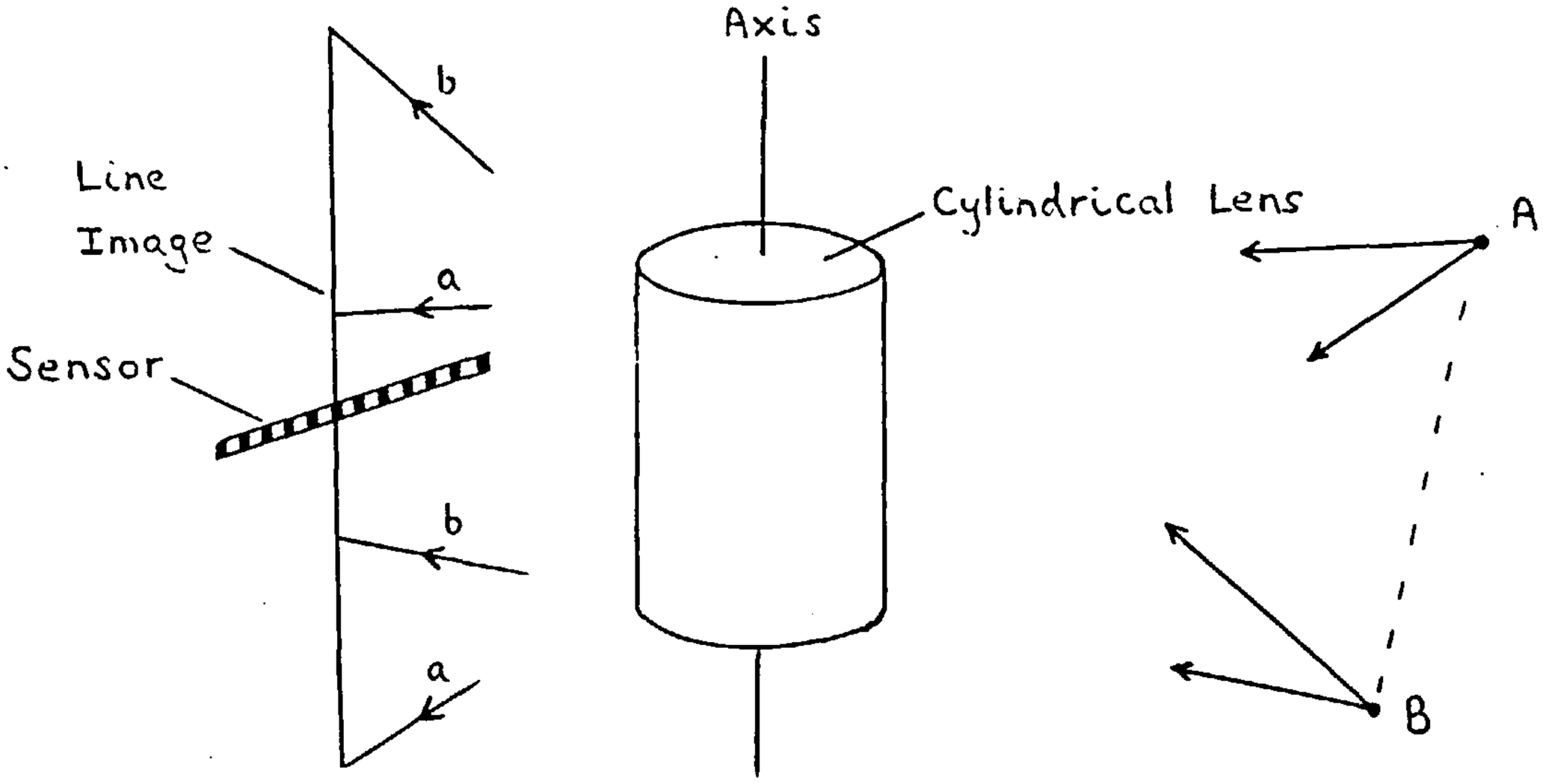

Figure 8.2 Cylindrical lens.

Yamashita et. al. offer another approach. This time the linear sensor is combined with a cylindrical lens. The sensor lies in the focal plane of the lens and at right angles to the axis of the cylinder. The lens converges incident light in one direction only, and a light source at point A will create a line image parallel to the cylinder axis. Once again, this is sufficient to place A on a plane defined by the image position on the sensor and the axis of the cylinder. Intersecting planes then locate the point in space.

Both systems have been made to work, but neither offer engineering accuracy. Discussions at NPL indicate that cylindrical lenses have some restrictions associated with them. In particular, the angle subtended by two points A and B in the direction of the axis cannot be very large, and this may limit the field of view.

My own approach to creating linear images is to use the property of diffraction.

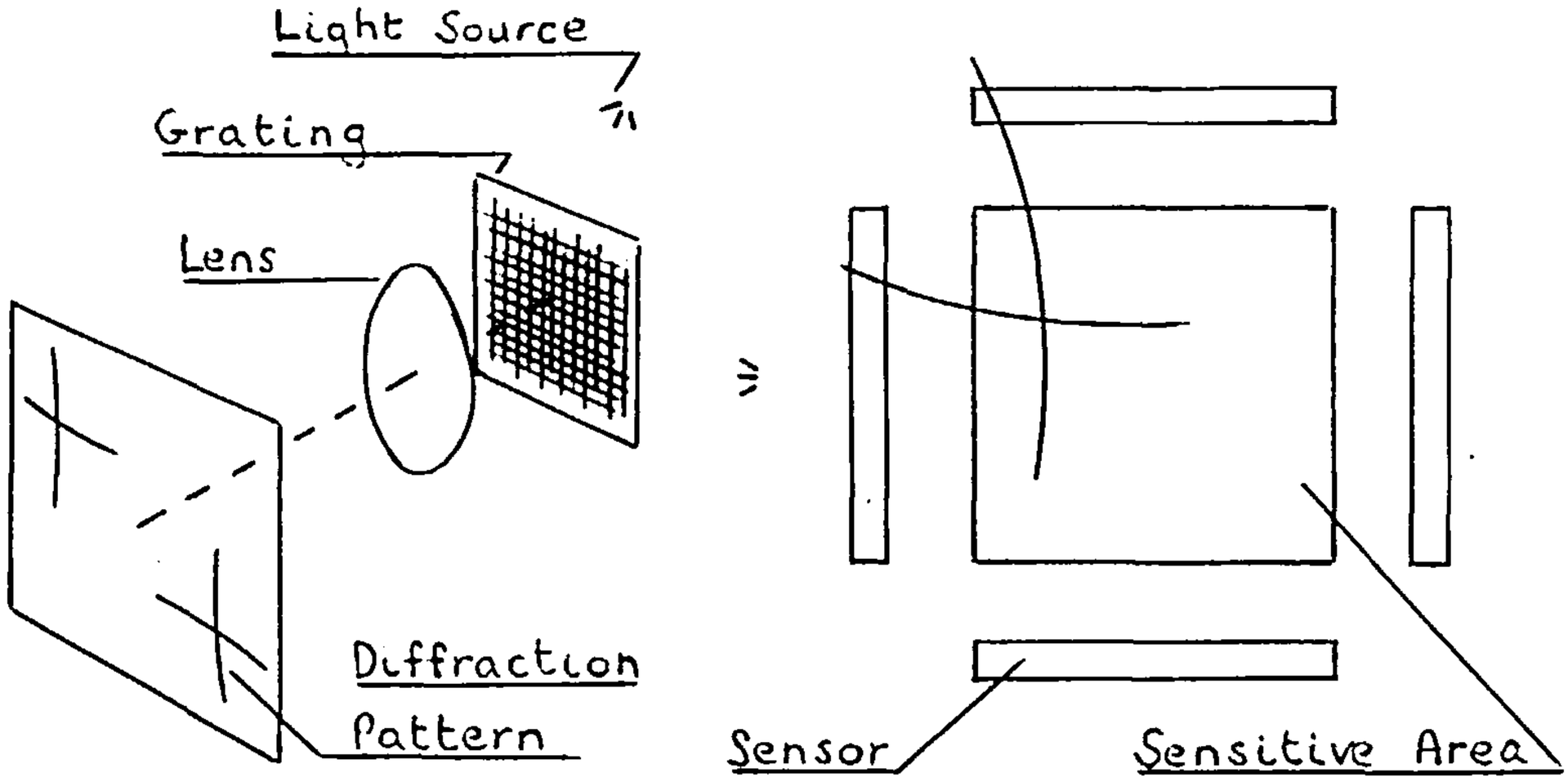

Figure 8.3 Starburst effect.

A conventional camera is used, and the target is bright white light source. A filter, similar to a photographer's "Starburst" filter, is placed in front of the lens. This filter is a crossed grating of randomly spaced, parallel lines. The image of the light source is diffracted by the filter into a cross, with very extended and curved arms. In the image plane are a number of linear arrays, fixed in position. The size of the cross is such that the arms will always intersect some of the arrays, irrespective of the target's position within the field of view. From the intersection positions and a knowledge of the form of the curved lines, the centre of the cross may be calculated. This is the required image position.

If each array is, say, 2000 elements long, the sensitive area would be approximately 2000 x 2000 elements, and this would be the size of the equivalent area array to do the same job. There is a very large saving in data storage with this approach. In the example only 8000 pixels are needed. Even a crude 100 x 100 area array has 25% more, i.e. 10000.

With the help of Dr. Jim Burch at NPL, several gratings were manufactured from good quality "perspex". The diffracting lines were made by drawing a pad of abrading material in a straight line across the surface. This was done for each surface. The two sets of abrasions were at right angles to one another, and the abrading material ensured that the lines were randomly spaced. A similar effect is created by a windscreen wiper on a dirty windscreen, and many people will be familiar with the way this causes lamps at night to be diffracted into long lines.

There are a number of issues to be resolved, and important points to be noted, before the idea can be implemented in a successful instrument.

1) The positions of the linear arrays within the image plane must obviously be known from an initial calibration procedure, otherwise the image coordinates of the intersection points cannot be determined.

2) The rulings of the grating must be randomly spaced in order to create a homogeneous image. If they are regularly spaced, a normal diffraction grating is obtained which will disperse the component colours of the image. A monochromatic target spot, which may be needed for identification purposes, will then diffract into curved lines of dots and not solid lines. Solid lines are needed to ensure that there is always an intersection with the linear arrays.

3) Laser light does not give as good an image as monochromatic or white light. There is still some residual "structure" in the rulings which gives a cross with rough and broken lines, rather than smooth solid lines.

4) The arms of the cross are only straight lines if they pass through the principal point of the image, otherwise they are curved.

The family of curves resembles "pin- cushion" distortion, and must be evaluated and modelled in order to achieve the correct intersection of the arms. Dr. Burch has suggested that the curves may be simple circular arcs.

5) Other arrangements of linear arrays may be more suitable. For instance, several could be set parallel to one another and at approximately 45 deg. to the diffracted arms of the cross.

6) The light energy from the target is imaged along two lines, rather than into a single spot, and the image may be very weak. If background illumination is significant, a problem will exist in distinguishing the signal. Devices such as LEDs may not be adequately bright, and a very high intensity, self luminous target may be required. It may also help to modulate and colour code the target.

This problem will be compounded if the target is moving rapidly and a very short exposure is required to freeze the motion.

7) There is a potential problem if multiple targets must be tracked simultaneously. One solution is to diffract in three directions rather than two, i.e. create a cross with three arms. Alternatively, it may be possible to design a set-up so that the intersections for each cross are always separate. An initial, sequential illumination of each target will identify to the instrument which intersections belong to which target. Several targets can then be tracked by extrapolating from the last position. Yet again, sequential illumination, as employed in the Selspot system, may be sufficient.

Regretably, the funds to follow up the idea were not available. It is easier to gain access to CCD cameras with area arrays, although this was not successful either.

Nevertheless, Dr. Roger Hunt at NPL pointed out that with an area array camera, a grid of linear arrays can be simulated simply by designating certain rows or columns as defining the grid. The further advantage is that the actual image position is available for comparison with that derived from the intersections of the selected rows or columns. With an area array camera there is scope to design a comprehensive research program to investigate both the electronic photo-theodolite and the Starburst effect.

The Starburst has also prompted another thought. When observing isolated targets with a photo-theodolite, would pointing accuracy improve if the image were diffracted by a conventional crossed diffraction grating? Take the case of a single retro-reflective target, illuminated by mono-chromatic light. In addition to the normal, zero-order image, higher order images are obtained above, below and to either side of this. More pixels are now "sensitive" to the target, which should make it easier to detect a smaller shift in target position. From another point of view, the higher order images can be used to interpolate the zero order. In a sense, a beneficial averaging effect is introduced.

This feature may enable a photo-theodolite to be converted back into a theodolite of higher accuracy, simply by replacing a cover glass with the same refracting properties as a diffracting filter. This variation is described as a theodolite because it would directly point at every target by centring its diffracted image within the field of view.

8.4 Calibrating the photo-theodolite.

When functioning as a theodolite, an electronic photo-theodolite can avoid instrumentation errors by measuring on both faces. As a photo-theodolite, a full camera calibration is necessary. I suggest that this be done by a development of Scott's method, presented in [B10].

This is a method of calibrating cameras focussed at close range, by determining the object space ray corresponding to any image point. A mathematical model may then be chosen which converts image coordinates into space directions.

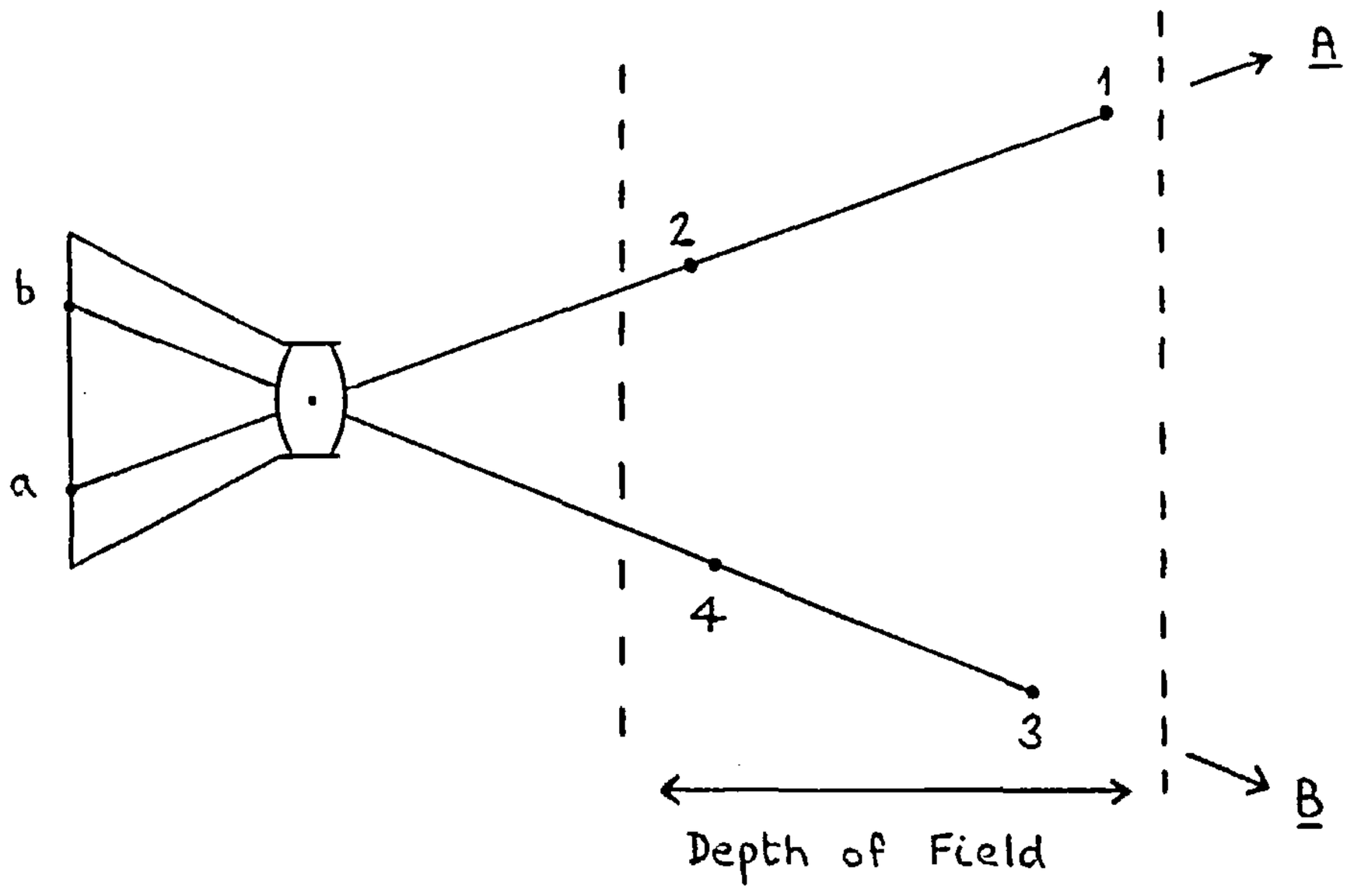

Figure 8.4 Scott's calibration method.

In Scott's original method, a control point field was set up which radiated away from the perspective centre. The objective was to ensure that pairs of targets had the same image position.
As fig. 8.4 shows, such targets therefore define the ray in space corresponding to a particular image position.

Using conventional photography, careful setting up of the targets is required to achieve the imaging condition. In fact, targets must be deliberately mis-aligned to ensure that they are all visible on the photograph. However, with an electronic camera it is possible to achieve exactly the condition that two or more points have the same image position. Furthermore, the proposed development of the method does not require a large control point field. In fact, a single target on a "linear" rig will suffice. Consider the following sequence of diagrams.

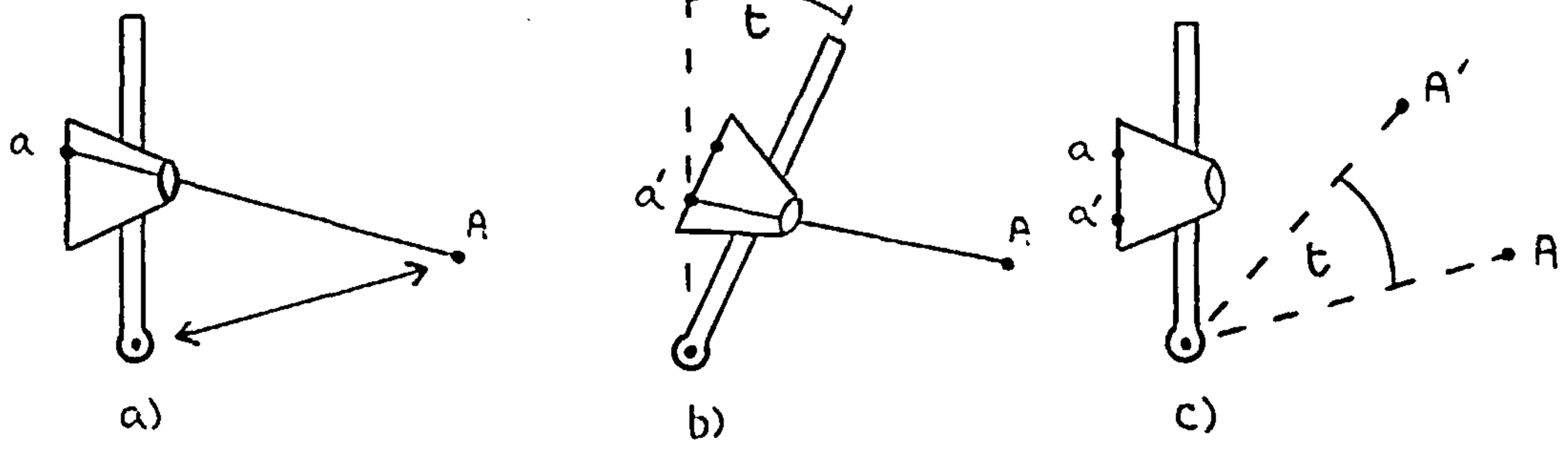

Figure 8.5 Electronic camera calibration.

A camera is located on a rig so that it may be rotated about two axes. The centre of rotation and the projection centre do not have to coincide, although it will be convenient if they are close. In fact, the electronic photo-theodolite could function as its own calibration rig.

The diagram shows only one rotation for convenience. A single target is located at a known distance, D, from the centre of rotation, fig. 8.5 (a). The direction from the rotation centre to the target is a datum direction which must be known.

A control point field is built up by rotating the camera so that the target is imaged in a new position, fig. 8.5 (b). Clearly, this is equivalent to rotating the target through the reverse angle, whilst keeping the camera fixed in position, fig. 8.5(c). From the angles of rotation and the distance, D, a series of new target coordinates can be derived, considering the camera to be held fixed.

After generating an array of image positions which cover the field of view, the separation of the target and calibration rig is altered and the process repeated. However, this time the same image positions are used. The steps are :

1) Set the approximate image position using the same angles as before.

2) Compare this with the required position and compute correction angles if necessary.
3) Iterate this process until the same image position as before has been found.

Obviously this can be done manually, but it could equally well be automated. By repeating the process for several values of D, the object space rays can be determined to a good accuracy.

Several points can be made concerning the method.

1) The closer the perspective centre is to the rotation centre, the less accurately D must be measured. In fact, if they coincide, D need not be measured at all! Since the determination of the perspective centre is part of the problem, this condition cannot be achieved initially.

2) The closer the centres are, the easier it is to iterate to common image positions.

3) Despite these facts, a simple rig would be obtained by attaching a camera to a theodolite telescope. This is the arrangement proposed by Wester-Ebbinghaus.

4) A datum direction must be known at each distance setting. If a theodolite is used as a calibration rig, face left and right observations, prior to attaching the camera, should provide this. The same applies to the photo-theodolite if the same image position is used for the face left and right observations.

5) If a photo-theodolite supplies its own calibration, it should be possible to correct for any offset of the best fitting projection centre from the centre of rotation. It is only necessary that the part which locates the lens in the rotating mount is large enough to permit additional machining to correct for the offset.

6) Although my preference is for a fixed focus camera, it may be acceptable to adopt "click stop" focussing. By this I mean a limited number of well defined focal settings for the CCD array. For each of these a calibration would be executed as described, applying the most appropriate camera model each time. From the discussion in Ch. 2, I do not expect any significant change in the optimum position of the projection centre, which can remain fixed at the rotation centre. The camera must therefore be focussed by moving the sensor away from the lens, rather than moving the lens out of the camera body, as is usual.

This calibration technique may well prove to be very accurate, and it may be possible to investigate two issues raised in Ch. 2.
Firstly, any variation of the perspective centre should be observable.
Secondly, if several points are used to define object space rays, it will be possible to see if these rays define straight lines.

Both these tests would be more accurate with a wide angle camera, and it would be interesting to apply the technique to the calibration of Rollei's electronic camera.

Finally, it should be noted that this calibration relates to the camera geometry, and not the sensor array itself, which must be calibrated by other methods.

Reference list.

Where possible, this reference list has been arranged in subject groups, which may help to locate information in a particular field. Not every reference is necessarily mentioned in the text. Any which are not, are included here to avoid potential gaps in information. Where several references have been available, the ones I judge to be most relevant are given. The comments associated with each are my own brief summary of contents, or are designed to draw attention to some particular aspect of the material.

Abbreviations.

Phot. Rec.	Photogrammetric Record
L&MS	Land and Minerals Surveying
PE&RS	Photogrammetric Engineering and Remote Sensing
ISPRS	International Society for Photogrammetry and Remote Sensing
SPIE	Society of Photo-Optical Instrumentation Engineers. (The International Society for Optical Engineering).
ACSM	American Congress on Surveying and Mapping.
ASPRS	American Society for Photogrammetry and Remote Sensing
AVN	Allgemeine Vermessungs-Nachrichten
ZfV	Zeitschrift fuer Vermessungswesen
DGK	Deutsche Geodaetische Kommission
FIG	Federation Internationale des Geometres.

Quoted accuracies should be taken as standard errors.

A) UNCLASSIFIED

A1 Mapping from aerial photographs.
C D Burnside, Granada Publishing, 1979.

A comprehensive treatment of conventional photogrammetry. Describes the node as projection centre (1.2) and lens distortion as a variable principal distance (1.4). Field calibration is explained (1.3). Cross ratios discussed in 3.6. Explains how a fifth point can be transfered between planes, via a projective transformation, provided 4 points are known in both.
An example of using several equations which are not independent is given in appendix A7, p279.

A2 Photogrammetric/Survey tests at the british National Engineering Laboratory.
S A Kyle, Wild Heerbrugg A.G.

An internal document prepared for Wild Heerbrugg, based on tests carried out with the assistance of NEL. Basically a feasibility study. Describes the results of comparing dual camera and dual theodolite coordinates against a 3-axis measuring machine. Some practical measurements simulated.

A3 Factors defining precision in close range photogrammetry.
Gates J W C, Oldfield S, Forno C, Scott P J, Kyle S A.
Proc. of ISPRS Comm. V, "Precision and Speed in Close Range Photogrammetry", York, 1982.

Gives the results of comparing dual camera intersections against a CMM, and shows how humidity changes cause bowing on photographic plates.

A4 The NPL Centrax - A new lens for photogrammetry.
Burch J M, Forno C.
Proc. SPIE Vol. 399 "Optical System Design, Analysis and Production". 1983, pp 412 - 417.

Describes the construction of the Centrax lens, with purely spherical components. For small luminous point targets, a ring image is obtained in the lens/object range 300mm to infinity. The camera is a true central projection and offers the possibility of specifying directions to better than 0.2 arc secs.

A5 STARS, A turnkey system for close range photogrammetry.
Brown D C. International Archives of Photogrammetry, Vol. 24, Part V/1, pp 68 - 87. (ISPRS Conf. "Precision and speed in close range photogrammetry", York, 1982)

Describes the CRC-1 camera, the back projected reseau platen, and the software package for processing measurements. Retro- reflective targets are mentioned, and a potential accuracy of 1: 500 000.

A6 CRISP. A software package for close range photogrammetry for the Kern DSR-1 Analytical Plotter.
Fuchs H, Leberl F. Ibid, pp 175 - 184.

A package for metric and non-metric cameras. The DLT is used for deriving an approximate solution.

A7 Three dimensional metrology at CERN.
C Lasseur, D Veal, CERN metrology group.
Presented at IAPI course, University College London, Sept. 1986. Contact Dept. of Photogrammetry and Surveying, UCL.

An overview of the precision survey techniques in use at CERN, with particular application to measurement of large structures (order 10m) for the physics experiments. Some discussion of computations.

A8 CERN Technology Note S1, May 1979. Self-aligning reflector for laser interferometer.
Available from the publications group, CERN.

Describes a hand held instrument which is a retro-reflector (corner of cube), driven by servo motors to stay on the line of a laser beam. The reflector is easily moved along the line to be re-located at another point, without losing the beam reference.

A9 Dual axis differential electronic level allows new options for solving alignment and monitoring problems.

Brunson D E. SPIE, vol. 483 "Optical Alignment II" 1984, pp 41-44.

The use of electronic levels to compensate for a ship's motion whilst afloat.

A10 The reflex plotters : measurement without photographs.
Scott, P J. Phot. Rec. 10(58): 435-446 (October 1981)

Describes how the Metrograph functions.

A11 K&E surveying instrument used aboard Columbia space flight.
Report in ACSM Bulletin, June 1982, p59.

<u>B) OPTICS AND CAMERA CALIBRATION</u>

B1 Geometrical Optics.
W T Welford. North-Holland Publishing Co. 1962.

Explains that nodal points are coincident with principal points for the same refractive indicies in object and image space, p36
Explains that exit pupils are often coincident with principal planes, and describes how a telecentric stop functions, p52.

B2 Decentred lens systems.
Conrady A. Monthly Notices of the Royal Astronomical Society, Vol. 79, 1919, pp 384-390

Explains how tangential distortion arises from the lack of correct centring of lens elements. An analytical formulation and description of the effect are given.

B3 Photogrammetrie.
Finsterwalder R. Published by Walter Gruyter & Co., Berlin 1952. In german.

Identifies centres of pupils as projection centres (p35).

B4 An outline of photogrammetry.
Schwidefsky K. Published by Pitman, London, 1959. English translation.

Identifies the centres of the pupils as the physical projection centres (p 10, 38, 48).

B5 Close range photogrammetry and surveying :
State of the art.
Workshop proceedings, ASP convention Sept. 1984.

P201 explains how distortion varies with f-stop.

B6 Thoughts on a standard algorithm for camera calibration.
Ziemann H. Proc. Comm. V, Vol. 26, ISPRS, "Real time photogrammetry - a new challenge", Ottawa, June 1986, pp 85-93.

Can be taken as a current summary. The assumption of a single projection centre for cameras is made, and attention is drawn to the pupil.

B7 Close range camera calibration.
Brown D C. PE&RS, Vol. 37, No. 8, Aug. 1971, pp 855 - 866.

Extends Magill's formula to compute radial distortion at a given focussing distance from known distortion at 2 planes on either side. Makes use of simple Gaussian lens formula, and assumes a single projection centre in the image space. On this basis a distortion function is simply re-scaled to determine its effects on other image planes.

B8 Lens distortion for close-range photogrammetry.
Freyer J G, Brown D C. PE&RS, Vol. 52, No. 1, Jan. 1986, pp 51-56.

Describes a physical camera model and the use of plumb wires for calibration purposes. Indicates that the distortion characteristic changes with object distance, an gives a formulation to account for this.

B9 A study on analytical calibration for non metric camera and accuracy of three dimensional measurement.
Murai, Matsuoka, Okuda. ISPRS Comm. V Proceedings, Rio de Janiero, June 1984. pp 570-579.

Evaluates different camera models applied to metric and non-metric cameras. Indicates a preference for a physical model. Non-metric cameras give an accuracy similar to metric, without allowing for variation of distortion with distance.

B10 Close range camera calibration : a new method.
Scott P J. Phot. Rec. 8(48): 806-812 (October 1976)

A method which directly identifies the perspective by arranging for control targets to have almost the same image position. Useful plumb-wire targets described.

B11 The pupil in perspective.
Scott P J. Phot. Rec. 9(49): 83-92 (April 1977)

A photogrammetrist's view of how a camera creates images, and the consequences for camera calibration. Indicates a shifting perspective centre.

B12 The geometrical theory of the camera and its application in photogrammetry.
Thompson E H. Phot. Rec. (1957), 2(10) : 240-263

Discusses calibration for cameras at infinity focus. Regards projections centres as poorly defined and avoids their use. A definition of pupil abberation is given.

C) OPTICAL ALIGNMENT

C1 Optical Tooling for precise manufacture and alignment.
Philip Kissam, McGraw-Hill, 1962.

This book is regrettably out of print. It provides some very useful on the techniques of optical alignment. Discusses autocollimation (7-6), autoreflection (7-7), and reciprocal telescope pointing using cross hairs (7-10).

C2 Optical Alignment.
Published by Rank Taylor Hobson, PO Box 36, Guthlaxton St., Leicester LE2 OSP, England. Available direct from RTH.

Optical alignment using Taylor Hobson equipment. Much of the book is an equipment specification, although even this can be useful to those who are only familiar with theodolites, levels and cameras. Some good discussions of practical measurements, as well as autocollimation and reflection (chapter 5).

C3 NPL, lasers and large scale alignment.
Burch J M. Paper presented in UK at Laser '78 Conference, organized by Engineers' Digest Ltd.

Discusses the 3-point alignment technique with zone plates, refraction effects and the possible use of pipes to eliminate them.

D) POLARIMETRY

D1 Schactverformungen. Vermessung und Auswertung.
Stelling W und Schmidt G. Das Markscheidewesen 90 (1983),
Nr 3

In german. The authors outline the SVP method, german for shaft measurement with polarized light. The polarized light is used to transfer a horizontal direction down the shaft, to an accuracy of 0.3 gon. With this, points on the shaft can be measured to +/- 2cm. Accuracy improvements are planned, but sub-millimetre accuracy is not expected.

D2 Errors in polarimetry caused by magnetic fields.
Gates J W. The International Sugar Journal, 1958, 60, pp 200-201.

Briefly discusses the rotational effect on the plane of polarization of polarized light, when passing through a magnetic field with a component parallel to the direction of movement.

D3 Sensitive method for measuring small rotations of a distant object.
King R J, et al. Journal of Scientific Instruments, vol. 38, pp 207 - 208, May 1961

The relative rotation between 2 instruments separated by 2000 ft, was determined by polarimetry with a sensitivity of 0.1 arc min (6 arc secs). The potential adverse influence of the earths magnetic field is estimated to cause errors of about 0.04 arc min per 1000 ft (about 5 arc secs total in this case). A suggested application is orientation transfer in mining.

D4 Polarimetry applied to alignment and angle measurement.
King R J, Raine K W. Optical Engineering, 20(1), 39-43, 1981

Polarimetry with an He-Ne laser is discussed, and its application to straightness measurement explained. The paper concludes that the relative rotation of units separated by some hundreds of metres could be measured to a few arc secs.

E) MATHEMATICAL ANALYSIS

E1 Least squares computations by Givens transformations without square roots.
Gentleman W. J. Inst. Maths. Applics. (1973) 12, 329-336

E2 A note on modifications to the Givens plane rotation.
Hammerling S. J. Inst. Maths. Applics. (1974) 13, 215-218

E3 The least squares solution of over-determined linear equations having band or augmented band structure.
Cox M G. IMA Journal of Numerical Analysis (1981) 1, 3-22.

E4 Mikhail E M, Gracie G. Analysis and adjustment of survey measurements. Van Nostrand Reinhold Co., New York.

A good presentation of the least squares solution and statistical analysis of survey networks. The notation used may be unfamiliar to UK readers, but is clearly defined.

E5 An introduction to the algebra of matrices, with some applications.
Thompson E H. Published by Adam Hilger, London.

Chapter 8, "Rotation in 3 dimensions." is particularly useful.

E6 Adaptation of the bundle method for triangulation of observations made by digital theodolites.
Brown D C. Presented paper no. 43, Conf. of South African Surveyors, Durban, May 1985.

Describes how theodolite observations are processed by GSI's bundle adjustment software, STARS, by conversion to pseudo- photographs (fictitious photos). Indicates that Brown and Trotter first used the method in 1969.

E7 Buendeltriangulation mit gemeinsamer Ausgleichung photogrammetrischer und geodaetischer Beobachtungen.
Wester-Ebbinghaus W. ZfV, 110. Jahrgang, Heft 3, March 1985.

In german. Describes a comprehensive adjustment program which accepts mixed photographic and theodolite data. Theodolites may be non-levelled. Briefly explains how to use theodolites in the non-levelled condition.

E8 Bundle adjustment methods in engineering photogrammetry.
Granshaw S I. Phot. Rec. 10(56): 181-207 (Oct. 1980)

A detailed presentation of multi-station photogrammetry. Covers formulation of the solution, error estimates, free network adjustment, self-calibration of cameras, and control requirements. The rotation matrix is developed as the product of two rotation sequences.

E9 Relative orientation problems.
Granshaw S I. Ibid., 9(53): 669-675 (April 1979)

Discusses the poor quality of a relative orientation when the target points do not have a conventionally "good" distribution within the field of view.

E10 Das Problem der "gefaehrlichen Flaechen" in Theorie und Praxis.
Hofmann W. DGK, Reihe C, No. 3, 1953.

In german. The failure cases in photogrammetric relative orientation are described. This is done in both geometrical and analytical terms, and the two cases of a multiplicity of solutions and ill conditioned solutions are explained.

E11 Estimation of initial values before bundle adjustment of close range data.
Hunt R A. Proc. of Comm. V, ISPRS, Rio de Janeiro, June 1984.

An analytical method of resection derived from a graphical procedure, and a direct solution for the rotation matrix avoiding the use of three parameters.

E12 The explicit solution of the single picture resection problem, with a least squares adjustment to redundant control.
Smith A D N. Phot. Rec., Vol. V, No. 26, Oct. 1965.

A general algebraic solution to 3-D resection. Based on photography, but the concept is equally applicable to theodolites.

E13 Space resection : failure cases.
Thompson E H. Phot. Rec., Vol. V, No. 27. April 66, pp 201 - 204.

A mathematical derivation of the danger cylinder in resection.

E14 Spatial positioning, vector notation and coordinates.
Michael Cooper, letter to L&MS, Dec. 1986, pp 623-625.

Discusses the application of vector algebra to both photogrammetry and surveying, emphasizing the common geometrical problem. Gives the solution to a 3-D intersection.

E15 Direct linear transformation from comparator coordinates into object space coordinates in close-range photogrammetry. Abdel-Aziz, Karara. ASP Symposium on close range photogrammetry, Urbana, Illinois, Jan. 1971.

E16 Die gegenseitige Orientierung von zwei Strahlenbuendeln bei Uebereinstimmung, bei unbekannten Naeherungswerten und durch ein nichtiteratives Verfahren.
Hofmann-Wellenhof B. DGK, Reihe C, Nr. 257, 1979

In german. Describes a method of orienting two photographs (without reciprocal observations), if 6 common points are imaged. It is a direct method which does not require starting values. The analysis is not particularly simple. Other approaches to deriving direct solutions are reviewed. Note particularly the methods requiring 8 common points. The method of von Sanden is discussed, in which the reciprocal observation is effectively established. The reference to von Sanden dates from 1908.

E17 A computer algorithm for reconstructing a scene from two projections.
Longuet-Higgins H C. Nature Vol. 293, 10 Sept. 1981.

A paper in english describing the direct linear solution of a relative photo orientation, using 8 common points.

F) SURVEYING

F1 Surveying with non-levelled theodolites.
Kyle S A. Survey Review, Vol. 27, 207, Jan. 1983, pp 39-42.

Outlines the basic method, and suggests how gravity measurements might otherwise be processed.

F2 Measurements in 3 dimensions without reference to the vertical.
Kyle S A, Dec. 1982. Thesis submitted to the Royal Institution of Chartered Surveyors, 12 Great George St., London SW1P 3AD, England.

A more comprehensive treatment of the material presented in the preceeding reference. Explains how to use a theodolite in a non-levelled way. A mathematical solution is explained which follows a bundle adjustment. A listing of program SURV3D is given. The inclusion of gravity information is discussed.

F3 Use of a theodolite and gyro on vessel when ships vertical plane not truly vertical.
Davis A. Presented at IAPI course, University College London, 15-18 April 1980. Contact Dept. of Photogrammetry and Surveying, UCL.

Explains how theodolites are set into tilted reference systems so that subsequent procedures are equivalent to working in a levelled system.

F4 Fehlertheoretische Untersuchung des elektronischen Mess- und Berechnungssystem ECDS 1 von KERN.

Bill R et al. ZfV, 10 Jahrgang. Heft 9. September 1985. pp 399-407

In german. General error analysis, optimum intersection and systematic error effects are discussed, using an electronic, dual theodolite system from KERN. Reciprocal pointing is described by the method of using the telescope cross-hairs. Sp

F5 AVN, issue 6, June 1985

In german. This issue is principally devoted to describing currently available coordinate measurement systems based on (dual) electronic theodolites. The 4 manufacturing sources describe their hardware, and give some examples of applications. The following appear : Sp

AIMS from Keuffel & Esser.

ECDS1 from Kern.

IMS from Zeiss (Oberkochen)

RMS 2000 from Wild.

G) SURVEYING CONCEPTS IN PHOTOGRAMMETRY.

G1 Tunnel calibration by photogrammetry.

Ethrog U and Schmutter B. Photogrammetria, 38 (1982) 103-113

Two cameras used for tunnel profiling faced one another. The authors used an exchangeable target and camera, with forced centring, and developed a solution for orientation based on the reciprocal pointing. The targetting system is not described.

G2 A parallel case of photogrammetry and its application in narrow transits.

Foud A Ahmed. PE&RS, vol 50, no. 10, Oct. 1984, pp 1443-1448.

Another application where the cameras point along the baseline, but they are apparently not targetted, nor is the reciprocal observation used. Similar to the photo-theodolite.

G3 Contemporary problems in terrestrial photogrammetry.
Erlandson J P, Veress, S A. ASP workshop proceedings, "Close range photogrammetry and surveying : State of the art", Sept. 1984.

Explains control problems associated with linear structures such as bridges. Resection is rejected and a photo-theodolite used. Assumes it is possible to define the projection centre to a high accuracy (within 10 microns) and recommends the facility to level the camera to within 5 arc secs.

G4 A direct method of orientation using scaling lengths.
Kyle S A. To be published in L&MS, Feb. or March 1988.

Explains how two scaling lengths can provide a direct means of relative orientation in the absence of reciprocal observations.

H) GENERAL PHOTOGRAMMETRIC APPLICATIONS

H1 Industrial photogrammetry: New developments and recent applications.
Fraser C S and Brown D C. Phot. Rec. 12(68): 197-217, Oct. 1986

Latest state of STARS system reviewed. Mentioned are CRC-1 camera (240mm focal length, 23 x 23 cm format) and Autoset mono-comparator with video imaging.
Several applications of multi-station photogrammetry in this paper including : antenna and aircraft engine measurement, thermal deformation of a compressor, periodic tool inspection and robot control. Retro-reflective targetting in use.

Antenna measurement suggests typical residuals around 1 micron, or approx. 1 arc sec with a 240mm focal length lens.

H2 Photogrammetry in engineering.
Welch N. Phot. Rec. 12(67): 25-44, April 1986.

Pipe deformation with single photo (UMK10) measurement, to
3 - 5 mm.
Robot calibration with dual cameras (UMK 10), point accuracy 0.25mm.
Comparison of photogrammetry (UMK 10) and theodolites (Wild TC1) against a 3-axis machine. Use made of pseudo-photographs to process the theodolite measurements with the photogrammetric software.
Large strain measurement with Hasselblad cameras.

J) ROBOTICS.

J1 The surveying of industry robots.
Bill R. and Staiger R. AVN international edition 2/1985, pp 2-10.

Theodolites are used to determine robot movement.

K) ANTENNAE.

K1 Hochpraezise photogrammetrische vermessung von Industrie- objekten.
Fritsch et al, IX Internationaler Kurs fuer Ingenieur-vermessung, Graz. Sept 1984.

Theory and results of measuring a 2m parabolic antenna.
Theodolite intersection gave standard errors :
56 micron (x), 64 micron (y), 13 micron (z).
Multi station photogrammetry with 10 photos gave :
53 micron (x), 54 micron (y), 57 micron (z).
Photogrammetry used a Wild P31 treated as a true metric camera (no additional parameters).

K2 Measurement of electrostatically formed antennas using photogrammetry and theodolites.
Goslee, Hinson,Kenefick, Mihora. ACSM - ASPRS Annual Convention, Washington D.C, March 1984, pp 424 - 433. (See also, Ibid, March 86, Vol. 2, pp 92 - 96.)

A 1/20 scale model of membrane antenna was measured. The model was 5m in diameter. Dual theodolite and triple camera setups, and a laser sensor were all compared. The camera was probably a Wild P31 metric camera, as JFK Associates are known to work with this.

K3 Audit profile check on a tropospheric scatter antenna.
Hepburn R M. South African Journal of Photogrammetry, Remote Sensing and Cartography, 13 (5), 1983: 315-320.

Theodolite and photogrammetric methods used and compared on large antenna. Antenna size around 25 m, accuracy requirement of 3.2 mm r.m.s. was met. 3 theodolites and stereo photographs, taken with a metric UMK 10 camera. Photo residuals around 3 microns (about 6 arc secs) with camera/object distances around 25m.

K4 Photogrammetric determination of the form of a 10m radio antenna.
Oldfield S. ISPRS Comm. V, Rio de Janiero, 1984.

Targetted points coordinated on 10m antenna to a standard error of about 0.3mm using a UMK 10 metric camera. 2 measurements made, one with 4 photos at about 15 m from the dish, one with 3 about 10 m distant. Photo residuals around 5 micron (10 arc sec) assuming metric properties (no self-calibration).
The paper also compares a standard and fine grain emulsion.

K5 Photogrammetric measurement of microwave antennae.
El-Hakim S F. PE&RS, Vol. 51, No. 10, Oct. 1985, pp 1577-1581.

A 4 photo measurement of an antenna's sub-assembly, about 1.5m x 3m. A Wild P31 at 2.5 m distance was used, and calibration parameters included in the processing. Accuracies were :
X - 0.12mm, Y - 0.13mm, Z - 0.15mm.
The additional calibration improved results by about 25 % compared with an uncalibrated (fully metric) procedure.

K6 Microwave antenna measurement.
Fraser C S. PE&RS, Vol. 52, No. 10, Oct. 1986, pp 1627-1635

5 antennae measurements are reviewed. Typical antennae sizes, 2 - 30 m. GSI's own (non-metric) cameras used, with full camera modelling in the processing. Accuracies all sub millimetre or sub 1/10 millimetre.

L) AEROSPACE.

L1 The use of photogrammetry in the manufacture of high performance aircraft.
Powell G E. ISPRS Comm. V, Rio de Janiero, 1984.

A master guaging technique to check aircraft tools (jigs) has been replaced by a system based on multi-station photogrammetry. The economic benefits of a greatly reduced tool "down time" are mentioned.

L2 Applications of photogrammetry to dimensional metrology.
Mallison J A. Measurement Science Conf., Irvine, Cal., USA, Jan. 1987.

Practical advantages of photogrammetry for the aircraft manufacturer are discussed, which include convenience and economy. An on-going measurement of a full aircraft is mentioned and target accuracies around 15microns are expected.

L3 Gageless tool fabrication.
Brochure from General Dynamics, Fort Worth Division, Texas, USA.

Describes the implementation of dual electronic theodolites for measurement and inspection.

M) NUCLEAR INDUSTRY

M1 Application of precision close range photogrammetry for quality control and documentation in power station construction.
Berg G. ISPRS Symposium (Real-time photogrammetry - a new challenge), Ottawa, 1986. Archives Vol. 26, part 5, pp 159-164.

Photogrammetric quality control of components manufactured for reactor pressure vessels. Wild P31 focussed on 4m gave standard errors better than 0.05 mm on two axes and 0.15 mm on the third axis. Additional parameters used in adjustment.

M2 Photogrammetry applied to nuclear reactor inspection.
Clayton R. SPIE vol. 599, Optics in engineering measurement, Cannes, Dec. 1985.

Measurement problems at very short range (<0.5m) and medium range (0.5m - 2m) discussed. Hasselblad non-metric cameras with reseau plates are used. Pre-calibration used.

N) AUTOMOBILE INDUSTRY.

N1 Photogrammetry at Regie Renault.
Wahl M. Phot. Rec. 11(62): 195-201 (October 1983).

The use of stereo photogrammetry to derive data on surface form for further processing by Renault's Unisurf method. Renault uses photogrammetry to measure styling models, body panels and in applications such as crash tests. Stereo photography with metric UMK 10 cameras is the basis. Accuracy is quoted as a function of image scale, around 0.005 mm x Scale. At close ranges of 4m (typical) this suggests errors around 0.2mm.

P) MARINE

P1 ARE Ship deformation measurements.
S A Kyle et. al., To be published.

Photo. survey and non-levelled use of theodolites on board floating ship.

P2 Submarine hull mapping and fixture set-out : an application of the ECDS system.
Bethel, Sedej. ASCM-ASPRS March convention 1986, Vol. 2, Surveying.

Describes the use of a Kern dual theodolite system to check the dimensions of a submarine hull in dry dock, using targetted points. A 25 station network and 100 points were coordinated to an estimated accuracy of about 0.25mm. Largest network dimension was about 80m. Setting out on the hull is also described, using a laser eyepiece.

P3 Close-range photogrammetry as a aid to measurement of marine structures.
Newton I. PE&RS, Vol. 41, No. 12, Dec. 1975, pp 1501-1512.

Applications of photogrammetry to measure parts of oil platforms and ship sections are given. The methods achieve accuracies of a few millimetres.

P4 Applications of photogrammetry in shipbuilding.
Kenefick J F, PE&RS, Vol. 43, No. 9. Sept. 1977. pp 1169-1175.

Several applications are described : the measurement of a ship's midship section which was roughly cubical, obtaining a piping diagram from a scale model, determining the section of a cylindrical tank of a liquid natural gas tanker and measuring the section of a ship's bow prior to mating with its counterpart. A metric Wild P31 was used. Typical coordinate accuracies for the large objects was around 1mm s.e.

P5 Photogrammetric surveys of Shell Offshore Inc. COGNAC Platform.
Heute D A. ASP Workshop proceedings, "Close range photogrammetry : State of the art", Sept. 1984.

The measurement of large sections of oil platforms.

P6 Joining ships built in halves using close range photogrammetry.
Peel D D. Ibid.

Q) MEASUREMENT OF PROCESS PLANT

Q1 Klement U R and Bracewell P A. Easier routes to "as-built" records. Process Engineering (UK magazine), March 1982.

Q2 Bracewell P A and Klement U R. The use of photogrammetry in piping design. Proc. of the Institution of Mechanical Engineers (Process industries div.), 1983, Vol. 197, No. 30.

These papers describe how stereo-photogrammetry has been used by ICI to obtain dimensional information on complex pipework and associated machinery. Metric UMK 10 cameras used, giving target accuracies of 3 - 10 mm.

R) OTHER LARGE STRUCTURES

R1 Photogrammetry for dimensional control of bridges.
Veress S A. Photogrammetria, 36 (1981) 193 - 206

The use of a Hasselblad 60mm metric camera to measure concrete bridge sections to an accuracy around 1mm.

R2 Photogrammetry as a tool in structural research.
Pries R A, Veress S A. ASP Workshop proceedings "Close range photogrammetry : State of the art", Sept. 1984.

The measurement of power transmission lines.

S) ELECTRONIC IMAGES

S1 Megaplus camera specification.
Published by Videk (a Kodak company), 1100 Corporate Drive, Canandaigua, New York 14425-9597.

A commercially available, solid state camera, with 1320 x 1035 pixels. Pixels are square, 6.8 x 6.8 microns. The camera is non-interlaced, and the active image area is approx. 9 x 7 mm.

S2 Star sensors for space satellites.
An article in "Measurement and Automation News", July 1984, No. 53. Published quarterly by SIRA.

A pointing device based on a 385 x 288 CCD sensor achieves an accuracy of about 15 arc secs, or 1/3000 of the 12 deg field of view. A defocussed and abberated image is used to achieve this interpolation accuracy of about 0.1 pixels.

S3 Ultra-precise star tracking using charge coupled devices (CCDs).
Dennison E W, Stanton R H. Jet Propulsion Lab. SPIE vol. 252, Smart Sensors ii (1980) pp 54 - 63

Concludes that star images could be tracked with a CCD imager to better than 1/50 pixel.

S4 Low cost smart camera.
Buechli F, Heeb E, Knop K. Proc. SPIE Vol. 595 "Computer Vision for Robots", Cannes, 1985.

A standard CCD camera finds the centre of a circular target (diameter 40mm) to about 5 microns normal to the camera axis, and 100 microns along the axis. Viewing distance is less than 1m, and the pixel interpolation factor is about 1/300.

S5 Accurate determination of ellipse centres in digital imagery.
Zhou G. ACSM-ASPRS March Convention 1986, Vol. 4, Photogrammetry, pp 256 - 264.

A development by Kern for automatic pointing, to determine the centre of a circular target with an electronic camera. Pixel interpolation to better than 0.05 pixels is reported.

S6 Automatic point determination in a reseau scanning system.
Luhmann T. Proc. of ISPRS, "Real time photogrammetry - a new challenge", Ottawa, June 1986, pp 400 - 408.

Describes the automatic determination of target centres (crosses and circles) to an accuracy of 0.1 pixels, using the CCD camera in the Rollei mono-comparator.

S7 High resolution digital object recording with small format matrix sensors.
Wester-Ebbinghaus. Proc. Intercommission Conf. on Fast processing of photogrammetric data. Interlaken, Switzerland, June 2-4, 1987. pp 90-98.

Outlines two approaches to obtain high resolution imagery over wide angles with small format CCD sensors. One is the reseau system incorporated in the Rollei system, the other is to use narrow field of view electronic cameras attached to theodolite telescopes. This is an external attachment and different from the approach which uses the camera to sight down the telescope. There is a distinct separation of camera perspective centre and theodolite rotation centre. Currently only a proposal.

T) LINE IMAGES.

T1 3-Dimensional position measuring systems.
Abelseth L, Rotvold O. Norwegian Hydrodynamic Lab., Ship and Ocean Lab. Division, Hakon Hakonsons gt 34, P.O.B. 4118-Valentinlyst, N-7001, Trondheim, Norway.

Cameras with single linear CCD arrays are used to sense the position of LED targets within the plane defined by the linear array and the camera perspective centre. Cameras are set up to make measurements in horizontal and vertical planes. Cylindrical lenses are used to maintain image sensing for small target movements out of the defining plane.

T2 Acquisition and modelling of human body form data.
Fuchs, Duran, Johnson, Kedem. University of Texas. SPIE Vol. 166, 1978.

Linear CCD arrays are used with a razor blade (knife edge) positioned a short distance in front, to form a "shadow sensor". An active point target (LED) throws a shadow of the edge on the array, enabling the array to position the point on a plane. Intersection of a minimum of 3 planes gives XYZ.

T3 Three-dimensional stereometric measurement system using optical scanners, cylindrical lenses, and line sensors. Yamashita Y, et. al. Proc. SPIE, Vol. 361, 1982, pp 67-73.

For measuring the human body form, a scanning laser spot is imaged by 4 instruments. These are cylindrical lenses with line sensors, with a relatively narrow (10 deg) field of view. These generate planes which are intersected to give object points to an accuracy of about 1 mm. The speed advantages of linear arrays are mentioned.

U) AUTOMATED TRIANGULATION SYSTEMS

U1 Kern system for positioning and automated coordinate evaluation. A real-time system for industrial measurement.
Roberts T P, Moffitt N M.

U2 The new Kern system for positioning and automated coordinate evaluation. Advanced technology for automated 3-D coordinate determination.

Both above are Kern publications reprinted from 1987 annual convention of ASPRS-ACSM.

The papers describe how Kern have included automated pointing of their electronic theodolites, by incorporating a CCD camera into the telescope.

U3 Automation of electronic angle-measuring instruments.
Katowski O. FIG/ISPRS Proc. of the 2nd. industrial and engineering survey conference, London, Sept. 1987, pp 230-240.

The equivalent Wild development. The CCD camera has both a wide angle view and a view down the telescope. Applications are discussed.

U4 Mapvision : The photogrammetric machine vision system.
Haggren H H, Leikas E. PE&RS, Vol. 53, No. 8, Aug. 1987, pp 1103-1108.

4 CCD cameras with images digitized to 512 x 512 pixels, view an object identified by specific targets and and a scanning laser spot. Set up is by resection on targets coordinated by theodolite. Pixel interpolation is around 0.05 pixels, and object space accuracy is estimated between 1:5000 and 1:10 000.

U5 Image recording with opto-electronic matrix sensor - possibilities for on-line processing.
Luhmann T, Wester-Ebbinghaus W. FIG/ISPRS Proc. of 2nd industrial and engineering survey conference, London, Sept. 1987, pp 122 - 133.

Describes the system being developed in conjunction with Rollei, in which a small area CCD array is used together with a reseau, either when digitizing an existing photographic image, or directly in the back of a small format camera.

U6 A flexible machine vision guidance system for 3-dimensional control tasks.
Pinkney H F L, Perratt C I. Proc. of ISPRS, "Real time photogrammetry - a new challenge", Ottawa, June 1986, pp 414-423.

A system based on a single video camera is under development to enable robots to grapple objects. A specific application is the robot arm of the space shuttle. The positioning of the robot is based on a resection, using marked targets on the object to simplify the task of identification.

U7 Photogrammetric application of a video system in 3 dimensional recording.
Foud A Ahmed. PE&RS, Vol. 50, No. 5, May 1984. pp 593-596.

Scanning system using 2 narrow field video cameras (4 deg), each located in rotating mounts. Each camera scans object on horiz. and vert. planes, including a pointing at the other camera position. Points of interest are subsequently located in the video recording, from which horiz. and vert. angles are deduced.

U8 Ein lernfahiges tachymetrisches Vermessungssystem zur Uberwachung kinematischer Vorgange ohne Beobachter.
Kahmen H, Suhre H, (Hannover), Zeitschrift fuer Vermessungswesen, 8/1983.

U9 Ein "intelligentes" polares Vermessungssystem fur die Beobachtung statischer Punktfelder und kinematischer Vorgange.
Kahmen H, Schwable R, Suhre H, (Hannover), ibid. 11/1984.

GEOROBOT, an automated system for civil engineering work and detail survey is described. Angular pointings are combined with edm measurements to targetted points to derive coordinates.

U10 CODA 3.
Movement Techniques Ltd, Unit 5, The Technology Centre, Epinal Way, Loughborough, Leicestershire LE11 0QE. Tel (0509) 267637.

Scanning system using white-light, fan-shaped beams reflected off object targets which are small corner cube reflectors. Reflectors are combined with colour filters for i/d purposes. Scanning unit is a fixed, rigid device. 2 mirrors scan beams in the horizontal plane (XY fix) and a 3rd mirror scans vertically (Z fix).

U11 VICON system.

Oxford Metrics Ltd. Unit 8, 7 West Way, Botley, Oxford OX2 OJB. Tel (0865) 244656

Vidicon cameras view passive targets. Typically, 4 cameras view subject. Each camera has infra-red ring strobe around lens and ir filter over lens. Targets made from retro-reflective material (eg Scotchlite). Each camera image shows bright target points against dark background, hence image and target coordinates by photogrammetric algorithms.

U12 Medical applications of close-range photogrammetry.

Macleod A. Phot. Rec. 12(68): 155-165 (October 1986)

Mentions VICON and CODA 3 systems. Not industrial accuracy but the principle is the same.

U13 SELSPOT II.

Selcom, Selective Electronic Co. AB, Box 250,
S-433 25 Partille 1, Sweden. Tel 031-44 74 40

Solid state cameras with position sensing elements view active light sources. Up to 16 cameras and 128 targets Targets are LEDs which are sequentially illuminated.

Note also : SELSPINE ROBOT CHECK. This is a dual camera system, using the same imaging technology as in SELSPOT, but the software is specifically tailored to robot analysis. In use at British Leyland Robotics Section, BL Technology Ltd., Cowley Body Plant, Cowley, Oxford OX4 5NL, England. Tel (0865) 777701

U14 Stereo vision for robotic seam sealant spraying.
Johnstone P. Proc. of 2nd. Intl. Conf. on Robots in the Auto Industry, Birmingham, May 1985.
See also : The Industrial Robot, Vol 12, No. 2, June 1985, p 103 and The Engineer, 12 June 1986, p 78.

System used in car manufacture to position body shell for spraying, etc. Appears to work by having camera pairs defining points in space. Presumably calibrated by a test object. Car body located within system defined by cameras, and check points can be measured to 0.1 mm.

U15 Automatic laser tracking interferometer system for robot metrology.
Lau K, Hocken R J, Haight W C. Precision Engineering, Jan. 1986, Vol. 8, No. 1, pp 3 - 8.

A tracking system under development. A laser is reflected off a mirror to point at a target mirror fixed to a moving robot. The target mirror is controlled to reflect the beam back to the tracker. The 2 tracking angles and interferometrically measured distance give the coordinates of the target. It is hoped to obtain an accuracy of 40 microns in a 3 x 3 x 3 m volume.

U16 Enhancing robot performance measurement.
A report in "The Industrial Robot" (UK magazine), March 1986.

An overview of laser tracking systems under development and investigation at NBS, including the one above. In addition to a system using spherical coordinates, other configurations are discussed.

U17 Laser tracking system to measure robot arm performance.

Gilby J H, Parker G A, Dept. of Mech. Eng., University of Surrey, Guildford. Sensor Review, Oct 1982.

U18 Dynamic performance measurement of Robot Arms.
Gilby et al. Robot Technology and Applications, Proc. of 1st Robotics Europe Conference, Brussels, June 27-28, 1984.

U17 and U18 describe a scanning system which tracks a single passive target on a robot arm. 2 scanning units are used. Each has 2 mirrors to deflect a laser beam about 2 axes and onto the target. The target is a corner cube reflector. The scanning system detects the reflected beam and uses feedback control to keep the beam on target. Beam intersections give target coordinates.

U19 Optical considerations in a 3D laser tracking instrument.
Mayer R and Parker G A. 6th. Intl. Conf. on Robot Vision & Sensory Controls, Paris, June 1986, pp 217 - 228.

More detail on the instrument under development at Surrey. Gives information on system calibration and target design. A "cats eye" retro-reflector designed by Dr Jim Burch is very interesting. Mathematics are also outlined for triangulation procedures which do not involve a unique projection centre.

U20 Position and orientation measurement of a moving object by CCD photo array sensors.
Arai T, Endoh T, Minokoshi S. Proc. of 4th Intl. Conf. on Assembly Automation. Tokyo Oct. 1983.

2 scanning sensors track a 3rd sensor fixed to object. Each scanner has 2 rotating mirrors plus feedback system to direct a cross-shaped laser beam onto the 3rd sensor. 3rd sensor has ring- shaped CCDs which deduce angular orientation of the sensor from the imaged position of the cross-shaped beams. This system avoids the need to coordinate at least 3 object targets, if angular orientation of object is required.

V) AUTOMATED SYSTEMS BASED ON LENGTH MEASUREMENT

V1 Development of the "Tetrabot" robotic manipulator.
GEC Techbrief, from GEC Research, Cambridge Rd., Whetstone, Leicester LE8 3LH, UK.
(See also : "The Engineer", 12 June 1986, p 37.)

Describes a robot manipulator to which 3 linear actuators are directly attached. Manipulator position is controlled by controlling the length of the actuators.

V2 Coordinate measurement with a tracking laser interferometer.
Brown L B, Merry J B, Wells D N. Lasers and Applications, Oct. 1986.

3 separate interferometers track a retro-reflecting prism on a robot. This positions the robot which then coordinates points of interest on an object. The objective is to replace CMMs. Coordinate accuracies in the range 10 - 100 microns are expected.

W) ROBOT PERFORMANCE MEASUREMENT

W1 A review of industrial robot performance measurement.
Gilby, Parker, University of Surrey. Second Intl. Metal Cutting Conf., May 14-18 1985, Wuhan, China.

Mentions Renault's use of theodolite intersection, and Peugeot's use of the trilateration method. Wires attached to the robot are wrapped around drums fixed in position. As they unwind, potentiometers register the changes in length.

W2 Performance Characteristics and Performance Testing of Industrial Robots - State of the Art.
Warnecke, Schiele. Robot Technology and Applications. Proc. of 1st Robotics Europe Conf., Brussels, June 27-28 1984.

This also mentions the possibility of a trilateration method.

W3 Project for development of a photogrammetric method for the evaluation of the dynamic performance of industrial robots.
Priel, Schatz, LNE Paris. Ibid.

Describes a current method for static calibration, and proposes the use of video cameras in dynamic cases.

APPENDIX

The appendix is a collection of tables of data which have been processed by the TRIGFIX package.

The following items are presented :

DATA SETS 1.
Comparison of dual theodolite intersection.

DATA SETS 2.
Comparison of conventional levelling with direct observation of the gravity vector.

DATA SETS 3.
Resection test with a levelled camera.

DATA SETS 4.
Orientation by distance ranging : theodolite test.

DATA SETS 5.
Orientation by distance ranging : camera test.

DATA SETS 6.
4-point camera target.

DATA SETS 7.
Measurement of a basement test field.

DATA SETS 8.
Measurement of untargetted points on UCL portico.

DATA SETS 1.

COMPARISON OF DUAL THEODOLITE INTERSECTION
LEVELLED THEODOLITES versus NON-LEVELLED THEODOLITES

File <RSC-1 > Obs. from theod. T1

NAME	HORIZ	VERT
150	144 27 34.5	-35 49 52.5
1450	168 45 49.0	-26 50 31.5
BALL-C	255 11 26.0	0 41 49.5
BALL-LL	253 51 30.0	-2 22 48.0
BALL-LR	256 16 37.5	-2 24 29.0
CAM	255 7 47.1	-0 50 10.6
T2 (recip. ob)	205 10 33.0	0 7 24.0
U1	103 43 4.0	37 13 28.5
U2	101 35 20.5	6 18 53.5
U3	114 43 54.5	-42 36 9.5
V1	124 14 14.0	22 37 8.5
V2	122 55 34.5	-5 46 33.0
W1	140 3 37.0	9 50 58.5
W2	156 33 33.0	-0 4 15.5
W3	145 21 4.0	-16 39 46.5
W4	172 21 45.0	11 27 48.5
W5	169 52 25.5	-15 11 3.0

Remarks. Conventionally levelled theodolite.

DATA SETS 1.

File <RSC-2 > Obs. from theod. T2.

NAME	HORIZ	VERT
150	74 11 17.5	-26 32 59.5
1450	96 35 30.5	-36 23 1.5
BALL-C	346 4 15.0	0 33 2.5
BALL-LL	345 4 26.5	-2 39 57.5
BALL-LR	347 29 35.5	-2 31 10.5
CAM	346 11 35.4	-1 0 15.3
T1 (recip. ob)	37 16 23.0	-0 7 25.0
U1	61 52 22.5	17 47 28.0
U2	62 13 50.5	2 39 3.0
U3	60 39 28.0	-20 9 10.5
V1	93 40 27.5	19 17 12.5
V2	91 41 48.0	-4 49 51.5
W1	112 28 5.0	10 23 52.0
W2	124 58 45.5	-0 12 25.0
W3	110 57 31.0	-18 28 30.0
W4	144 38 58.5	19 31 19.0
W5	140 30 53.0	-24 41 0.5

Remarks. Conventionally levelled theodolite.

DATA SETS 1.

OPTIMAL ORIENTATION of <RSC-1 > with <RSC-2 >

NAME	Resid 1 ARC SEC	Resid 2 ARC SEC	Weight 1	Weight 2
150	1.1	1.1	1.00	1.00
1450	0.5	0.5	1.00	1.00
BALL-C	0.4	0.4	1.00	1.00
BALL-LL	1.0	1.0	1.00	1.00
BALL-LR	1.5	1.5	1.00	1.00
CAM	temp. deletion			
U1	0.6	0.6	1.00	1.00
U2	0.0	0.0	1.00	1.00
U3	0.4	0.4	1.00	1.00
V1	0.5	0.5	1.00	1.00
V2	0.9	0.9	1.00	1.00
W1	1.9	1.9	1.00	1.00
W2	2.5	2.5	1.00	1.00
W3	1.2	1.2	1.00	1.00
W4	2.0	2.0	1.00	1.00
W5	1.6	1.6	1.00	1.00

RMS residual angle = 1.3 ARC SEC

Posn. at <T1	> =	0.000000	0.000000	0.000000
Rotn. at <T1	> =	1.000000	0.000000	0.000000
		0.000000	1.000000	0.000000
		0.000000	0.000000	1.000000

Gravity resid. = 0.0 ARC SEC, Recip. resid. = 2.4 ARC SEC

Posn. at <T2	> =	-1.384359	-2.945086	0.007037
Rotn. at <T2	> =	0.977794	-0.209568	0.000000
		0.209568	0.977794	0.000000
		0.000000	0.000000	1.000000

Gravity resid. = 0.0 ARC SEC, Recip. resid. = 1.2 ARC SEC

Remarks. Coordinate data file X-3AUG created.

DATA SETS 1.

File <RSC-5 > Obs. from theod. T1.

NAME	HORIZ	VERT
150	144 27 37.0	-35 49 55.5
1450	168 45 52.0	-26 50 36.0
A	253 44 4.5	0 40 34.5
B	256 54 53.5	0 48 28.5
C	256 41 25.5	-2 29 18.5
D	253 30 28.0	-2 26 2.0
T2 (recip. ob)	205 10 33.0	0 7 18.5
U1	103 43 21.5	37 13 27.0
U2	101 35 29.5	6 18 57.0
U3	114 43 55.5	-42 36 8.0
V1	124 14 19.5	22 37 7.5
V2	122 55 35.5	-5 46 31.0
W1	140 3 42.0	9 51 0.0
W2	156 33 34.5	-0 4 14.5
W3	145 21 4.0	-16 39 44.0
W4	172 21 45.0	11 27 43.5
W5	169 52 24.5	-15 11 4.5

Remarks. Non-levelled theodolite.

DATA SETS 1.

File <RSC-6 > Obs. from theod. T2.

NAME	HORIZ	VERT
150	74 11 20.0	-26 33 9.0
1450	96 35 33.5	-36 23 6.5
A	344 23 19.5	0 33 28.0
B	347 35 13.0	0 37 49.5
C	347 53 12.5	-2 34 1.5
D	344 41 1.5	-2 44 51.5
T1 (recip. ob)	37 16 23.5	-0 7 29.5
U1	61 52 28.0	17 47 19.5
U2	62 13 54.0	2 38 56.0
U3	60 39 29.0	-20 9 12.5
V1	93 40 29.5	19 17 6.5
V2	91 41 52.0	-4 49 59.5
W1	112 28 3.5	10 23 52.5
W2	124 58 46.0	-0 12 32.0
W3	110 57 32.5	-18 28 30.5
W4	144 39 0.5	19 31 19.5
W5	140 30 53.5	-24 41 6.0

Remarks. Non-levelled theodolite.

DATA SETS 1.

OPTIMAL ORIENTATION OF <RSC-5 > with <RSC-6 >

NAME	Resid 1 ARC SEC	Resid 2 ARC SEC	Weight 1	Weight 2
150	1.0	1.0	1.00	1.00
1450	1.7	1.7	1.00	1.00
A	2.1	2.1	1.00	1.00
B	1.6	1.6	1.00	1.00
C	0.2	0.2	1.00	1.00
D	1.9	1.9	1.00	1.00
U1	1.1	1.1	1.00	1.00
U2	0.8	0.8	1.00	1.00
U3	1.4	1.4	1.00	1.00
V1	0.1	0.1	1.00	1.00
V2	0.6	0.6	1.00	1.00
W1	0.6	0.6	1.00	1.00
W2	0.9	0.9	1.00	1.00
W3	0.9	0.9	1.00	1.00
W4	0.3	0.3	1.00	1.00
W5	0.5	0.5	1.00	1.00

RMS residual angle = 1.1 ARC SEC

Posn. at <T1	> =	0.000000	0.000000	0.000000
Rotn. at <T1	> =	1.000000	0.000000	0.000000
		0.000000	1.000000	0.000000
		0.000000	0.000000	1.000000

Recip. resid. = 1.7 ARC SEC

Posn. at <T2	> =	-1.384386	-2.945169	0.006943
Rotn. at <T2	> =	0.977791	-0.209582	-0.000047
		0.209582	0.977791	-0.000035
		0.000053	0.000025	1.000000

Recip. resid. = 2.8 ARC SEC

Remarks. Coordinate data file X-7AUG created.

DATA SETS 1.

DIFFERENCES of Fixed <X-3AUG > Transf. <X-7AUG >

NAME	X m	Y m	Z m
T1	0.000000	0.000000	0.000000
	0.000000	0.000000	0.000000
	0.000000	0.000000	0.000000
T2	-1.384359	-2.945086	0.007037
	-1.384386	-2.945169	0.006943
	0.000028	0.000084	0.000094
U1	1.627875	-0.397369	1.273030
	1.627842	-0.397508	1.273006
	0.000033	0.000139	0.000024
U2	1.719823	-0.352686	0.194283
	1.719814	-0.352762	0.194306
	0.000009	0.000077	-0.000023
V1	3.306815	-2.250451	1.666563
	3.306786	-2.250561	1.666570
	0.000029	0.000110	-0.000007
V2	3.237799	-2.096731	-0.390160
	3.237882	-2.096808	-0.390163
	-0.000083	0.000077	0.000003
W1	3.162732	-3.777256	0.855302
	3.162568	-3.777250	0.855352
	0.000164	-0.000006	-0.000049
W2	1.873034	-4.319876	-0.005776
	1.873012	-4.319914	-0.005829
	0.000021	0.000038	0.000053

Remarks. Sample only to show stability of instruments in test area. Levelled and non-levelled data sets observed on 3/8/87 and 7/8/87 resp. Theodolites were not moved.

DATA SETS 1.

3-D BEST FIT : Fixed <X-3AUG > Transf. <X-7AUG >

NAME	X m	Y m	Z m	x mm	y mm	z mm
150	1.146306	-1.604659	-1.423901			
	1.146294	-1.604675	-1.423965	0.012	0.016	0.064
1450	0.548081	-2.758838	-1.423426			
	0.548051	-2.758839	-1.423441	0.030	0.002	0.015
T1	0.000000	0.000000	0.000000			
	0.000015	0.000053	0.000005	-0.015	-0.053	-0.005
T2	-1.384359	-2.945086	0.007037			
	-1.384367	-2.945119	0.007031	0.008	0.033	0.005
U1	1.627875	-0.397369	1.273030			
	1.627885	-0.397429	1.272982	-0.010	0.060	0.048
U2	1.719823	-0.352686	0.194283			
	1.719834	-0.352703	0.194280	-0.011	0.018	0.003
U3	1.282459	-0.590728	-1.298498			
	1.282435	-0.590699	-1.298460	0.024	-0.029	-0.038
V1	3.306815	-2.250451	1.666563			
	3.306841	-2.250472	1.666543	-0.026	0.022	0.020
V2	3.237799	-2.096731	-0.390160			
	3.237892	-2.096757	-0.390191	-0.093	0.026	0.031
W1	3.162732	-3.777256	0.855302			
	3.162608	-3.777176	0.855356	0.124	-0.080	-0.053
W2	1.873034	-4.319876	-0.005776			
	1.873034	-4.319859	-0.005787	-0.001	-0.017	0.011
W3	2.448366	-3.542645	-1.288962			
	2.448361	-3.542615	-1.288886	0.004	-0.030	-0.076
W4	0.644717	-4.807823	0.983652			
	0.644772	-4.807925	0.983682	-0.055	0.102	-0.030
W5	0.841256	-4.710210	-1.298529			
	0.841249	-4.710141	-1.298533	0.007	-0.069	0.004

RMS residuals : x = 0.046 mm, y = 0.048 mm, z = 0.037 mm

Weighted rms = 0.044 mm

Remarks. Best fit with a shift and rotation only. Scale factor fixed at unity.

COMPARISON OF CONVENTIONAL LEVELLING AGAINST DIRECT OBSERVATION OF THE GRAVITY VECTOR.

File <TILT-REFL >

NAME	HORIZ	VERT
C1	87 31 26.5	26 43 47.0
C2	84 43 40.0	7 52 44.5
C3	84 44 1.0	-11 24 34.0
C4	83 48 26.5	-28 44 53.0
C5	97 56 5.5	-22 3 28.0
F1	48 30 26.5	-28 10 32.5
F2	48 27 1.0	-2 9 55.0
L1	20 40 28.5	11 22 58.0
L2	23 48 44.5	-1 12 39.5
L3	23 53 45.5	-23 58 44.5
R1	78 24 3.5	5 52 49.0
R2	91 29 15.5	7 21 52.5
R3	110 9 28.0	8 18 46.0
R4	110 12 2.5	-18 48 57.5
RIGHT	141 26 23.0	-0 2 10.5
S-1450	85 54 27.5	13 4 32.0
S-150	87 59 42.0	-9 16 22.5

Remarks. Conventionally levelled theodolite.

DATA SETS 2.

File <TILT-REFR >

NAME	HORIZ	VERT
C1	48 44 51.0	27 22 50.5
C2	49 55 21.5	7 58 4.0
C3	49 50 53.5	-11 25 58.0
C4	36 0 22.5	-23 59 30.5
C5	57 11 9.5	-27 56 49.0
F1	26 44 37.0	-16 42 4.0
F2	43 25 37.5	-1 39 22.5
L1	28 41 26.0	7 51 46.0
L2	21 47 40.0	-0 38 29.0
L3	21 49 18.5	-13 42 51.5
LEFT	352 39 33.0	0 2 15.0
R1	78 0 21.0	6 35 28.5
R2	81 17 55.0	9 36 35.5
R3	89 44 21.0	15 39 13.0
R4	89 51 14.0	-33 3 35.0
S-1450	53 58 16.0	13 55 13.0
S-150	56 31 16.5	-10 18 5.5

Remarks. Conventionally levelled theodolite.

Separation of S-150 -> S-1450 = 1.3 metres.

Coords. from <TILT-REFL> and <TILT-REFR> in <TILT-REF>.

DATA SETS 2.

File <TILT-L >

NAME	HORIZ	VERT
C1	241 46 35.5	27 3 50.0
C3	223 49 59.0	-6 50 49.5
C4	213 20 27.0	-21 3 31.0
DOWN	136 48 4.0	-67 9 59.5
L2	172 35 28.0	21 39 18.0
L3	168 1 28.0	1 19 21.5
R2	240 10 12.0	5 17 41.5
R4	247 2 38.5	-26 37 8.5
TILT-R	284 26 10.5	-15 13 43.0

File <TILT-R >

NAME	HORIZ	VERT
C1	311 49 13.5	27 11 11.5
C3	312 28 2.0	-12 59 14.5
C4	297 41 14.0	-25 30 38.0
L2	285 2 37.5	-1 16 24.5
L3	284 46 22.0	-14 27 45.0
R2	345 41 25.0	8 35 57.5
R4	354 37 14.5	-36 22 32.5
TILT-L	250 33 6.0	-4 3 44.5

Remarks.

Data in <TILT-L> were recorded by a non-levelled theodolite which observed a downward gravity vector by autocollimation off an oil pool. See observation "DOWN", which indicates a tilt of some 23 degs. The reflection in the oil was faint. The equivalent upward unit vector representing the direction of gravity was (-0.265636 0.282884 0.921637).

Data in <TILT-R> were recorded by a non-lev. theodolite.

Scale was not measured.

Coords. from <TILT-L> and <TILT-R> in <TILT>.

DATA SETS 2.

3-D BEST FIT : FIXED <TILT-REF >, TRANSF. <TILT >

NAME	X m	Y m	Z m	x mm	y mm	z mm
C1	2.897167	0.125268	1.460396			
	2.897303	0.125220	1.460263	-0.136	0.048	0.133
C3	3.005566	0.277036	-0.609147			
	3.005588	0.277043	-0.609130	-0.022	-0.007	-0.017
C4	2.282425	0.247656	-1.259421			
	2.282437	0.247545	-1.259483	-0.012	0.111	0.062
L2	1.177532	2.668263	-0.061612			
	1.177501	2.668196	-0.061564	0.031	0.067	-0.048
L3	1.180665	2.664818	-1.296400			
	1.180661	2.664979	-1.296474	0.004	-0.157	0.074
R2	4.961100	-0.128831	0.641350			
	4.961039	-0.128766	0.641474	0.060	-0.066	-0.125
R4	3.902828	-1.436020	-1.417016			
	3.902754	-1.436024	-1.416937	0.074	0.005	-0.079

Scale factor : 2.907076

Rotn matrix : -0.893624713 -0.448814964 0.000000000
0.448814964 -0.893624713 0.000000000
0.000000000 0.000000000 1.000000000

Rotn origin : -0.131513E+01 -0.284053E+00 -0.412182E+00
Shift : 0.390275E+01 -0.143602E+01 -0.141694E+01

RMS residuals : x = 0.065 mm, y = 0.083 mm, z = 0.086 mm

Remarks. All coordinates transformed with unit weights.
Transformation uses a 3-D shift, a scale change, and a rotation about the vertical Z axis only.
The top line of every pair represents coordinates computed from data sets <TILT-REFL> and <TILT-REFR>.
The lower line give the transformed coordinates computed from data sets <TILT-L> and <TILT-R>.

DATA SETS 3.

RESECTION TEST WITH A LEVELLED CAMERA.

File <FC0808 P > Photo-coordinates.

NAME	X mm	Y mm
PA1	-26.910	14.093
PA2	-27.015	9.904
PA3	-27.104	6.117
PA4	-27.303	-1.756
PA5	-27.454	-7.588
PA6	-27.609	-13.650
PA7	-27.792	-20.761
PA8	-28.038	-30.885
PB1	32.661	14.867
PB2	33.373	6.287
PB3	33.922	-0.424
PB4	34.547	-8.026
PB5	35.007	-13.629
PB6	35.442	-18.935
PB7	35.846	-23.835
PB8	36.119	-27.147
U1	-33.523	14.470
U2	-34.975	-3.941
U3	-31.472	-32.910
V1	-10.383	10.596
V2	-11.757	-11.403
W1	4.708	1.771
W2	17.850	-6.397
W3	7.045	-21.612
W4	33.646	7.681
W5	32.839	-24.274

Remarks.

Observations PAn and PBn are points along the image of 2 plumbwires.

The data is reduced to the p.p, and p.d = 63.96 mm.

Gravity vector is (-0.022534 0.993493 -0.111646).

DATA SETS 3.

Object coordinates in a levelled system.

File <X-3AUG >

NAME	X m	Y m	Z m
U1	1.627875	-0.397369	1.273030
U2	1.719823	-0.352686	0.194283
U3	1.282459	-0.590728	-1.298498
V1	3.306815	-2.250451	1.666563
V2	3.237799	-2.096731	-0.390160
W1	3.162732	-3.777256	0.855302
W2	1.873034	-4.319876	-0.005776
W3	2.448366	-3.542645	-1.288962
W4	0.644717	-4.807823	0.983652
W5	0.841256	-4.710210	-1.298529

DATA SETS 3.

NAME	Resid. (degs)	
U1	0.006	LEVELLED
U2	0.004	RESECTION
U3	0.007	
V1	0.004	Gravity vector defines
V2	0.000	Z axis.
W1	0.003	
W2	0.002	RMS fit = 15.2 arc secs.
W3	0.004	
W4	0.003	
W5	0.005	

Position (m)	-2.495812	-0.660632	-0.038355
Posn s.e	0.000424	0.000574	0.000097
Rotation :	-0.413289575	-0.110942420	-0.903816080
	-0.910320793	0.025775524	0.413100079
	-0.022533989	0.993492527	-0.111645947

NAME	Resid. (degs)	
U1	0.005	NON-LEVELLED
U2	0.005	RESECTION
U3	0.006	
V1	0.004	
V2	0.001	
W1	0.002	RMS fit = 13.8 arc secs.
W2	0.001	
W3	0.004	
W4	0.002	
W5	0.004	

Position (m)	-2.495922	-0.660757	-0.037738
Posn s.e	0.000417	0.000563	0.000492
Rotation :	-0.413264920	-0.110834296	-0.903840619
	-0.910331493	0.025701052	0.413081141
	-0.022553903	0.993506525	-0.111517293

DATA SETS 4.

ORIENTATION BY DISTANCE RANGING : THEODOLITE TEST.

File <CAL-REF 1 >. non-levelled theodolite.

NAME	HORIZ	VERT
B01	301 21 41.5	28 52 17.5
B02	300 33 52.5	4 23 43.5
B03	313 17 33.0	-28 40 6.5
B11	305 39 24.0	22 40 30.5
B12	303 10 48.0	11 32 31.5
B13	304 48 46.5	-3 48 14.5
B20	317 17 13.0	17 3 15.5
B22	315 25 33.5	8 18 36.0
B23	316 30 4.0	-2 24 9.0
B24	322 1 29.5	-15 34 9.0
B31	328 9 14.5	9 17 21.5
B32	328 7 33.0	2 38 27.0
B33	332 22 33.5	-13 34 3.5
B41	341 54 41.5	11 21 14.0
B42	343 22 51.0	1 50 22.0
B43	342 31 23.5	-11 39 57.0
B51	356 25 44.5	11 1 26.0
B52	356 40 54.0	3 14 4.0
B53	353 56 52.0	-12 36 15.5
G1-A	329 39 57.5	-1 10 3.0
G1-B	332 17 56.5	-1 14 56.5
G1-C	332 24 52.0	-4 33 45.0
G1-D	329 47 7.5	-4 37 31.5
G2-A	15 9 42.0	-9 20 4.5
G2-B	16 30 47.5	-8 59 9.0
G2-C	16 44 56.5	-10 53 23.5
G2-D	15 22 55.0	-11 15 8.5
SA-00	322 44 52.5	-24 9 4.0
SA-14	322 18 23.0	1 34 47.5
SA-26	321 54 6.5	22 33 19.5
SB-00	346 57 45.0	-14 22 36.0
SB-14	345 58 57.0	1 27 25.5
SB-26	345 9 43.0	14 53 7.5

DATA SETS 4.

File <CAL-REF 2 >, non-levelled theodolite.

NAME	HORIZ	VERT
B01	42 10 2.5	12 42 13.5
B02	42 50 42.5	0 15 39.5
B03	45 13 26.5	-17 18 57.5
B11	55 50 28.5	13 56 1.0
B12	53 36 60.0	5 45 47.5
B13	55 25 5.5	-4 6 35.0
B20	70 27 47.5	13 3 33.5
B22	67 53 30.0	5 19 4.5
B23	69 44 14.0	-3 19 54.5
B24	68 9 26.5	-14 15 26.5
B31	81 38 21.0	7 50 41.5
B32	81 52 19.0	1 25 3.5
B33	81 11 8.5	-14 32 57.0
B41	90 14 58.5	11 45 21.5
B42	91 47 17.5	1 3 44.0
B43	91 38 51.5	-14 18 26.5
B51	103 34 30.0	14 39 39.5
B52	104 21 24.5	3 42 11.0
B53	102 1 21.5	-17 53 41.0
G1-A	39 3 4.5	-2 36 35.0
G1-B	40 12 32.5	-2 41 8.0
G1-C	40 6 30.0	-4 12 58.5
G1-D	38 57 20.0	-4 6 49.0
G2-A	61 13 33.5	-17 58 36.0
G2-B	62 59 40.0	-18 37 34.0
G2-C	62 43 59.0	-21 52 7.0
G2-D	60 57 4.0	-21 0 12.0
SA-00	55 35 8.5	-18 20 50.5
SA-14	56 12 22.5	-0 41 46.0
SA-26	56 32 11.0	14 8 15.0
SB-00	90 48 8.5	-18 12 22.0
SB-14	89 47 39.5	0 32 8.5
SB-26	88 54 39.0	16 6 49.5

Remarks. Pts. SA- and SB-, on approx. straight line.

Separations are 00 -> 14 = 1.4 m and 14 -> 26 = 1.2 m

DATA SETS 4.

RELATIVE ORIENTATION of <CAL-REF 1> with <CAL-REF 2>
based on distance ranging to linear scales.

NAME	Ins Agl. DEC DEG	Angle 1 DEC DEG	Angle 2 DEC DEG	Resid 1 ARC SEC	Resid 2 ARC SEC
B01	51.0	97.9	31.1	11.2	5.8
B02	51.5	100.2	28.3	20.8	10.0
B03	58.1	88.2	33.7	3.6	2.0
B11	41.6	94.5	43.9	29.1	20.2
B12	42.9	97.4	39.7	22.9	14.8
B13	43.2	96.1	40.7	24.0	15.7
B20	39.0	83.6	57.4	33.8	28.6
B22	40.9	85.4	53.7	29.0	23.4
B23	40.6	84.4	55.0	30.1	24.8
B24	46.4	79.5	54.2	16.0	13.2
B31	39.6	72.8	67.5	21.8	21.1
B32	40.0	72.7	67.3	20.5	19.8
B33	43.9	69.3	66.8	5.7	5.6
B41	44.2	59.5	76.4	0.4	0.5
B42	45.3	57.5	77.2	10.8	12.5
B43	43.9	59.2	76.9	10.5	11.9
B51	45.2	45.3	89.5	20.8	29.2
B52	45.9	44.2	89.8	33.8	48.5
B53	44.7	48.4	86.8	33.6	44.9
G1-A	84.4	71.2	24.4	113.9	49.7
G1-B	85.9	68.6	25.5	109.2	50.6
G1-C	85.9	68.6	25.5	108.1	50.0
G1-D	84.4	71.2	24.3	111.2	48.4
G2-A	104.2	27.5	48.3	117.2	189.5
G2-B	103.7	26.1	50.1	118.4	206.3
G2-C	102.6	26.7	50.7	115.6	199.5
G2-D	103.1	28.0	48.9	114.1	182.8
SA-00	57.3	79.5	43.3	0.0	0.0
SA-14	59.9	78.5	41.6	19.8	13.4
SA-26	55.9	79.5	44.6	1.3	0.9
SB-00	48.4	55.4	76.2	20.9	24.6
SB-14	50.0	54.9	75.2	21.3	25.2
SB-26	47.7	56.8	75.5	4.3	4.9

DATA SETS 4.

OPTIMAL ORIENTATION of <CAL-REF 1> with <CAL-REF 2>
treating all targets as unknowns.

NAME	Resid 1 ARC SEC	Resid 2 ARC SEC	Weight 1	Weight 2
B01	1.1	1.1	1.00	1.00
B02	0.5	0.5	1.00	1.00
B03	1.4	1.4	1.00	1.00
B11	1.7	1.7	1.00	1.00
B12	1.9	1.9	1.00	1.00
B13	1.0	1.0	1.00	1.00
B20	0.5	0.5	1.00	1.00
B22	0.4	0.4	1.00	1.00
B23	1.0	1.0	1.00	1.00
B24	1.2	1.2	1.00	1.00
B31	0.2	0.2	1.00	1.00
B32	1.6	1.6	1.00	1.00
B33	2.0	2.0	1.00	1.00
B41	0.1	0.1	1.00	1.00
B42	0.1	0.1	1.00	1.00
B43	0.8	0.8	1.00	1.00
B51	0.9	0.9	1.00	1.00
B52	0.5	0.5	1.00	1.00
B53	0.9	0.9	1.00	1.00
G1-A	1.0	1.0	1.00	1.00
G1-B	0.3	0.3	1.00	1.00
G1-C	0.4	0.4	1.00	1.00
G1-D	0.0	0.0	1.00	1.00
G2-A	0.8	0.8	1.00	1.00
G2-B	0.3	0.3	1.00	1.00
G2-C	0.5	0.5	1.00	1.00
G2-D	0.5	0.5	1.00	1.00
SA-00	0.6	0.6	1.00	1.00
SA-14	1.4	1.4	1.00	1.00
SA-26	0.4	0.4	1.00	1.00
SB-00	0.9	0.9	1.00	1.00
SB-14	0.8	0.8	1.00	1.00
SB-26	0.7	0.7	1.00	1.00

DATA SETS 5.

ORIENTATION BY DISTANCE RANGING : PHOTO TESTS.

PHOTO DATA SETS <FC0913 P> AND <FC0914 P> ARE ORIENTED BY APPROXIMATE AND OPTIMAL MEANS. THEY CREATE TARGET COORDINATES IN FILE <FC-13-14 > WHICH ARE COMPARED WITH REFERENCE COORDINATES IN FILE <BUL-DEC >.

File <FC0913 P >

NAME	X mm	Y mm
B01	-29.358	17.677
B02	-30.824	-4.276
B03	-20.595	-35.178
B11	-22.702	13.541
B12	-25.689	2.654
B13	-24.329	-11.864
B21	-8.972	10.203
B22	-12.315	-0.161
B23	-11.133	-10.438
B24	-6.815	-23.509
B31	0.806	1.219
B32	0.936	-5.303
B33	4.685	-21.864
B41	13.858	4.078
B42	15.891	-5.660
B43	15.749	-20.297
B51	30.108	5.525
B52	31.217	-3.452
B53	29.206	-22.452
L1	-29.221	-19.808
L2	-20.506	3.827
L3	-15.168	18.627
R1	23.488	-25.010
R2	19.464	-6.334
R3	16.533	7.385

DATA SETS 5.

File <FC0914 P >

NAME	X mm	Y mm
B01	-35.409	14.563
B02	-35.035	-0.980
B03	-31.695	-22.723
B11	-19.013	14.484
B12	-21.876	5.273
B13	-20.110	-5.861
B21	-1.407	14.411
B22	-6.215	4.102
B23	-4.571	-5.081
B24	-6.060	-17.028
B31	8.338	6.276
B32	8.371	-0.514
B33	7.456	-17.630
B41	18.145	9.902
B42	19.533	-1.664
B43	18.855	-18.269
B51	34.198	12.926
B52	34.820	0.292
B53	31.100	-24.197
L1	-32.465	-11.483
L2	-24.033	5.770
L3	-17.675	19.269
R1	17.790	-25.102
R2	17.456	-2.967
R3	17.134	13.665

Remarks.

Each group of 3 points, Ln and Rn, lies approximately on a straight line, with separations :

1 -> 2 = 1.4 m

2 -> 3 = 1.2 m

DATA SETS 5.

RELATIVE ORIENTATION of <FC0913 P> with <FC0914 P>
based on distance ranging to linear scales.

NAME	Ins Agl. DEC DEG	Angle 1 DEC DEG	Angle 2 DEC DEG	Resid 1 ARC SEC	Resid 2 ARC SEC
B01	40.2	96.1	43.8	311.1	216.4
B02	40.1	98.2	41.7	191.9	128.9
B03	43.2	91.5	45.3	166.4	118.3
B11	33.0	91.3	55.7	28.3	23.4
B12	33.8	94.1	52.0	20.1	15.9
B13	33.6	93.6	52.7	119.1	95.0
B21	29.5	80.0	70.5	219.8	210.3
B22	31.6	83.3	65.1	193.4	176.7
B23	31.1	82.8	66.1	250.5	230.8
B24	35.0	80.2	64.8	261.4	240.1
B31	30.2	71.6	78.2	273.4	282.1
B32	30.4	71.9	77.8	277.3	285.2
B33	33.1	70.4	76.5	285.1	294.3
B41	33.2	60.0	86.8	235.3	271.2
B42	33.9	58.9	87.2	216.8	253.0
B43	33.0	61.1	85.9	252.0	287.2
B51	34.0	47.1	99.0	180.2	243.0
B52	34.4	46.7	98.9	146.1	198.5
B53	33.8	51.4	94.7	186.9	238.3
L1	39.1	97.4	43.5	0.0	0.0
L2	39.6	90.0	50.4	82.1	63.2
L3	37.2	85.1	57.7	0.7	0.6
R1	39.0	56.1	84.9	156.3	187.6
R2	38.6	56.0	85.4	168.8	203.0
R3	36.1	57.8	86.2	196.3	231.6

DATA SETS 5.

OPTIMAL ORIENTATION of <FC0913 P> with <FC0914 P>
treating all targets as unknowns.

NAME	Resid 1 ARC SEC	Resid 2 ARC SEC	Weight 1	Weight 2
B01	7.7	7.7	1.00	1.00
B02	3.5	3.5	1.00	1.00
B03	3.6	3.6	1.00	1.00
B11	3.1	3.1	1.00	1.00
B12	8.1	8.1	1.00	1.00
B13	0.9	0.9	1.00	1.00
B21	9.5	9.5	1.00	1.00
B22	0.0	0.0	1.00	1.00
B23	3.1	3.1	1.00	1.00
B24	6.1	6.1	1.00	1.00
B31	3.4	3.4	1.00	1.00
B32	0.2	0.2	1.00	1.00
B33	1.8	1.8	1.00	1.00
B41	2.8	2.8	1.00	1.00
B42	1.2	1.2	1.00	1.00
B43	0.7	0.7	1.00	1.00
B51	0.4	0.4	1.00	1.00
B52	3.8	3.8	1.00	1.00
B53	3.7	3.7	1.00	1.00
L1	6.2	6.2	1.00	1.00
L2	1.3	1.3	1.00	1.00
L3	2.8	2.8	1.00	1.00
R3	2.7	2.7	1.00	1.00

RMS residual angle = 4.2 ARC SEC

Posn. at <FC0913 P > =	0.000000	0.000000	0.000000
Rotn. at <FC0913 P > =	1.000000	0.000000	0.000000
	0.000000	1.000000	0.000000
	0.000000	0.000000	1.000000
Posn. at <FC0914 P > =	3.190568	0.187947	-1.018838
Rotn. at <FC0914 P > =	0.795759	-0.019575	0.605297
	-0.052496	0.993486	0.101143
	-0.603334	-0.112262	0.789547

DATA SETS 5.

3-D BEST FIT : Fixed <BUL-DEC > Transf. <FC-13-14 >

NAME	X m	Y m	Z m	x mm	y mm	z mm
B01	-1.956958	1.192731	1.263634			
	-1.956909	1.192582	1.263728	-0.049	0.150	-0.093
B02	-2.047127	1.208961	0.182738			
	-2.047085	1.208352	0.183285	-0.042	0.609	-0.546
B03	-1.641753	1.546704	-1.233261			
	-1.642111	1.546087	-1.233407	0.358	0.616	0.146
B11	-3.079289	2.209162	1.583403			
	-3.078598	2.209277	1.582736	-0.690	-0.114	0.667
B12	-3.028811	1.980487	0.739065			
	-3.029562	1.981086	0.739296	0.751	-0.599	-0.231
B13	-3.078345	2.140536	-0.249318			
	-3.078318	2.140729	-0.249270	-0.027	-0.193	-0.048
B23	-3.412473	3.596137	-0.207975			
	-3.411904	3.595951	-0.208030	-0.570	0.186	0.055
B31	-2.970378	4.782160	0.920807			
	-2.970044	4.782176	0.920773	-0.334	-0.017	0.034
B32	-2.982777	4.796853	0.260579			
	-2.982237	4.796502	0.260388	-0.541	0.351	0.191
B33	-2.352093	4.494561	-1.224261			
	-2.352232	4.494654	-1.224238	0.139	-0.092	-0.023
B41	-1.671544	5.117582	1.081023			
	-1.672041	5.117847	1.080920	0.498	-0.265	0.103
B42	-1.543697	5.171912	0.173335			
	-1.543646	5.171626	0.173274	-0.051	0.286	0.061
B43	-1.628231	5.171400	-1.119425			
	-1.628396	5.171988	-1.119394	0.165	-0.588	-0.031
B51	-0.339305	5.437135	1.061309			
	-0.339376	5.436776	1.061347	0.071	0.359	-0.038
B52	-0.316791	5.463757	0.309299			
	-0.317037	5.463819	0.309795	0.246	-0.063	-0.496
B53	-0.575191	5.425069	-1.219899			
	-0.575267	5.425695	-1.220149	0.075	-0.626	0.250

RMS residuals : x = 0.377 mm, y = 0.385 mm, z = 0.273 mm

Weighted rms = 0.349 mm

DATA SETS 6.

4-POINT CAMERA TARGET.

COORDINATES OF A 4-POINT CAMERA TARGET, ADJUSTED SUCH THAT THE 4 TARGETS AND THE ENTRANCE PUPIL ARE COPLANAR.

THE TARGET POINTS ARE A,B,C,D AND CENTRE OF ENTRANCE PUPIL IS P. TWO SETS OF MEASUREMENTS MADE AT DIFFERENT TIMES ON DIFFERENT METROGRAPHS.

BEST FITTING PLANES

Data set : <4PT-SEP > Units : MILLIMETRES

NAME	X	Y	Z	resid.
A	48.045	53.710	202.380	0.033
B	232.800	53.805	199.735	-0.004
C	229.020	53.530	53.500	0.032
D	44.380	53.365	58.100	-0.005
P	137.734	53.533	129.114	-0.056

Unit vector : -0.000747 0.999997 -0.002111
Offset dist. : 53.214
RMS offset : 0.033 (MM)

Data set : <4PT-NOV > Units : MILLIMETRES

NAME	X	Y	Z	resid.
A	4.550	57.500	-24.750	0.006
B	189.320	59.220	-22.460	-0.003
C	185.740	77.240	122.680	0.006
D	1.220	75.280	118.300	-0.003
P	94.590	67.210	47.620	-0.006

Unit vector : 0.007659 -0.992321 0.123453
Offset dist. : -60.085
RMS offset : 0.005 mm

DATA SETS 6.

3-D BEST FIT : Fixed <4PT-NOV > Transf. <4PT-SEP >

NAME	X mm	Y mm	Z mm	x mm	y mm	z mm
A	4.550	57.500	-24.750			
	4.664	57.468	-24.794	-0.114	0.032	0.044
B	189.320	59.220	-22.460			
	189.416	59.213	-22.528	-0.096	0.007	0.068
C	185.740	77.240	122.680			
	185.779	77.204	122.600	-0.039	0.036	0.080
D	1.220	75.280	118.300			
	1.140	75.291	118.384	0.080	-0.011	-0.084
P	94.590	67.210	47.620			
	94.421	67.273	47.728	0.169	-0.063	-0.108

Scale factor : 1.000000

Rotn matrix : 0.999964206 0.008402740 -0.000995523
0.008219806 -0.992573464 -0.121368670
-0.002007956 0.121356142 -0.992606994

Rotn. origin : 0.443800E+02 0.533650E+02 0.581000E+02
Shift : 0.113984E+01 0.752915E+02 0.118384E+03

RMS residuals : x = 0.108 mm, y = 0.036 mm, z = 0.080 mm
Weighted rms = 0.080 mm

DATA SETS 7.

MEASUREMENT OF BASEMENT TEST FIELD.

RELATIVE ORIENTATION OF 2 PHOTOS USING RECIPROCAL OBSERVATIONS TO A COMMON THEODOLITE STATION.

CAMERA POSITIONS C1 AND C2 ARE TARGETTED WITH A 4-POINT CAMERA TARGET. THE REDUCED POINTING FROM THE THEODOLITE IS COMPUTED FROM THESE.

CAMERA OBSERVATIONS REDUCED TO PRINCIPAL POINT.
PRINCIPAL DISTANCE = 63.96 mm.

File <RECIP 1T> Theodolilte station T1.

NAME	HORIZ	VERT
B12	333 24 0.5	9 27 19.5
B22	353 38 14.5	9 16 55.5
B31	15 21 54.0	14 24 16.0
C1-A	237 16 0.0	3 33 50.5
C1-B	239 37 48.5	3 33 27.0
C1-C	239 40 42.5	1 31 19.0
C1-D	237 18 52.5	1 31 1.0
-> C1 (recip. ob)	238 28 33.5	2 33 13.0
C2-A	279 53 59.0	3 54 50.5
C2-B	281 39 44.5	3 50 48.0
C2-C	281 40 48.0	2 19 41.0
C2-D	279 54 54.0	2 23 33.5
-> C2 (recip. ob)	280 47 25.5	3 7 50.5

DATA SETS 7.

File <RECIP-411 > Camera station C1.

NAME	X mm	Y mm
B01	-33.159	11.783
B02	-33.102	-3.404
B03	-29.227	-24.859
B11	-18.613	11.647
B12	-21.381	2.727
B13	-19.723	-8.177
B20	-3.876	9.566
B22	-6.541	1.634
B23	-4.943	-7.244
B24	-5.644	-18.805
B31	7.334	3.740
B32	7.459	-2.684
B33	7.361	-18.998
B41	17.181	7.127
B42	18.772	-3.536
B43	18.425	-19.136
B51	32.424	9.752
B52	33.333	-1.479
B53	30.517	-23.930
T1 (recip. ob)	29.992	-4.500

DATA SETS 7.

File <RECIP-421 > Camera station C2.

NAME	X mm	Y mm
B01	-27.711	16.971
B02	-29.999	-7.100
B03	-18.939	-40.085
B11	-24.934	13.786
B12	-28.083	1.933
B13	-27.213	-13.666
B20	-13.568	8.239
B21	-12.402	10.111
B22	-15.726	-0.759
B23	-14.985	-11.422
B24	-9.859	-25.233
B31	-3.011	0.452
B32	-3.123	-6.142
B33	0.744	-22.988
B41	10.383	2.442
B42	11.966	-7.179
B43	11.245	-21.307
B51	25.866	2.736
B52	26.474	-5.763
B53	23.821	-23.438
T1 (recip. ob)	30.570	-8.154

DATA SETS 7.

ORIENTATION PARAMETERS AND TARGET COORDINATES.

Rotn. at C1	0.833840	0.006969	-0.551962
----------	-0.551062	-0.047932	-0.833086
	-0.032263	0.998826	-0.036128
Rotn. at C2	0.252169	-0.064786	-0.965512
----------	-0.967678	-0.020097	-0.251386
	-0.003118	0.997697	-0.067760
Rotn. at T1	1.000000	0.000000	0.000000
----------	0.000000	1.000000	0.000000
	0.000000	0.000000	1.000000

NAME	X m	Y m	Z m
C1	-0.851578	-0.522332	0.044542
C2	-1.311706	0.249995	0.073029
T1	0.000000	0.000000	0.000000
B01	-0.715922	0.722399	0.310111
B02	-0.716031	0.743228	0.044112
B03	-0.676663	0.625326	-0.306376
B11	-0.396900	0.919336	0.377515
B12	-0.462206	0.923011	0.171922
B13	-0.430088	0.924707	-0.072576
B20	-0.020627	0.898717	0.354474
B22	-0.100989	0.905674	0.148940
B23	-0.062978	0.905214	-0.076172
B24	-0.183546	0.733944	-0.312541
B31	0.197826	0.719933	0.191751
B32	0.196263	0.722398	0.029148
B33	0.068350	0.594198	-0.331795
B41	0.190944	0.389985	0.230737
B42	0.186928	0.356680	0.007248
B43	0.180423	0.377222	-0.310662
B51	0.176160	0.053216	0.225693
B52	0.174105	0.046488	0.040637
B53	0.168617	0.111082	-0.335618

3-D BEST FIT ; Fixed <BUL-DEC > Transf. <RECIP 1 >

NAME	X m	Y m	Z m	x mm	y mm	z mm
B01	-1.956958	1.192731	1.263634			
	-1.956622	1.193275	1.263359	-0.336	-0.544	0.275
B02	-2.047127	1.208961	0.182738			
	-2.046805	1.208988	0.182778	-0.322	-0.027	-0.040
B03	-1.641753	1.546704	-1.233261			
	-1.641646	1.546180	-1.233805	-0.107	0.523	0.544
B11	-3.079289	2.209162	1.583403			
	-3.079870	2.209490	1.583803	0.581	-0.327	-0.400
B12	-3.028811	1.980487	0.739065			
	-3.028272	1.980773	0.738834	-0.539	-0.285	0.230
B13	-3.078345	2.140536	-0.249318			
	-3.078906	2.140512	-0.249373	0.561	0.024	0.055
B22	-3.364020	3.414417	0.700119			
	-3.364166	3.414247	0.700372	0.146	0.170	-0.253
B23	-3.412473	3.596137	-0.207975			
	-3.412296	3.596539	-0.208181	-0.177	-0.403	0.206
B24	-2.616834	3.352396	-1.184966			
	-2.616358	3.351759	-1.185042	-0.476	0.637	0.076
B31	-2.970378	4.782160	0.920807			
	-2.970089	4.782182	0.921111	-0.289	-0.022	-0.304
B32	-2.982777	4.796853	0.260579			
	-2.983419	4.797398	0.260424	0.642	-0.545	0.155
B33	-2.352093	4.494561	-1.224261			
	-2.351784	4.494316	-1.223888	-0.309	0.245	-0.373
B41	-1.671544	5.117582	1.081023			
	-1.671574	5.117692	1.081212	0.031	-0.109	-0.189
B42	-1.543697	5.171912	0.173335			
	-1.544408	5.172256	0.173157	0.711	-0.344	0.178
B43	-1.628231	5.171400	-1.119425			
	-1.628073	5.170991	-1.119231	-0.158	0.409	-0.194
B51	-0.339305	5.437135	1.061309			
	-0.339068	5.436471	1.061342	-0.237	0.664	-0.033
B52	-0.316791	5.463757	0.309299			
	-0.316672	5.463350	0.309460	-0.119	0.407	-0.161
B53	-0.575191	5.425069	-1.219899			
	-0.575590	5.425542	-1.220127	0.399	-0.473	0.228

DATA SETS 7.

3-D BEST FIT : Fixed <BUL-DEC > Transf. <RECIP 1 >

Scale factor : 4.064455

Rotn matrix : -0.274414256 -0.961576342 0.008231198
0.960888539 -0.274529752 -0.036422987
0.037283189 -0.002085722 0.999302564

Rotn. origin : -0.715922E+00 0.722399E+00 0.310111E+00
Shift : -0.195662E+01 0.119328E+01 0.126336E+01

RMS residuals : x = 0.395 mm, y = 0.397 mm, z = 0.252 mm
Weighted rms = 0.354 mm

Remarks.
Point B20 removed from best fit due to bad residuals.

DATA SETS 8.

MEASUREMENT OF UNTARGETTED POINTS ON THE UCL PORTICO.

File <PORTICO TH> Theodolite station THEOD.

NAME	HORIZ	VERT
CAM1 (recip. ob)	245 18 45.8	-0 24 6.1
CAM2 (recip. ob)	185 10 0.1	-0 18 55.0
TAR1	339 39 34.5	11 57 33.0
TAR2	88 39 40.0	12 42 50.5

File <PORTICO 31> Camera station CAM1.

NAME	X mm	Y mm
220	-18.335	-21.845
221	23.370	-25.718
222	-1.464	-23.458
224	-30.934	-0.542
225	-5.217	-0.414
226	-0.984	-0.417
227	26.970	-0.628
500	2.669	-31.878
503	-33.012	0.714
TAR1	29.827	-7.936
TAR2	-30.924	-6.244
THEOD (recip. ob)	-17.285	1.226

File <PORTICO 33> Camera station CAM2.

NAME	X mm	Y mm
220	-24.372	-26.664
221	17.045	-21.130
222	-3.836	-23.977
224	-27.197	-1.038
225	3.652	-0.259
226	7.691	-0.179
227	29.648	0.127
500	0.773	-31.310
503	-30.710	0.585
TAR1	30.160	-5.474
TAR2	-30.039	-8.570
THEOD (recip. ob)	14.829	1.603

DATA SETS 8.

ORIENTATION PARAMETERS AND TARGET COORDINATES.

Rotn. at CAM1	-0.640254	0.017012	-0.767975
----------	0.768125	0.024132	-0.639845
	0.007648	-0.999564	-0.028518
Rotn. at CAM2	-0.949864	0.002122	-0.312657
----------	0.312578	0.029863	-0.949423
	0.007322	-0.999552	-0.029029
Rotn. at THEOD	1.000000	0.000000	0.000000
----------	0.000000	1.000000	0.000000
	0.000000	0.000000	1.000000

NAME	X m	Y m	Z m
CAM1	-0.909	-0.418	-0.007
CAM2	-0.088	-0.978	-0.005
THEOD	0.000	0.000	0.000
220	1.089	0.451	0.769
221	0.038	1.217	0.770
222	0.621	0.791	0.771
224	0.770	0.000	0.045
225	0.286	0.423	0.043
226	0.205	0.481	0.043
227	-0.293	0.774	0.044
500	0.495	0.846	1.002
503	0.818	-0.035	0.014
TAR1	-0.314	0.848	0.192
TAR2	0.861	0.020	0.194

DATA SETS 8.

3-D BEST FIT : Fixed <PORTICO > Transf. <PORTICO A >

NAME	X m	Y m	Z m	x mm	y mm	z mm
220	26.413	14.274	-42.102			
	26.420	14.250	-42.087	-7.975	24.243	-14.909
221	3.469	14.283	-41.823			
	3.456	14.273	-41.821	12.768	10.110	-1.794
222	16.210	14.290	-41.962			
	16.214	14.280	-41.949	-3.939	10.237	-12.021
224	26.668	1.429	-32.357			
	26.676	1.445	-32.357	-8.498	-15.853	0.208
225	15.358	1.411	-33.207			
	15.357	1.414	-33.222	1.005	-3.288	15.111
226	13.594	1.412	-33.188			
	13.595	1.413	-33.197	-0.664	-0.705	8.922
227	3.478	1.422	-32.093			
	3.457	1.429	-32.086	20.639	-7.027	-6.598
500	13.841	18.359	-41.388			
	13.845	18.366	-41.389	-3.944	-7.651	0.915
503	27.714	0.887	-32.363			
	27.723	0.897	-32.373	-9.391	-10.065	10.166

Scale factor : 17.660921

Rotn matrix : 0.801348784 -0.598197360 0.000148504
0.001002400 0.001591085 0.999998239
-0.598196543 -0.801347234 0.001874636

Rotn. origin : 0.377168E-01 0.121714E+01 0.770122E+00

Shift : 0.345623E+01 0.142729E+02 -0.418212E+02

RMS residuals : x = 9.693 mm, y = 11.863 mm, z = 9.578 mm
Weighted rms = 10.431 mm

Remarks. Reference coords. in file <PORTICO >.